3.0 THERMAL EVALUATION

Provides an evaluation of the package to protect the fuel during varying thermal conditions.

3.1 DESCRIPTION OF THERMAL DESIGN

The RAJ-II package is designed to provide thermal protection as described in Subpart F of 10 CFR 71 for transport of two BWR fuel assemblies with negligible decay heat. Compliance is demonstrated with 10 CFR 71 subpart F in the following subsections. The RAJ-II protects the fuel through the use of an inner and outer container that restricts the exposure of the fuel to external heat loads. The insulated inner container further restricts the heat input to the fuel through its insulation. The fuel requires very little thermal protection since similar fuel has been tested to the 800°C temperature without rupture.

Given negligible decay heat, the thermal loads on the package come solely from the environment in the form of solar radiation for Normal Conditions of Transport (NCT), as described in Section 3.4 or a half-hour, 800°C (1,475°F) fire for Hypothetical Accident Conditions (HAC), described in Section 3.5.

Specific ambient temperatures and solar heat loads are considered in the package thermal evaluations. Ambient temperatures ranging from -40°C to 38°C (-40°F to 100°F) are considered for NCT. The HAC fire event considers an ambient temperature of 38°C (100°F), with solar heat loading (insulation) before and after the HAC half-hour fire event.

Details and assumptions used in the analytical thermal models are described with the thermal evaluations.

3.1.1 Design Features

The primary features that affect the thermal performance of the package are 1) the materials of construction, 2) the inner and outer containers and 3) the thermal insulation of the inner container. The stainless sheet metal construction of the structural components of the inner and outer containers influences the maximum temperatures under normal conditions. The material also ensures structural stability under the hypothetical accident conditions as well as provides some protection to the fuel. Likewise the zirconium alloy cladding has also been proven to be stabile at the high temperatures potentially seen during the Hypothetical Accident Conditions (HAC).

The multi walled construction of the single walled outer container and the double walled inner container reduces the heat transfer as well as provides additional stability. The multi walled construction also reduces the opportunity for the fire in the accident conditions to impinge directly on the fuel.

The thermal insulation also greatly reduces the heat transfer to the fuel from external sources. The insulation consists of alumina silicate around most of the package plus the use of wood on the ends that both provide some insulation as well as shock absorbing capabilities.

3.1.2 Content's Decay Heat

Since the contents are unirradiated fuel, the decay heat is insignificant.

3.1.3 Summary Tables of Temperatures

Since the decay heat load is negligible, the maximum NCT temperature of 171°F (77°C, 350 K) occurs on the package exterior, and the maximum HAC temperature of 1198°F (648°C, 921 K) occurs at the inner surface of the inner container at the end of the fire. These analyses demonstrate that the RAJ-II package provides adequate thermal protection for the fuel assembly and will maintain the maximum fuel rod temperature well below the fuel rod rupture temperature of 800+°C under all transportation conditions.

3.1.4 Summary Tables of Maximum Pressures

The maximum pressure within the containment, the fuel rods during normal conditions of transport is 1.33 MPa (192.9 psia).

The maximum pressure during the hypothetical accident conditions is 3.50 MPa (508 psia).

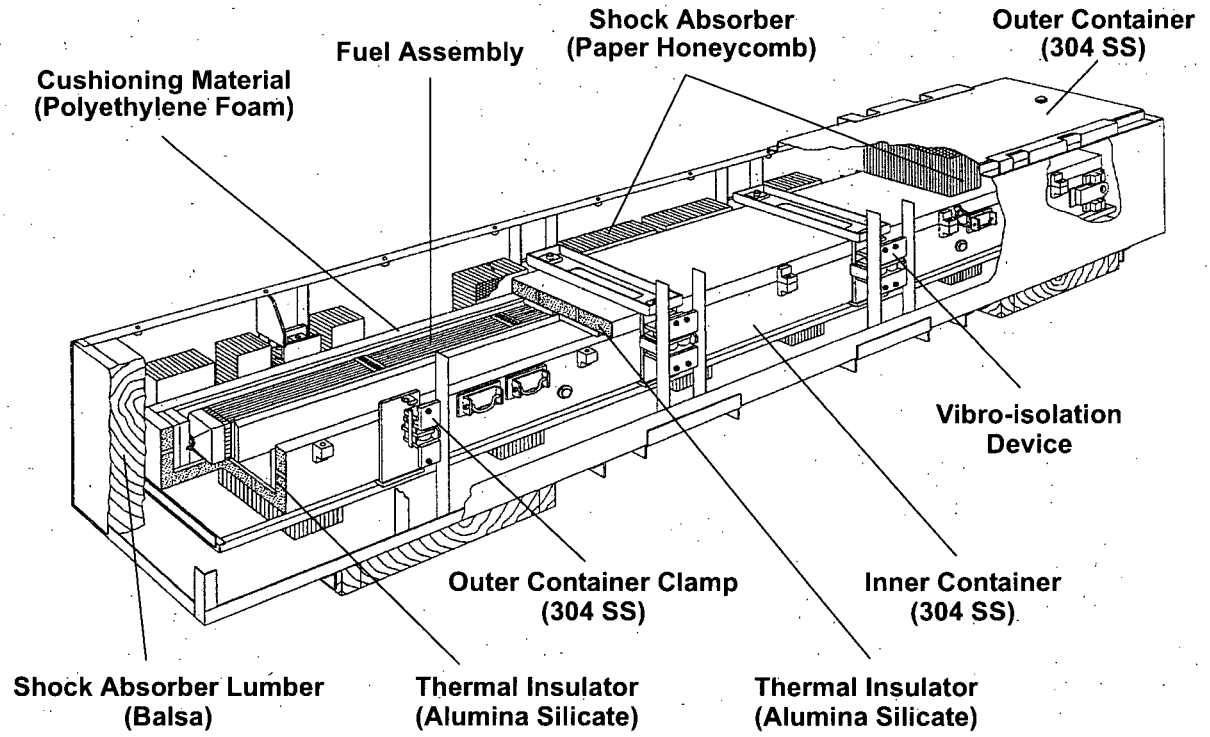

Figure 3-1 Overall View of RAJ-II Package

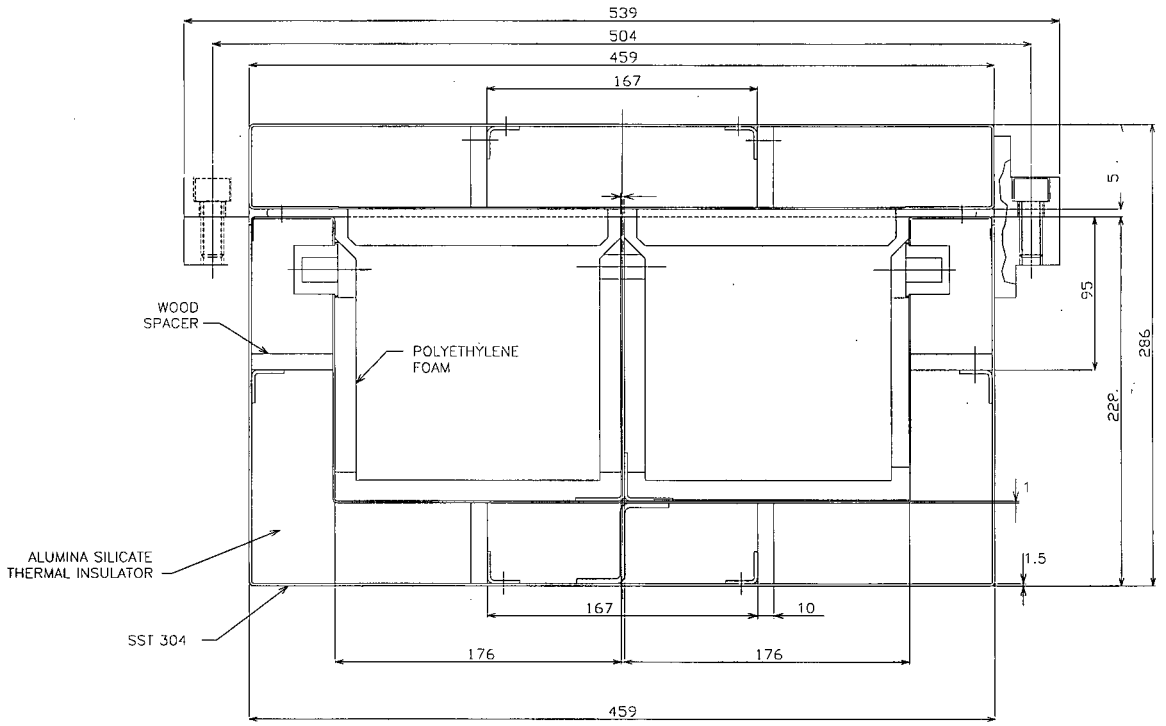

Figure 3-2 Transverse Cross-Sectional View of the Inner Container

3.2 MATERIAL PROPERTIES AND COMPONENT SPECIFICATIONS

3.2.1 Material Properties

The RAJ-II inner container is constructed primarily of Series 300 stainless steel, wood, and alumina silicate insulation. The void spaces within the inner container are filled with air at atmospheric pressure. The outer container is constructed of series 300 stainless steel, wood, and resin impregnated paper honeycomb. The thermal properties of the principal materials used in the thermal evaluations are presented in Table 3-1 and Table 3-2. Where necessary, the properties are presented as functions of temperature. Note that only properties for materials that constitute a significant heat transfer path are defined. A general view of the package is depicted in Figure 3-1. A sketch of the inner container transversal cross-section with the dimensions used in the calculation is presented in Figure 3-2.

For the Alumina Silicate, maximum values are specified because the maximum conductivity is the controlling parameter. This is because there is no decay heat in the payload and the only consideration is the material's ability to block of heat transfer to the fuel during the fire event.

Table 3-1 Material Properties for Principal Structural/Thermal Components

Material	Temperature, K	Thermal Conductivity, W/m-K	Specific Heat, J/kg-K	Density, kg/m^3	Notes
Wood	300	0.240	2,800	500	①
Series 300 Stainless Steel	300	15	477	7,900	②
	400	17	515		
	500	18	539		
	600	20	557		
	800	23	582		
	1,000	25	611		
Alumina Silicate Insulation	673	≤ 0.105	1,046 (Nominal)	250 (Nominal)	③
	873	≤ 0.151			
	1,073	≤ 0.198			④
	1,273	≤ 0.267			④

Notes:
① The material specified for the wood spacers. The properties have been placed with typical values for generic softwood.
② [Reference 2. p.809, 811, 812, and 820]
③ The values shown are based on published data for Unifrax Duraboard LD [11] and include compensation for the possible variation in test data (see discussion in Section 3.2.1).
④ Values at higher temperatures than 1,000 K are linearly extrapolated.

Table 3-2 Material Properties for Air

Temperature (K)	Thermal Conductivity (W/m·K)	Density (kg/m^3)	Specific Heat (J/kg·K)	Coefficient of Kinematic Viscosity $\nu(m^2/s)$	Prandtl Pr
300	0.0267	1.177	1005	15.66 E-06	0.69
310	0.0274	1.141	1005	16.54 E-06	0.69
320	0.0281	1.106	1006	17.44 E-06	0.69
330	0.0287	1.073	1006	18.37 E-06	0.69
340	0.0294	1.042	1007	19.32 E-06	0.69
350	0.030	1.012	1007	20.30 E-06	0.69
360	0.0306	0.983	1007	21.30 E-06	0.69
370	0.0313	0.956	1008	22.32 E-06	0.69
380	0.0319	0.931	1008	23.36 E-06	0.69
390	0.0325	0.906	1009	24.42 E-06	0.69
400	0.0331	0.883	1009	25.50 E-06	0.69
500	0.0389	0.706	1017	37.30 E-06	0.69
600	0.0447	0.589	1038	50.50 E-06	0.69
700	0.0503	0.507	1065	65.15 E-06	0.70
800	0.0559	0.442	1089	81.20 E-06	0.70
900	0.0616	0.392	1111	98.60 E-06	0.70
1000	0.0672	0.354	1130	117.3 E-06	0.70

Source: Reference 2, p. 824

3.2.2 Component Specifications

None of the materials used in the construction of RAJ-II package, such as series 300 stainless steel and alumina silicate insulation, are sensitive to temperatures within the range of -40°C to 800°C (-40°F to 1,475°F) that spans the NCT and HAC environment. Stainless steel has a melting point above 1,400°C (2,550°F), and maximum service temperature of 427°C (800°F). Similarly, the ceramic fiber insulation has a maximum operating temperature of 1,300°C (2,372°F). Wood is used as dunnage and as part of the inner package wall in the RAJ-II package. Before being consumed in the HAC fire, the wood would insulate portions of the inner container from exposure to the flames. However, the HAC transient thermal analyses presented herein conservatively neglects the wood's insulating effect, and assumes that all of the wood is consumed in the fire generating heat for all of its total mass.

The temperature limit for the fuel assembly's rods is greater than 800°C (1,472°F), based on the pressure evaluation provided in Section 3.5.3.2.

3.3 GENERAL CONSIDERATIONS

3.3.1 Evaluation by Analysis

The normal conditions of transport thermal conditions are evaluated by closed form calculations. The details of this analysis and supporting assumptions are found in that evaluation. The evaluation finds the maximum temperature for the outside of the package due to the insulation and uses that temperature for the contents of the package.

The transient hypothetical accident conditions are evaluated using an ANSYS finite element model. The model does not take credit for the outer container or the wood used in the inner container. Details of the model and the supporting assumptions maybe found in Section 3.5.

3.3.2 Evaluation by Test

Thermal testing was performed on fuel rods to determine the ability of the cladding (primary containment) to withstand temperatures greater than 800°C. The testing was performed for a range of fuel rods of different diameters, clad thickness and internal pressure. Since some of the current fuel designs for use in the RAJ-II are outside the range of parameters tested, additional thermal analyses have been performed to demonstrate the fuel rod's ability to withstand the HAC fire. In these tests, the fuel rods were heated to various temperatures from 700°C to 900°C for periods over one hour to determine the rupture temperature and pressure of the fuel. It was found that the fuel cladding did not fail at 800°C the temperature of the hypothetical accident conditions. This temperature associated pressure and resulting stress were used to provide the allowable conditions of the fuel which is used for containment.

3.3.3 Margins of Safety

For the normal condition evaluation the margins of safety are qualitative, based on comparisons to the much higher temperatures the fuel is designed for when it is in service in the reactors. There is no thermal deterioration of the packaging components at normal condition temperatures therefore no margins for the package components are calculated.

The margins of safety for the accident conditions are evaluated in Section 3.5 and are based on the testing discussed in Section 3.3.2.

3.4 THERMAL EVALUATION UNDER NORMAL CONDITIONS OF TRANSPORT

This section presents the results of thermal analysis of the RAJ-II package for the Normal Conditions of Transport (NCT) specified in 10 CFR 71.71. The maximum temperature for the normal conditions of transport is used as input (initial conditions) in the Hypothetical Accident Condition (fire event) analysis.

3.4.1 Heat and Cold

Per 10 CFR 71.71(c)(1), the maximum environmental temperature is 100°F (311 K), and per 10 CFR 71.71(c)(2), the minimum environmental temperature is -40°F (233 K).

Given the negligible decay heat of the fuel assembly, the thermal loads on the RAJ-II package come solely from the environment in the form of solar radiation for NCT as prescribed by 10 CFR 71.71(c)(1). As such, the solar heat input into the package is 800 g·cal/cm^2 for horizontal surfaces and 200 g·cal/cm^2 for vertical surfaces for a varying insolation over a 24-hour period).

3.4.1.1 Maximum Temperatures

For the analysis, the applied insolation is modeled transiently as sinusoidal over a 24-hour period, except when the sine function is negative (the insolation level is set to zero). The timing of the sine wave is set to achieve its peak at 12:00 PM and peak value of the curve is adjusted to ensure that the total energy delivered matched the regulatory values (800 g·cal/cm^2 for horizontal surfaces, 200 g·cal/cm^2 for vertical surfaces). As such, the total energy delivered in one day by the sine wave model is given by:

$$\int_{6\cdot hr}^{18\cdot hr} Q_{peak} \cdot \sin\left(\frac{\pi t}{12\cdot hr} - \frac{\pi}{2}\right) dt = \left(\frac{24\cdot hr}{\pi}\right) \times Q_{peak}$$

Using the expression above for the peak rate of insolation, the peak rates for top and side insolation may be calculated as follows:

Based on these inputs, the maximum NCT temperature on the inside surface of the inner container, as calculated in Appendix 3.6.3, is 350 K (77°C, 171°F).

Given negligible decay heat, the maximum accessible surface temperature of the RAJ-II package in the shade is the maximum environment temperature of 38°C (100°F), which is less than the 50°C (122°F) limit established in 10 CFR 71.43(g) for a non-exclusive use shipment.

3.4.1.2 Minimum Temperatures

The minimum environmental temperature that the RAJ-II package will be subjected to is -40°F, per 10 CFR 71.71(c)(2). Given the negligible decay heat load, the minimum temperature of the RAJ-II package is -40°F.

3.4.2 Maximum Normal Operating Pressure

The fuel rods are pressurized with helium to a maximum pressure of 1.145 MPa (absolute pressure (161.7 psia) helium at ambient temperature prior to sealing. Hence, the Maximum Normal Operating Pressure (MNOP) at the maximum normal temperature is:

$$\text{MNOP} = (P_1)\frac{T_{max}}{T_{ambient}} = 1.1145 \times \frac{350}{293} = 1.33 \text{ MPa} = 192.9 \text{ psia}$$

Since there is no significant decay heat and the fuel composition is stable, MNOP calculated above would not be expected to change over a one year time period.

3.4.3 Maximum Thermal Stresses

Due to the construction of the RAJ-II, light sheet metal constructed primarily of the same material, 304 SS, there are no significant thermal stresses. The package is constructed so that there is no significant constraint on any component as it heats up and cools down. The fuel cladding which provides containment is likewise designed for thermal transients, greater than what is found in the normal conditions of transport. The fuel rod is allowed to expand in the package. The fuel within the cladding is also designed to expand without interfering with the cladding.

3.5 THERMAL EVALUATION UNDER HYPOTHETICAL ACCIDENT CONDITIONS

This section presents the results of the thermal analysis of the RAJ-II package for the Hypothetical Accident Condition (HAC) specified in 10 CFR 71.73(c) (4).

For the purposes of the Hypothetical Accident Conditions fire analysis, the outer container of the RAJ-II package is conservatively assumed to be not present during the fire. This allows the outer surface of the inner container to be fully exposed to the fire event. The wood used in the inner container is conservatively assumed to combust completely. By ignoring the outer container and

applying the fire environment directly to the inner container, the predicted temperature of the fuel rods is bounded. To provide a conservative estimate of the worst-case fuel rod temperature, the fuel assembly and its corresponding thermal mass are not explicitly modeled as well as the polyethylene foam shock absorber. The maximum fuel rod temperature is conservatively derived from the maximum temperature of the inside surface of the inner stainless steel wall. The analysis considering the insulation and multi-layers of packaging is very conservative because as discussed in Section 3.3.2 the bare fuel has been demonstrated to maintain integrity when exposed to temperatures that equal those found in the hypothetical accident conditions.

Thermal performance of the RAJ-II package is evaluated analytically using a 2-D model that represents a transversal cross-section of the inner container (Figure 3-2) in the region containing the metallic and wood spacers. The 2-D inner container finite element model was developed using the ANSYS computer code [3]. ANSYS is a comprehensive thermal, structural and fluid flow analysis package. It is a finite element analysis code capable of solving steady state and transient thermal analysis problems in one, two or three dimensions. Heat transfer via a combination of conduction, radiation and convection can be modeled.

The solid entities were modeled in the present analysis with PLANE55 two-dimensional elements and the radiation was modeled using the AUX12 Radiation Matrix method. The developed ANSYS input file is included as Appendix 3.6.2.

The initial temperature distribution in the inner container prior to the HAC fire event is a uniform 375 K conservatively corresponding to the outer surface temperature of the inner container per the normal condition calculations presented in Appendix 3.6.3.

3.5.1 Initial Conditions

The environmental conditions preceding and succeeding the fire consist of an ambient temperature of 38°C (311 K) and insulation per the normal condition thermal analysis. The solar absorptivity coefficient of the outer surface has been increased for the post-fire period to 1 to include changes due to charring of the surfaces during the fire event.

3.5.2 Fire Test Conditions

The Hypothetical Accident Condition fire event is specified per 10 CFR 71.73(c) (4) as a half-hour, 800°C (1,073 K) fire with forced convection. For the purpose of calculation, the value of the package surface absorptivity coefficient (0.8) is selected as the highest value between the actual value of the surface (0.42) and a value of 0.8 as specified in 10 CFR 71.73(c) (4).

A value of 1.0 for the emissivity of the flame for the fire condition is used in the calculation. The rationale for this is that 1.0 maximizes the heating of the package. This value exceeds the minimum value of 0.9 specified in 10 CFR 71.73(c) (4). The Hypothetical Accident Condition (HAC) fire event is specified per 10 CFR 71.73(c)(3) as a half-hour, 800°C (1,475°F) fire with forced convection and an emissivity of 0.9. The environmental conditions preceding and succeeding the fire consist of an ambient temperature of 100°F and insulation per the NCT thermal analyses.

To model the combustion of the wood, the wood elements of the model are given a heat generation rate based on the high heat value of Western Hemlock of 3630 Btu/lb (8.442×10^6 J/kg) from Reference 8, Section 7, Table 9. It is conservatively assumed that the entire mass of the wood will burn. Moreover, the wood will burn across its thinnest section from opposite faces. Using data burn rate data for redwood which has approximately the same density as hemlock [8], each face will burn 5 mm at a minimum rate of 0.543 mm/min [10] resulting in a 9.2 minute time of combustion. This conservatively results in the longest burn time for the hemlock, and the greatest effect on temperature. The resulting heat generation rate in the wood spacers is equal to:

$$\dot{Q} = (8.42\times10^6) \times (500 \text{ kg / m}^3) / (9.2 \text{ sec} \times 60) = 7.63\times10^6 \text{ W/m}^3\text{/sec.}$$

3.5.2.1 Heat Transfer Coefficient during the Fire Event

During a HAC hydrocarbon fire, the heating gases surrounding the package will achieve velocities sufficient to induce forced convection on the surface of the package. Peak velocities measured in the vicinity of the surfaces were under 10 m/s [4].

The heat transfer coefficient takes the form [Reference 4, p. 369]:

$$h = k/D \cdot C \cdot (u \cdot D/\upsilon:)^m \cdot Pr^{1/3} \qquad (8)$$

Where:

D: average width of the cross-section of the inner container (0.373 m)

k: thermal conductivity of the fluid

υ: kinematic viscosity of the fluid

u: free stream velocity

C, m: constants that depend on the Reynolds number ($Re=u\cdot D/\upsilon$)

Pr: Prandtl number for the fluid

The property values of k, υ and Pr are evaluated at the film temperature, which is defined as the mean of the wall and free stream fluid temperatures. At the start of the fire the wall temperature is 375 K (101.7°C, 215°F) and the stream fluid temperature is 1,073 K (1,475°F). The film temperature is therefore 710.5 K, and the property values for air at this temperature (interpolated from Table 3-2) are k=0.0509 W/m·K, υ=66.84E-06 m^2/s and Pr= 0.70. Assuming a maximum stream velocity of 10 m/s this yields a Reynolds number of 55.8E03. At this value of Re, the constants C and n are 0.102 and 0.675 respectively [Reference 4, Table 7.3].

$$h = \frac{0.0509 \cdot 0.102 \cdot (10 \cdot 0.373/66.84 \cdot 10^{-6})^{0.675} \cdot (0.70)^{1/3}}{0.373}$$

$$h = 19.8\ W/m^2 \cdot K$$

A value of 19.8 $W/m^2 \cdot K$ was conservatively used in the analysis of the regulatory fire.

3.5.2.2 Heat Transfer Coefficient during Post-Fire Period

During the post-fire period of the HAC, it is conservatively assumed that there is negligible wind and that heat is transferred from the inner container to the environment via natural convection. Natural heat transfer coefficients from the outer surface of the square inner container are calculated as follows.

Reference 4 recommends the following correlations for the Nusselt number (Nu) describing natural convection heat transfer to air from heated vertical and horizontal surfaces:

Vertical heated surfaces [Reference 4, p. 493]:

$$Nu = \left(0.825 + \frac{0.387 \cdot (Gr \cdot Pr)^{1/6}}{(1 + (0.492/Pr)^{9/16})^{8/27}}\right)^2 \quad \text{For entire range of } Ra = Gr \cdot Pr \tag{9}$$

Where:

Nu: Nusselt number

Gr: Grashof number

Pr: Prandtl number

Horizontal heated surfaces facing upward [Reference 4, p. 498]:

$$Nu = 0.54 \cdot (Gr \cdot Pr)^{1/4} \quad \text{for } (10^4 < Gr \cdot Pr < 10^7) \tag{10}$$

$$Nu = 0.15 \cdot (Gr \cdot Pr)^{1/3} \quad \text{for } (10^7 < Gr \cdot Pr < 10^{11}) \tag{11}$$

and, for horizontal heated surfaces facing downward:

$$Nu = 0.27 \cdot (Gr \cdot Pr)^{1/4} \quad \text{for } (10^5 < Gr \cdot Pr < 10^{10}) \tag{12}$$

The correlations for the horizontal surfaces are calculated using a characteristic length defined by the relation L=A/P, where A is the horizontal surface area and P is the perimeter [Reference 4, p. 498]. The calculated characteristic length for the horizontal surfaces of the inner container is L=0.209 m (A=2.14812 m^2 and P=10.278 m).

The following convective heat transfer coefficients (Table 3-1) have been calculated using Eq. (5), (6), (9), (10), (11) and (12). The corresponding characteristic length used in calculating the Nusselt number for each surface is also used in Eq. 5 for calculating the heat transfer coefficient. The thermal properties of air have been evaluated at the mean film temperature (=(T_s+$T_{ambient}$)/2).

The effects of solar radiation are included during the post-fire period by specifying the equivalent heat flow for each node of the surfaces exposed to fire for an additional 3.5 hours, i.e. the fire starts at the time of the peak temperature in the inner container (8 hours after sunrise) and is 0.5 hours in duration. This results in an additional 3.5 hours of solar insolation. Using the peak rates calculated in Section 3.4.1.1, the nodal heat flows at 2:30 PM are equal to:

$$\dot{q}_{top} = \frac{1{,}218\frac{W}{m^2}\left(Sin\left(\frac{\pi\times(6+8.5)}{12}-\frac{\pi}{2}\right)\right)(0.459\,m)}{(155-1)} = 2.88\,W/m$$

$$\dot{q}_{side} = \frac{305\frac{W}{m^2}\left(Sin\left(\frac{\pi\times 14.5}{12}-\frac{\pi}{2}\right)\right)(0.281\,m)}{99-1} = 0.69\,W/m$$

where 0.459 m is the width of the inner container, 0.281 m is its height, and the model is 155 nodes in width by 99 nodes in height. For the remaining 3.5 hours of solar insolation, these heat fluxes are conservatively applied as bounding constant values rather than varying with time.

The solar absorptivity coefficient of the outer surface is conservatively assumed to be 1. The duration of the post-fire period has been extended to 12.5 hr to investigate the cool-down of the inner container.

3.5.3 Maximum Temperatures and Pressure

3.5.3.1 Maximum Temperatures

The peak fuel rod temperature, which is conservatively assumed to be the same as the inner wall temperature of the package, response over the course of the HAC fire scenario is illustrated in Figure 3-3. The temperature reaches its maximum point of 921 K or 648°C (1198°F) at the end of the fire or 1,800 seconds after the start of the fire. This peak temperature occurs at top corners of the inner wall.

The maximum temperature even when applied to the fuel directly is well below the maximum temperature the fuel can withstand. Similar fuel with no thermal protection has been tested in fire conditions at over 800°C (1,475°F) for more than 60 minutes without failures.

3.5.3.2 Maximum Internal Pressure

The maximum pressure for the fuel can be determined by considering that the fuel is pressurized initially with helium. As the fuel is heated, the internal pressure in the cladding increases. By applying the perfect gas law the pressure can be determined and the resulting stresses in the cladding can be determined. Since the temperatures can be well above the normal operating range of the fuel the cladding performance can best be determined by comparison to test data.

Similar fuel with similar initial pressures has been heated in an oven to over 800°C for over an hour without failures [6]. The fuel that was tested in the oven was pressurized with 10 atmospheres of helium. When heated to the 800°C it had an equivalent pressure of:

$$P_{\max} = (P_1)\frac{T_{\max}}{T_{ambient}} = 1.1145 MPa * \frac{1073}{293} = 4.08 MPa = 592 psia$$

This results in an applied load to the cladding of 3.98 MPa or 577.3 psig. The fuel that was tested had an outer diameter of 0.4054 inch (10.30 mm). Since the fuel when tested to 850°C had some ruptures but did not rupture at 800°C when held at those temperatures for 1 hour, the stresses at 800°C are used as the conservative allowable stress. Both the tested fuel and the fuels to be shipped in the RAJ-II have similar zirconium cladding. The stress generated in the cladding of the test fuel is:

$$\sigma = \frac{pr}{t} = \frac{3.98\text{MPa} \times 4.56\text{mm}}{0.584\text{mm}} = 31.1\text{MPa} = 4510\text{psi}$$

Recognizing that the properties of the fuel cladding degrade as the temperature increases the above calculated stress is conservatively used as the allowable stress for the fuel cladding for the various fuels to be shipped. The fuel is evaluated at the maximum temperature the inner wall of the inner container sees during the Hypothetical Accident Condition thermal event evaluated above. Table 3-5 shows the maximum pressure for each type of fuel and the resulting stress and margin. The limiting design properties of the fuel, maximum cladding internal diameter, minimum cladding wall thickness and initial pressurization for each type of fuel are considered in determining the margin of safety. Positive margins are conservatively determined for each type of fuel demonstrating that containment would be maintained during the Hypothetical Accident events. The minimum cladding thickness does not include the thickness of the liner if used.

The results of the transient analysis are summarized in Table 3-4. The temperature evolution during the transient in three representative locations on the inner wall and one on the outer wall is included. The maximum temperature on the inner wall is 921 K (648°C, 1198°F) and is reached at the upper inner corners of the container, 1,800 seconds after the beginning of the fire. The graphic

evolution of the temperatures listed in Table 3-4 is represented in Figure 3-3. Representative plots of the isotherms at various points in time are depicted in Figure 3-4 through Figure 3-7.

The temperatures and resulting pressures are within the capabilities of the fuel cladding as shown by test. Therefore the fuel cladding and closure welds maintain containment during the Hypothetical Accident Conditions.

The temperatures and resulting pressures are within the capabilities of the fuel cladding as shown by test. Therefore the fuel cladding and closure welds maintain containment during the Hypothetical Accident Conditions.

3.5.4 Accident Conditions for Fissile Material Packages for Air Transport

Approval for air transport is not requested for the RAJ-II.

Table 3-3 Convection Coefficients for Post-fire Analysis

T_s (surface temperature)		$T_{ambient}$		H (vertical surface)	h (horizontal surface facing upward)	h (horizontal surface facing downward)
°F	K	°F	K	($W/m^2 \cdot K$)	($W/m^2 \cdot K$)	($W/m^2 \cdot K$)
150	338.71	100	311	4.68	5.19	2.34
200	366.48	100	311	5.61	6.34	2.74
250	394.26	100	311	6.18	7.05	2.99
300	422.04	100	311	6.60	7.55	3.17
350	449.82	100	311	6.90	7.92	3.30
400	477.59	100	311	7.13	8.18	3.41
600	588.71	100	311	7.64	8.74	3.67
900	755.37	100	311	8.00	9.07	3.89
1,375	1,019.26	100	311	8.25	9.17	4.09

Table 3-4 Calculated Temperatures for Different Positions on the Walls of the Inner Container Walls

Time (s)	Inner Wall Temperature (top right corner) (K)	Inner Wall Temperature (bottom) (K)	Inner Wall Temperature (top) (K)	Outer Wall Temperature (K)
0.1	375	375	375	377
911	750	667	546	1,062
1,800	921	821	696	1,067
1,900	918	823	710	807
2,000	905	817	723	686
2,200	868	797	742	583
2,600	803	761	760	509
3,268	723	715	758	463
4,280	639	662	727	437
27,973	354	335	369	378
45,000	349	324	358	377

Table 3-5 Maximum Pressure

Parameter	Units	8 × 8 Fuel	9 × 9 Fuel	10 × 10 Fuel
Initial Pressure	MPa absolute	0.608	1.1145	1.1145
Fill temperature	°C	20	20	20
Temperature during HAC	°C	648	648	648
Outside Diameter Maximum	mm	12.5	11.46	10.52
	inches	.492	.4512	.4142
Minimum Allowable Cladding Thickness	inches	0.0268	0.0224	0.0205
	mm	.68	0.570	0.520
Cladding Inside Diameter Maximum	mm	11.14	10.32	9.48
	inches	.439	.406	.373
Pressure @ HAC	MPa (absolute)	1.91	3.50	3.50
	Psia	277	508	508
Applied Pressure @ HAC	MPa	1.81	3.40	3.40
	Psig	262	493	493
Stress Pr/t	MPa	14.82	30.8	31.0
	Psi	2,149	4,467	4,498
Margin	(allowed stress/actual stress)-1	1.10	0.01	0.003
Max allowed cladding	Inside Radius/Thickness	20.20	9.14	9.14

Note: Table values for cladding thickness and diameters are for example purposes and represent current limiting fuel designs. However, all fuel to be shipped must have a maximum pre-pressure times the maximum Inside Radius/Thickness product of 9.14 × 1.1145 MPa = 10.18653 MPa or less. Thus, all products must meet the maximum product of allowed pressure multiplied by Inside Radius/Thickness of 10.18653 MPa.

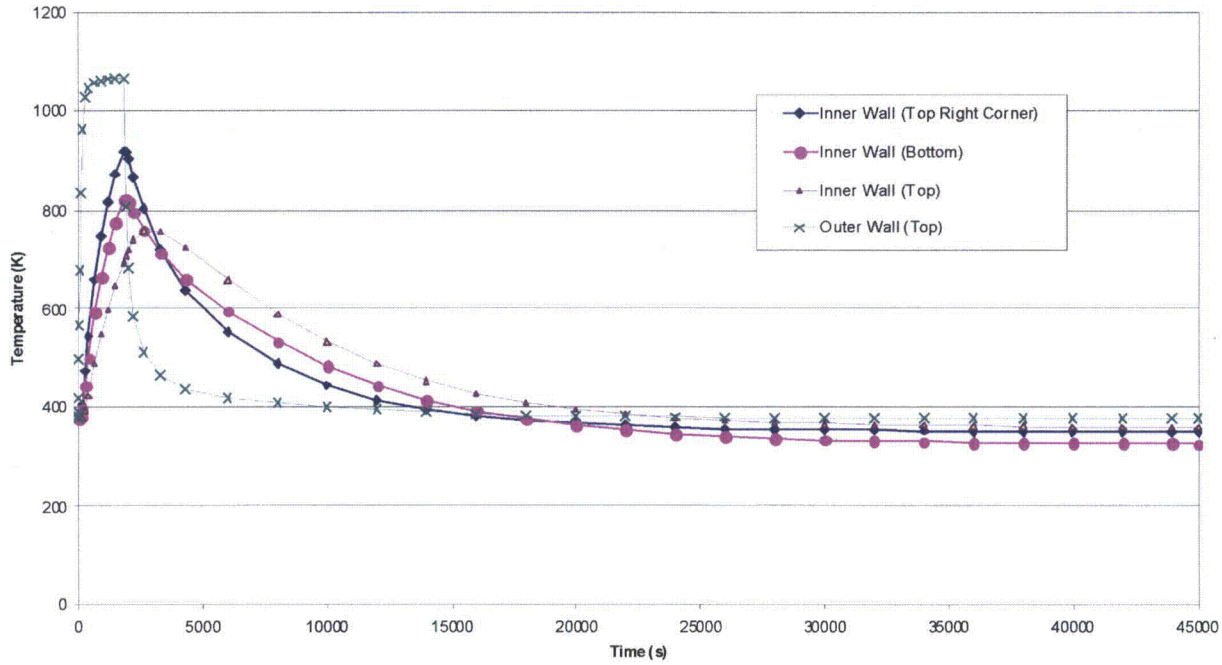

Figure 3-3 Calculated Temperature Evolution During Transient

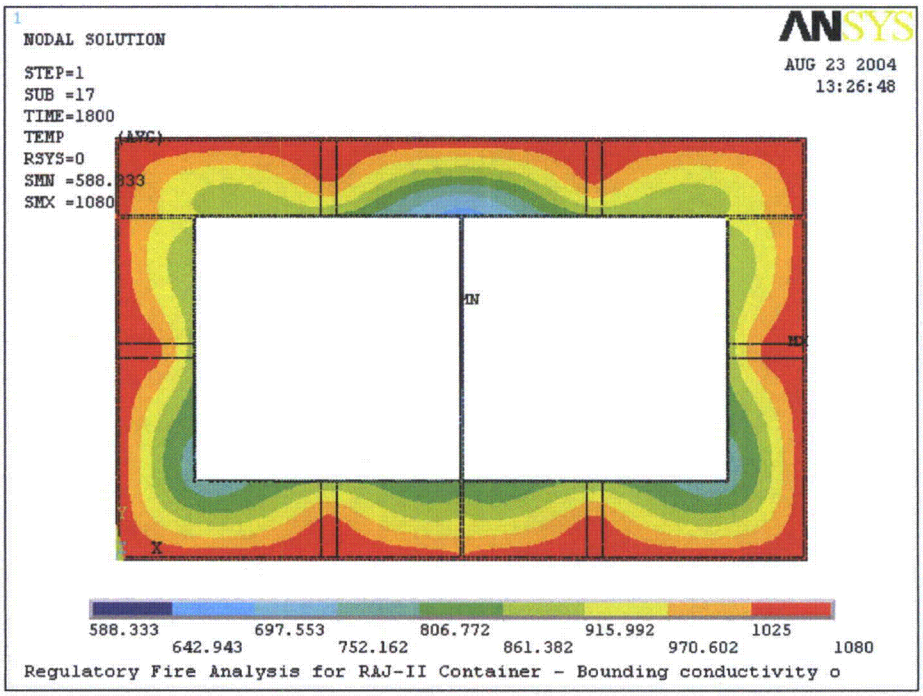

Figure 3-4 Calculated Isotherms at the End of Fire Phase (1,800 s)

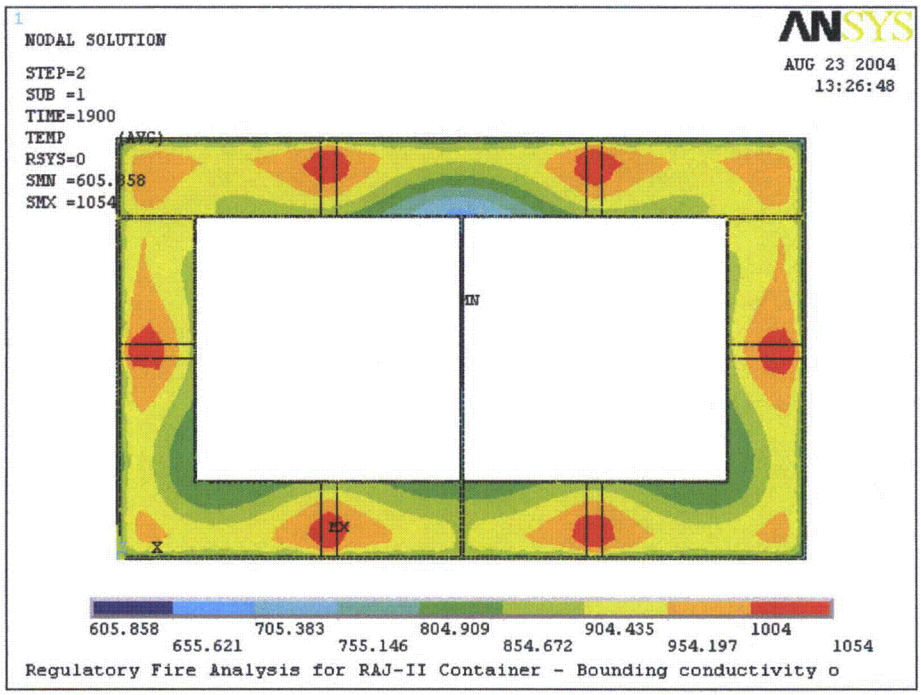

Figure 3-5 Calculated Isotherms at 100s After the End of Fire

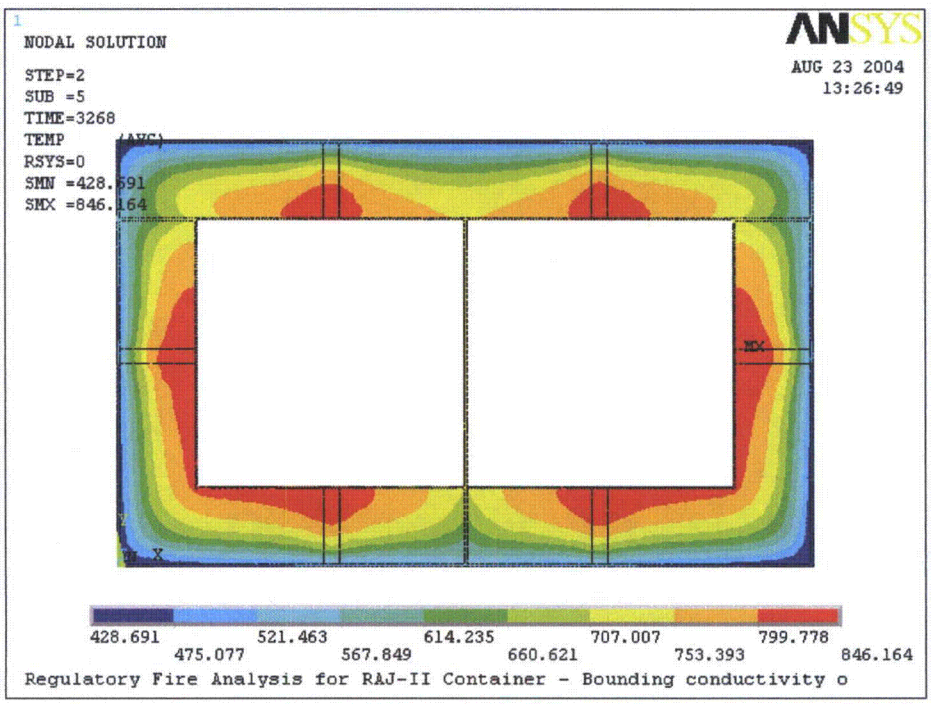

Figure 3-6 Calculated Isotherms at 1,468s After the End of Fire

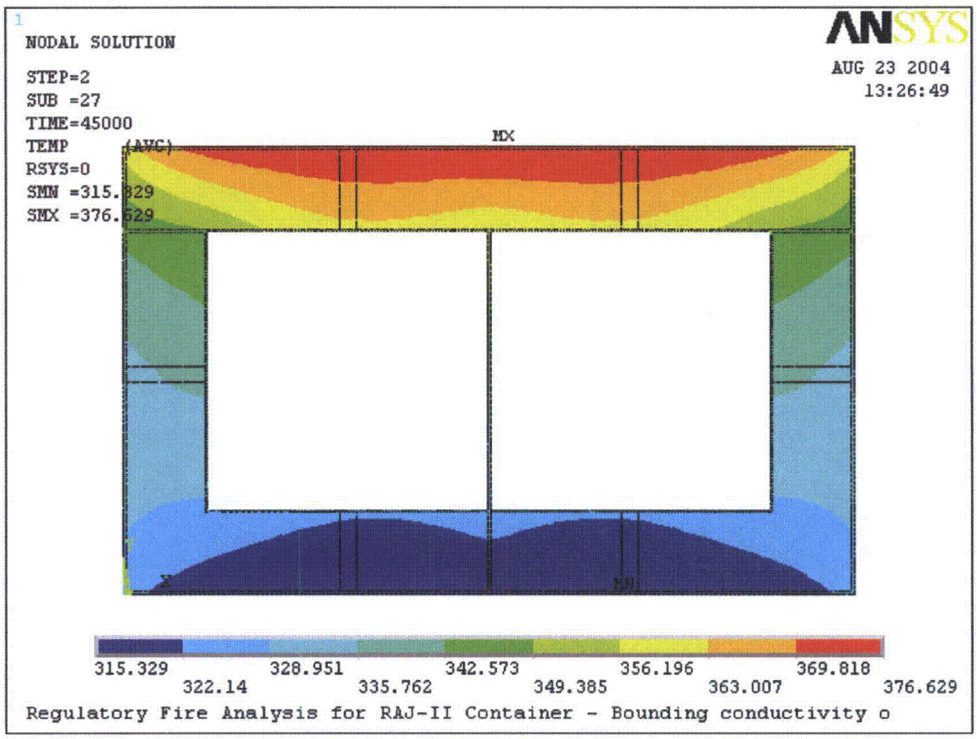

Figure 3-7 Calculated Isotherms at 12 hr After the End of Fire

3.6 APPENDIX

3.6.1 References

1. 10 CFR 71, Packaging and Transportation of Radioactive Material

2. Mills, A.F., Heat Transfer, Irwin, Inc., Homewood, Illinois, 1992

3. ANSYS Finite Element Computer Code, Version 5.6, ANSYS, Inc., 2000

4. McCaffery, B.J., Purely Buoyant Diffusion Flames – Some Experimental Results, Report PB80-112113, U.S. National Bureau of Standards, Washington, D.C., 1979

5. Incropera, F.P., Dewitt, D.P., Fundamentals of Heat and Mass Transfer, John Wiley and Sons, Inc., New York, New York, 1996.

6. GNF-2 Fuel Rod Response to An Abnormal Transportation Event (proprietary) (30 Minute Fire)

7. Handbook of Heat Transfer, Warren M. Rohsenow, James P. Hartnett, McGraw Hill book company.

8. Standard Handbook for Mechanical Engineers, Baumeister, Marks, McGraw Hill book company, Seventh edition.

9. Thermal Properties of Paper, PTN149, Charles Green, Webster New York, 2002 (http://www.frontiernet.net/~charmar/).

10. Tran, H.C., and White, R. H., Burning Rate of Solid Wood Measured in a Heat Release Calrimeter, Fire and Materials, Vol. 16, pp 197-206,1992.

11. "Pactec Specification: Regarding Global Nuclear Fuel Specification for Alumina Silicate for use in the RAJ-II Shipping container," Unifrax Corporation, 6/3/04.

12. Ragland, Aerts, "Properties of Wood for Combustion Analysis," Department of Mechanical Engineering, University of Wisconsin-Madison.

13. EthaFoam 220", Dow Chemical Company.

14. Gaur, Wunderlich, "Heat Capacity and Other Thermodynamic Properties of Linear Macromolecules. II. Polyethylene," Department of Chemistry, Renssalaer Polytechnic Institute.

15. Walters, Hackett, and Lyon, "Heats of Combustion of High Temperature Polymers," Federal Aviation Administration.

16. Hopkins, "Predicting the Ignition Time and Burning Rate of Themoplastics in the Cone Calorimeter," Department of Fire Protection Engineering, University of Maryland.

17. "Delrin Acetal Resin," Dow Chemical Company.

18. "EU-Material Safety Data Sheet: Delrin. Issue 250/05,"Dow Chemical Company.

19. Steinberg, Newton, and Beeson, ed, "Flammability and Sensitivity of Materials in Oxygen-Enriched Atmospheres," ASTM STP 1395, p.98.

20. Perry, R.H. and Green, D.W., Perry's Chemical Engineers' Handbook, 7th Edition, McGraw-Hill, 1997, Table 27-4.

3.6.2 ANSYS Input File Listing

Listing of the ANSYS input file (file: model_fl_heat.inp)

```
fini
/clear
/filnam,model_f1_heat,
/outp, model_f1_heatout,out
/PREP7
/TITLE, Regulatory Fire Analysis for RAJ-II Container -
Bounding conductivity of Alumina
/UNITS,SI
/SHOW,JPEG
!*
!*set element types
!*
ET,1, PLANE55,1
ET,2,LINK32
ET,3,MATRIX50,1
!*
!* define keypoints
!*
K,1,0,0,0,
K,2,0.459,0,0,
K,3,0,0.0015,0,
K,4,0.0015,0.0015,0,
K,5,0.136,0.0015,0,
K,6,0.146,0.0015,0,
K,7,0.2285,0.0015,0,
K,8,0.2305,0.0015,0,
K,9,0.313,0.0015,0,
K,10,0.323,0.0015,0,
K,11,0.4575,0.0015,0,
K,12,0.459, 0.0015, 0,
K,13,0.0015,0.0515 0,
K,14,0.0515,0.0515,0,
K,15,0.136,0.0515,0,
K,16.0.146,0.0515,0,
K,17,0.2285,0.0515,0,
K,18,0.2305,0.0515,0,
K,19,0.313,0.0515,0,
K,20, 0.323,0.0515, 0,
K,21,0.4075,0.0515,0,
K,22,0.4575,0.0515,0,
K,23,0.0515,0.0525,0,
K,24,0.0525,0.0525,0,
K,25,0.2285,0.0525,0,
K,26,0.2305,0.0525,0,
K, 27,0.4065,0.0525,0,
K,28,0.4075,0.0525,0,
K,29,0.0525,0.0705,0,
K,30,0.0705,0.0705,0,
K,31,0.2105,0.0705,0,
K,32,0.2285,0.0705,0,
K,33,0.2305,0.0705,0,
K,34,0.2485,0.0705,0,
```

K,35,0.3885 0.0705,0,

K,36,0.4065,0.0705,0,

K,37,0.0015,0.1335,0,

K,38,0.0515,0.1335,0,

K,39,0.4075, 0.1335,0,

K,40,0.4575,0.1335,0,

K,41,0.0015,0.1435,0,

K,42,0.0515,0.1435,0,

K,43,0.4075,0.1435,0,

K,44,0.4575,0.1435,0,

K,45,0.0705,0.1975,0,

K,46,0.2105,0.1975,0,

K,47,0.2485,0.1975, 0,

K,48,0.3885,0.1975,0,

K,49,0.0525,0.2155,0,

K,50,0.060,0.2115,0,

K,51,0.066,0.2055,0,

K,52,0.2175,0.2055,0,

K,53,0.2235 0.2115,0,

K,54,0.2285,0.2155,0,

K,55,0.2305,0.2155,0,

K,56,0.2355,0.2115,0,

K,57,0.2415,0.2 055,0,

K,58,0.393,0.2055,0,

K,59,0.399,0.2115,0,

K,60,0.4065,0.2155,0,

K,61,0.,0.2275,0,

K,62,.0.0015,0.2275,0,

K,63,0.0515,0.2275,0,

K,64,0.0525,0.2275,0,

K,65,0.4065,0.2275,0,

K,66,0.4075,0.2275,0,

K,67,0.4575,0.2275,0,

K,68,0.459,0.22 75,0,

K,69,0.,0.2285,0,

K,70,0.0525,0.2285,0,

K,71,0.06,0.2285,0,

K,72,0.2235,0.2285,0,

K,73,0.2285,0.2285,0,

K,74,0.2305,0.2285,0,

K,75,0.2355,0.2285,0,

K,76,0.399,0.2285,0,

K,77,0.4065,0.2285,0,

K,78,0.459,0.2285,0,

K,79,0.,0.2295,0,

K,80,0.0015,0.2295,0,

K,81,0.136,0.2295,0,

K,82,0.146,0.2295,0,

K,83,0.313,0.22 95,0,

K,84,0.323,0.2295,0,

K,85,0.4575,0.2295,0,

K,86,0.459,0.22 95,0,

K,87,0.,0.2795,0,

K,88,0.0015,0.2795,0,

K,89,0.136,0.2795,0,

K,90,0.146,0.2795,0,

K,91,0.313,0.2795,0,

K,92,0.323, 0.2795, 0,

```
K,93,0.4575,0.2 795,0,
K,94,0.459,0.2795,0,
K,95,0.,0.281,0,
K,96,0.459,0.281,0,
SAVE
!*
!* define material properties
!*
!*
!* STAINLESS STEEL (SS304)
!*
MP,DENS,1,7900
MPTEMP,1,300,400,500,600,800,1000
MPDATA,kxx,1,1,15,17,18,20,23,25
MPDATA,c,1,1,477,515,539,557,582,611
!*
!* THERMAL INSULATOR
!*
MP,DENS,2,260
MP,C,2,1046
MPTEMP
MPTEMP,1,673,873,1073,1273
MPDATA,KXX,2,1,0.105,0.151,0.198,0.267 !MAX VALUES
!*
!*
!* WOOD (generic softwood)
!*
UIMP,3,EX, , , ,
UIMP,3,NUXY, , , ,
UIMP,3,ALPX, , , ,
UIMP,3,REFT, , , ,
UIMP,3,MU, , , ,
UIMP,3,DAMP, , , ,
UIMP,3,DENS , , , 500,
UIMP,3,KXX , , , 0.24,
UIMP,3,C , , , 2800,
UIMP,3,ENTH, , , ,
UIMP,3,HF, , , ,
UIMP,3,EMIS, , , ,
UIMP,3,QRATE, , , ,
UIMP,3,VISC, , , ,
UIMP,3,SONC, , , ,
UIMP,3,MURX, , , ,
UIMP,3,MGXX, , , ,
UIMP,3,RSVX, , , ,
UIMP,3,PERX, , , ,
!*
!* define areas
!*
FLST,2,12,3
FITEM,2,1
FITEM,2,2
FITEM,2,12
FITEM,2,11
FITEM,2,10
FITEM,2,9
FITEM,2,8
FITEM,2,7
```

FITEM,2,6

FITEM,2,5

FITEM,2,4

FITEM,2,3

A,P51X

FLST,2,7,3

FITEM,2,3

FITEM,2,4

FITEM,2,13

FITEM,2,37

FITEM,2,41

FITEM,2,62

FITEM,2,61

A,P51X

FLST,2,5,3

FITEM,2,4

FITEM,2,5

FITEM,2,15

FITEM,2,14

FITEM,2,13

A,P51X

FLST,2,4,3

FITEM,2,5

FITEM,2,6

FITEM,2,16

FITEM,2,15

A,P51X

FLST,2,4,3

FITEM,2,6

FITEM,2,7

FITEM,2,17

FITEM,2,16

A,P51X

FLST,2,4,3

FITEM,2,7

FITEM,2,8

FITEM,2,18

FITEM,2,17

A,P51X

FLST,2,4,3

FITEM,2,8

FITEM,2,9

FITEM,2,19

FITEM,2,18

A,P51X

FLST,2,4,3

FITEM,2,9

FITEM,2,10

FITEM,2,20

FITEM,2,19

A,P51X

FLST,2,5,3

FITEM,2,10

FITEM,2,11

FITEM,2,22

FITEM,2,21

FITEM,2,20

A,P51X

FLST,2,7,3

FITEM,2,11

FITEM,2,12

FITEM,2,68

FITEM,2,67

FITEM,2,44

FITEM,2,40

FITEM,2,22

A,P51X

FLST,2,5,3

FITEM,2,13

FITEM,2,14

FITEM,2,23

FITEM,2,38

FITEM,2,37

A,P51X

FLST,2,8,3

FITEM,2,23

FITEM,2,24

FITEM,2,29

FITEM,2,49

FITEM,2,64

FITEM,2,63

FITEM,2,42

FITEM,2,38

A,P51X

FLST,2,14,3

FITEM,2,14

FITEM,2,15

FITEM,2,16

FITEM,2,17

FITEM,2,18

FITEM,2,19

FITEM,2,20

FITEM,2,21

FITEM,2,28

FITEM,2,27

FITEM,2,26

FITEM,2,25

FITEM,2,24

FITEM,2,23

A,P51X

FLST,2,8,3

FITEM,2,25

FITEM,2,26

FITEM,2,33

FITEM,2,55

FITEM,2,74

FITEM,2,73

FITEM,2,54

FITEM,2,32

A,P51X

FLST,2,8,3

FITEM,2,27

FITEM,2,28

FITEM,2,39

FITEM,2,43

FITEM,2,66

```
FITEM,2,65
FITEM,2,60
FITEM,2,36
A,P51X
FLST,2,5,3
FITEM,2,21
FITEM,2,22
FITEM,2,40
FITEM,2,39
FITEM,2,28
A,P51X
FLST,2,4,3
FITEM,2,37
FITEM,2,38
FITEM,2,42
FITEM,2,41
A,P51X
FLST,2,4,3
FITEM,2,39
FITEM,2,40
FITEM,2,44
FITEM,2,43
A,P51X
FLST,2,4,3
FITEM,2,41
FITEM,2,42
FITEM,2,63
FITEM,2,62
A,P51X
FLST,2,4,3
FITEM,2,43
FITEM,2,44
FITEM,2,67
FITEM,2,66
A,P51X
SAVE
FLST,2,6,3
FITEM,2,61
FITEM,2,62
FITEM,2,63
FITEM,2,64
FITEM,2,70
FITEM,2,69
A,P51X
FLST,2,6,3
FITEM,2,65
FITEM,2,66
FITEM,2,67
FITEM,2,68
FITEM,2,78
FITEM,2,77
A,P51X
FLST,2,18,3
FITEM,2,69
FITEM,2,70
FITEM,2,71
FITEM,2,72
FITEM,2,73
```

```
FITEM,2,74
FITEM,2,75
FITEM,2,76
FITEM,2,77
FITEM,2,78
FITEM,2,86
FITEM,2,85
FITEM,2,84
FITEM,2,83
FITEM,2,82
FITEM,2,81
FITEM,2,80
FITEM,2,79
A,P51X
FLST,2,4,3
FITEM,2,79
FITEM,2,80
FITEM,2,88
FITEM,2,87
A,P51X
FLST,2,4,3
FITEM,2,80
FITEM,2,81
FITEM,2,89
FITEM,2,88
A,P51X
FLST,2,4,3
FITEM,2,81
FITEM,2,82
FITEM,2,90
FITEM,2,89
A,P51X
FLST,2,4,3
FITEM,2,82
FITEM,2,83
FITEM,2,91
FITEM,2,90
A,P51X
FLST,2,4,3
FITEM,2,83
FITEM,2,84
FITEM,2,92
FITEM,2,91
A,P51X
FLST,2,4,3
FITEM,2,84
FITEM,2,85
FITEM,2,93
FITEM,2,92
A,P51X
FLST,2,4,3
FITEM,2,85
FITEM,2,86
FITEM,2,94
FITEM,2,93
A,P51X
SAVE
FLST,2,10,3
```

```
FITEM,2,87
FITEM,2,88
FITEM,2,89
FITEM,2,90
FITEM,2,91
FITEM,2,92
FITEM,2,93
FITEM,2,94
FITEM,2,96
FITEM,2,95
A,P51X
SAVE
!*
!* glue all areas
!*
FLST,2,31,5,ORDE,2
FITEM,2,1
FITEM,2,-31
AGLUE,P51X
!*
/PNUM,KP,0
/PNUM,LINE,0
/PNUM,AREA,1
/PNUM,VOLU,0
/PNUM,NODE,0
/PNUM,TABN,0
/PNUM,SVAL,0
/NUMBER,0
!*
/PNUM,ELEM,0
/REPLOT
!*
APLOT
FLST,5,14,5,ORDE,10
FITEM,5,1
FITEM,5,-2
FITEM,5,6
FITEM,5,10
FITEM,5,12
FITEM,5,-15
FITEM,5,21
FITEM,5,-24
FITEM,5,30
FITEM,5,-31
ASEL,S , , , P51X
/REPLOT
FLST,5,14,5,ORDE,10
FITEM,5,1
FITEM,5,-2
FITEM,5,6
FITEM,5,10
FITEM,5,12
FITEM,5,-15
FITEM,5,21
FITEM,5,-24
FITEM,5,30
FITEM,5,-31
CM,_Y,AREA
```

```
ASEL, , , ,P51X
CM,_Y1,AREA
CMSEL,S,_Y
!*
CMSEL,S,_Y1
AATT,   1, ,  1,   0
CMSEL,S,_Y
CMDELE,_Y
CMDELE,_Y1
!*
ALLSEL,ALL
FLST,5,11,5,ORDE,11
FITEM,5,3
FITEM,5,5
FITEM,5,7
FITEM,5,9
FITEM,5,11
FITEM,5,16
FITEM,5,19
FITEM,5,-20
FITEM,5,25
FITEM,5,27
FITEM,5,29
ASEL,S , , , P51X
FLST,5,11,5,ORDE,11
FITEM,5,3
FITEM,5,5
FITEM,5,7
FITEM,5,9
FITEM,5,11
FITEM,5,16
FITEM,5,19
FITEM,5,-20
FITEM,5,25
FITEM,5,27
FITEM,5,29
CM,_Y,AREA
ASEL, , , ,P51X
CM,_Y1,AREA
CMSEL,S,_Y
!*
CMSEL,S,_Y1
AATT,   2, ,  1,   0
CMSEL,S,_Y
CMDELE,_Y
CMDELE,_Y1
!*
ALLSEL,ALL
FLST,5,6,5,ORDE,6
FITEM,5,4
FITEM,5,8
FITEM,5,17
FITEM,5,-18
FITEM,5,26
FITEM,5,28
ASEL,S , , , P51X
FLST,5,6,5,ORDE,6
FITEM,5,4
```

```
FITEM,5,8
FITEM,5,17
FITEM,5,-18
FITEM,5,26
FITEM,5,28
CM,_Y,AREA
ASEL, , , ,P51X
CM,_Y1,AREA
CMSEL,S,_Y
!*
CMSEL,S,_Y1
AATT,   3, ,  1,   0
CMSEL,S,_Y
CMDELE,_Y
CMDELE,_Y1
!*
ALLSEL,ALL
SAVE
!*
!* mesh the areas
!*
ALLSEL,ALL
APLOT
SMRT,10
FLST,5,31,5,ORDE,2
FITEM,5,1
FITEM,5,-31
CM,_Y,AREA
ASEL, , , ,P51X
CM,_Y1,AREA
CHKMSH,'AREA'
CMSEL,S,_Y
!*
AMESH,_Y1
!*
CMDELE,_Y
CMDELE,_Y1
CMDELE,_Y2
!*
/PNUM,KP,0
/PNUM,LINE,0
/PNUM,AREA,0
/PNUM,VOLU,0
/PNUM,NODE,0
/PNUM,TABN,0
/PNUM,SVAL,0
/NUMBER,0
!*
/PNUM, MAT,1
/REPLOT
ALLSEL,ALL
!* select nodes on the outer sufaces
NSEL, S, LOC,X,0.,0.0001
NSEL,A, LOC,X,0.4589,0.459
NSEL,A, LOC,Y,0.,0.0001
NSEL,A, LOC,Y,0.2809,0.281
!* define element for outer surface
!*
```

```
TYPE,  2
MAT,     1
NPLOT
esurf
!*
!* create space node
N, 50000, 0.3, 0.5, 0, , , ,
!* select the nodes and elements that
!* make up the radiation surfaces
ESEL,S,TYPE,, 2
NSLE,R
NSEL, S, LOC,X, 0., 0.0001
NSEL,A, LOC,X, 0.4589, 0.459
NSEL,A, LOC,Y,0.,0.0001
NSEL,A, LOC,Y,0.2809,0.281
ESLN,R
NSEL,a,node,,50000
FINISH
!* define radiation matrix
/AUX12
EMIS,1,0.8,
STEF,5.67e-08,
GEOM,1,0,
SPACE,50000,
!*
VTYPE,0,20,
MPRINT,0
WRITE,rad
!*
ALLSEL,ALL
FINISH
/PREP7
!*
!*
TYPE, 3
MAT,     1
REAL,
ESYS,     0
SECNUM,
TSHAP,LINE
!*
SE,rad, , ,0.0001,
ESEL,S,TYPE,, 2
EDELE,ALL
SAVE
!* Define effective heat transfer coeficients for
!* post-fire (vert-20,horiz-up-25, horiz-down-35)
MPTEMP
M PTEMP,1,338.71,366.48,394.26,422.04,449.82,477.59,
M PTEMP,7,588.71,755.37,1019.26,
MPDATA,HF,20,1,4.68,5.61,6.18,6.60,6.90,7.13,
MPDATA, HF, 20, 7, 7.64, 8.00, 8.25,
MPDATA,HF,25,1,5.19,6.34,7.05,7.55,7.92,8.18,
MPDATA,HF,25,7,8.74,9.07, 9.17,
MPDATA,HF,35,1,2.34,2.74,2.99,3.17,3.30,3.41,
MPDATA, HF, 35, 7, 3.67, 3.89, 4.09,
MPLIST
SAVE
```

```
FINISH
/SOLU
!* setup convection coefficients for fire case
ALLSEL,ALL
NSEL,S,LOC,X, 0., 0.0001
NSEL,A,LOC,X, 0.4589, 0.459
NSEL,A,LOC,Y,0.,0.0001
NSEL,A,LOC,Y,0.2809,0.281
SF,ALL,CONV,19.8,1073
NSEL,ALL
!*****************************************************************
******
!* Test Heat Generation modelling wood burning
ASEL,S,MAT,,3
ESLA,S
/GO
!*
*DIM,burning,TABLE,5,1,0,TIME
!*
BFE,ALL,HGEN, , %burning%
!*
!*********BFA,ALL,HGEN, %burning%
*SET,BURNING(1,0,1), 0.0
*SET,BURNING(2,0,1), 0.1
*SET,BURNING(3,0,1), 0.2
*SET,BURNING(4,0,1), 552.2
*SET,BURNING(5,0,1), 552.3
*SET,BURNING(1,1,1), 0.0
*SET,BURNING(2,1,1), 0.0
*SET,BURNING(3,1,1), 7.63e6
*SET,BURNING(4,1,1), 7.63e6
*SET,BURNING(5,1,1), 0.0
ALLSEL,ALL
SAVE
!*****************************************************************
******
D,50000,TEMP, 1073
!*****************************************************************
******
TUNIF,375,!REVISED FOR NEW NCT
NUMBER (IC OUTER SHELL)
!*****************************************************************
******
SAVE
!*
!* set up run parameters for fire case
!*
ANTYPE,4
!*
TRNOPT,FULL
LUMPM,0
!*
TIME,1800
AUTOTS,-1
DELTIM,0.1,0.1,600,1
KBC,1
!*
TSRES,ERASE
```

```
!*
OUTRES,ALL,ALL,
!*
LSWRITE,2,
!*
!* change boundary conditions for post fire case
!*
ALLSEL,ALL
NSEL,S, LOC,X,0.000,0.0001
NSEL,A, LOC,X, 0.4589, 0.459
SF,ALL,CONV,-20, 311
ALLSEL,ALL
NSEL,S, LOC,Y,0.0,0.0001
SF,ALL,CONV,-35, 311
ALLSEL,ALL
NSEL,S, LOC,Y,0.2809,0.281
SF,ALL,CONV,-25, 311
ALLSEL,ALL
D,50000,TEMP,311
!*
!* apply solar heat flux
!*
ALLSEL,ALL
!* select vertical lines and nodes on the left side
nsel,s,loc,x,0
!FLST,5,4,4,ORDE,4
!FITEM,5,18
!FITEM,5,76
!FITEM,5,94
!FITEM,5,97
!LSEL,S , , , P51X
!NSLL,S,1
! FLST,2,97,1,ORDE,9
!FITEM,2,12
!FITEM,2,17
!FITEM,2,56
!FITEM,2,70
!FITEM,2,72
!FITEM,2,447
!FITEM,2,-521
!FITEM,2,2039
!FITEM,2,-2055
/GO
!*
F,all,HEAT,0.69

ALLSEL,ALL
!* select lines and nodes on the right side
nsel,s,loc,x,.459,.460
!FLST,5,4,4,ORDE,4
!FITEM,5,35
!FITEM,5,77
!FITEM,5,86
!FITEM,5,108
!LSEL,S , , , P51X
!NSLL,S,1
!FLST,2,97,1,ORDE,9
!FITEM,2,3
```

```
!FITEM,2,27
!FITEM,2,57
!FITEM,2,63
!FITEM,2,78
!FITEM,2,795
!FITEM,2,-869
!FITEM,2,2240
!FITEM,2,-2256
!/GO
!*
F,all,HEAT,0.69

!* select nodes on upper surface
ALLSEL,ALL
NSEL,S, LOC,Y,0.2809,0.281
!FLST,2,155,1,ORDE,4
!FITEM,2,79
!FITEM,2,-80
!FITEM,2,2257
!FITEM,2,-2409
!/GO
!*
F,all,HEAT,2.88
ALLSEL,ALL
!* set up run parameters for post fire
TIME,14400 !was 9000
AUTOTS,-1
DELTIM,0.5,0.1,2000,1
KBC,1
!*
TSRE S,ERASE
!*
TINTP,0.005, , ,-1,0.5,-1
!*
OUTRES,ALL,ALL,
TIME,45000
DELTIM,100,10,2000,1
LSWRITE,3,
SAVE
FINISH
/SOLU
/STATUS,SOLU
LSSOLVE,2,3,1
FINISH
SAVE
/POST26
!*
!* plot temperature evolution at specified nodes
!*
!*
!* inner wall, top right corner
NSOL,2,58,TEMP, ,inn_wtr
!*
!*
!* inner wall, bottom mid position
NSOL,3,1185,TEMP, ,inn_wbm
!*
!*
```

```
!* inner wall, top mid position
NSOL,4,1720,TEMP, ,inn_wtm
!*
!*
!* outer wall, top mid position
NSOL,5,2333,TEMP, ,out_wtm
!*
!*
PLVAR,2,3,4,5,,, , , , ,
PRVAR,2,3,4,5,,,
FINISH
!* plot isothermes at certain moments in time
/POST1
SET,LIST,2
SET, , , 1 , , , , 17,
/EFACE,1
!*
PLNSOL,TEMP, ,0,
FINISH
/POST1
SET, , , 1 , , , , 18,
/EFACE,1
!*
PLNSOL,TEMP, ,0,
SET, , , 1 , , , , 20,
/EFACE,1
!*
PLNSOL,TEMP, ,0,
SET, , , 1 , , , , 22,
/EFACE,1
!*
PLNSOL,TEMP, ,0,
SET, , , 1 , , , , 30,
/EFACE,1
!*
PLNSOL,TEMP, ,0,
SET, , , 1 , , , , 43,
/EFACE,1
!*
PLNSOL,TEMP, ,0,
SET,PREVIOUS
FINISH

! ********************************NEW
allsel
/post1

Tmax=0
TimeMAX=0
nmax=0

nsel ,s,loc, x, 0.0525, .4065,
nsel, r,loc,y,0.0525,.2285,
!nsel, u, loc,y,0.053, .2280

nplot
*GET, ncount, NODE, 0, count
cm,icnodes,node
```

```
set, 1,1

*do,t,1,46
tmaxn=0
cmsel,s,icnodes

*do, i,1, ncount
nodei=node(0,0,0)
*get,tempi,node, nodei,temp
*if,tempi, gt,tmaxn,then
tmaxn=tempi
nmaxn=nodei
*endif
nsel,u ,,, nodei
*enddo
*if,tmaxn, gt,tmax,then
tmax=tmaxn
nmax=nmaxn
*GET,timemax, ACTIVE, 0, set, time
*endif
set,next
*enddo

tmax=tmax
nmax=nmax
timemax=timemax

allsel

/show,term
/post1,
! Reverse Video
/rgb, index,100,100,100,0
/rgb, index,80,80,80,13
/rgb, index,60,60,60,14
/rgb,index,0,0,0,15
set, 1,17
plnsol,temp
/image, save,fig3-4(1800),wmf
set,2,1
/replot
/image, save,fig3-5(1900),wmf
set,2,5
/replot
/image, save,fig3-6(3268),wmf
set,last
/replot
/image, save,fig3-7(45000),wmf
!*******************************NEW
! /EXIT,ALL
```

3.6.3 NCT Transient Analysis

The transient analysis uses a one dimensional model of the vertical face of the packaging (thinner part of the packaging) as described in the figure below:

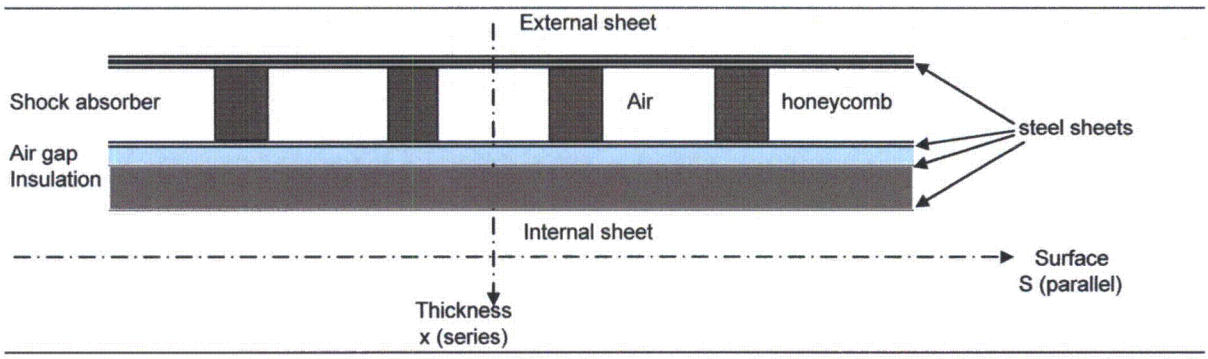

Figure 3-8 Vertical Face Model

The heat flux is set as a sine wave function:

$$Q = \pi/2 \times 800 \sin(\omega\ \theta) \qquad 0 < (\omega\ \theta) < \pi$$

$$Q = 0 \qquad \pi < (\omega\ \theta) < 2\pi$$

With:

Q = heat energy in g-cal/cm^2

ω = $2\pi / 24$ pulsation

θ = time in hour

Note that the peak value of ($\pi/2 \times 800$) complies with 10 CFR 71.71(c)(1), conservatively assuming the highest value of 800 g-cal/cm^2 for the insolation.

$$\int_0^{24\text{hours}} Q\, d\theta = 800 \text{ g-cal/cm}^2$$

Assuming that at each time step, the external surface of the package achieves steady state conditions, the energy balance between the solar heat load, and the convection and radiation exchanges (see Section 3.4.1.1), results time dependant solution for the external surface temperature.

The result is plotted on the Figure 3-9 (blue curve) and is close to a sine wave function. Indeed, when calculating the energy balance equation, it appears that the convention term represents 65%

of the exchange, and the radiation term 35%. As the convection term is linearly proportional to the external temperature, this curve is nearly proportional to the solar heat load.

Assume that the external temperature is a sine function with respect to time as follows (and as plotted on Figure 3.6.3-1):

$$Ts = T_{avg} + T^{+} \sin(\omega\ \theta)$$

With:

$T_{avg} = 420$ K (maximum value of the blue curve)

$T^{+} = (420\text{-}311) = 109$ K

The system is thus modeled as a one dimensional model of conduction, with a sinusoidal wave temperature on the external surface as a boundary condition.

Using equation 4-22 of the "Handbook of Heat Transfer," [7], the heat equation through a layer of material leads to a temperature of:

$$T(x,\theta) = T_{avg} + T^{+} \exp(-L\ x/d) \sin[L(2\ L\ Fo - x/d)]$$

Using the reference's notation, it becomes:

$$T(x,\theta) = T_{avg} + T^{+} \exp[-(\omega/2\alpha)^{1/2}\ x] \sin[\omega\ \theta - (\omega/2\alpha)^{1/2} x]$$

With:

$\alpha = K / \rho\ C$ = thermal diffusivity,

K = conductivity if material,

ρ = density of material,

C = specific heat of the material,

x = thickness thru the material.

Through each layer of material "i" in the RAJ-II packaging, the temperature of the external surface is so decreased by a factor η and lagged by a factor ϕ:

$$\eta_i = \exp[-(\omega/2\alpha_i)^{1/2}\ x_i]$$

$$\phi_i = (\omega/2\alpha_i)^{1/2} x_i$$

Table 3.6.3-1 summarizes the material properties for each component layer through the thickness of the model.

Equivalent Properties of Material

The thermal properties (K, ρ, C) of a material equivalent to materials of a system are following the rules:

Materials in series $K = \dfrac{e_T}{\sum_i \dfrac{e_i}{K_i}}$ Materials in parallel $K = \dfrac{1}{S_T}\sum_i S_i K_i$

Materials in series $\rho C = \dfrac{\sum_i \rho_i C_i e_i}{e_T}$ Materials in parallel $\rho C = \dfrac{\sum_i \rho_i C_i S_i}{S_T}$

The maximum temperature of the cavity surface of the packaging resulting from solving the one dimensional model occurs at ten hours into the cycle and is equal to 350 K. The maximum temperature on the outer surface of the inner container occurs at 8 hours and is equal to 375K. Temperatures are summarized on Figure 3-7.

Table 3-6 Material Properties

Component	Material	Thickness x (m)	Surface S (m)	Conductivity K (W/m-K)	Density r (kg/m^3)	Specific heat C (J/kg-K)	Diffusivity a (m^2/s)
OC outer sheet	steel	0.004	–	15	7900	477	3.981E-06
Honeycomb①	paper	–	0.084①	0.13595	700①	1531①	3.932E-07
	air	–	0.916①	0.0267	1.177	1005	
Shock absorbers	honeycomb	0.108	0.64	0.0359	60	1522	1.737E-06
	air		3.186	0.0267	1.177	1005	
OC inner sheet	steel	0.001	–	15	7900	477	3.981E-06
Air gap	air	0.01	–	0.0267	1.177	1005	2.257E-05
IC outer sheet	steel	0.0015	–	15	7900	477	3.981E-06
IC insulation	Alumina	0.048	–	0.09	250	1046	3.442E-07
IC inner sheet	steel	0.001	–	15	7900	477	3.981E-06

Note:

① The honeycomb is assumed to be a combination of paper and air in a parallel system (see below). The proportion of paper and air is determined by the ratio of the densities:

Honeycomb density = 60 kg/m^3
Paper density = 700 kg/m^3 8.4%
Air density = 1.177 kg/m^3 91.6%

Thermal properties of resin impregnated kraft paper (density, conductivity, specific heat) are conservatively assumed to correspond to that of ordinary paper. [9]

Table 3-7 NCT Temperatures through the Package Thickness

Time (hour)	Surface temp sin wave Ts (K)	T thru OC Outer Shell	T thru Honeycomb and Air	T thru OC Inner Steel	T thru Air Gap	T thru IC Inner Shell	T thru Alumina Silicate
0	311	311	311	311	311	311	311
0.5	325	324	311	311	311	311	311
1	339	338	311	311	311	311	311
1.5	353	351	311	311	311	311	311
2	366	364	312	312	311	311	311
2.5	377	376	321	320	320	319	311
3	388	386	329	329	328	327	311
3.5	397	396	337	337	336	335	311
4	405	404	345	345	343	343	312
4.5	412	410	352	352	350	350	317
5	416	415	358	358	357	356	322
5.5	419	418	364	364	362	362	327
6	420	419	368	368	367	367	332
6.5	419	418	372	372	371	370	336
7	416	415	375	375	373	373	340
7.5	412	411	376	376	375	375	343
8	405	405	377	376	376	**375**	346
8.5	397	397	376	376	375	375	348
9	388	388	374	374	373	373	349
9.5	377	378	371	371	371	371	**350**
10	366	366	367	367	367	367	350
10.5	353	353	362	362	362	362	350
11	339	340	357	357	357	357	349
11.5	325	326	350	350	350	350	347
12	311	312	343	343	343	343	344
12.5	311	311	335	335	336	336	342
13	311	311	327	327	328	328	338
13.5	311	311	318	319	319	320	334
14	311	311	311	311	311	311	330
14.5	311	311	311	311	311	311	325
15	311	311	311	311	311	311	320
15.5	311	311	311	311	311	311	315
16	311	311	311	311	311	311	311
16.5	311	311	311	311	311	311	311

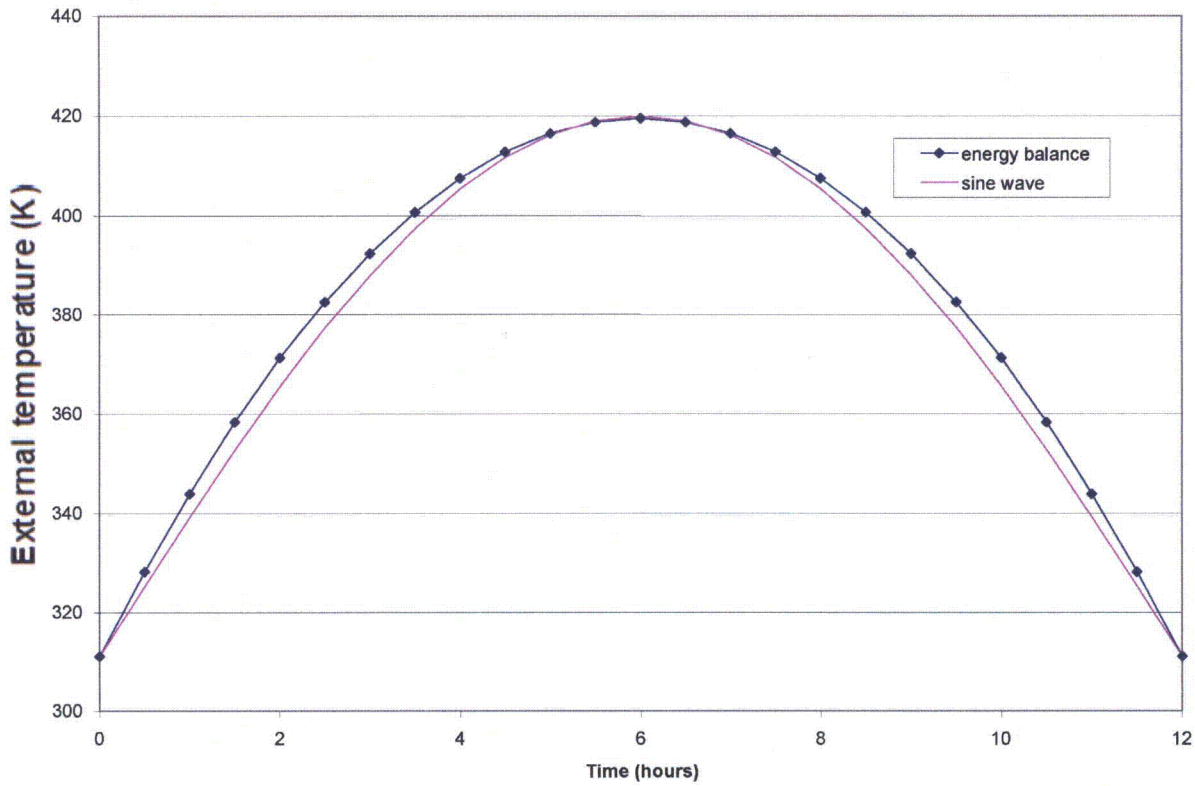

Figure 3-9 Comparison between Energy Equation Solution with a Sine Wave Equation

3.6.4 HAC 3D Transient Fire Analysis

A new 3-D finite element model is used to evaluate the performance of the RAJ-II when exposed to the NRC/IAEA regulatory fire conditions. The new model includes the complete geometry of the RAJ-II outer and inner containers. Boundary conditions include preheating of the container, combustion of the honeycomb paper, charring of the balsawood, charring of hemlock and the phase change of the polyethylene foam (both melting and vaporizing) within the inner container. Also included are the combustible materials located at the ends of the RAJ-II package.

3.6.4.1 Finite Element Model Description

The 3-D finite element model includes both transverse and longitudinal heat transfer and end effects, e.g., burning of Delrin® (polyacetal). In order to decrease computing time, geometric symmetries were used, requiring only one-half of the transverse cross section to be modeled. Similarly, only a portion of the overall length was required. The finite element model is shown in Figure 3-10.

All solid components within the RAJ-II container, as well as the air encased between the inner and outer container walls, are modeled with 81,216 nodes and 75,578 ANSYS Type 70 Thermal Solid elements.

The fuel assembly is modeled as a single monolith of appropriate envelope. The "law of mixtures" is used to estimate the material properties of this monolith.

For purposes of analysis, an equivalent volume of honeycomb shock absorber is calculated. This equivalent volume shock absorber is located at the centeroid of the summed volumes. The equivalent volume is 0.0848 m^3 with a centroid at 477 mm from the end of the internal package.

Radiation heat transfer between the outer container wall and the surrounding environment is modeled with a Matrix 50 element utilizing the 7,064 surface nodes on the outer container and a single environment node.

Radiation heat transfer between the outer container wall and the inner container wall is modeled using the radiosity solver capability of ANSYS. This method allows for symmetries to be used to reduce the overall model size, and superimposes thermal surface elements over existing solid elements. The parameters used in the modeling create 15,988 ANSYS Type 252 3D Thermal Surface elements and 8,404 nodes.

3.6.4.2 Assumptions

The following are the assumptions made for the 3-D model:

- Combustion is simulated by heat generation rates in the appropriate combusting elements.

- Paper honeycomb shock absorbers in the outer compartment are exposed to enough oxygen to fully combust. The combustion rate of the honeycomb is based on the rate of consumption of wood in free air modified by the flame front propagation rate in the model when loaded only by external sources. The resulting flame front propagation rate is 0.785 mm per minute. The resin impregnating the honeycomb is assumed to contribute negligibly to the heat of combustion of the honeycomb.

- Delrin® (polyacetal) guides in the outer compartment are exposed to enough oxygen to fully combust. The Delrin® material is assumed to burn for one hour with resulting flame front propagation rate of 0.582 mm per minute.

- The end compartment houseing the balsawood impact absorber are oxygen starved, resulting in pyrolysis (charring) of the balsa wood components only. Thermal experiments documented in Appendix 3.6.5 support this assumption.

- The volume between the inner container shell walls is oxygen starved, resulting in pyrolysis (charring) of the hemlock wood components only. The drop testing result support this assumption.

- If any polyethylene foam reaches ignition temperature, it is allowed to fully combust.

- The system is conservatively assumed to be to be essentially closed, with the only method of heat escaping the package being through the outer compartment wall radiating to the environment, or by the free convection cooling modeled on the outer wall, both of which are included in the model. No accounting was made for "chimney effects" where hot gasses are evacuated from the enclosure through any enclosure opening.

3.6.4.3 Boundary Conditions

For the initial state, the bulk temperature is fixed at 311 K (38°C). The surface heat flux for horizontal surfaces is 387.4 W/m^2, while the surface heat flux for vertical surfaces is 96.9 W/m^2, both as described and calculated in Section 3.5.

Combustion is simulated by applying heat generation rates in the appropriate combusting elements. Elements that were allowed to combust include the paper honeycomb, polyacetal inserts, and polyethylene foam.

For the transient state time t=0 was considered the start of the external fire. To simulate the external fire, the environment node was fixed at 1073 K (800°C) for thirty minutes. The paper honeycomb material was calculated to begin burning 30 seconds after the start of the external fire, continuing for 200 minutes. The polyacetal was calculated to begin burning 21 minutes after the start of the external fire, continuing for 60 minutes. After the end of the external fire, the bulk temperature

was fixed at 311 K (38°C) and a temperature dependent heat transfer coefficient, as calculated in Section 3.5, was applied to the outer container. An external heat flux, representing solar radiation was applied to the package for 3.5 hours after the HAC fire, then removed for the duration of the transient analysis. The boundary conditions are summarized in Table 3-8.

Radiation heat transfer is modeled between the outer container wall and the surrounding environment and between the outer container wall and the inner container. The ANSYS program internally calculates view factors between components. Emissivity in all radiation cases is conservatively chosen as 1.

The convection heat transfer from the outer container wall to the environment is also modeled. The mixing effects of convection are included in the enclosure between the outer container wall and the inner container wall, equalizing temperature in all air elements.

3.6.4.4 Material Properties

The RAJ-II inner container is constructed primarily of Series 300 stainless steel, wood, and alumina silicate insulation. The void spaces within the inner container are filled with air at atmospheric pressure. The outer container is constructed of series 300 stainless steel, wood, and resin impregnated paper honeycomb. The thermal properties of the principal materials used in the thermal evaluations are presented in Table 3-1 and Table 3-2. Where necessary, the properties are presented as functions of temperature. Note that only properties for materials that constitute a significant heat transfer path are defined. A general view of the package is depicted in Figure 3-1. A sketch of the inner container transversal cross-section with the dimensions used in the calculation is presented in Figure 3-2.

For the Alumina Silicate, maximum values are specified because the maximum conductivity is the controlling parameter. This is because there is no decay heat in the payload and the only consideration is the material's ability to block of heat transfer to the fuel during the fire event.

The possible ignition of polyethylene foam is of primary concern due to the relatively great heat energy potentially released during combustion. Somewhat associated with this capacity are relatively high latent heats, both fusion and in particular vaporization. In order to better predict the behavior of the polyethylene foam, this latent heat was considered as part of the transient problem. The ANSYS FEA package allows this phase change, but requires the use of enthalpy change when doing so, rather than the typical simplification of using specific heat. There is no restriction on using enthalpy with one material and specific heat with a second material within the same analysis. Therefore, the RAJ-II material properties are specific heat based except for the polyethylene foam, which is enthalpy based as required to account for the phase changes. The material properties for the Fuel Assembly are defined in Table 3-10. The material properties for the RAJ-II packaging is presented in Table 3-11.

The heat of combustion for polyacetal is 20.05 MJ/kg [19] and ignition temperature is 595 K (322°C) [17] [18]. The heat of combustion for the paper honeycomb is 17.6125 MJ/kg [20] and ignition temperature is assumed the same as ignition for paper, 505 K (232°C). The heat of

combustion for the polyethylene form is 44.6 kJ/g [15], and ignition temperature is 573 K (300°C) [16].

3.6.4.5 Evaluation

3.6.4.5.1 Steady State Analysis

The transport normal steady-state condition for ambient exposure was calculated by hand in Section 3.5. In the type of transient problem that exists with consideration of this Hypothetical Accident Condition, where steady state conditions exist before some upset condition, the analyst establishes initial conditions for the transient upset by judicious use of the load stepping capabilities of the ANSYS program. By doing so, an additional measure of accuracy in the transient case is ensured, as the initial temperature gradients are also necessarily calculated.

3.6.4.5.2 Transient Analysis

Heat generation rates in ANSYS are on a volumetric basis, and the program internally creates a heat energy transfer out of the nodes loaded. In the case of an interface where a single node is shared by elements of two substantially differing materials, the potential to artificially transfer too much heat energy across the interface to the material with the lower capacity exists. This leads to artificially high indications of temperature. As such, when combustion is simulated in this analysis, only the nodes and elements completely internal to the volume of interest are loaded with a heat generation rate. The total energy released by this generation is, however, calculated on the basis of the total volume.

The transient conditions for heat generation rates were calculated as follows:

The equivalent paper honeycomb volume is 0.0848 m^3. The heat of combustion of the paper honeycomb is 17.6125 MJ/kg. The density is 18 kg/m^3. The combustion rate of the honeycomb was assumed 200 minutes, based on the propagation speed of the ignition temperature front through the honeycomb paper in the model with only external loads. The heat generation rate (W/m^3) was then calculated from:

$$(17.6125\ MJ/kg)(18\ kg/m^3)(84.84 \times 10^{-3}\ m^3) = 26.90\ MJ \qquad \text{(total energy released)}$$

$$(26.90\ MJ) / (84.84 \times 10^{-3}\ m^3) / (12000\ s) = 26.4 \times 10^3\ W/m^3 \qquad \text{(heat generation rate for paper honeycomb)}$$

The Delrin® (polyacetal) insert volume is 2.2×10^{-3} m^3. The heat of combustion of polyacetal is 20.05 MJ/kg [19]. The density of polyacetal is 1420 kg/m^3 [17]. The combustion of the polyacetal was assumed to require one hour, based on the propagation of the temperature front with no internal heat generation of the polyacetal. The heat generation rate (W/m^3) was then calculated from:

$$(20.05\ MJ/kg)(1420\ kg/m^3)(1.1 \times 10^{-3} m^3) = 62.64\ MJ \qquad \text{(total energy released)}$$

$(62.64\ MJ) / (2.2 \times 10^{-3}\ m^3) / (3600\ s) = 7.91 \times 10^6\ W/m^3$ (heat generation rate for polyacetal)

From Section 3.5, the polyethylene (EthaFoam®) heat of combustion of is 46.4 MJ/kg. The density of polyethylene is 35 kg/m^3. Based on data from hydrocarbon combustibles, a combustion rate of 0.5mm per minute for the polyethylene is used. For a typical element size of (0.01m × 0.01m × 0.01m) used in this analysis, the heat generation rate (W/m^3) is estimated from:

$(44.6\ MJ/kg)(35\ kg/m^3)(1.0x10^{-6}\ m^3) = 1561\ J$ (total energy released per element)

$(1561\ J) / (1.0x10^{-6}\ m^3) / (1200\ s) = 1.3x10^6\ W/m^3$ (typical heat generation rate for polyethylene)

Beginning with the initial steady-state analysis followed by the fire transient, it was determined that the onset of combustion in the honeycomb paper occurs at approximately 30 seconds and the propagation of the ignition temperature front through the thickness of the honeycomb takes 200 minutes. Following the combustion progression of the paper honeycomb, it was determined that the Delrin® (polyacetal) ignited at approximately 21 minutes thus inputting addition heat into the inner container. However, no polyethylene reached ignition temperature over the span of the thermal transient. Therefore, and it is concluded that this material did not ignite or combust.

3.6.4.5.3 Results

Temperature time-history plots of the transient analysis are presented in Figure 3-11 and Figure 3-12. Figure 3-13 shows the post fire thermal response of the RAJ-II package at 4 hours and 9 minutes. For comparison Figure 3-14 shows the temperatures in the inner container at the 4 hour and 9 minute time. Figure 3-15 shows the temperatures in the inner container at 1 hour and 21 minutes, the time at which the maximum temperatures occur and at the end of the polyacetal fire.

Results of the transient analysis shows that the temperatures inside of the inner container reached the melting point of the polyethylene foam but not the combustion temperature. Therefore, only the melting and vaporization of the polyethylene foam contributes to the internal temperature of the fuel bundle. The analysis shows that the peak temperature of the polyethylene is ~225°C below the combustion temperature that occurs at 300°C and the fuel assembly is ~200°C.

Based on these results, the fuel cladding temperature is below the mechanical limit for the material and the pressure stresses are below the values previously presented in this safety analysis report. Therefore, the existing 2-D thermal analysis presented in Section 3.5 bounds the worst-case thermal conditions and no further analysis is required.

Table 3-8 Summary of Transient Boundary Conditions

	Time Regime	Environment*	Force Convection on External Surface	Heat Flux on External Surface	Internal Heat Generation
Initial Conditions		311 K (38° C)	4.8 W/m²-K	387.4 W/m²(h) 96.9 W/m² (v)	—
HAC	0–30 min	1073 K (800°C)	19.8 W/m²-K	—	(see specific items)
Immed. Post HAC	30 min–4 hr	311 K (38° C)	Table 3-3	966.27 W/m²(h) 260.64 W/m² (v)	(see specific items)
Post HAC	4 hr–18 hr	311 K (38° C)	Table 3-3	—	(see specific items)
Honeycomb Burn	30 sec– ~200min	HAC	HAC	HAC	18.762×10^3 W/m³
Polyacetal Burn	~21 in– 1 hr 21 min	HAC	HAC	HAC	7.91×10^3 W/m³

*Bulk temperatures for radiative and convective loads.

Table 3-9 Ignition Temperatures and Heat Generation Rates

Material	Ignition Temperature	Typical Heat Generation Rate
Paper Honeycomb	505 K (232°C)	26.4×10^3
Polyacetal	595 K (322°C)	7.91×10^6
Polyethylene	573 K (300°C)	1.30×10^6

Table 3-10 Fuel Assembly Material Properties

Material	Density (g/m³)	Mass (kg)	Thermal Conductivity (W/m-K)	Specific Heat (J/kg-K)
Zirconium	6,550	105.5	—	335
UO_2	11,200	189.0	—	243
Fuel Assembly	$= (M_{Zr}+M_{UO2}) / \text{Cavity Volume}$ $= (105.5+189.0) / (140\times140\times4580)$ $= (294.5) / (0.090)$ $= 3280$	—	16.8	$= [(CP_{UO2})\times(M_{UO2}) + (CP_{Zr})\times(M_{Zr})]/(M_{UO2} + M_{Zr})$ $= [(243)\times(189) + (335)\times(105.5)]/(189 + 105.5)$ $= 276$

Table 3-11 RAJ-II Thermal Properties Summary

Material	Temperature (K)	Density (kg/m^3)	Thermal Conductivity (W/m-K)	Specific Heat (J/kg-K)	Reference
Stainless Steel	300	7900	15	477	Table 3-1
	400		17	525	
	500		18	539	
	600		20	557	
	800		23	582	
	1000		25	611	
Alumina Silicate	673	250	0.0697	1046	Table 3-1
	873		0.1046		
	1073		0.1512		
	1273		0.2092		
Wood	300	500	0.12	2800	Table 3-1
	500		0.12	2800	
Char	550		0.26	1588	[12]
	600		0.26	1606	
	800		0.26	1678	
	1000		0.26	1750	
	1073		0.26	1776	
	1273		0.26	1848	
Polyacetal (Delrin)	(all)	1420	0.40	1465	[17]
Paper Honeycomb	(all)	18	0.24	2800	
Air	300	1.177	0.0267	1005	Table 3-2
	400	0.883	0.0331	1009	
	500	0.706	0.0389	1017	
	600	0.589	0.0447	1038	
	800	0.442	0.0559	1089	
	1000	0.354	0.0672	1130	
	1073	0.354	0.0672	1130	
	1273	0.354	0.0672	1130	
Polyethylene Foam	200	35	0.33	11.1	Section 3.5
	250			14.6	[13]
	300			18.3	[14]
	350			22.3	
	400			26.5	
	410			27.4	
	415			(melt temp)	
	420			38.5	
	450			41.3	
	500			46.1	
	550			51.1	
	560			53.3	
	575			(vaporization temp)	
	590			186.5	
	600			188.7	
	620			190.9	
	660			195.4	

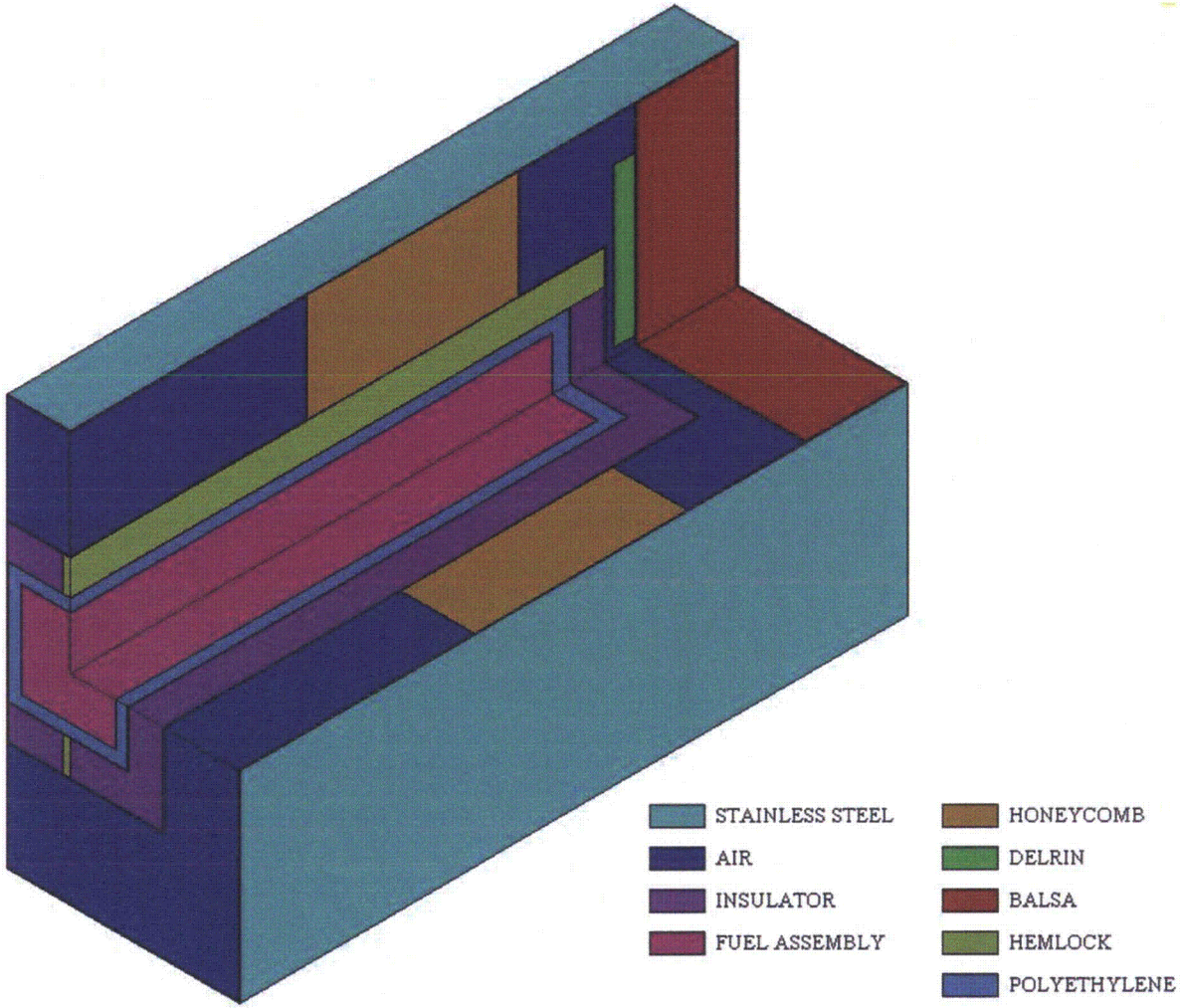

Figure 3-10 ANSYS Model with Cutaway

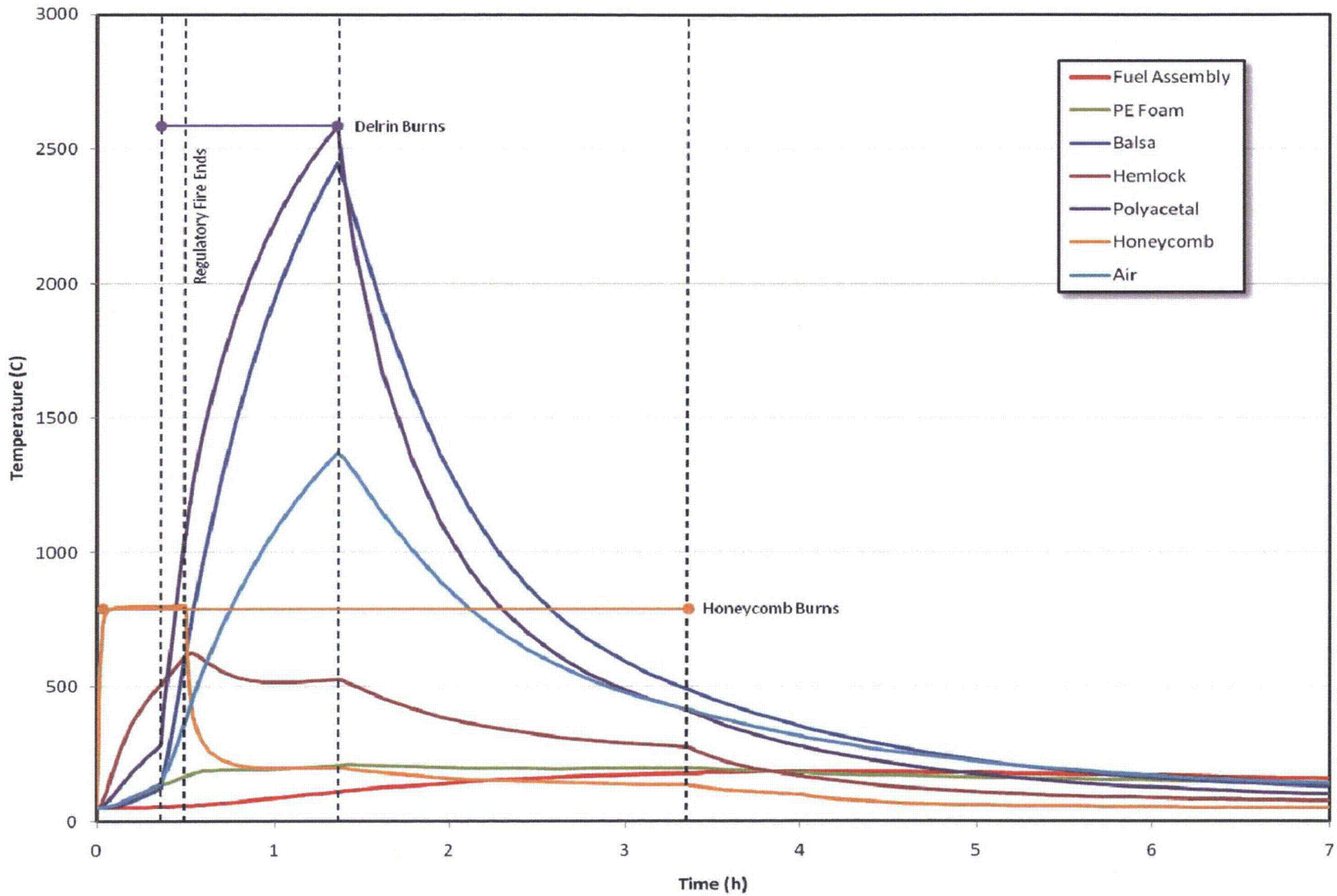

Figure 3-11 Fire Analysis Transient Response RAJ-II Inner and Outer Container Components

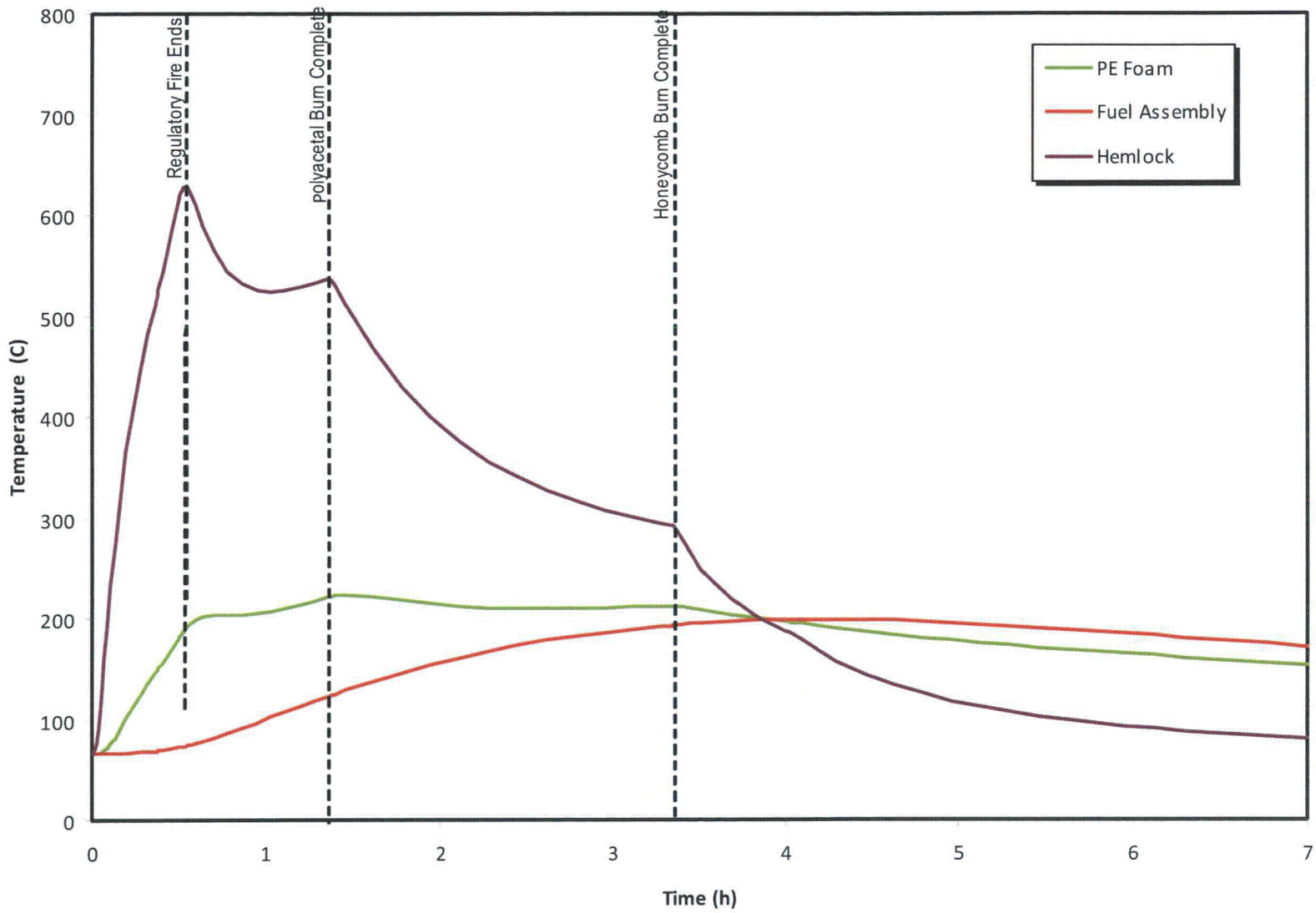

Figure 3-12 Fire Analysis Transient Response RAJ-II Inner Container Components

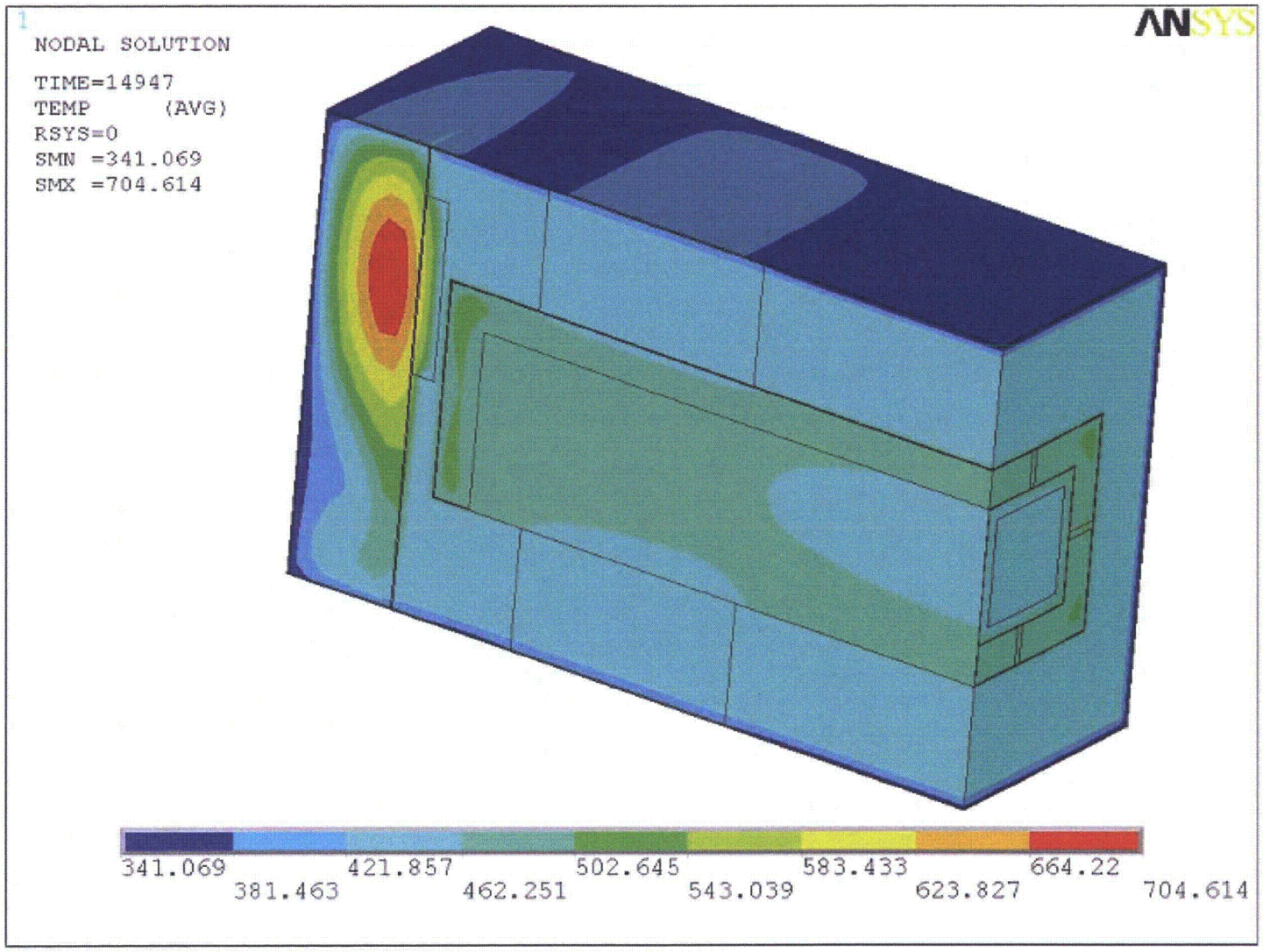

Figure 3-13 Package Temperature (°K) Distribution, t = 4 hr 9 min

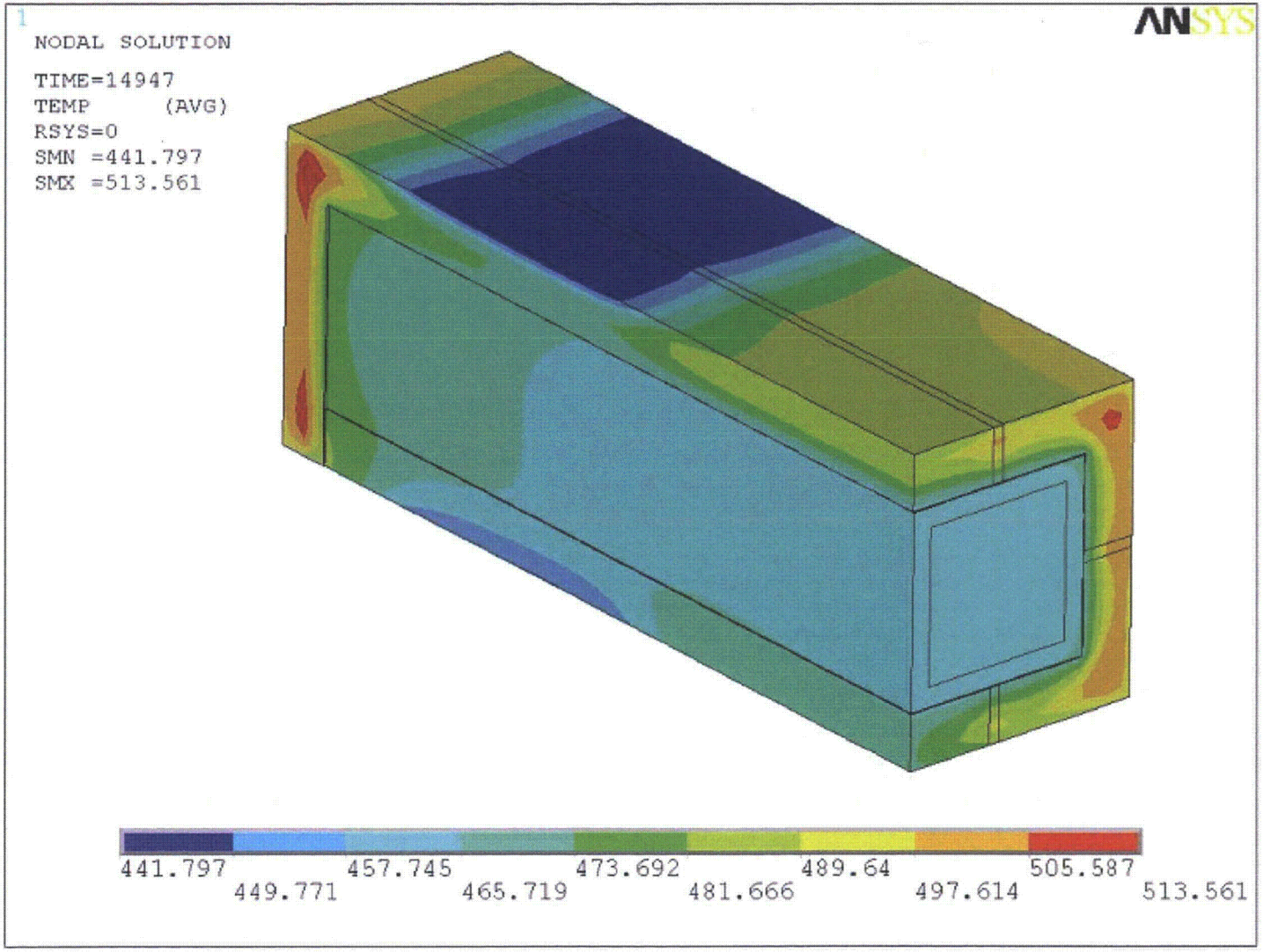

Figure 3-14 Inner Container Temperature (°K) Distribution, t = 4 hr 9 min

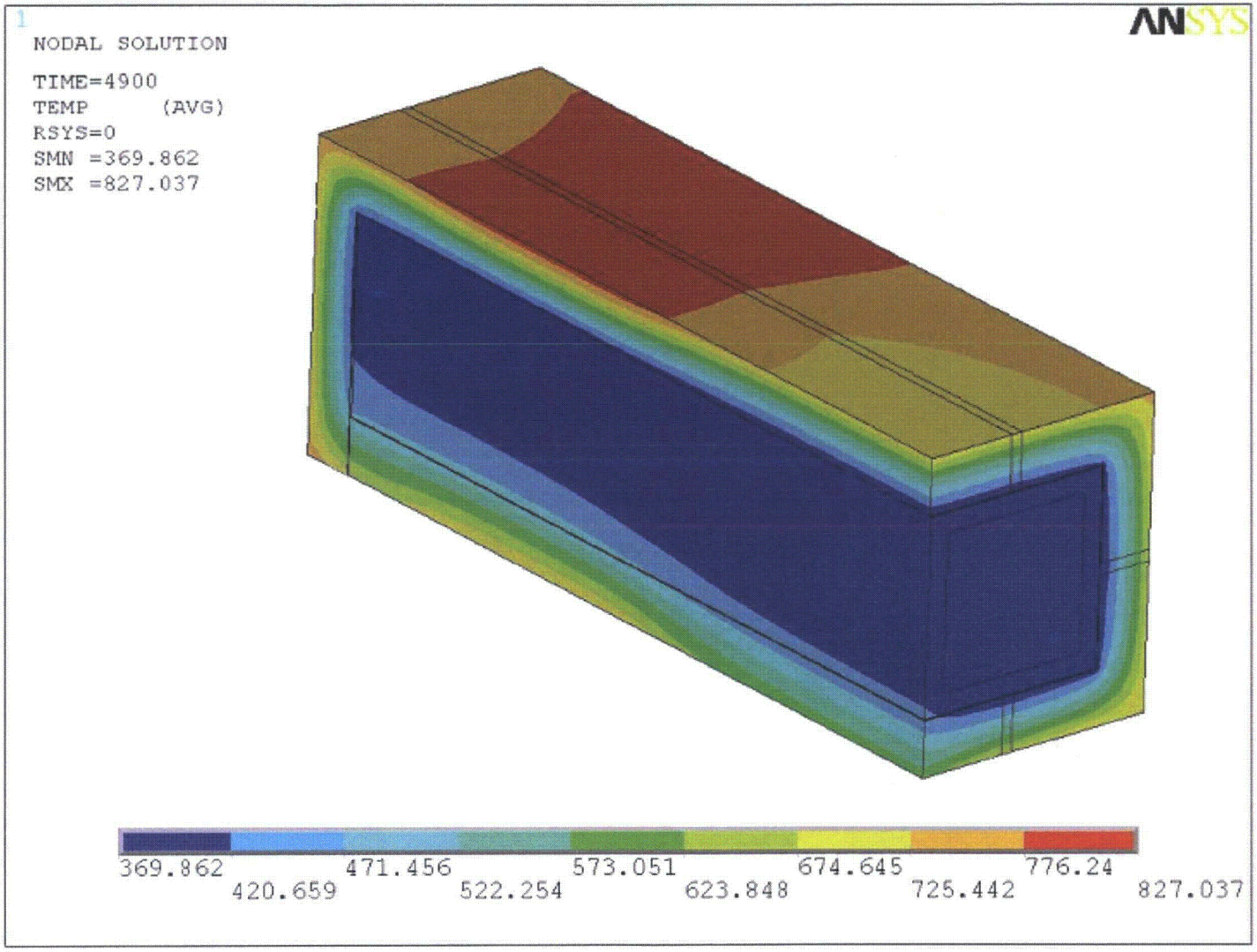

Figure 3-15 Inner Container Temperature (°K) Distribution, t = 1 hr 21 min

3.6.5 Thermal Test of Balsa Wood

Reference No.AT793016
P.No.NNH21141

Attention to:
Transnuclear,LTD.
Engineering Dept.

TEST REPORT

Thermal Test of Balsa Wood

(Translation)

April 2009

KOBELCO RESEARCH INSTITUTE, INC.
Applied Chemistry Division
Technology Dept.

1-5-5 Takatsukadai, Nishi-ku Kobe, 651-2271 JAPAN
TEL: 81-78-992-5193
FAX: 81-78-993-4403

Approved	Prepared

Thermal test of Balsa Wood

Kobelco Research Institute, Inc.
Applied Chemistry Division
Technology Dept.

1. Subject: Thermal test of Balsa Wood

2. Purpose
   In order to demonstrate the behavior of Balsa wood under thermal test conditions.

3. Specimen
   Balsa wood covered by stainless steel plate (an extremity is opened)
   2 lateral surfaces of stainless steel are cut off as the following figures.

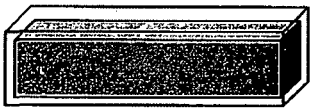

Dimensions: 58 x 58 x 150 mm

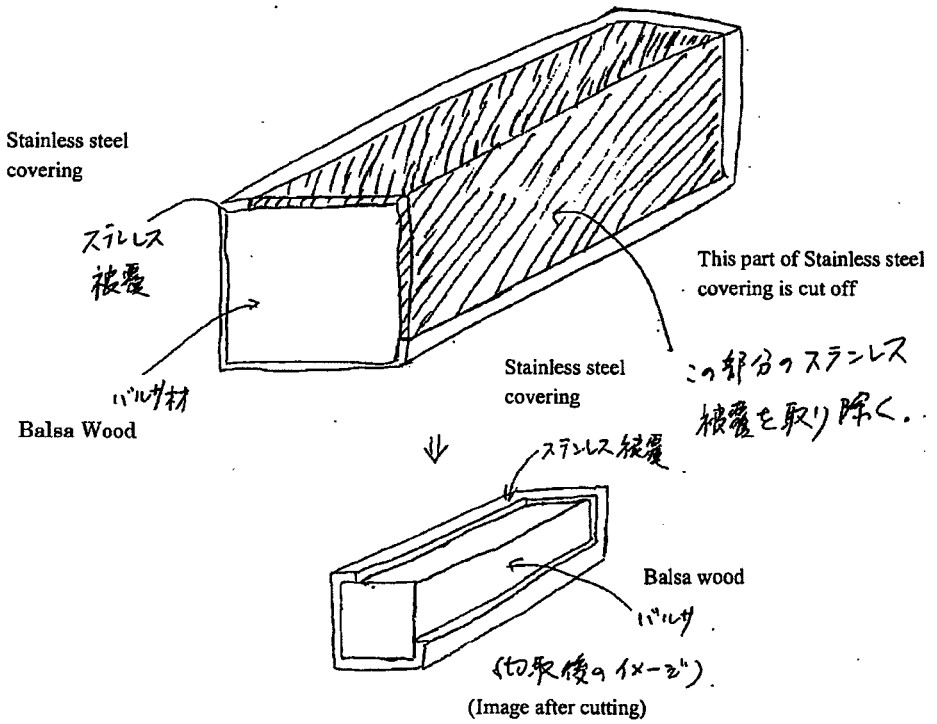

Fig. 1 Procedure of cutting for stainless steel covering

4. Test method
   An oven (Dimensions: 800x800x800 mm) is used in Kakogawa plant.
   Ambient temperature in the oven is set at 800 °C.
   After specimen is loaded in the oven and the ambient temperature is reached at 800 °C, thermal test is started and maintained during 30minutes. And then, specimen is

taken out of the oven, and is left for cooling.
After cooling, the specimen is observed.

①Heating: Ambient temperature in the oven is set at 800 °C. The specimen is heated during 30 minutes after the temperature in the oven reach at 800 °C.
Temperatures near the specimen and itself are measured.
Oxygen rate in the oven is measured continuously.

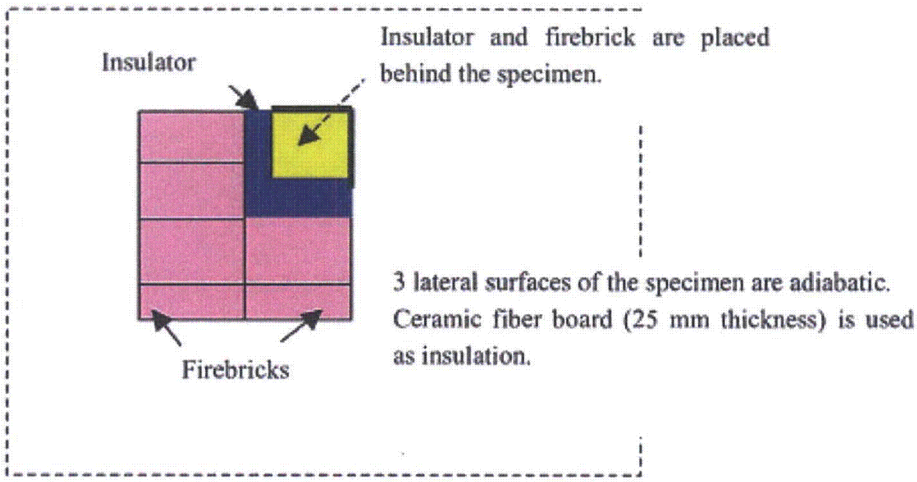

(Oven)

②Cooling: The specimen is cooled outside the oven.
Measurement of specimen temperature during cooling

③Observation: Balsa wood is taken out of stainless steel covering, and is observed

5. Date of testing
13:00 to 16:00 of March 19, 2009

6. Results
Just after the specimen is loaded in the oven, it looks combustion. Oxygen rate decrease down to 17% temporarily.
And then, oxygen rate recover to around 20%.
After the specimen is hold under 800 °C during 30 minutes, it is taken out the oven, cooled, and observed.
As the results, the Balsa wood is carbonized, but almost its shape is maintained. All Balsa wood is not burned to ashes.
Refer to the attachment-1 as the detail of the test results.

<Attachment-1>

Thermal Test of Balsa Wood

1. Subject: Thermal test of Balsa Wood
2. Purpose: In order to demonstrate the behavior of Balsa wood under thermal test conditions
3. Specimen:

   Balsa wood covered by stainless steel plate (an extremity is opened)
   2 lateral surfaces of stainless steel are cut off as the following figures.

Specimen (58 × 58 × 150)

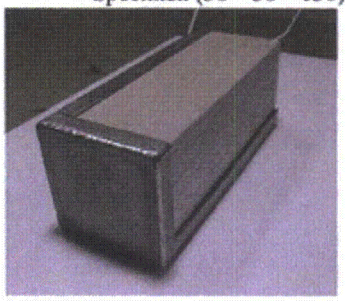

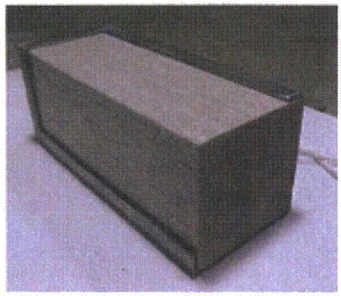

4. Test Method

   An oven (Dimensions: 800x800x800 mm) is used in Kakogawa plant.
   Ambient temperature in the oven is set at 800 °C.
   After specimen is loaded in the oven and the ambient temperature is reached at 800 °C, thermal test is started and maintained during 30minutes. And then, specimen is taken out of the oven, and is left for cooling.
   After cooling, the specimen is observed.

   ① Heating: Ambient temperature in the oven is set at 800 °C. The specimen is heated during 30 minutes after the temperature in the oven reach at 800 °C.
   Temperatures near the specimen and itself is measured.
   Oxygen rate in the oven is measured continuously.

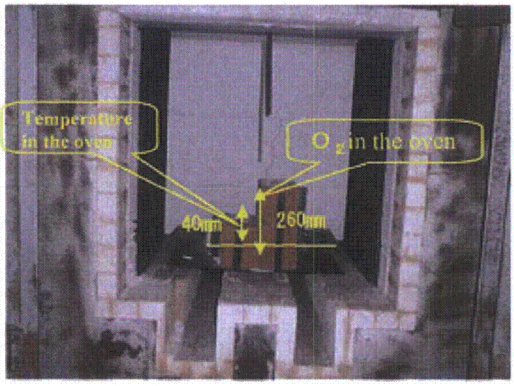

Electric oven (Mizukami Electric Works)
RT～1300℃、60kw

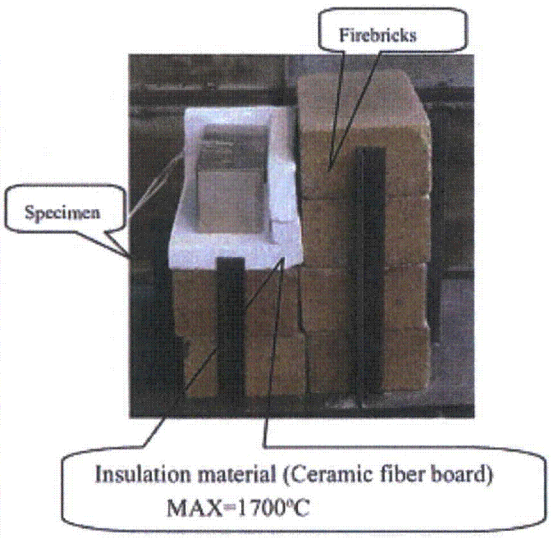

②Photos of specimen before and after test

Before test	After test
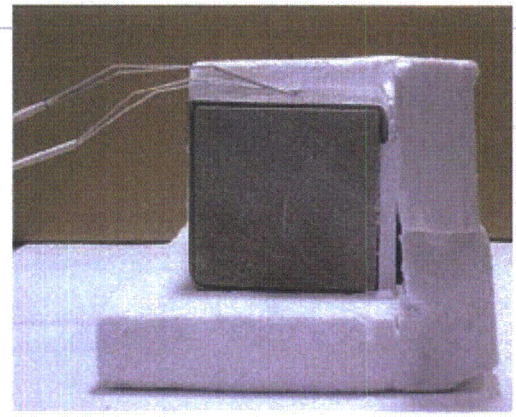	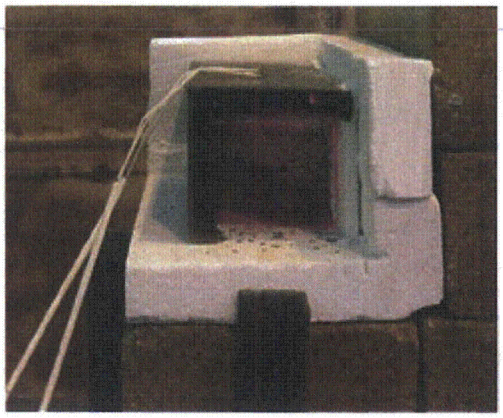

5. Test results

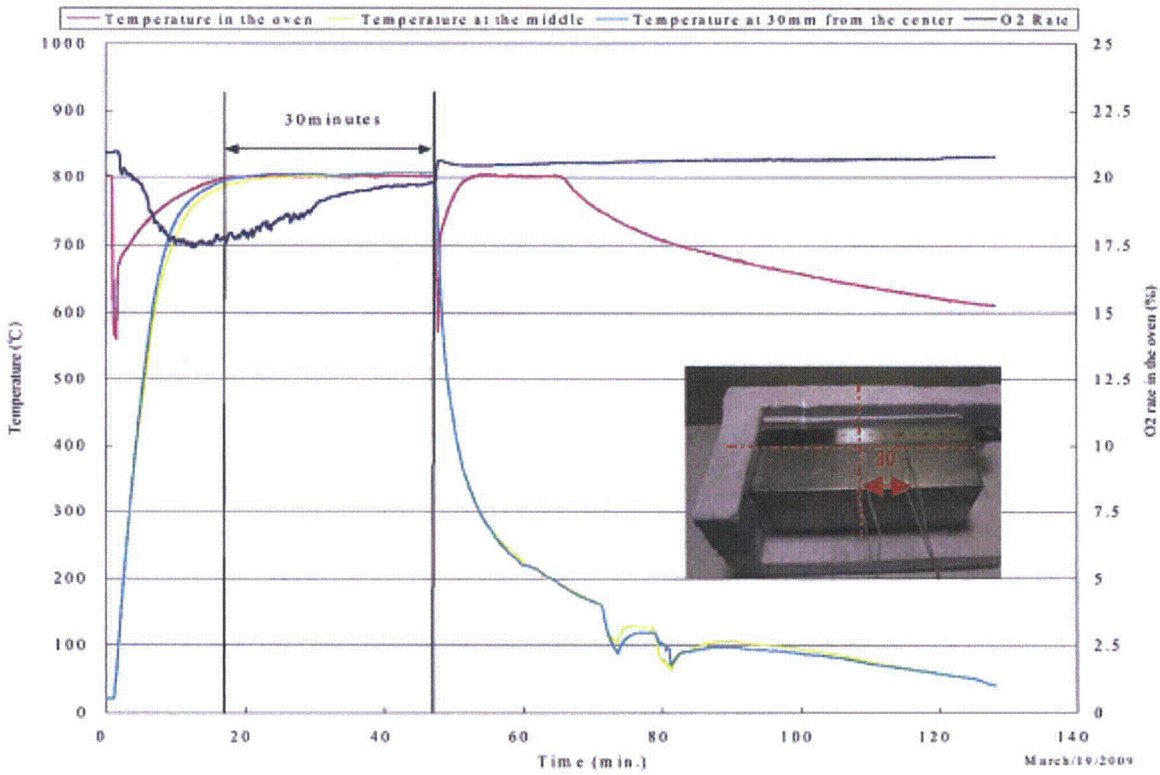

6. Items of data recorded

① Temperature in the oven : R-Thermo couples (Yamari Industries, Limited)

② Temperature of specimen (Center, 30 mm from the center) : K (ϕ0.3) Thermo couples (Asahi Pyro Industrial Co. Ltd.)
JIS C1602−1995 Grade 2 (±2.5℃) adapted

③ Environment in the oven : O_2 Analyzer (POT−101)

④ Data collection and processing : Data logger (GL800, GRAPHTEC)
Interval: Every 0.5 sec

6. Observation after test

Balsa wood and stainless steel covering after test

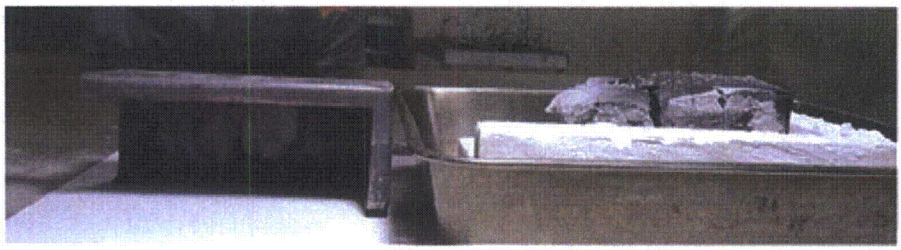

Stainless steel covering after test

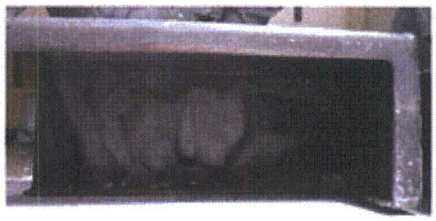

Direction of an open extremity

Adiabatic side (lateral surface)

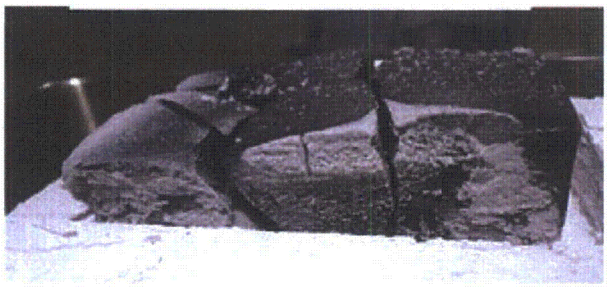

Adiabatic side (Rear)

Side of cutting covering

Photos after thermal test

4.0 CONTAINMENT

4.1 DESCRIPTION OF THE CONTAINMENT SYSTEM

Fuel rod cladding and welded end plugs form the containment vessel for the containment of radioactive material in the contents that is transported in the RAJ-II package. Design and fabrication details for fuel rod are described in Section 1.0. Compliance with the containment requirements does not rely upon either filters or mechanical cooling systems. The RAJ-II package does not incorporate a feature intended to allow continuous venting of the containment vessel under normal conditions of transport.

4.2 CONTAINMENT UNDER NORMAL CONDITIONS OF TRANSPORT

The RAJ-II package is constructed, and prepared for shipment so that there is no loss or dispersal of the radioactive contents and no substantial reduction in the effectiveness of the packaging during normal conditions of transport. The nature of the contained radioactive material and the structural integrity of the fuel rod cladding including the closure welds are such that there will be no loss or dispersal of radioactive material under normal conditions of transport. Each rod is pressurized with helium gas to a nominal internal pressure of approximately 1.1 MPa (160 psi) and undergoes a leak check during fabrication. A helium leak test is done during the fabrication of each fuel rod to demonstrates that the fuel rod is leak tight ($<1 \times 10^{-7}$ std-cm^3/s). The release rate limit for normal transport condition is less than 10^{-6}A2 in a period of one week. Details for the calculation of the release rate limit are in Appendix 4.5.2.

4.3 CONTAINMENT UNDER HYPOTHETICAL ACCIDENT CONDITIONS

The containment requirement of 10 CFR 71.51(a)(2) requires that no escape of other radioactive material exceeding a total amount A_2 in 1 week. [1] Following the drop test, a fuel bundle was leak tested and shown to have a leak rate of He equivalent to a rate of 5.5×10^{-6} atm cm^3/s. Fuel rods were also heated to 800°C for over 30 minutes and remained leaktight. The release rate limit for the accident condition is less than an A2 in the period of one week following the accident transport conditions. Details for the calculation of the release rate limit are in Appendix 4.5.2.

4.4 LEAKAGE RATE TESTS FOR TYPE B PACKAGES

During manufacturing each fuel rod is He leak tested to demonstrate that it is leak tight ($<1 \times 10^{-7}$atm-cm^3/s). The fabrication leakage rate test for each fuel rod satisfies the requirement for the pre-shipment leakage rate test. There are no maintenance or periodic leakage rate tests for the fuel rods.

4.5 APPENDIX

4.5.1 References

1. 10 CFR 71, Packaging and Transport of Radioactive Materials

2. NUREG/CR-6487 Containment Analysis for Type B Packages Used to Transport Various Contents

3. ASTM C 1295-05 Standard Test Method for Gamma Energy Emission from Fission products in Uranium Hexafluoride and Uranyl Nitrate Solution

4. ANSI N14.5-1997 American National Standard for Radioactive Materials – Leakage Tests on Packages for Shipment

5. Petersen, Helge, Riso Report No. 224, The properties of Helium: Density, Specific Heats, Viscosity, and Thermal Conductivity at Pressures from 1 to 100 bar and from Room Temperature to about 1800 K, Danish Atomic Energy Commission, September, 1970

4.5.2 Determination of Allowable Release Rates

Allowable release rates are determined for both normal conditions of transport and hypothetical accident conditions as follows:

Step 1: Identify the radioactive contents.

The radioactive contents is limited to commercial grade or reprocessed uranium in solid form as ceramic uranium oxide that is enriched to no more than 5.00 wt%. The uranium and other nuclides are considered to be dispersible solids that have a homogeneous distribution.

The total activity contained in the radioactive material contents is calculated for a maximum allowed payload of two fuel assemblies containing 550 kg UO_2 (484 kg U) with nuclide specification for enriched reprocessed uranium.

The basic radionuclide values from 10 CFR 71, Appendix A [1], (A_2 and specific activity) for the enriched reprocessed uranium contents described in Section 1.2.2 are summarized in Table 4-1.

Table 4-1 Basic Radionuclide Values

Symbol of Radionuclide	Element and Atomic Number	A_2(TBq)	A_2(Ci)	Specific Activity (TBq/g)	Specific Activity (Ci/g)
U-232 (slow lung absorption)	Uranium (92)	1.0×10^{-3}	2.7×10^{-2}	8.3×10^{-1}	2.2×10^{-1}
U-234 (slow lung absorption)		6.0×10^{-3}	1.6×10^{-1}	2.3×10^{-4}	6.2×10^{-5}
U-235 (all lung absorption types)		Unlimited	Unlimited	8.0×10^{-8}	2.2×10^{-6}
U-236 (slow lung absorption)		6.0×10^{-3}	1.6×10^{-1}	2.4×10^{-6}	6.5×10^{-5}
U-238 (all lung absorption types)		Unlimited	Unlimited	1.2×10^{-8}	3.4×10^{-7}
Tc-99	Technetium(43)	9.0×10^{-1}	2.4×10^{1}	6.3×10^{-4}	1.7×10^{-2}
Alpha emitting	Neptunium(93) Plutonium(94)	9.0×10^{-5}	2.4×10^{-3}		
Gamma emitting	Fission Products	2.0×10^{-2}	5.4×10^{-1}		

Step 2: Determine the total releasable activity.

Releasable airborne materials can originate from the radionuclides within the individual fuel rods. The contribution of the fuel to the overall release rate largely depends on its initial pre-transport condition and on subsequent fuel rod response to transportation events. Loose radioactive particles may originate from spallation of material from the surface of the pellets during normal transport conditions. The uranium oxide pellets may fracture and crumble due to handling, vibration, or accident conditions. These conditions will tend to cause the fuel pellets inside the fuel rod to

produce a powder aerosol in the helium fill gas. To estimate the source terms under normal and accident conditions, an assumption is made that of the total fuel rod inventory is fine fuel particles. A reasonable bounding value for the mass density of a powder aerosol is 9×10^{-6}g/cm^3. [2]

The activity of the radioactive material in the contents is summarized in Table 4-2.

Table 4-2 Activity of Radioactive Material

			Activity	
Nuclide	**Maximum Content**	**Mass (g)**	**TBq**	**Ci**
U-232	0.050 μg/gU	2.42×10^{-2}	2.01×10^{-2}	5.32×10^{-1}
U-234	2000 μg/gU	$9.68\times10^{+2}$	2.23×10^{-1}	6.00
U-235	50000 μg/gU	$2.42\times10^{+4}$	1.94×10^{-3}	5.32×10^{-2}
U-236	2500 μg/gU	$1.21\times10^{+3}$	2.90×10^{-3}	7.78×10^{-2}
U-238	9.23×10^{5} μg/gU	$4.47\times10^{+5}$	5.36×10^{-3}	2.47×10^{-1}
Tc-99	5 μg/gU	2.42	1.52×10^{-3}	4.11×10^{-2}
Np/Pu	3300 Bq/kgU	---------	1.60×10^{-6}	4.31×10^{-5}
Gamma Emitters[1]	4.4 X 10^5 MeV Bq/kgU	---------	3.45×10^{-2}	9.30×10^{-2}
Total activity			**2.58×10^{-1}**	**6.95**

Note:
1. The mean gamma energy per disintegration for the gamma emitting measured by the standard test method for gamma energy emission from fission products ranges from 0.0618 to 0.766 [3]. The gamma energy production specification for reprocessed uranium (4.4 X 105 MeV Bq/kg) is divided by the lowest mean gamma energy (0.0618 MeV) to conservatively estimate the activity of the gamma emitters.

The specific activity of the solid uranium oxide pellets is

$$S_A = 6.95 \text{ Ci} / 550 \text{ kg } UO_2 = 1.27\ 10^{-5} \text{ Ci/g } UO_2$$

The total releasable activity inside an individual fuel rod is

$$C = S_A \times \rho$$

where:

C is the releasable activity concentration inside the fuel rod [Ci/cm^3],

S_A is the specific activity of the fines in fuel rods [Ci/g UO_2],

ρ is the aerosol mass density [g/cm^3].

The release activity for the reprocessed enriched uranium for both normal and accident conditions is

$$C_N = C_A = (1.27 \times 10^{-5}\ \text{Ci/g}\ UO_2)\ (9\times10^{-6}\text{g/cm}^3) = 1.14 \times 10^{-11}\text{Ci/ cm}^3$$

Step 3: Determine an A2 value for the releasable activity.

Table 4-3 A_2 for Mixture

Nuclide	Fraction of Activity f(i)	f(i)/A2(i) A2/TBq	f(i)/A2(i) A2/Ci
U-232	7.66×10^{-2}	$7.79\times10^{+1}$	2.84
U-234	8.64×10^{-1}	$1.44\times10^{+2}$	5.40
U-235	7.66×10^{-3}	0	0
U-236	1.13×10^{-2}	1.88	7.08×10^{-2}
U-238	2.12×10^{-2}	0	0
Tc-99	5.92×10^{-3}	6.57×10^{-3}	2.47×10^{-4}
Np/Pu	6.21×10^{-6}	6.88×10^{-2}	2.59×10^{-3}
Gamma Emitters	1.34×10^{-2}	6.68×10^{-1}	2.48×10^{-2}
Totals	**1.0**	**224**	**8.34**

The release fraction of the individual radionuclide is assumed to be the same for all nuclides. The A2 value for a mixture of releasable radionuclides can be derived using 10 CFR Part 71, Appendix A from the expression.

$$A_2 \text{ for mixture} = \frac{1}{\sum_i \frac{f(i)}{A2(i)}}$$

where f(i) is the releasable activity fraction of radionuclide (i). The A_2 for mixture is 0.12 Ci (4.46×10^{-3} TBq).

Step 4: Determine the release rate for normal conditions of transport, R_N, and for hypothetical accident conditions, R_A.

Standard methods described in ANSI N14.5 [4] are used to determine the package release limits. Leaktightness is the specified containment criterion for the design, fabrication, and preshipment leakage rate of the fuel rod containment. Leaktightness is defined as 10^{-7} cm^3/s, based on dry air at 1 atm abs and 298 K leaking to a 0.01 atm abs ambient. The maximum fuel rod conditions are 350 K (77°C, 171°F) and 1.33 MPa (192.9 psia, 13.1 atm abs) for normal conditions, and 1073 K (800°C, 1472°F) and 4.08 MPa (592 psia, 40.3 atm abs) assuming no rod deformation for accident conditions.

The volume leakage rate at the upstream conditions is estimated by the following equation:

$$L_u = (F_c + F_m)(P_u - P_d)(P_a / P_u)\, cm^3 / s$$

$$F_c = [2.49\times10^6\ D^4]/(a\times\mu)\ cm^3/atm\times s$$

$$F_m = [3.81\times10^3\ D^3\ (T/M)^{0.5}]/(a\times P_a)\ cm^3/atm\times s$$

where

- a is leakage hole length, cm
- D is leakage hole diameter, cm
- F_c is coefficient of continuum flow conductance per unit pressure, cm^3/atm s,
- F_m is coefficient of free molecular flow conductance per unit pressure, cm^3/atm s,
- M is molecular weight, g/mol
- P_u is fluid upstream pressure, atm abs,
- P_d is fluid downstream pressure, atm abs,
- P_a is average stream pressure = 1/2 (Pu+Pa), atm abs
- T is fluid absolute temperature, K, and
- μ is fluid viscosity, cP (centipoises).

The correlation for the coefficient of dynamic viscosity [5] for helium is

$$\mu = 3.674\times10^{-7}\ T^{0.7}\ kg/m\times s = 3.674\times 10^{-4}T^{0.7}\ cP$$

Normal Transport

A reference air leakage rate corresponding to normal transport conditions is $L_{R,N}=1\times10^{-7}$ std cm^3/s (air at 25°C and 1.0 atm abs leaking to a 0.01 ambient). A 1.0-cm path length is assumed. The corresponding leakage rate for helium, $L_{u,He}$, at 77°C and 13.1 atm abs leaking to 1.0 atm abs ambient is calculated to determine the allowable leak rate for helium.

For the air flow, a = 1.0 cm, T = 298 K, u(air, 298 K) = 0.0198 cP, Pu = 1 atm, Pd = 0.01 atm, M=29 g/mol, and Pa = 0.505 atm,

$$F_c = [2.49\times10^6\ D^4]/(1.0\times0.0185) = 1.34\times10^8\ D^4\ cm^3/atm\times s$$

$$F_m = [3.81\times10^3\ D^3\ (298/29)^{0.5}]/(1.0\times0.505) = 2.41\times10^4\ D^3\ cm^3/atms$$

$$L_u = (F_c + F_m)(P_u - P_d)(P_a / P_u)\, cm^3 / s$$

$L_{R,N} = L_{u=}1\times10^{-7}$ atm cm^3/s

1×10^{-7} atm × cm^3/s = $[1.34\times10^8 D+2.41\times10^4](D^3)(0.99)(0.505)$

Solving implicitly for D gives,

$D = 1.63\times10^{-4}$ cm

For the helium leak flow conditions: Pu = 13.1 atm, Pd = 1.0 atm, T = 350 K, μ(helium, 350 K) =0.02218 cP, Pu – Pd = 12.1 atm, Pa = 7.1 atm, a (fuel rod cladding thickness) = 0.2 cm, M=4.0 g/mol, and

Pa/Pu = 0.525.

$F_c = [2.49\times10^6 (1.63\times10^{-4})^4]/(0.2\times0.02218) = 3.96\times10^{-7}$ cm^3/atm×s

$F_m = [3.81\times10^3 (1.63\times10^{-4})^3 (350/4)^{0.5}]/(0.2\times7.1) = 1.09\times10^{-7}$ cm^3/atm×s

Then, the helium flow rate equivalent to the leaktightness criteria 10^{-7} cm^3/s based on air is:

$L_{u,He} = (3.96\times10^{-7}+1.09\times10^{-7})(13.1-1.0)(0.542) = 3.31\times10^{-6}$ cm^3/s

The helium flow rate for the package contents based on 2 fuel bundles with 92 fuel rods per fuel bundle is:

$\mathbf{L_N} = 2\times92\times(3.31\times10^{-6}$ cm^3/s) = 6.09×10^{-4} cm^3/s

The release rate for normal transport conditions based on the contents of 2 fuel bundles is:

$\mathbf{R_N} = \mathbf{L_N C_N} = (6.09\times10^{-4}$ cm^3/s) × $(1.14 \times 10^{-11}$Ci/ cm^3) = 6.94×10^{-15} Ci/s

where:

L_N is the time-averaged volumetric gas flow rate for normal transport conditions [cm^3/s], and

C_N is the curies per unit volume of the releasable radioactive material within the containment vessel normal transport conditions [Ci/cm^3].

The maximum allowed release rate for normal conditions in units of curies per second assuming a time-averaged constant flow rate is:

$A_2\times10^{-6}$/hour = ($A_2\times10^{-6}$/hour)/3600 seconds/hour) =A_2 2.78×10^{-10}/second

$A_2\times2.78 \times10^{-10}$/second = (0.12 Ci)($2.78 \times 10^{-10}$/second) = 3.34×10^{-11} Ci/s

The release rate for normal transport conditions, $\mathbf{R_N}$ is less than $A_2\times10^{-6}$/hour.

Accident Conditions

The reference air leakage rate corresponding to accident conditions for a single fuel bundle subject is $L_{R,A}=5.5\times10^{-6}$ atm cm^3/s (air at 25°C and 1.0 atm abs leaking to a 0.01 ambient). The corresponding leakage rate for helium at 25°C and 36 atm abs leaking to 1.0 atm abs ambient is calculated to determine the allowable leak rate for helium.

For the air flow, a = 1.0 cm, T = 298 K, u(air, 298 K) = 0.0198 cP, Pu = 1 atm, Pd = 0.01 atm, M=29 g/mol, and Pa = 0.505 atm,

$$F_c = [2.49\times10^6\ D^4]/(1.0\times0.0185) = 1.34\times10^8\ D^4\ cm^3/atm \times s$$

$$F_m = [3.81\times10^3\ D^3\ (298/29)^{0.5}]/(1.0\times0.505) = 2.41\times10^4\ D^3\ cm^3/atms$$

$$L_u = (F_c + F_m)(P_u - P_d)(P_a / P_u)\, cm^3 / s$$

$$L_{R,A} = L_u = 5.5\times10^{-6}\ atm\ cm^3/s$$

$$5.5\times10^{-6}\ atm \times cm^3/s = [1.34\times10^8\ D + 2.41\times10^4](D^3)(0.99)(0.505)$$

Solving implicitly for D gives,

$$D = 4.95\times10^{-4}\ cm$$

For the helium leak flow conditions: Pu = 40.3 atm, Pd = 1.0 atm, T = 1073 K, μ(helium, 1073 K) = 0.0486 cP, Pu – Pd = 39.3 atm, Pa = 20.2 atm, a (fuel rod cladding thickness) = 0.2 cm, M=4.0 g/mol, and Pa/Pu = 0.501.

$$F_c = [2.49\times10^6\ (4.95\times10^{-4})^4]/(0.2\times0.0486) = 1.54\times10^{-5}\ cm^3/atm \times s$$

$$F_m = [3.81\times10^3\ (4.95\times10^{-4})^3\ (1073/4)^{0.5}]/(0.2\times20.2) = 1.87\times10^{-6}\ cm^3/atm \times s$$

Then, the helium flow rate equivalent to the measured leak rate $5.5\text{x}10^{-6}$ cm^3/s based on air is:

$$L_{u,He} = (1.54\times10^{-5} + 1.87\times10^{-6})(40.3-1.0)(0.501) = 3.40\times10^{-4}\ cm^3/s$$

The helium flow rate for the package contents based on 2 fuel bundles with 92 fuel rods per fuel bundle is:

$$\mathbf{L_A} = 2\times(3.40\times10^{-4}) = 6.80\times10^{-4}\ cm^3/s$$

$$\mathbf{R_A} = \mathbf{L_A C_A} = (6.80\times10^{-4}\ cm^3/s) \times (1.14 \times 10^{-11} Ci/cm^3) = 7.75\times10^{-15}\ Ci/s$$

where:

L_A is the time-averaged volumetric gas flow rate for accident transport conditions [cm^3/s], and

C_A is the curies per unit volume of the releasable radioactive material within the containment vessel accident transport conditions [Ci/cm^3].

The maximum allowed release rate for accident conditions in units of curies per second assuming a time-averaged constant flow rate is:

$$A_2 \text{ /week} = (A_2 \text{ /week})/6.048 \text{ seconds/week}) = A_2\ 1.65\times10^{-6}\text{/second}$$

$$A_2\ 1.65\times10^{-6}\text{/second} = (0.12 \text{ Ci})(1.65\times10^{-6}\text{/second}) = 1.98\times10^{-6} \text{ Ci/s}$$

The release rate for accident conditions, $\mathbf{R_A}$, is less than A_2 /week.

5.0 SHIELDING EVALUATION

The contents of the RAJ-II require no shielding since unirradiated fuel gives off no significant radiation either gamma or neutron. Hence the RAJ-II provides no shielding. The minimal shielding provided by the stainless steel sheet is not required. The dose rate limits established by 10 CFR 71.47(a) for normal conditions of transport (NCT) are verified prior to shipping by direct measurement.

Since there is no shielding provided by the package, there is no shielding change during the Hypothetical Accident Conditions (HAC). Therefore, the higher dose rate allowed by 10 CFR 71.51(a)(2) will be met.

6.0 CRITICALITY EVALUATION

6.1 DESCRIPTION OF CRITICALITY DESIGN

6.1.1 Design Features

A principle safety function of the RAJ-II is to provide criticality control. The inner and outer containers retain the contents within a fixed geometry relative to other such packages in an array. The fuel assembly structure or fuel rod container retains the fuel rods within a fixed geometry. Individual fuel rods retain the fuel pellets within a fixed geometry of the fuel rod tube. The *confinement system* consists of the inner and outer containers, fuel assembly structure or fuel rod container, and the fuel rod tube. Neutron absorption is provided by packaging structural materials and gadolinium oxide in the uranium oxide fuel mixture. Neutron moderation is provided from external sources consistent with the normal or accident transport conditions. Packaging materials, such as paper honeycomb, wood, and polyethylene, also provides neutron moderation, but none of these materials is intended to provide the neutron moderation required for effective neutron absorption. Dimensions and tolerances of the confinement system for fissile material, floodable void spaces, and overall package that affect the physical separation of fissile contents in package arrays are described in Section 1.

6.1.2 Summary Table of Criticality Evaluation

A criticality evaluation is done for each of the type and form of contents that includes fuel rods, fuel bundles, and fuel assemblies. Each fuel rod, fuel bundle, and fuel assembly design as described in Section 1 is considered in the evaluation of the package. A demonstration of maximum reactivity determined the most reactive package configuration for each type and form of contents.

The criteria to establish subcriticality of the package includes an allowance for uncertainties in the calculated multiplication factor k_{eff} of the package or array of packages and margin for uncertainty in the mean k_{eff} that results from calculation of the benchmark criticality experiments [1].

$$k_p + \Delta k_p \leq k_c - \Delta k_c - \Delta k_m$$

where:

k_p is the calculated multiplication factor k_{eff} of the individual package or package array for normal and accident transport conditions;

k_c is the mean k_{eff} that results from the calculation of the benchmark criticality experiments;

Δk_p is an allowance for statistical uncertainty in the calculation of k_p, material and fabrication tolerances, and uncertainties due to limitation in the geometric or material representations used in the computational method;

Δk_c is a margin for uncertainty in k_c that includes allowances for uncertainties in the critical experiments, statistical uncertainties in the computation of k_c, uncertainties due to extrapolation of k_c outside the range of experimental data, and uncertainties due to limitation in the geometric or material representations used in the computational method;

Δk_m is an administrative margin to ensure the subcriticality of k_p.

The maximum multiplication factor (*Maximum* k_{eff}) is the maximum value of $k_p+\Delta k_p$ for the contents and transport condition that is used to demonstrate that criteria for subcriticality is satisfied. The statistical uncertainty for k_p is 2 times the standard deviation for the calculation method ($2\sigma_p$). The total uncertainty Δk_p also includes allowances for other uncertainties (Δk_u) that depend on package assessment such that $\Delta k_p = 2\sigma_p + \Delta k_u$. The upper subcritical limit (USL) is defined as the value for $k_c - \Delta k_c - \Delta k_m$, where Δk_m is 0.05. Table 6-1 provides a summary of the USL for the package configurations. The criterion for all package configurations is as follows:

Maximum $k_{eff} \leq$ USL

where:

Maximum $k_{eff} = k_p + 2\sigma_p + \Delta k_u$, and

USL= $k_c - \Delta k_c - \Delta k_m$

Table 6-1 Summary of Upper Subcritical Limits

Package Configuration	$USL = k_c - \Delta k_c - \Delta k_m$
Individual Package, Fuel Bundle or Fuel Assembly, no BA Rods	0.9424
Package Array, Fuel Bundle or Fuel Assembly, with BA Rods	0.9361
Package Array, Fuel Bundle or Fuel Assembly, no BA Rods	0.9436
Individual Package, Fuel Rods or Fuel Rod Container	0.9396
Package Array, Fuel Rods or Fuel Rod Container	0.9275

6.1.2.1 Fuel Bundle or Fuel Assembly

A criticality evaluation is done for fuel bundles that have no BA rods and fuel bundles that have a minimum number of BA rods. A fuel assembly is the fuel bundle with the fuel channel installed. The credible rearrangement of the fuel bundle due to accident conditions of transport is limited by the fuel channel for a fuel assembly, where as, the inner container limits the fuel rod rearrangement for a fuel bundle. A minimum of eight (8) BA rods meeting the following constraints is assumed in the criticality evaluation of the fuel bundles and fuel assembly contents:

1. BA rods shall be in positions that are symmetric across the major geometric diagonal from the control blade corner.

2. No BA rod shall be in the outermost edge or corner location of the fuel rod lattice.

3. Partial length fuel rods shall not be BA rods.

4. At least one BA rod shall be in three of the four fuel lattice quadrants.

5. No BA rods are required in fuel lattices that do not have fissile material (natural uranium defined as uranium containing a mass percentage of uranium-235 that does not exceed 0.72%) or is fissile excepted (uranium enriched in uranium-235 to a maximum of 1 percent by weight).

Table 6-2 Individual Package, Fuel Bundle or Fuel Assembly, no BA Rod (USL=0.9424)

Condition of Transport	Contents	*Maximum* k_{eff}	Reference
Normal	Fuel Assembly or Fuel Bundle	0.8126	Table 6-25
Accident	Fuel Assembly	0.8437	Table 6-25
	Fuel Bundle	0.9372	Table 6-25

Table 6-3 Package Array, Fuel Bundle or Fuel Assembly, with BA Rods (USL=0.9361)

Condition of Transport	Contents	Array Size	*Maximum* k_{eff}	Reference
Normal	Fuel Assembly	5N = 529	0.6390	Table 6-31
	Fuel Bundle	5N = 361	0.6236	Table 6-31
Accident	Fuel Assembly	2N = 196	0.9337	Table 6-44
	Fuel Bundle	2N = 100	0.9345	Table 6-44

Table 6-4 Package Array, Fuel Bundle or Fuel Assembly, no BA Rods (USL=0.9436)

Condition of Transport	Contents	Array Size	*Maximum* k_{eff}	Reference
Normal	Fuel Assembly	5N = 169	0.6227	Table 6-31
	Fuel Bundle	5N = 100	0.5891	Table 6-31
Accident	Fuel Assembly	2N = 49	0.9361	Table 6-44
	Fuel Bundle	2N = 25	0.9358	Table 6-44

6.1.2.2 Fuel Rods

Fuel rods may be transported either packaged in a rod container or as a cluster of fuel rods without a rod container. Each individual fuel rod may be protected by a polyethylene sleeve. The routine and normal condition of transport is for the fuel rods to be close packed. During accident conditions the rod container confines the fuel rods to fixed geometry whereas a cluster of fuel rods are confined only by the inner container. For fuel rod shipment without a rod container, a maximum of 25 fuel rods in each compartment of the inner container is permissible. For a rod container, the number of fuel rods is limited by the capacity of the rod container (protective case, rod pipe, or rod box).

Table 6-5 Individual Package, Fuel Rods or Fuel Rod Container (USL=0.9396)

Condition of Transport	Contents	*Maximum* k_{eff}	Reference
Normal	Fuel Rods without Rod Container	0.3817	Table 6-25
	Fuel Rod with Rod Container	0.5679	Table 6-25
Accident	Fuel Rods without Rod Container	0.6589	Table 6-25
	Fuel Rod with Rod Container	0.6199	Table 6-25

Table 6-6 Package Array, Fuel Rods or Fuel Rod Container (USL=0.9275)

Condition of Transport	Contents	Array Size	*Maximum* k_{eff}	Reference
Normal	Fuel Rods without Rod Container	5N = 361	0.9381	Table 6-31
	Fuel Rod with Rod Container	5N = 361	0.9086	Table 6-31
Accident	Fuel Rods without Rod Container	2N = 144	0.8054	Table 6-44
	Fuel Rod with Rod Container	2N = 144	0.9106	Table 6-44

6.1.3 Criticality Safety Index

CSI = 50/N where the number of undamaged packages in an array is 5N and number of damaged packages in an array is 2N. The CSI is rounded up to the nearest tenth decimal place. BA Rods refers to a minimum number and positions of BA Rods assumed in the evaluation. If a minimum number of eight BA rods meeting the constraints is not satisfied by the actual fuel bundle design, the CSI for a fuel assembly or fuel bundle without BA rods must be used. For fuel rod shipment without a rod container, a maximum of 25 fuel rods in each compartment of the inner container is permissible. For a rod container, the number of fuel rods is limited by the capacity of the rod container (protective case, rod pipe, or rod box).

Table 6-7 Summary of Criticality Safety Index

	Transport Conditions		
	Normal	Accident	
Contents	5N	2N	CSI
Fuel Assembly, without BA Rods	169	49	2.1
Fuel Assembly with BA Rods	529	196	0.6
Fuel Bundle, without BA Rods	100	25	4.0
Fuel Bundle with BA Rods	361	144	0.7
Fuel Rods or Fuel Rod Container	361	144	0.7

6.2 FISSILE MATERIAL CONTENTS

The contents are evaluated using nominal mass, density and dimensions described in Section 1.0 with the following exceptions to the uranium enrichment, fuel pellet density, and gadolinium oxide content in the BA rods.

1. The fissile material in fuel pellets is assumed to be uranium enriched up to a maximum of 5.0 wt% uranium-235 in all fuel rods.

2. Theoretical density for uranium dioxide (10.96 g/cm^3), and

3. A minimum number of eight gadolinium oxide fuel rods with a minimum 2.0 weight percent is assumed for the BA rods in every lattice zone of the fuel bundle.

6.3 GENERAL CONSIDERATIONS

6.3.1 Model Configuration

Figure 6-1 and Figure 6-2 show a comparison between actual packaging and model configuration used for the k_{eff} calculations. The actual packaging configurations shown in Figure 6-1 and Figure 6-2 are a summary of dimensions from the engineering drawings in Section 1.0. The model configuration represents the actual packaging with the following exception:

Gasket gap of about 5 to 8 mm, between the inner container upper lid and inner container box is not included in the model. Omitting the gap results in the height dimension of the inner wall of the inner container and the overall height of the inner container in the model that is less than the dimensions shown on engineering drawings. The inner container lid deformation during accident condition impacts results in an increase in the inner container height dimension. The inner wall of the inner container is a confinement feature that limits

fuel rearrangement, and increase in the inner wall height due to gasket gap and other impacts is considered in the assessment of the contents for accident transport conditions.

Wooden thermal insulator replaced with alumina silicate insulator. The wooden thermal insulator is a 10 mm thickness along the length of the package that provides support between the inner container outer wall and inner wall.

Container stainless steel structure is partially omitted (outer container 50 mm stainless steel angles that make the framework angle, inner and outer container tightening blocks and closure bolts, inner container hold down bar boss, partition plate angle). Structural stainless steel is a criticality feature that provides neutron absorption. Stainless steel sheet in the inner container and outer container provides significant neutron absorption for package array configurations. The effect of omitting angles that make the framework and other components results is less neutron absorption in the model.

Figure 6-3 shows typical configurations for the fuel bundle contents. There are four groups of fuel bundles 1) GE11 and GE13, 2) GE12B, GE14C, and GE14G, 3) GNF2, and 4)SVEA. The GE11 and GE13 fuel bundles are 9 by 9 lattice of fuel rods, and all other fuel bundles are 10 by 10 lattice of fuel rods. Detailed description of the fuel bundle configurations is found in Section 1.0. Fuel bundles are modeled explicitly in three-dimensions including the partial length fuel rods and water rods. The fuel bundle spacers, finger springs, upper tie plate, lower tie plate, lower fuel support piece, transition nosepiece, fuel channel and other hardware (i.e., springs, nuts, etc.) are not included in the model. These components are either stainless steel or a zirconium alloy that would insert additional neutron absorption, displace water moderation from the fuel lattice, or displace water reflector from the fuel bundle envelope in the model. The net effect of omitting the fuel assembly components has no significant effect of the neutron multiplication factor.

Although loose rods are in reality unconstrained by spacers or other fixtures when loaded into the product containers for storage or shipment, they have been conservatively modeled in fixed lattices with constant spacings between individual rods for optimum moderation.

6.3.1.1 Protective Case

Square lattices have been considered with the intent of identifying the most reactive arrangement and determining the maximum allowable number of loose rods inside the product protective case that can be transported within the RAJ-II package. Figure 6-4 shows the SCALE model of the protective case. This approach to modeling the fuel rods is conservative, since it permits the rods to be spaced in optimally moderated configurations within the cylindrical pipe and eliminates any restriction on the number of rods that can be transported in a rod container. Actual shipments will utilize the full rod container capacity such that the rods will be nearly close-packed in the rod container; however, there a partially loaded rod container is credible.

The protective case is a SS body holding the fuel rods, surrounded by a poly urethane cushioning material. The length of the body has exterior dimensions of 9.7 cm wide by 84 cm tall by 417.6 cm long, composed of 0.4 cm thick SS. The top lid is installed on top of the body and run the length

of the case, composed of 0.5 cm thick SS, resulting in an overall case height of 93 cm. The end plates are 0.5 cm thick SS, and result in a modeled case length of 418.6 cm. Assembly pieces such as the lumber shock absorbers, exterior cushioning materials, and structural steel components are conservatively neglected.

6.3.1.2 Rod Pipe

Triangular lattices have been considered with the intent of identifying the most reactive arrangement and determining the maximum allowable number of loose rods that can be transported within the RAJ-II package inside the product container of a 5 in. rod pipe. Figure 6-5 shows the SCALE model of the rod pipe. This approach to modeling the fuel rods is conservative, since it permits the rods to be spaced in optimally moderated configurations within the cylindrical pipe and eliminates any restriction on the number of rods that can be transported in a rod container. Actual shipments will utilize the full rod container capacity such that the rods will be nearly close-packed in the rod container; however, there a partially loaded rod container is credible.

The 5 inch schedule 40 pipe container, composed of 304 SS, has an outer diameter of 5.563 in. (14.13 cm) with a 0.258 in. (0.65532 cm) thickness. The pipe has a length 424.18 cm plus the end caps, which are 0.5 in. (1.27 cm) thick and modeled with the same exterior dimensions of the pipe body.

6.3.1.3 WEC Rod Box

Square lattices have been considered with the intent of identifying the most reactive arrangement and determining the maximum allowable number of loose rods inside the product WEC container that can be transported within the RAJ-II package. Figure 6-6 show the SCALE model of the WEC rod box. This approach to modeling the fuel rods is conservative, since it permits the rods to be spaced in optimally moderated configurations within the cylindrical pipe and eliminates any restriction on the number of rods that can be transported in a rod container. Actual shipments will utilize the full rod container capacity such that the rods will be nearly close-packed in the rod container; however, there a partially loaded rod container is credible.

The WEC rod box is a rectangular box, composed of an external shell and internal steel bars limiting the contents spacing. Although not modeled, the shell has large punched holes to avoid water moderation buildup within the container. Since the shell is modeled solid, the internal spacing is fully moderated for hypothetical accident transport conditions.

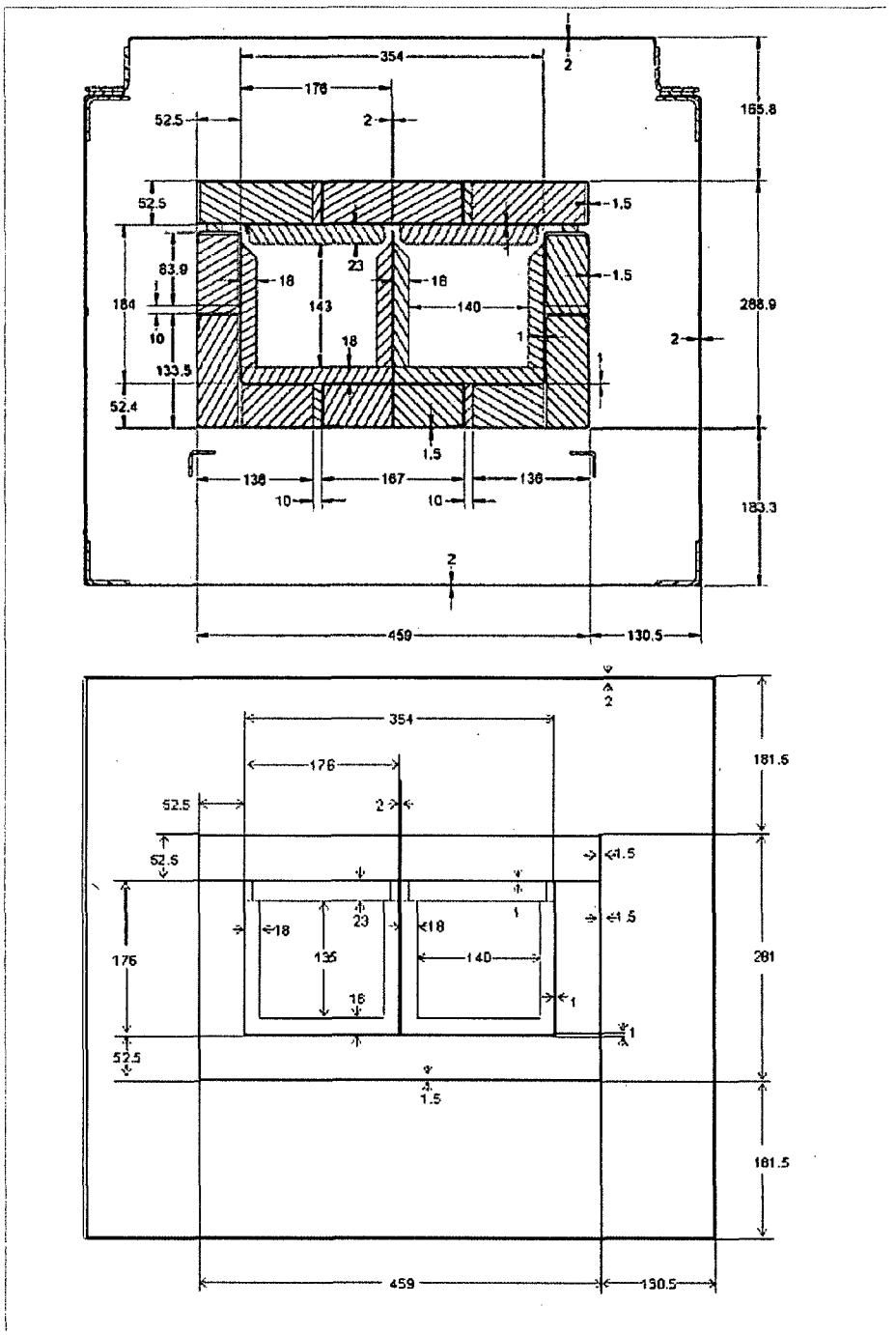

Figure 6-1 End View Cross Section Comparison of Actual Packaging (Top) and Model Geometry (Bottom), (Units in mm)

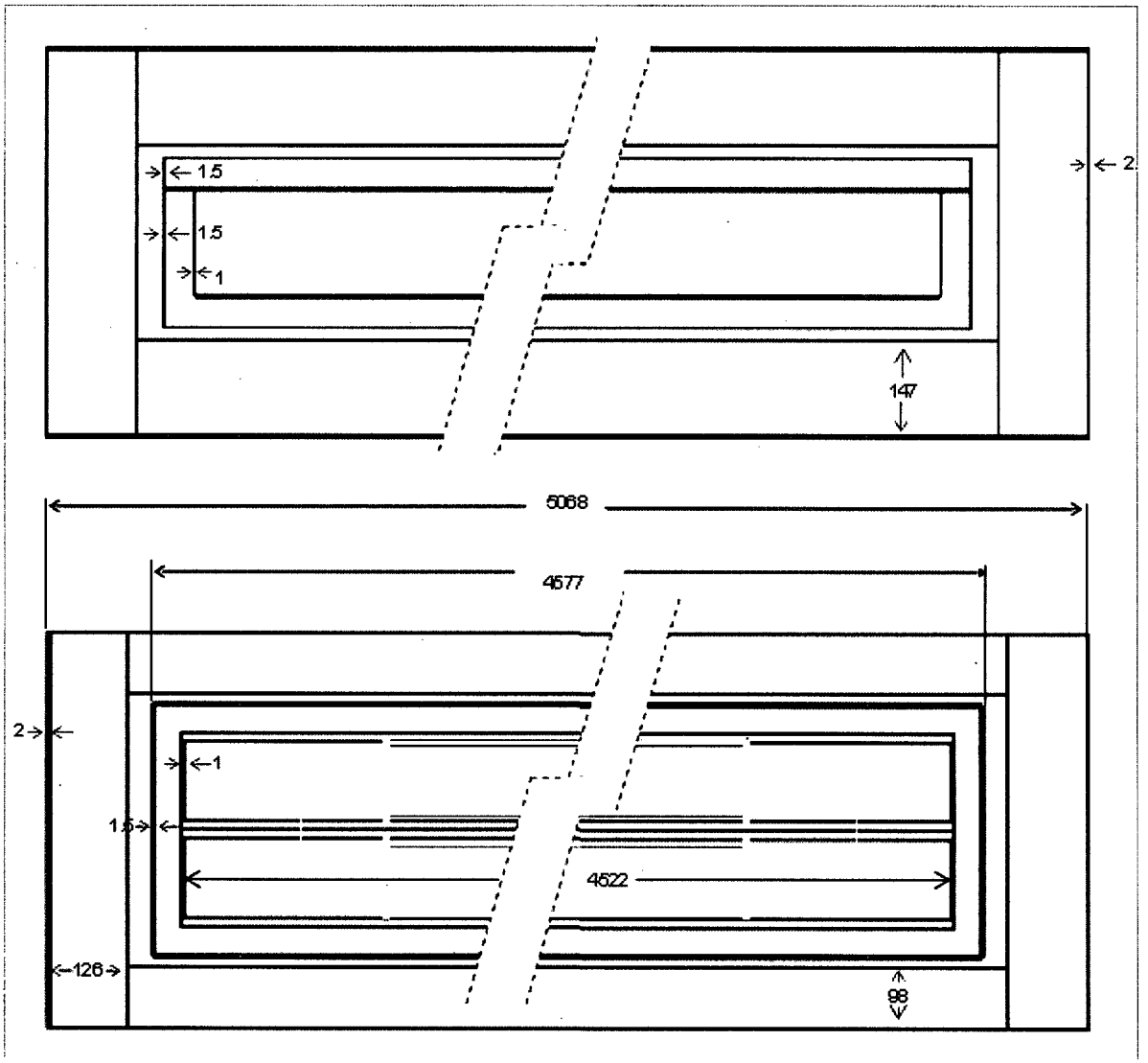

Figure 6-2 Side View (Top) and Top View (Bottom) Cross Section of Model Geometry, (Units in mm)

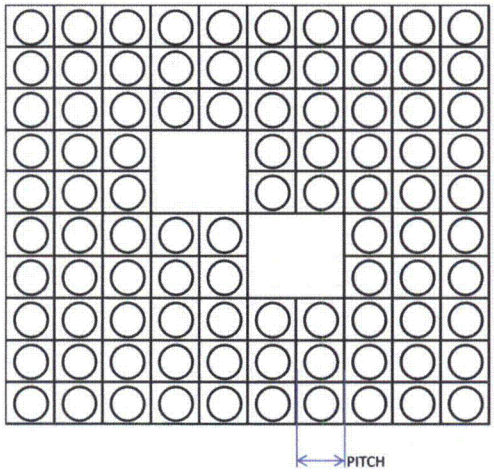

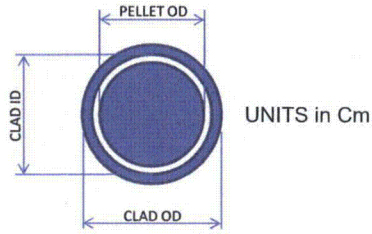

FUEL TYPE	PELLET OD	CLAD ID	CLAD OD	PITCH
GE11 GE13	0.9560	0.975	1.118	1.438
GE12B GE14C GE14G	0.876	0.894	1.026	1.295
GNF2 GNF4	0.888	0.906	1.026	1.295

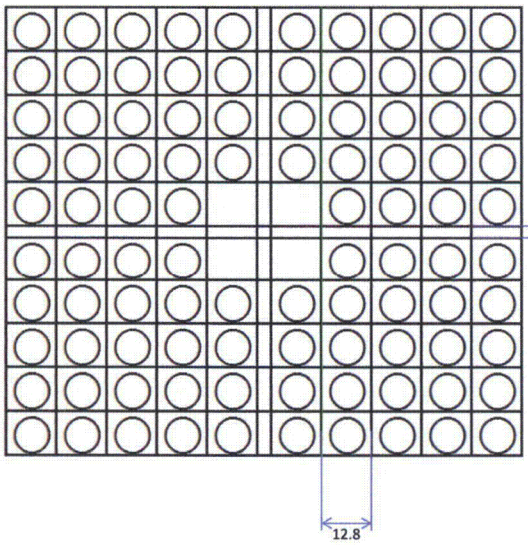

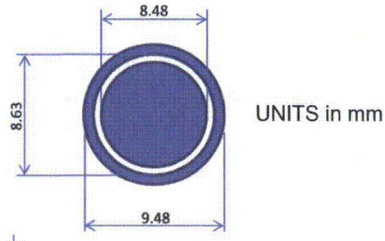

Figure 6-3 Fuel Bundle Model – GE12B (Top) and Westinghouse SVEA (Bottom)

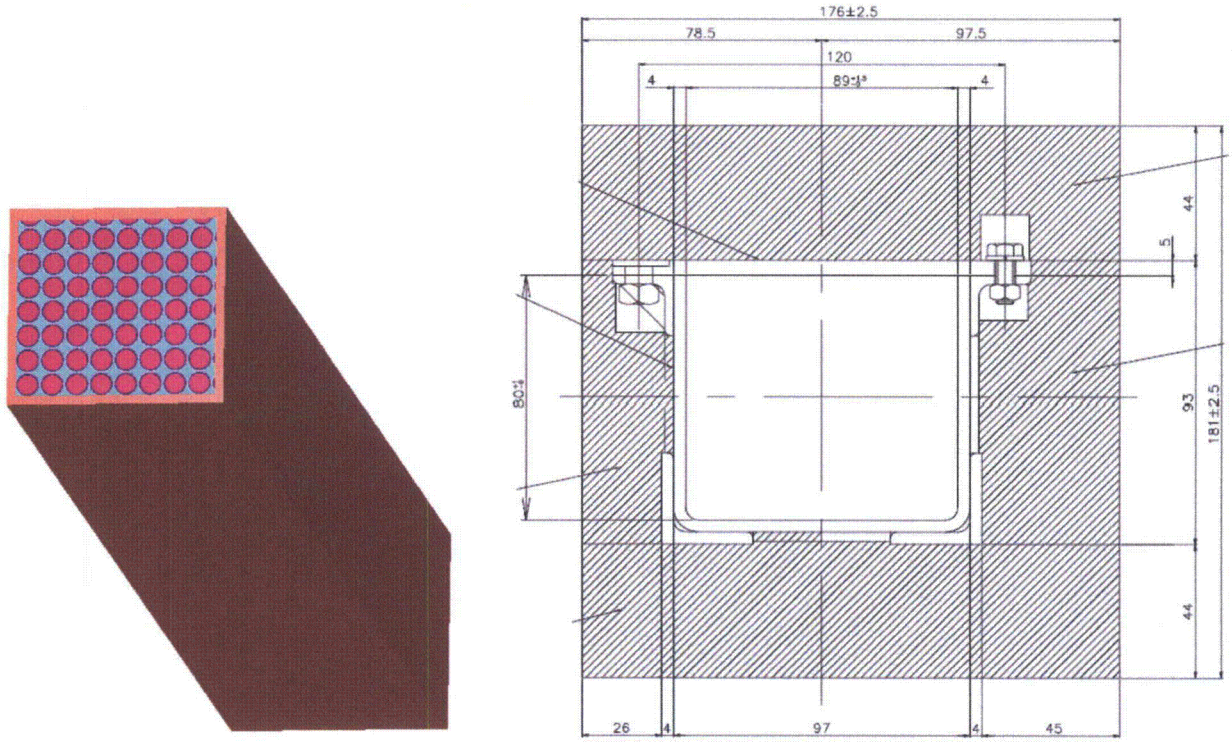

Figure 6-4 Protective Case: SCALE Model slice (left), Licensing Drawing (right)

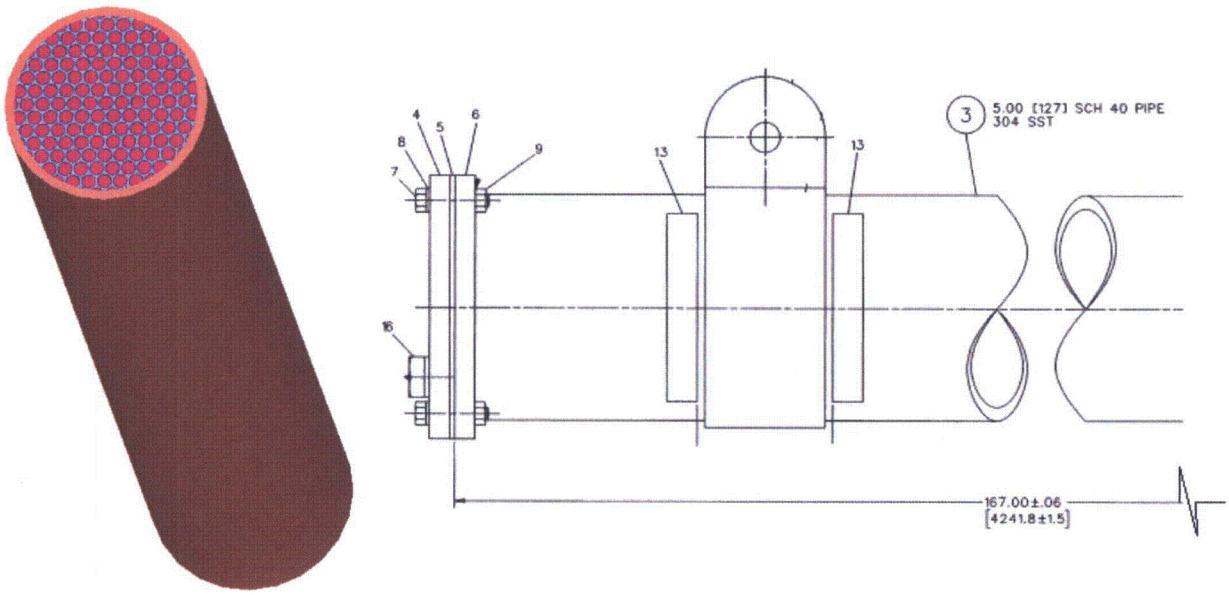

Figure 6-5 Rod Pipe: SCALE Model slice (left), Licensing Drawing (right)

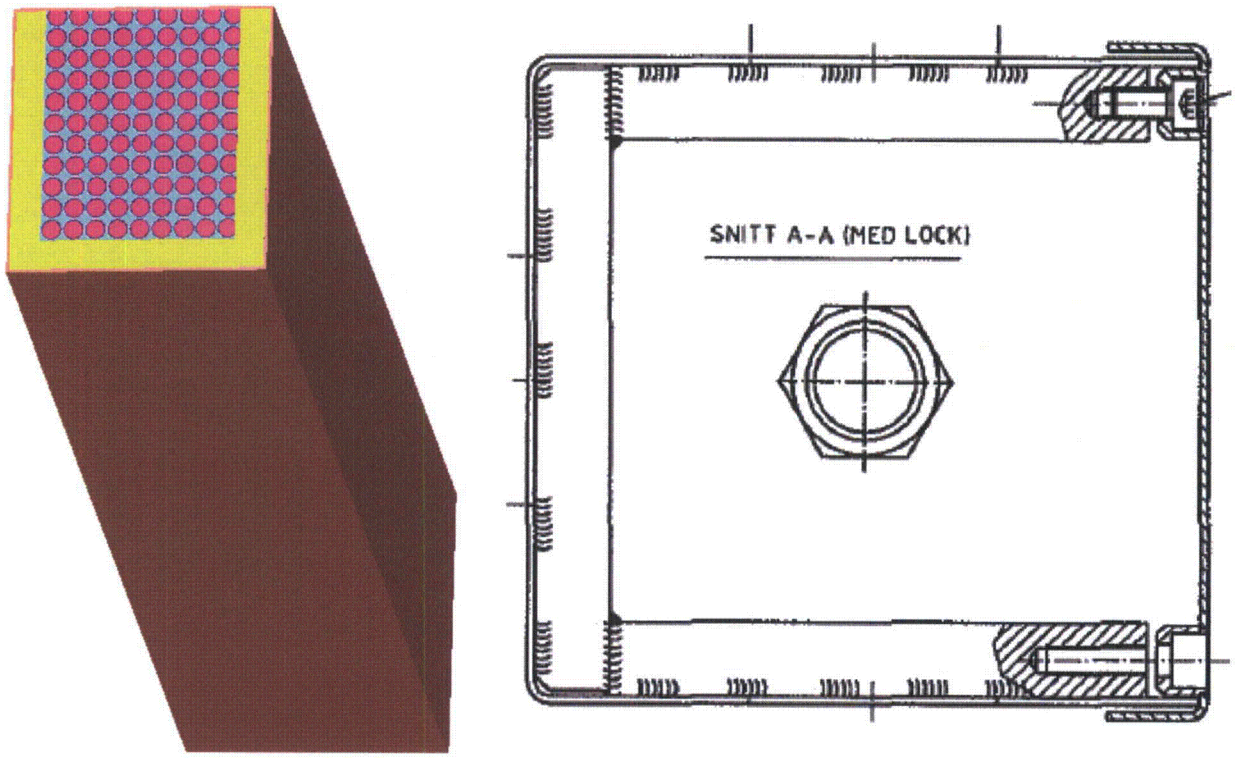

Figure 6-6 WEC Rod Box: SCALE Model slice (left), Licensing Drawing (right)

6.3.2 Material Properties

6.3.2.1 UO_2

A mixture defining UO_2 has a density of 10.96 g/cm^3 that is the theoretical density for the compound. Actual density of UO_2 fuel pellets is between 95% and 97% of theoretical density to provide porosity for fuel performance in the reactor. The uranium is 5 wt% ^{235}U and 95 wt% ^{238}U. Reprocessed enriched uranium specification [2] allows 5.0E-06 wt% ^{232}U, 0.2 wt% ^{234}U, and 0.25 wt% ^{236}U. Any ^{232}U, ^{234}U, or ^{236}U is assumed to be ^{238}U since these uranium isotopes are not fissile, present in small amounts and have total neutron cross sections that tend to be greater than the total neutron cross section for ^{238}U (Figure 6-7). The maximum actual nominal enrichment is 4.95 wt% ^{235}U. The density is incorporated into the density multiplier, VF, rather than using the DEN=keyword. The generic input specification for this standard composition is

SC MX VF TEMP (IZAi WTPi) END

where

SC is the standard composition component name (UO2).

MX is the mixture number (1).

VF is the density multiplier (the density multiplier is the ratio of actual to theoretical density (10.96/10.96 = 1).

TEMP is the temperature in Kelvin (300).

IZA is the isotope ID number (92235 for ^{235}U and 92238 for ^{238}U).

WTP is the weight percent of the isotope in the material (5 for ^{235}U and 95 for ^{238}U).

The input data for the UO_2 are given below.

```
UO2     1 1 300  92235 5  92238 95  end
```

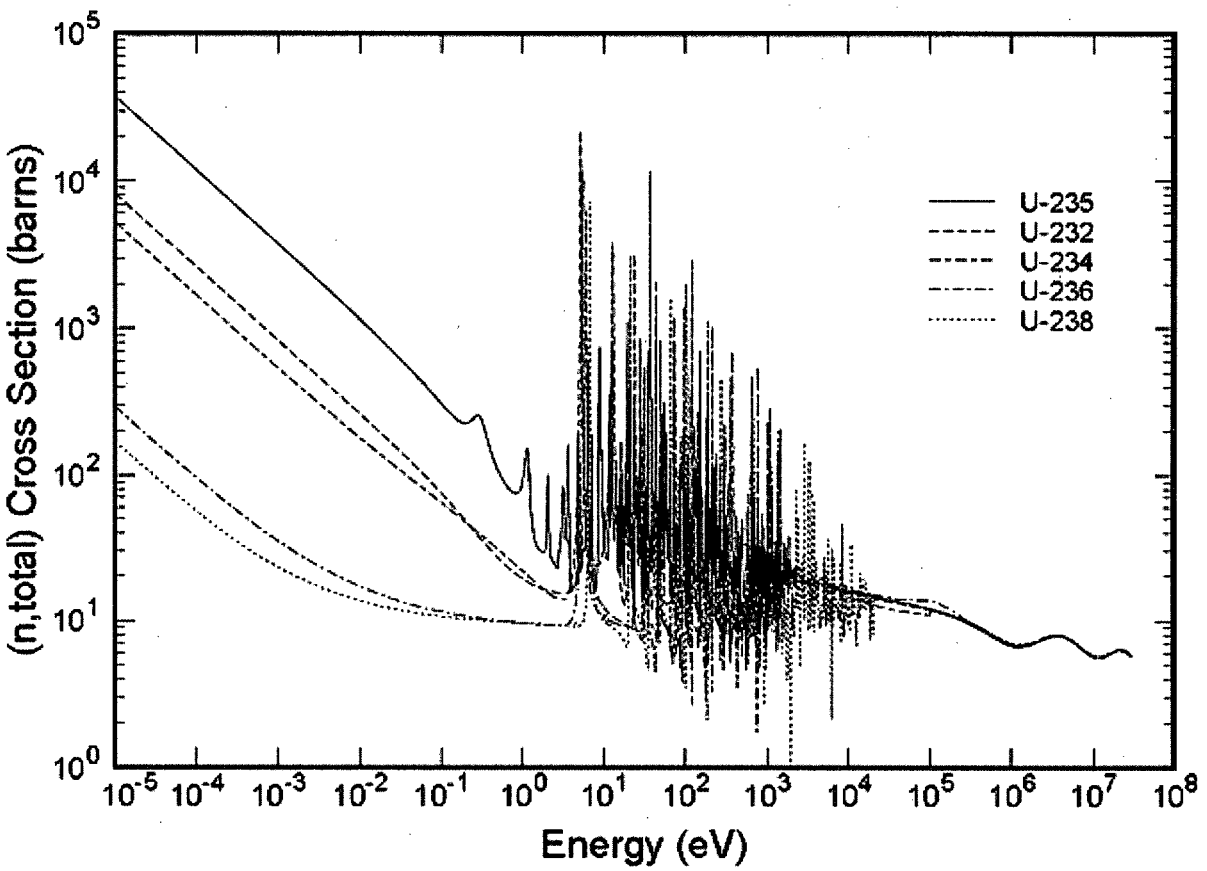

Figure 6-7 Uranium (n, total) Cross Section

6.3.2.2 UO_2 - Gd_2O_3

The design objective for gadolinia oxide is to suppress reactivity during the beginning of a reactor cycle. A uniform distribution of burnable absorber (BA) contents allow for depletion from the outer surface of the pellet inward as the exposure increases. The number density for the elements in Gd_2O_3 is calculated using 75 percent of Gd for a nominal 2.0 wt% Gd_2O_3 content and an actual BA pellet density of 10.53 ± 0.015 g/cm^3. The theoretical density is used for the UO_2 in the urania-gadolinia mixture.

$$10.53\ g/cm^3 \times 0.02 = 0.1827\ g/cm^3\ Gd_2O_3$$
$$\mathrm{M(Gd2O3)} = 362.504$$
$$\mathrm{A(Gd-NAT)} = 157.256$$
$$2\ \mathrm{Gd/mole\ Gd2O3} \times \frac{157.256\ \mathrm{g/mole\ Gd-NAT}}{362.504\ \mathrm{g/mole\ Gd2O3}} \times 0.1827\ g/cm^3\ Gd_2O_3 \times 0.75 = 0.1370\ g/cm^3\ Gd$$
$$0.2106\ g/cm^3\ Gd_2O_3 - 0.1370\ g/cm^3\ Gd = 0.0736\ g/cm^3\ O$$

$$N = \frac{\rho \cdot N_A}{M}$$
$$N_{Gd} = \frac{0.1370\ g/cm^3\ Gd \cdot 0.6022 \times 10^{24}\ atoms/mole \cdot 10^{-24}\ cm^3/b}{157.256\ g/mole} = 5.2463 \times 10^{-4}\ atoms/b \cdot cm$$
$$N_O = \frac{0.0736\ g/cm^3\ O \cdot 0.6022 \times 10^{24}\ atoms/mole \cdot 10^{-24}\ cm^3/b}{16.000\ g/mole} = 2.7701 \times 10^{-3}\ atoms/b \cdot cm$$

The generic standard composition specification is

SC MX VF ADEN END

where

SC is the standard composition component name (GD and O).

MX is the mixture number (6).

VF is the density multiplier (enter 0 because the number density is to be used).

ADEN is the number density of the standard composition (GD 5.2463E-04, O 2.7701E-03).

The input data for the Gd_2O_3 are given below:

```
GD    6 0 5.2463E-04 end
O     6 0 2.7701E-03 end
```

The input data for UO_2 component of the mixture is the same as for the UO_2 and is given below:

```
UO2    6 1 300  92235 5  92238 95  end
```

6.3.2.3 Zircaloy-2

Zircaloy is the material of the fuel rod cladding represented by Zr-2 for BWR rods and Zr-4 for PWR rods.

Zircaloy-2

Standard composition of ZIRC2 is used to represent the Zircaloy-2 for the fuel rod cladding material. The standard density is 6.56 g/cm^3 and composition is as follows:

98.250 wt% zirconium
1.45 wt% tin
0.100 wt% chromium
0.135 wt% iron
0.055 wt% nickel
0.01 wt% hafnium

Zircaloy-4

Standard composition of ZIRC4 is used to represent the Zircaloy-4 for the fuel rod cladding material. The standard density is 6.56 g/cm^3 and composition is as follows:

98.23 wt% zirconium
1.45 wt% tin
0.100 wt% chromium
0.210 wt% iron
0.01 wt% hafnium

6.3.2.4 Stainless Steel-304

Several specifications of stainless steel as apply to Grade 304/304L are provided in Section 1.0, Appendix 1.3.4. The stainless steel 304 (SS304) composition from the SCALE standard composition library is used to represent all specifications for stainless steel. The standard density is 7.94 g/cm^3 and composition is as follows:

68.375 wt % iron
19 wt % chromium
9.5 wt % nickel
2 wt % manganese
1 wt % silicon
0.08 wt % carbon
0.045 wt % phosphorus

6.3.2.5 Polyethylene

Standard material POLY(H2O) is used to represent all polyethylene packaging materials in normal and accident transport conditions (plastic sheathing, foam cushions, and melted foam). The POLY(H2O) is polyethylene CH_2, 0.92 g/cc that uses hydrogen in the water with a S(α,β) thermal kernel.

The modeled densities of the polyethylene materials are as follows:

Cluster separator fingers (LDPE)	0.925 g/cm^3
Cluster separator holders (HDPE)	0.959 g/cm^3
Protective sheath	0.919 g/cm^3
Foam cushion	0.080 g/cm^3

The polyethylene material is represented as a mixture of the actual densities as follows,

$$\frac{1}{\rho_T} = \sum_i \frac{\omega_i}{\rho_i}$$

where,

ω_I is the weight fraction of material *I*,

ρ_I is the density of the mixture, and

ρ_T is the density of the mixture.

Instead of representing the actual material distribution within the contents, an equivalent mass of material is distributed uniformly around each of the fuel rods. For the normal transport condition a volume weighted mixture density of the polyethylene is specified, where as the standard material density is used for an accident transport condition where melting of the polyethylene is credible.

6.3.2.5.1 Cluster Separator and Protective Sheath

Polyethylene inserts or polyethylene cluster separators are positioned between fuel rods at various locations along the axis of the fuel assembly to avoid stressing the axial grids during transportation. The separators are shown in Figure 6-8. The cluster separator is composed of LDPE (0.925 g/cm^3) fingers and a High Density Polyethylene (HDPE, 0.959 g/cm^3) holder. For a 10x10 assembly piece, the LDPE fingers occupy an approximate volume of 38 cm^3 while the HDPE holder has an approximate volume of 85 cm^3. A weight average density of 0.949 g/cm^3 is calculated for the polyethylene cluster assembly is calculated as follows:

$$\omega_{LDPE} = \frac{V_{LPDE}\rho_{LPDE}}{V_{LPDE}\rho_{LPDE} + V_{HPDE}\rho_{HPDE}} = \frac{38\,cm^3 \times 0.925\,g/cm^3}{38\,cm^3 \times 0.925\,g/cm^3 + 85\,cm^3 \times 0.959\,g/cm^3} = 0.30$$

$$\omega_{HDPE} = 1 - \omega_{LDPE} = 1 - 0.30 = 0.70$$

$$\frac{1}{\rho_T} = \frac{\omega_{LDPE}}{\rho_{LDPE}} + \frac{\omega_{HDPE}}{\rho_{HDPE}} = \frac{0.30}{0.925} + \frac{0.70}{0.959} = 1.054$$

$$\rho_T = 0.949\,g/cm^3$$

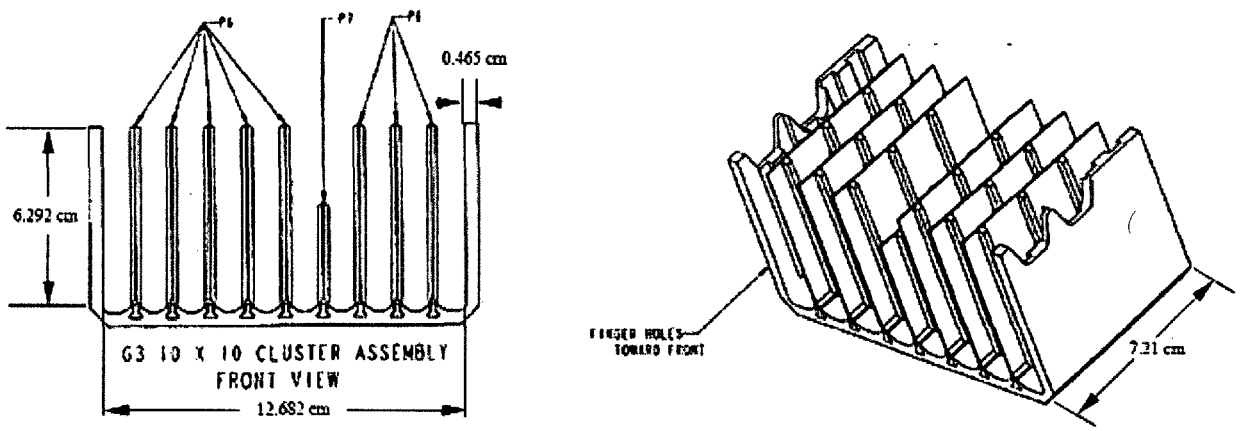

Figure 6-8 Polyethylene Cluster Separator

The fuel bundle or fuel assembly is wrapped in a polyethylene protective sheath (0.919 g/ cm^3). Including the protective sheath further reduces the density of the polyethylene mixture used to represent the polyethylene packaging material that is part of the contents during normal transport conditions. The volume of sheath varies with the fuel design, but is in the range of 600 to 700 cm^3. Where as the volume of the cluster separators is approximately 8000 cm^3, the effect of the protective sheath on the polyethylene mixture density is small. For example:

$$\omega_{CLUSTER\,SEP} = \frac{V_{CLUSTER\,SEP}\,\rho_{CLUSTER\,SEP}}{V_{CLUSTER\,SEP}\,\rho_{CLUSTER\,SEP} + V_{SHEATH}\,\rho_{SHEATH}} =$$

$$\frac{8000\,cm^3 \times 0.949\,g/cm^3}{8000\,cm^3 \times 0.949\,g/cm^3 + 700\,cm^3 \times 0.919\,g/cm^3} = 0.92$$

$$\omega_{SHEATH} = 1 - \omega_{CLUSTER\,SEP} = 1 - 0.93 = 0.08$$

$$\frac{1}{\rho_T} = \frac{\omega_{CLUSTER\,SEP}}{\rho_{CLUSTER\,SEP}} + \frac{\omega_{SHEATH}}{\rho_{SHEATH}} = \frac{0.92}{0.949} + \frac{0.08}{0.919} = 1.056$$

$$\rho_T = 0.947\,g/cm^3$$

6.3.2.5.2 Foam Cushion

The range of nominal, densities includes Ethafoam 400 (0.058 g/cc), Ethafoam HS-45 (0.062 g/cc), and Suntec <15> (0.068 g/cc). A maximum density of 0.080 g/cc is used to evaluate moderating effect of packaging materials. Specifications for the foam material are provided in Appendix 1.3.4.

6.3.2.6 Alumina Silicate

Fiberfrax® Duraboard® products are a family of rigid, high temperature ceramic fiber boards manufactured in a wet forming process using Fiberfrax alumina-silica fibers and binders. Board type LD is a higher quality surface finish and tighter dimensional tolerances make this board suitable for use in situations where aesthetic quality, as well as performance, is important with a nominal density of 258 kg/m^3 (16 lb/ft^3) consisting of 100% Fiberfrax, which is Unifrax's patented 2300°F/1260°C amorphous alumina-silica fiber. Specifications for Fiberfrax® Durabond® are provided in Appendix 1.3.4.

The arbitrary chemical compound specification is used to create a mixture that is a alumina silicate, Al_2O_3-SiO_2 where density and chemical equation are known.

ATOM MX ROTH NEL (NCZA$_i$ ATPM$_i$) VF TEMP END

where

ATOM is the standard composition component name (ATOMAL2O3SIO2).

MX is the mixture number (26).

ROTH is the theoretical density of the compound in g/cm^3 (3.247).

NCZA is the element ID number. (13000 for aluminum, 8016 for oxygen, and 14000 for silicon)

ATPM is the number of atoms of this element per molecule of user-defined compound. (2 for aluminum, 5 for oxygen, and 1 for silicon)

VF is the fraction of this user-defined compound in the mixture (0.077). (The actual density is RHO=ROTH × VF, RHO=3.247 × 0.077=0.250)

TEMP is the temperature in Kelvin (300).

The input data for Alumina Silicate are given below:

atomal2o3sio2 26 3.247 3 13000 2 8016 5 14000 1 0.077 300 end

6.3.2.7 Paper Honeycomb

Standard composition BALSA is used to represent the paper honeycomb for the shock absorber on the sides, bottom and top of the outer container. A density 0.08 g/cm^3 is specified for the material $C_6H_{10}O_5$.

6.3.2.8 Balsa Wood

Standard composition BALSA is used to represent the balsa wood for the shock absorber material on the ends of the outer container. The standard density is 0.125 g/cm^3 and composition is $C_6H_{10}O_5$.

6.3.2.9 Char

Char is material resulting from thermal decomposition of paper honeycomb or balsa wood. Char is produced in the absence of oxygen by the slow pyrolysis of organic material. Charring is a chemical process of incomplete combustion a solid when subjected to high heat. The resulting residue matter is called char. By the action of heat, charring removes hydrogen and oxygen from the solid, so that the remaining char is composed primarily of carbon. The resulting char is 85% to 90% carbon with the remainder consisting of volatile chemicals and ash. Char composition from the incomplete combustion of paper honeycomb or balsa wood is assumed to be 100% of the carbon content in the nominal material composition. Atomic density is assumed to be the number density of carbon in the paper honeycomb or balsa wood. Theoretical density of char is assumed to be 2.1 g/cc.

6.3.2.10 Full Density Water

Standard composition H2O is used to represent the water moderator and reflector. The standard density is 0.9982 g/cm^3 and uses hydrogen in the water S(α,B) thermal kernel.

Table 6-8 Summary of Material Compositions

Material	Density (g/cm^3)	Constituent	Atomic Density (atoms/b-cm)
UO_2	10.96	U-235	1.23762E-03
5 wt% uranium 235		U-238	2.32178E-02
		O-16	4.89109E-02
UO_2-Gd_2O_3	11.17	U-235	1.23762E-03
	(Note: Density is	U-238	2.32178E-02
5 wt% uranium 235	greater than UO2	O-16	5.16810E-02
1.5 wt% Gd_2O_3	due to assumption	Gd-152	1.04926E-06
	that Gd_2O_3 in the	Gd-154	1.14369E-05
	mixture does not	Gd-155	7.76452E-05
	reduce UO2	Gd-156	1.07392E-04
	density)	Gd-157	8.21046E-05
		Gd-158	1.30318E-04
		Gd-160	1.14684E-04
Zircaloy-2	6.56	Zr-90	2.18914E-02
		Zr-91	4.77399E-03
98.250 wt% zirconium		Zr-92	7.29714E-03
1.45 wt% tin		Zr-94	7.39501E-03
0.135 wt% iron		Zr-96	1.19137E-03
0.100 wt% chromium		Sn-112	4.68066E-06
0.055 wt% nickel		Sn-114	3.13652E-06
0.01 wt% hafnium		Sn-115	1.73715E-06
		Sn-116	7.01133E-05
		Sn-117	3.70592E-05
		Sn-118	1.16872E-04
		Sn-119	4.14021E-05
		Sn-120	1.57260E-04
		Sn-122	2.23417E-05
		Sn-124	2.79392E-05
		Fe-54	5.63467E-06
		Fe-56	8.75953E-05
		Fe-57	2.00556E-06
		Fe-58	2.67408E-07
		Cr-50	3.30123E-06
		Cr-52	6.36617E-05
		Cr-53	7.21788E-06
		Cr-54	1.79687E-06
		Ni-58	2.52754E-05
		Ni-60	9.66291E-06
		Ni-61	4.18356E-07
		Ni-62	1.32911E-06
		Ni-64	3.36906E-07

Table 6-8 Summary of Material Compositions (Continued)

Zircaloy-2 (continued)		Hf-174	3.58562E-09
		Hf-176	1.15227E-07
		Hf-177	4.11815E-07
		Hf-178	6.04177E-07
		Hf-179	3.01657E-07
		Hf-180	7.76885E-07
Zircaloy-4	6.56	Zr-90	2.18870E-02
		Zr-91	4.77302E-03
98.230 wt% zirconium		Zr-92	7.29566E-03
1.45 wt% tin		Zr-94	7.39350E-03
0.210 wt% iron		Zr-96	1.19113E-03
0.100 wt% chromium		Sn-112	4.68066E-06
0.01 wt% hafnium		Sn-114	3.13652E-06
		Sn-115	1.73715E-06
		Sn-116	7.01133E-05
		Sn-117	3.70592E-05
		Sn-118	1.16872E-04
		Sn-119	4.14021E-05
		Sn-120	1.57260E-04
		Sn-122	2.23417E-05
		Sn-124	2.79392E-05
		Fe-54	8.76505E-06
		Fe-56	1.36259E-04
		Fe-57	3.11976E-06
		Fe-58	4.15968E-07
		Cr-50	3.30123E-06
		Cr-52	6.36617E-05
		Cr-53	7.21788E-06
		Cr-54	1.79687E-06
		Hf-174	3.58562E-09
		Hf-176	1.15227E-07
		Hf-177	4.11815E-07
		Hf-178	6.04177E-07
		Hf-179	3.01657E-07
		Hf-180	7.76885E-07
Stainless steel-304	7.94	Fe-54	3.45421E-03
		Fe-56	5.36984E-02
68.375 wt% iron		Fe-57	1.22947E-03
19 wt% chromium		Fe-58	1.63929E-04
9.5 wt% nickel		Cr-50	7.59182E-04
2 wt% manganese		Cr-52	1.46402E-02
1 wt% silicon		Cr-53	1.65989E-03
0.08 wt% carbon		Cr-54	4.13226E-04
0.045 wt% phosphorus		Ni-58	5.28415E-03
		Ni-60	2.02016E-03

Table 6-8 Summary of Material Compositions (Continued)

Stainless steel-304 (continued)		Ni-61	8.74628E-05
		Ni-62	2.77869E-04
		Ni-64	7.04346E-05
		Mn-55	1.74072E-03
		Si-28	1.57022E-03
		Si-29	7.95072E-05
		Si-30	5.27778E-05
		P-31	6.94681E-05
		C-12	3.18477E-04
Polyethylene (Sheeting, Melted Foam)	0.92	H-1	7.89975E-02
		C-12	3.94988E-02
Polyethylene (Foam)	0.08	C-12	1.51126E-03
		H-1	3.02251E-03
Alumina Silicate Al_2O_3-SiO_2	0.25	Al-27	1.85853E-03
		Si-28	8.57060E-04
		Si-29	4.33966E-05
		Si-30	2.88072E-05
		O-16	4.64632E-03
Paper Honeycomb $C_6H_{10}O_5$	0.08	C-12	1.78300E-03
		H-1	2.97167E-03
		O-16	1.48583E-03
Char (Paper Honeycomb)	0.036	C-12	1.78300E-03
Balsa Wood $C_6H_{10}O_5$	0.125	C-12	2.78594E-03
		H-1	4.64323E-03
		O-16	2.32161E-03
Char (Balsa wood)	0.056	C-12	2.78594E-03
Full Density Water H2O	0.9982	H-1	6.67515E-02
		O-16	3.33757E-02

6.3.3 Computer Codes and Cross-Section Libraries

6.3.3.1 Computer Codes

SCALE Version 6 is used to perform the criticality evaluation [3]. Standardized automated procedures process cross sections to provide resonance-corrected library based on the physical characteristics of the RAJ-II package. CSAS6 (Criticality Safety Analysis Sequence with KENO-VI) and TSUNAMI (Tools for Sensitivity and Uncertainty Analysis Methodology Implementation) are used in the evaluation.

6.3.3.1.1 CSAS6 (Criticality Safety Analysis Sequence with KENO-VI)

CSAS6 calls BONAMI, to perform the unresolved resonance processing, CENTRM/PMC/ WORKER, to perform the resolved resonance processing for ENDF/B-VII cross-section library, and finally KENO-VI. CENTRM/PMC is used instead of NITAWL to address a limitation in NITAWL for the resonance processing for gadolinium in the urania-gadolinia oxide fuel rods. A major limitation of the analytical model used by the Nordheim integral treatment in NITAWL is a lattice system whose fuel or moderator contains an absorber that has rapidly varying cross sections across the resonance region that may be inadequately treated. The codes utilized in CSAS6 start with an AMPX master format cross-section library and generated a self-shielded, group-averaged library applicable to the RAJ-II package. These cross sections are then used KENO-VI Monte Carlo code to determine the neutron multiplication factor (k_{eff}). KENO-VI provides a geometry package known as SCALE Generalized Geometry Package (SGGP). This feature simplifies data input for the complex geometry of the RAJ-II package and benchmark experiments.

CSAS6

The CSAS6 sequence calculates the system k_{eff} for 3-D problems. This sequence uses the functional module BONAMI to process the required cross sections in the unresolved resonance region. By default for ENDF/B-V and ENDF/B-VII master libraries the functional modules WORKER, CENTRM, and PMC are used to process the required cross sections in the resolved resonance range.

Table 6-9 CSAS6 Parameter Values

Parameter	Value for TSUNAMI-3D	Value for KENO in CSAS Sequences or as Stand-alone Code	Description
CFX	YES	NO	collect fluxes
GEN	550	550	number of generations to be run
NSK	50	3	number of generations to be omitted when collecting results
PNM	3	0	highest order of flux moments tallies
TFM	YES	NO	perform coordinate transform for flux moment and angular flux calculations

6.3.3.1.2 TSUNAMI (Tools for Sensitivity and Uncertainty Analysis Methodology Implementation)

TSUNAMI-3D provides automated, problem-dependent cross sections using the same methods and input as the Criticality Safety Analysis Sequences (CSAS). TSUNAMI-3D sequence calls the cross-section processing codes BONAMIST and CENTRM/PMC/WORKER and accesses the SENLIB routines. After the cross sections are processed, the TSUNAMI-3D-K6 sequence performs two KENO-VI criticality calculations, one forward and one adjoint. Finally, the sequence

calls the SAMS module to calculate the sensitivity coefficients that indicate the sensitivity of the calculated value of k_{eff} to changes in the cross sections and the uncertainty in the calculated value of k_{eff} due to uncertainties in the basic nuclear data. SAMS prints energy-integrated sensitivity coefficients and their statistical uncertainties to the SCALE output file and generates a separate data file containing the energy-dependent sensitivity coefficients. TSUNAMI-3D-K6 is used to generate sensitivity data to study the relative worth of urania-gadolinia rods in the fuel assembly lattice and evaluate the applicability of benchmark experiments.

TSUNAMI-3D-K6

This sequence is used for sensitivity and uncertainty calculations with KENO-VI. By default, resonance self-shielding calculations are performed with BONAMIST and CENTRM/PMC/ WORKER with input to these codes generated with routines from SENLIB. The TSUNAMI-3D-K6 sequence can also be abbreviated as or TS3DK6.

Table 6-10 TSUNAMI Parameter Values

Parameter	Value for TSUNAMI-3D	Corresponding KENO Parameter	Description
ABK	APG × 2	NBK	number of positions in the neutron bank for the adjoint calculation
AGN	GEN=NSK +ASK	GEN	number of generations to be run for the adjoint calculation-default value produces the same number of active generations as the forward calculation
APG	NPG × 3	NPG	number of particles per generation
ASG	SIG (default SIG=0)	SIG	if > 0.0, this is the standard deviation at which the adjoint problem will terminate
ASK	NSK × 3	NSK	Number of generations to be omitted when collecting results for the adjoint calculation

Sensitivity data generated by TSUNAMI-3D is used to evaluate the relative importance of materials in the package. The sensitivity coefficient for the material is the percentage change in k_{eff} for a 1% increase in the total cross section of all nuclides applied to all energy groups and regions for the mixture.

TSUNAMI-IP (**T**ools for **S**ensitivity and **U**ncertainty **A**nalysis **M**ethodology **I**mplementation – **I**ndices and **P**arameters) uses sensitivity data generated by TSUNAMI-3D and cross section-covariance data to generate several relational parameters and indices that can be used to determine the degree of similarity between benchmark experiments and RAJ-II package evaluations.

6.3.3.2 Cross-Section Libraries

A 238-group ENDF/B-VII Release 0 library is used for general-purpose criticality analyses. The 238-group and continuous-energy ENDF/B-VII.0 libraries have 417 nuclides that include 19 thermal-scattering moderators. The ENDF/B-VII.0 library cannot be used with the NITAWL module for resonance self-shielding calculations in the resolved range. The CENTRM/PMC modules must be used for resonance self-shielding calculations in the resolved region with the ENDF/B-VII.0 library [4].

6.3.3.3 Uncertainty Evaluation for Material and Fabrication Tolerances

The effectiveness of a material at suppressing reactivity in the transport system is dominated by its absorption reaction rate. The absorption reaction rate of a material can be determined using the following equation:

$$R = \phi\Sigma = \phi N\sigma$$

Where:

R = absorption rate in absorptions/cm^3-s

ϕ = neutron flux in n/cm^2-s

Σ = macroscopic cross section in absorptions/cm^3

σ = absorption cross section in cm^2

N = Number Density in atoms/cm^3

This equation demonstrates that the reaction rate is proportional to both the absorption cross section and the number density of the material of interest. As this is the case, an equivalent change in either number density or absorption cross section will result in the same percentage change in reaction rate. In other words:

$$\Delta R = \phi\Delta N\sigma = \phi N\Delta\sigma$$

Number density can be determined with the following equation:

$$N = \frac{N_A}{M}\rho$$

Where:

N_A = Avogadro's Number

M = Atomic Mass

ρ = density (g/cm^3)

The number density changes proportionally with the material density, and therefore

$$\Delta N = \frac{N_A}{M}\Delta\rho$$

Replacing this in the reaction rate equation yields

$$\Delta R = \phi\frac{N_A}{M}\Delta\rho\sigma = \phi N\Delta\sigma$$

The equation above demonstrates that the reaction rate of a material, and therefore its relative effect on system reactivity, will change by the same amount given an identical percentage change in either material density or absorption cross section. TSUNAMI has been used to define the change in reactivity for a system on a 1% change in cross section basis for a given material. The change is defined as the sensitivity coefficient of the material, and is represented by the following equation.

$$\frac{\frac{\Delta keff}{keff}}{\frac{\Delta\Sigma}{\Sigma}}$$

Using the equations above, this can be related to changes in either cross section or material density as specified below:

$$\frac{\frac{\Delta keff}{keff}}{\frac{\Delta\Sigma}{\Sigma}} = \frac{\frac{\Delta keff}{keff}}{\frac{\frac{N_A}{M}\Delta\rho\sigma}{\Sigma}} = \frac{\frac{\Delta keff}{keff}}{\frac{\frac{N_A}{M}\rho\Delta\sigma}{\Sigma}}$$

For the tolerance values being studied in this system, the reactivity affect on the system must be determined based on a change in the total amount of the material of interest present. This can be accomplished in one of two ways:

- Study of an explicit change in material volume due to tolerance value
- Study of a change in material density proportional to the volume change assuming constant volume to match the volume based material change

As the geometric differences between the materials being studied are small compared to their total size in the system, it is reasonable to assume that a small change in material density will produce equivalent reactivity effects as a change in the material volume. In other words, a change in thickness of a material is effectively the same as a change in density for a fixed volume of the same material. This conservation of mass assumption can be written as:

$$\frac{\Delta V}{V} \equiv \frac{\Delta \rho}{\rho} \quad \text{for constant V}$$

Likewise, the sensitivity to total cross section is also equivalent to the sensitivity to material thickness provided the material is associated with a material region of approximately the same thickness. The effect of the uncertainty in material properties on k_{eff} can be estimated by multiplying the sensitivity coefficient for each material by a relative uncertainty in the material density or volume.

The uncertainty associated with each material region is calculated using the relative change in volume $\Delta V/V$ for the geometry of the region. The individual relative uncertainties are combined as a simple summation, not taking credit for the possibility of the uncertainties being independent of each other by using a statistical sum. Equations to relate changes in volume to applicable geometries and tolerances being studied are presented later in this section.

$$\left(\frac{\Delta keff}{keff}\right)_i = \left[\frac{\frac{\Delta keff}{keff}}{\frac{\Delta \Sigma}{\Sigma}}\right]_i \cdot \left(\frac{\Delta V}{V}\right)_i$$

The individual relative uncertainties are aggregated as a simple sum instead of combining using a statistical sum such as route mean square. This results in a conservative estimate of the uncertainty as the simple sum ignores the possibility that the material tolerances are independent of each other.

$$\left(\frac{\Delta keff}{keff}\right)_{TOTAL} = \sum_i \left(\frac{\Delta keff}{keff}\right)_i$$

The total absolute uncertainty associated with the material tolerance, Δk_u, is obtained by multiplying the relative uncertainty by $k_p = 1.0$ with the assumption that $\Delta k_{eff}/k_{eff}$ is independent of the absolute value of k_p that is calculated for the package system.

$$\Delta k_u = \left(\frac{\Delta keff}{keff}\right)_{TOTAL} \times \quad k_p$$

where

$k_p = 1.0$

Equations Relating Changes in Volume for Applicable Geometries to Material Tolerances

Slab Geometry

The relative change in volume for slab geometries, such are sheet or plate steel, is equivalent to the relative change in thickness of the material.

$$V = \ell \cdot A$$

where

$A = total\ area\ of\ the\ material$

$\ell = average\ thickness\ of\ the\ material$

$$dV = A\, d\ell$$

*where A is cons*tan*t*

$$\frac{dV}{V} = \frac{d\ell}{\ell}$$

Solid Cylinder Geometry

The relative change in volume for a solid cylindrical geometry, such as fuel pellets, is 2 times the relative change in radius.

$$V = \pi h r^2$$

where

$h = height\ of\ the\ material$

$r = average\ radius\ of\ the\ material$

$$dV = 2\pi\, h\, r\, dr$$

*where h is cons*tan*t*

$$\frac{dV}{V} = \frac{2\, r\, dr}{r^2}$$

$$dr = \omega r$$

where ω *is the tolerance for r*

$$\frac{dV}{V} = 2\,\omega$$

For example, a 0.2 percent tolerance on radius is a 0.4 percent change in volume.

Annular Cylinder Geometry

The relative change in volume for an annular cylindrical geometry, such as cladding, depends on whether the uncertainty is for the inner or outer radial dimension.

$$V = \pi \cdot H\,(r_o^2 - r_i^2)$$

where

$H = height\ of\ the\ material$

$r = average\ radius\ of\ the\ material$

$$dV = 2\pi \cdot H \cdot r_o dr_o$$

or

$$dV = -2\pi \cdot H \cdot r_i dr_i$$

$$\frac{dV}{V} = \frac{2 r_o dr_o}{(r_o^2 - r_i^2)}$$

$$dr = \omega\, r$$

$$\frac{dV}{V} = \frac{2\omega r_o^2}{(r_o^2 - r_i^2)}$$

The relative change in volume for a BWR 10X10 cladding with inside diameter of 9.8 mm and inside diameter of 8.6 mm with a 1% tolerance applied to either radius or thickness can result in approximately a 10% change in the volume.

Geometry Uncertainty with Associated Material Displacement

A change in cladding thickness or pellet thickness is associated with a change in the volume of water in the space between the fuel rods or within the diametric gap between the pellet and cladding. The increase in water moderation may result in either an increase or decrease in k_{eff} depending on whether the fuel rod contains a neutron absorber, such as a gadolinia oxide fuel rod. The uncertainty in the water volume is calculated as follows:

$$V_{\text{mod}} = h \cdot p^2 - V_{clad} - V_{pellet}$$

where

$p = fuel\ rod\ pitch$

$r = average\ radius\ of\ the\ pellet$

$r_o = average\ outer\ radius\ of\ the\ clad$

$r_i = average\ outer\ radius\ of\ the\ clad$

$$V_{clad} = \pi \cdot h \cdot (r_o^2 - r_i^2)$$

$$V_{pellet} = \pi \cdot h \cdot r^2$$

$$dV_{\text{mod}} = 2\pi \cdot h \cdot r_o dr_o + 2\pi \cdot h \cdot r\, dr$$

$$or$$

$$dV = 2\pi \cdot h \cdot r_i dr_i + 2\pi \cdot h \cdot r\, dr$$

$$\frac{dV_{\text{mod}}}{V_{\text{mod}}} = \frac{2\pi \cdot r_o dr_o + 2\pi \cdot r\, dr}{p^2 - \pi(r_o^2 - r_i^2) - \pi r^2}$$

$$dr = \omega r$$

$$\frac{dV}{V} = \frac{2\pi(\omega_o\, r_o^2 + \omega\, r^2)}{p^2 - \pi(r_o^2 - r_i^2) - \pi r^2}$$

For example, the relative change in volume for a BWR 10X10 with pitch of 12.8 mm, cladding with inside diameter of 9.8 mm and inside diameter of 8.6 mm with a 1% tolerance applied to either radius or thickness and a 8.5 mm pellet diameter with 0.2% tolerance could result as much as a 2% change in the moderator volume.

6.3.4 Demonstration of Maximum Reactivity

The configuration of the contents and packaging are considered to demonstrate the most reactive configuration for the package. Configurations of the contents that are consistent with each transportation case (single package, arrays of undamaged packages, and arrays of damaged packages) are evaluated. A most reactive configuration for the types of contents (fuel bundle, fuel assembly, fuel rods) is determined. The most reactive contents will be evaluated in the packaging to identify the optimum combination of internal moderation and interspersed moderation. This most reactive package configuration will be used to evaluate the individual package and package arrays.

6.3.4.1 Contents

The contents may be a fuel bundle, fuel assembly, or fuel rods. The most reactive configuration for each type of contents takes into consideration partial length fuel rods in fuel bundle and fuel assembly, neutron absorbing BA rods in the fuel bundle, rearrangement of the fuel bundle in the form of lattice expansion during accident transport conditions, and partial loadings of fuel rods. Fuel rearrangement is limited by the fuel bundle and fuel assembly structure, inner container body inner wall, or fuel rod container depending on the contents category Table 6-11 defines the confinement boundary for each of the contents categories.

Table 6-11 Confinement Boundary

Contents Category	Confinement Boundary
Fuel Assembly	Distance between two spacer grids and fuel channel
Fuel Bundle	Distance between two spacer grids and inner wall of inner container
Fuel Rods without Rod Container	Inner wall of inner container
Fuel Rods with Rod Container	Rod box, rod pipe or protective case

Three confinement boundaries are defined by the contents and packaging. First, the fuel bundle structure (tie plates, spacer grids) confines fuel rods to a nominal pitch during normal transport conditions. Second, rearrangement of the bundle lattice resulting from an impact consistent with accident transport conditions is confined by the fuel channel for fuel assembly contents. Third, the inner wall of the inner container provides confinement for fuel bundle contents or fuel rods without the rod container. Figure 6-9 shows the three confinement boundaries and the fuel rod pitch associated with each confinement dimension for each of the fuel types. An additional confinement boundary is provided by the rod container (rod box, rod pipe, or protective case) for the fuel rod contents.

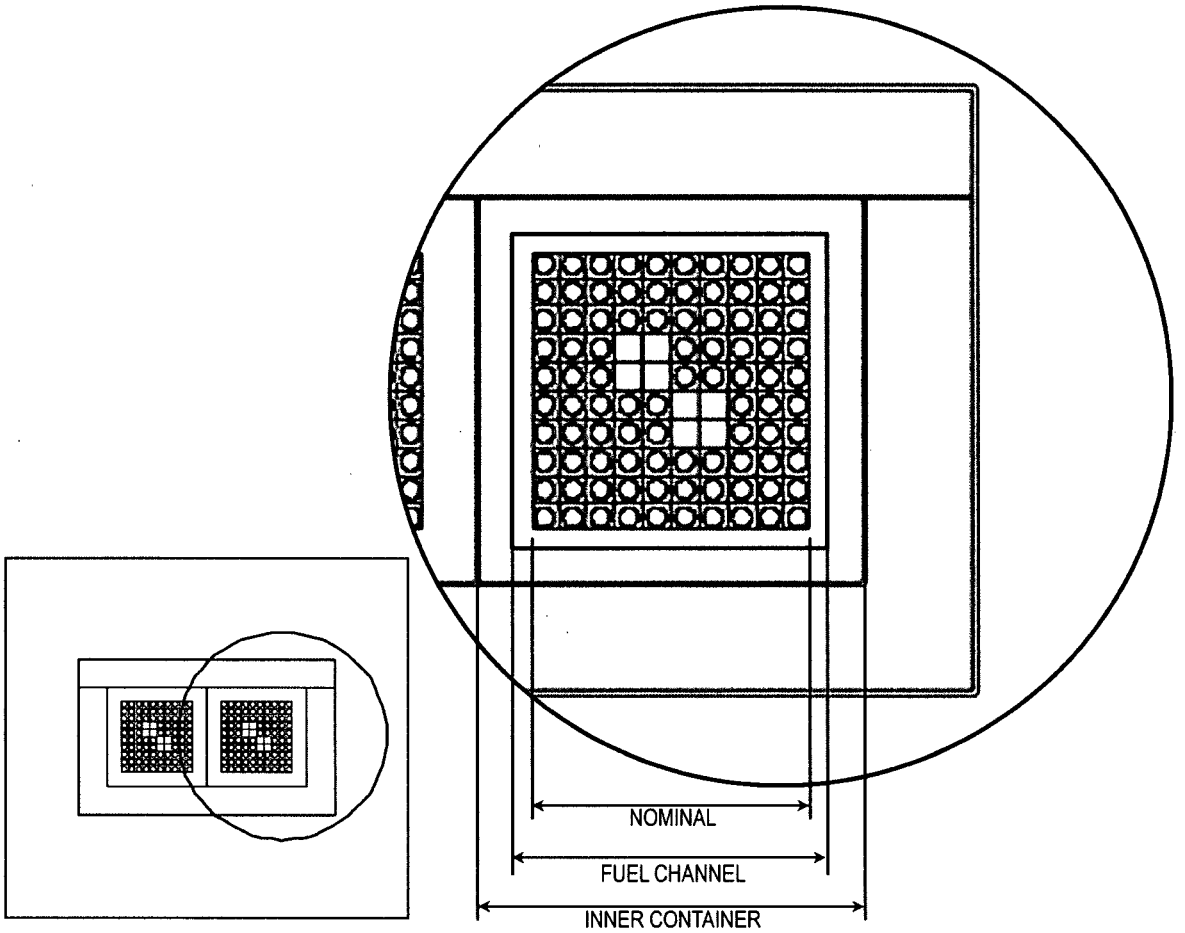

	Fuel Rod Pitch (cm)		
Fuel Type	**Nominal**	**Fuel Channel**	**Inner Container**
GE11, GE13	1.438	1.5378	2.0603
GE12B, GE14C, GE14G, GNF2, GNF4	1.295	1.3771	1.8416
SVEA	1.280	1.3796	1.8018

Figure 6-9 Fuel Rod Confinement Boundaries

6.3.4.1.1 Burnable Absorber Rods (Gd_2O_3)

Burnable absorber (BA) rods that are used to extend the life of the fuel bundle during the power generation cycle also provide neutron absorption for transport conditions that may result in moderation of the fuel bundle. Moderation of the fuel bundle is consistent with transport conditions for the single package, arrays of undamaged packages and arrays of damaged packages. Packaging materials, such as polyethylene foam, and packing materials, such as protective polyethylene spacers, cluster separators, and sheathing, or water from external environment are credible sources of moderation for the fuel bundle. The effectiveness of the BA rods as a neutron absorber is significant in a moderated fuel bundle, but the relative efficacy as a neutron absorber varies sensitively with the location of the BA rod within the fuel bundle lattice. In order to evaluate the relative efficacy of BA rods, neutron absorption in the gadolinium must be assessed at each location within a fuel bundle lattice.

A direct perturbation method could be used to evaluate the effectiveness of each possible arrangement for a fixed number of BA rods in the fuel bundle lattice. The rod worth of each combination would be determined by evaluating the multiplication factor with BA rods inserted and removed as $\rho_\omega = \frac{k_{in} - k_{out}}{k_{in}}$. The direct perturbation approach requires an exhaustive evaluation of every combination of BA rods for a specified number of BA rods. A more efficient methodology is to use analytical perturbation methods to calculate sensitivity coefficients, dk/k / $\Delta\Sigma/\Sigma$, of the absorber nuclides for each credible BA rod locations in the bundle lattice. This evaluation can be completed for all possible BA rod locations in a single calculation sequence. Analytical perturbation methods require calculating the forward and adjoint fluxes that are then used to calculate of sensitivity coefficients for each isotope in the system. The nuclide of interest for BA rods is the gadolinium, Gd, in the Gd_2O_3. The nuclide abundance, thermal neutron cross section, and resonance integral for each of the nuclides in natural gadolinium are shown in Table 6-12.

Table 6-12 Natural Gadolinium Isotope Specifications

Nuclide	Atom Percent Abundance	Thermal Neutron Capture Cross Section (barns)	Resonance Integral
Gd-152	0.20	7.0E2	7.0E2
Gd-154	2.18	6.0E1	2.3E2
Gd-155	14.80	6.1E4	1.54E3
Gd-156	20.47	2.0	1.0E2
Gd-157	15.65	2.53E5	8.0E2
Gd-158	24.84	2.4	7.0E1
Gd-160	21.86	1.0	8.0

Thermal neutron cross sections correspond to neutron energy of 0.0253 eV. In the intermediate energy range each of the Gd nuclides have similar resonance structure. The resonance integral (RI)

represents the probability of neutron reactions in the energy range above thermal energies. Gd-155 and Gd-157 have the largest thermal neutron capture cross sections. Total neutron cross section of the Gd nuclides as a function of the neutron energy in shown in Figure 6-10.

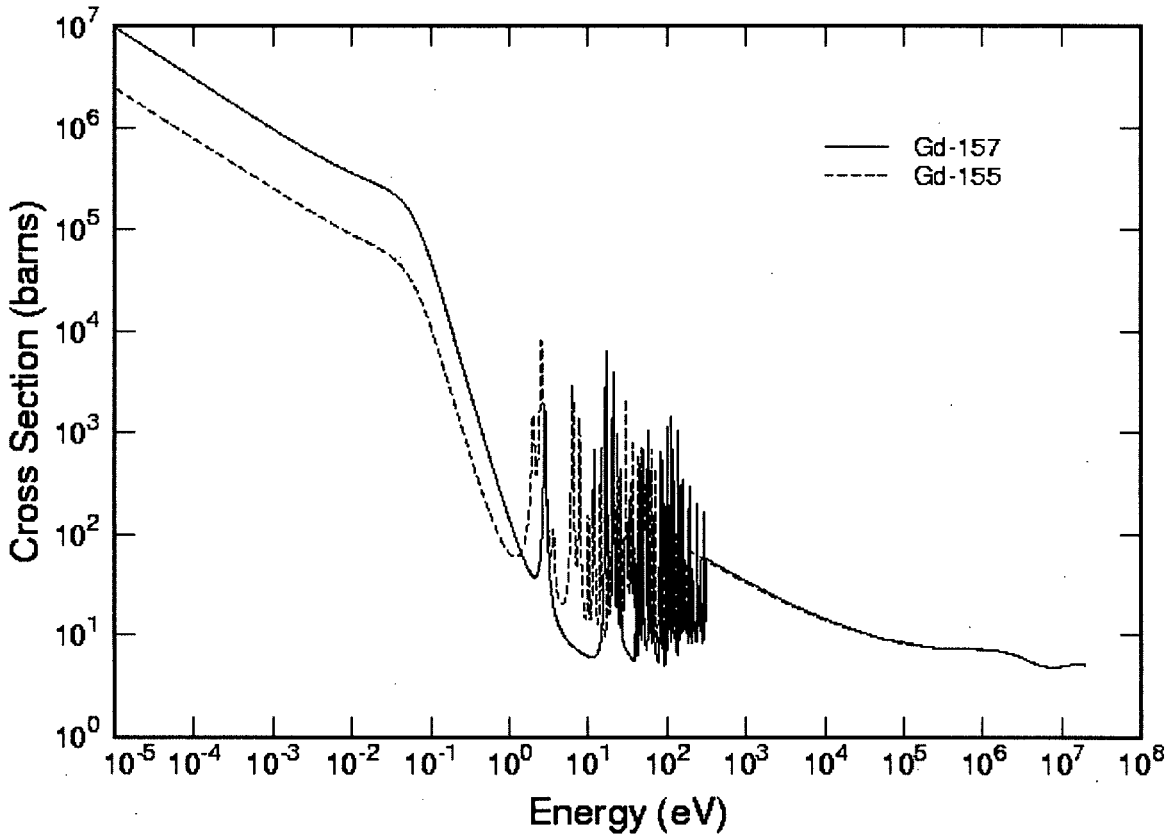

Figure 6-10 Gadolinium (n, total) Cross Section

A small quantity of Gd_2O_3 is included in the fuel mixture for each fuel rod and a unique material identifier is assigned for each fuel rod. The sensitivity coefficient for ^{157}Gd that is calculated by TSUNAMI is used to compare the worth of the BA rod in each lattice location. Gd-157 is used to trace the sensitivity coefficients because of its large abundance in natural gadolinium and large thermal neutron cross section.

A set of BA rod locations is chosen by considering the BA rod worth and constraints placed by design on BA rod locations. Details of the BA rod selection process are provided in Appendix 6.9.3. In general, the lower worth BA rods are found in lattice locations furthest from moderated regions (water hole, water channel or edge of lattice). The locations are determined for an infinite array of fuel bundles such as to represent the package array. There is no evaluation of BA rod positions for an isolated fuel bundle because the individual package is not evaluated with BA rods.

The positions are described using a convention of letters and numbers for the purpose of this evaluation where the positions are referenced to a lattice pattern as shown in Figure 6-11. The eight BA rods are in lattice positions such that three of the four fuel lattice quadrants contain at least one BA rod and the BA rod positions are in symmetric locations around the geometric diagonal. The BA rod locations determined for each of the water rod and partial rod arrangement associated with fuel bundle design as described in Section 1.0 are summarized in Table 6-13. The Gd_2O_3 content in a BA rod is 1.5 w/o.

GE12B

	A	B	C	D	E	F	G	H	I	J
1										
2		P		P			P		P	
3								B		
4		P				W	W		P	
5					P	W	W			
6				W	W	P		B		
7		P		W	W		B	B	P	
8			B			B	B	B		
9		P		P			P		P	
10										

SVEA

	A	B	C	D	E	F	G	H	I	J
1	P									P
2										
3				B			B	B		
4			B		P	P		B		
5				P	W	W	P			
6				P	W	W	P			
7			B		P	P				
8			B	B						
9										
10	P									P

Key: P Part length rod; B BA rod; W Water rod; Full length UO2 rod

Figure 6-11 Examples of the Most Reactive Credible Fuel Lattice Configurations

Table 6-13 Summary of BA Rod Locations for Fuel Bundle Configurations

Fuel Design	BA Rods			Water Rod			Partial Length Fuel Rod Short		Partial Length Fuel Rod Long			
GE11	G-3	G-6	H-6	E-4	F-4	D-5			B-2	E-2	H-2	B-5
	C-7	F-7	H-7	E-5	F-5	D-6			H-5	B-8	E-8	H-8
	F-8	G-8		E-6								
GE12B	H-3	H-6	G-7	F-4	G-4	F-5			B-2	D-2	G-2	I-2
	H-7	C-8	F-8	G-5	D-6	E-6			B-4	I-4	E-5	F-6
	G-8	H-8		D-7	E-7				B-7	I-7	B-9	D-9
									G-9	I-9		
GE13	G-2	G-3	G-6	E-4	F-4	D-5			B-2	E-2	H-2	B-5
	B-7	C-7	F-7	E-5	F-5	D-6			H-5	B-8	E-8	H-8
	H-7	G-8		E-6								
GE14C	C-3	D-3	E-3	F-4	G-4	F-5			B-2	D-2	G-2	I-2
	H-3	C-4	D-4	G-5	D-6	E-6			B-4	I-4	E-5	F-6
	C-5	C-8		D-7	E-7				B-7	I-7	B-9	D-9
									G-9	I-9		
GE14G	C-3	D-3	E-3	F-4	G-4	F-5			B-2	D-2	G-2	I-2
	H-3	C-4	D-4	G-5	D-6	E-6			B-4	I-4	E-5	F-6
	C-5	C-8		D-7	E-7				B-7	I-7	B-9	D-9
									G-9	I-9		
GNF2	B-2	C-2	B-3	F-4	G-4	F-5	E-4	D-5	E-1	F-1	A-5	J-5
	C-3	D-3	H-3	G-5	D-6	E-6	E-5	F-6	A-6	J-6	E-10	F-10
	C-4	C-8		D-7	E-7		G-6	F-7				
SVEA	D-3	G-3	H-3	E-5	F-5	E-6	E-4	F-4	A-1	J-1	A-10	J-10
	C-4	H-4	C-7	F-6			D-5	G-5				
	C-8	D-8					D-6	G-6				
							E-7	F-7				

6.3.4.1.2 Lattice Expansion

Fuel Bundles

Tests demonstrate that virtually all fuel rod deformations induced from an axial impact are due to interactions between the end of the fuel rod and the deformed nozzles. BWR fuels are designed to be under moderated, hence an impact event which increases the pin pitch can result in a general increase in reactivity. It has been observed that for end impacts on BWR designs of fuel, the lattice may contract near the impacted end but expand slightly in the adjacent intra-grid length, as shown in Figure 6-12. A mean lattice pitch change of less than 5 mm is predicted by static analysis methods between the second and third spacer grids from the bottom of the fuel assembly. Nominal dimension between the second and third grid is less than 50 cm for BWR fuel assemblies. Analyzed performance of the lower tie plate and cladding during an end impact as evaluated in Section 2.12.6 of the structural analysis, and predicts responses that are consistent with the testing. The analysis concludes that the lower tie plate will not fail during an end drop and the cladding will not rupture due to the rod bowing. The testing and analytical results justify the assumptions that the individual fuel pellets will be contained in the cladding and no water can lead into the void space between fuel pellet and cladding.

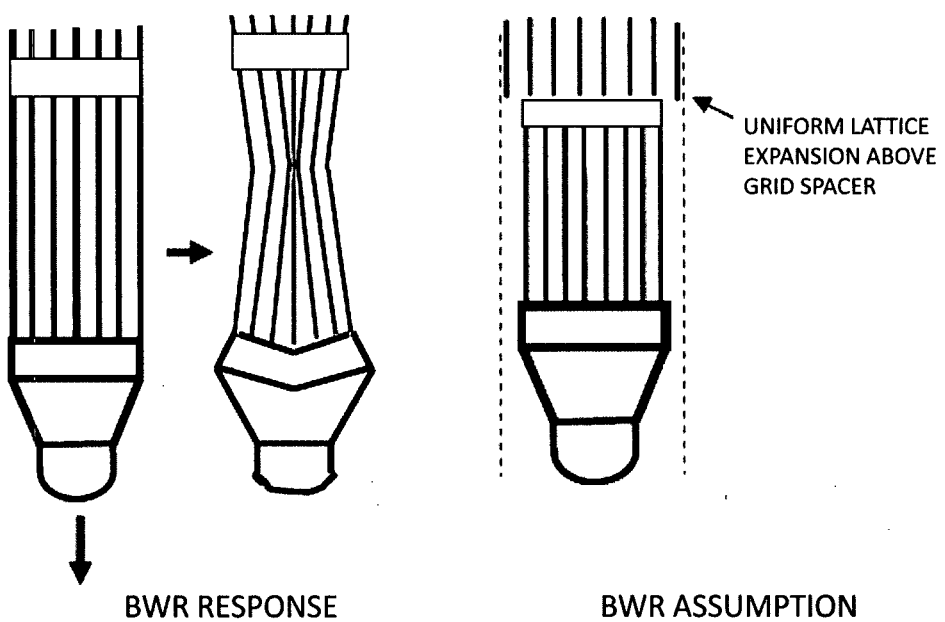

Figure 6-12 Effect of End Impact of BWR Fuel Bundle

The criticality analysis ignores lattice contraction near the end but does consider the uniform lattice expansion. Each BWR fuel assembly type is evaluated to determine the maximum reactivity due to an increase in lattice pitch that is confined to a length of 50 cm at the end of the fuel bundle with 20 cm of close fitting, full density water. Each fuel assembly type is evaluated using the spacing provided by the structure of the packaging, but not including the packaging materials. The

individual package is assessed using fuel bundles with no BA rods, with all void space filled with water and the package closely reflected by 20 cm of water. The package array is assessed as an infinite array using fuel bundles with the BA rod configuration determined previously in 6.3.4.1.1 and filling only the void space within the fuel bundle with water. This assessment is done for a range of fuel rod pitch that includes the dimension that is associated with each confinement boundary (nominal, fuel channel, inner container) for the fuel bundle.

In addition to the water moderation, polyethylene packing materials provide moderation of the contents consistent with the transport condition. Cluster separators, spacers, and wrap are considered for all transport conditions. The effect of moderation by packing materials that are part of the contents is evaluated by assuming that these materials are uniformly distributed on the fuel rod outer surface regardless of the condition of transport. The additional effect of foam cushion that may melt during accident conditions and provide moderation within the fuel bundle is considered in the evaluation of packaging materials. The lattice expansion is evaluated with and without packing materials (cluster separators, fuel rod spacers and wrap) to determine if there is any interaction for the effect on reactivity.

Polyethylene inserts or cluster separators, as utilized by GNF only, are positioned between fuel rods at various locations along the axis of the fuel bundle to avoid stressing the axial grids during transportation. Since the polyethylene cluster separators provide a higher volume average density polyethylene inventory than the inserts/spacers, they are chosen for the RAJ-II criticality analysis. Other types of inserts are acceptable provided that their polyethylene inventory is within the limits established using the cluster separators.

As a maximum limit, 64 separator cluster pieces (32 separator cluster units) are inserted into the bundle. The packing material is represented in the model as a polyethylene wrapped uniformly thick ($POLYR_N$ minus $CLADR$) around each fuel rod ($FUELR$) over the active fuel length. The volume of packing material assumed to be distributed within the fuel bundle is used to determine the uniform poly thickness ($POLYR_N$) around each fuel rod. This volume of material consists of the cluster separators (GNF fuel bundles only) and protective sheath for all transport conditions.

The density specified in the material composition is an apparent density of the polyethylene that is a volume weighted average of the cluster separator and plastic sheath. The apparent density is determined as follows:

Apparent polyethylene density for $POLYR_N$

$$\rho_{POLYR\,N} = \frac{\rho_{CLUSTER\ SEPARATOR} V_{CLUSTER\ SEPARATOR} + \rho_{PLASTIC\ SHEATH} V_{PLASTIC\ SHEATH}}{V_{POLYR_N}}, \text{ where}$$

V_{POLYR_N} *is total volume of packing material wrapped uniformly on each fuel rod*

The volume of packing material is used to determine a uniform poly thickness ($POLYR_N$) around each fuel rod is calculated as follows:

$$Area\ of\ fuel\ rod\ with\ polyethylene = Area\ of\ polyethylene + Area\ of\ fuel\ rod$$

$$\pi(POLYR_N)^2 = \frac{V_{POLY_N}}{\sum_i N_i H_i} + \pi(FUELR)^2,\ where$$

N *is number of fuel rods with active fuel height* H

V_T *is total volume of packaging material wrapped uniformly on each fuel rod*

$$POLYR_N = \sqrt{\frac{V_{POLY_N}}{\pi \sum_i N_i H_i} + (FUELR)^2}$$

The outer radius for the polyethylene ($POLYR_N$) used to represent the routine packing material for the contents (cluster separators and plastic sheath) and apparent densities are summarized in Table 6-14.

Table 6-14 Polyethylene for Routine and Normal Transport Conditions

Fuel Type	Cluster Separator Volume ρ=0.949 g/cc (cm^3)	Plastic Sheath Volume ρ=0.919 g/cc (cm^3)	Total V_{POLY-N} (cm^3)	$\sum_i N_i H_i$	Apparent Polyethylene Density, $\rho_{POLYR-N}$ (g/ cm^3)	$POLYR_N$ (cm)
GE12B	7872	730.88	8602.88	35263.4	0.947	0.5838
GE14C		689.81	8561.81	33131.2	0.947	0.5877
GE14G		672.71	8544.71	32297.8	0.947	0.5894
GNF2		689.81	8561.81	32614	0.947	0.5888
SVEA	0	704.89	704.89	34840	0.919	0.4985

In addition to the geometry representation in the model, the effect of polyethylene packing materials on resonance self shielding is accounted for in the cross-section processing by specifying a cylindrical multiregion unit cell as shown in Figure 6-13. The lattice effects are approximated by applying a white right boundary condition. The results for the lattice expansion evaluation are in Appendix 6.9.4

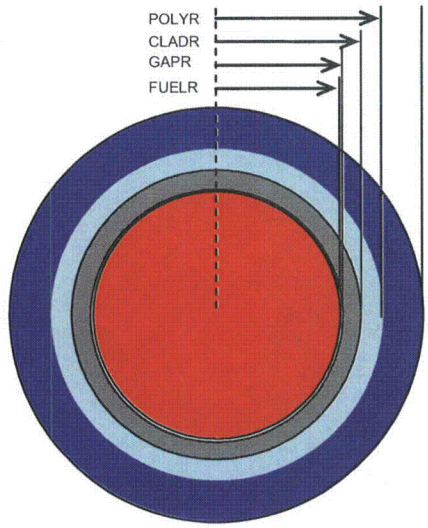


```
CELLTYPE  CS    RIGHT_BDY       FUELR    GAPR    CLADR     POLYR     MODR
multiregion cylindrical right_bdy=white end  1 0.444  0 0.453 3 0.513  21 0.5888  4 0.7306   end zone
```

Figure 6-13 SCALE Unit Cell Demonstration for Re-distribution of Polyethylene

Fuel Rods

The evaluation for fuel rods determines a pitch for the maximum keff for each of the fuel rod category, as defined in Appendix 6.9.5. The detailed evaluation used to determine the optimum pitch is in Appendix 6.9.5.

The optimum fuel rod configuration is most sensitive to the pitch and the maximum keff value is not sensitive to differences in the dimensions for fuel rod parameters characterized by the fuel designs as shown in Table 6-15. The keff values for the optimum pitch of the fuel rod configurations are not significantly different.

As shown in Table 6-15, the BWR_G3 fuel rod category at a pitch of 0.9 cm is the most reactive fuel rod configuration. Hence, the BWR_G3 rod configuration is evaluated in the package with confinement provided by the inner container (without rod container) or the rod container (rod pipe, rod box, or protective case) for the package transport evaluations.

In addition to the water moderation, polyethylene packing materials provide moderation of the contents consistent with the transport condition. For fuel rod transport polyethylene sheathing is considered for all transport conditions. The effect of moderation by packing materials that are part of the contents is evaluated by assuming that an equivalent mass of material is distributed uniformly around each of the fuel rods. This plastic sheathing has been conservatively included in

the model as 0.015 inch (0.0381 cm) thick high density polyethylene wrapped around the cladding at a 0.925 g/cm3 density, representing high density polyethylene.

Table 6-15 Optimum Pitch for Fuel Rod Configurations

Fuel Category	Pitch	Moderator/Fuel	k_{inf}
BWR_W1	0.85	3.0850	1.52685
BWR_G1	0.95	2.7851	1.52663
BWR_G2	0.90	3.2838	1.52616
BWR_G3	0.90	3.1957	1.52738
PWR_W1	0.90	3.3195	1.52656
PWR_W2	0.95	3.2784	1.52689
PWR_W3	0.95	2.9164	1.52731
PWR_W4	0.85	3.4037	1.52624
PWR_W5	0.85	3.2942	1.52641
PWR_W6	0.85	3.2942	1.52604
PWR_W7	0.85	3.2847	1.52608

6.3.4.1.3 Summary of Most Reactive Configuration for Contents

Fuel Bundle or Fuel Assembly

Structural features of the fuel bundle (grids, tie plates, handle) are considered to limit the lattice expansion, but only materials in the active length of the fuel rod (fuel pellet and cladding) are considered in the evaluation of reactivity. The other fuel bundle components are fabricated from materials (stainless steel, inconel, and zircalloy) that absorb neutrons by radiative capture or volume of the structure displaces moderator in the fuel lattice. Representing the fuel bundle components as water results in an increase in reactivity due to both a decrease in neutron absorption and increase in fuel rod lattice moderation. Partial length rods are a feature of the fuel bundle design, and as such are considered in the demonstration of the most reactive configuration.

The most reactive configuration for the fuel bundle and fuel assembly takes into consideration the Gd_2O_3 content in the BA rods, position of neutron absorbing BA rods in the fuel bundle, position of partial length rods, moderation by packing materials and lattice expansion as result of fuel bundle rearrangement during accident transport conditions.

The fuel rod lattice moderation is less than optimum for the extent of lattice expansion that is considered as limited by the confinement system. The 10X10 fuel lattice is the most reactive configuration for the fuel bundle within the range of fuel rod pitch limited by the confinement system for lattice expansion within a maximum credible fuel length of 50 cm. Lattice expansion

is uniform along a 50 cm axial length at one end of the fuel bundle. The maximum lattice pitch is a value that depends on the condition of transport and confinement boundary. The lattice pitch for an undamaged package is the nominal fuel rod pitch. For a damaged package the maximum fuel rod pitch is limited to the fuel channel for a fuel assembly or the inner container for a fuel bundle.

Although the reactivity of the 10X10 fuel bundle configurations are similar, three of the fuel bundle configurations that represent design differences are used in the package evaluation. These differences are characterized by partial length rod and water rod arrangements as follows:

GE14 is a GNF fuel design with only long partial length rods and central water rods.

GNF2 is a GNF fuel design with long and short partial length rods and central water rods.

SVEA is a Westinghouse fuel design with water cross and central water channel.

The GE14G, GNF2, and SVEA fuel bundle configurations are used for the evaluations without BA rods and GE14C, GNF2, and SVEA fuel bundle configurations are used for the evaluations with BA rods.

Fuel Rods

The BWR_G3 fuel rod category is used to represent the most reactive fuel rod configuration for the evaluation of the package transport conditions. The BWR_G3 rod configuration is evaluated in the package with confinement provided by only the inner container (without rod container) or the rod container (rod pipe, rod box, or protective case).

6.3.4.2 Packaging Materials

Interspersed moderation (moderation between packages) is limited to moderators no more effective than water from sources external to the package. There are packaging materials that are internal moderators (within the package) that may be more effective than water either in their normal condition or as degraded by combustion or melting in a thermal event such as a fire. Water can leak into all void spaces of the package, including those within the containment system. Four regions of the package, as shown in Figure 6-14, are considered to assess the effect of packaging materials inside the containment system and surrounding the confinement system.

The reference case for the individual package is to fill all regions that are normally void space or occupied by packaging material with full density water. The reference case for the package array is void in all space normally occupied by packaging material. In both the individual package and package array the void space within the fuel bundle is filled with full density water. Void space within the fuel bundle contents is assumed to always contain water, because the low enriched uranium requires moderation to have any significant neutron multiplication. Additional moderation from the redistribution of the normal packing materials (polyethylene sleeves and cluster separators) are present for all transport conditions.

Accident transport conditions (impact, fire, or water submersion) may degrade the packaging material or damage the package resulting in water filling the void space or saturating the packaging material. Water or void is replaced by nominal packaging material (AlSi insulation, polyethylene foam cushion, paper honeycomb and balsa wood impact limiter) to assess the effect on neutron multiplication.

Two regions (2 and 3) are within the boundary of the confinement system. The polyethylene foam cushion, represented as region 2 for normal transport conditions, may redistribute from region 2 to the fuel bundle due to melting at elevated temperature during a fire event. Region 3 defines polyethylene material from the normal package configuration of the polyethylene foam cushion material that is redistributed from region 2. Polyethylene material in the fuel bundle has the greatest effect on neutron multiplication when distributed uniformly as a full density, close fitting layer on each fuel rod [7].

The remaining two regions (1 and 4) are outside the boundary of the confinement system. Decomposition of the impact absorber material, region 4, is assessed by either assuming formation of char at elevated temperatures during a fire event or assuming complete combustion. The effect of material in region 1 is assessed as present or by assuming saturation of the thermal insulation during water immersion. Although decomposition of the impact absorber or saturation of thermal insulation is possible during accident transport conditions, it is important to assess package configuration assuming that a fire or water immersion does not have any effect on nominal packaging materials inside the containment or surrounding the confinement system.

A packaging configuration consistent with the transport condition that results in the maximum neutron multiplication is identified for further use in the package evaluation. The details of the packaging material evaluation are in Appendix 6.9.6.

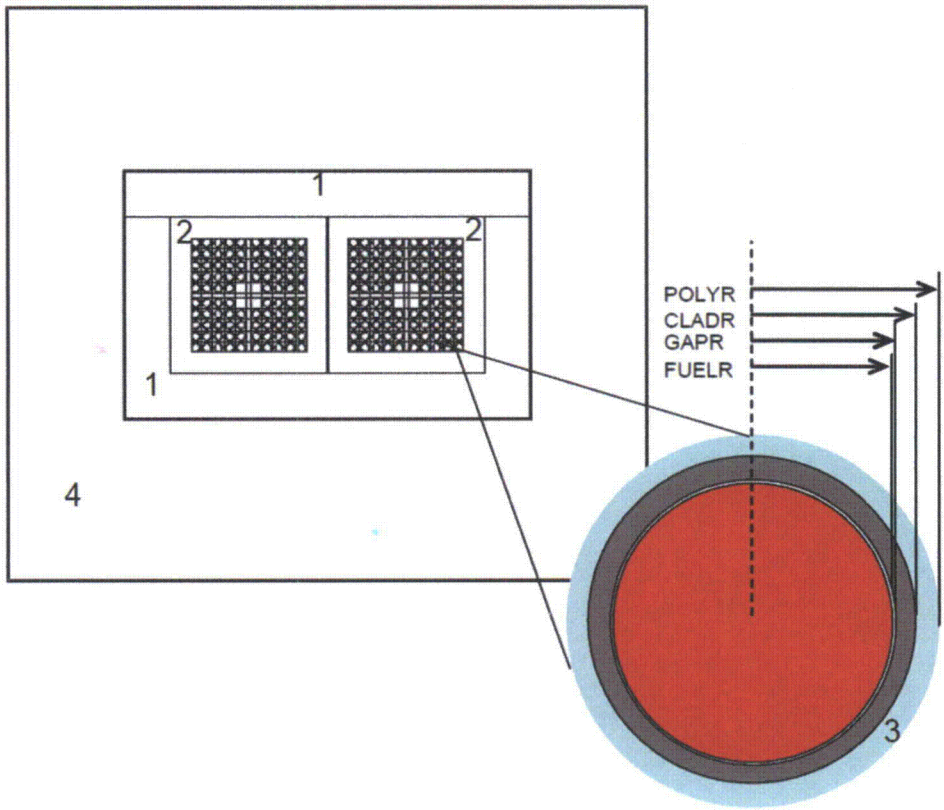

Region	Nominal Packaging Material
1	Alumina Silica (AlSi)
2	Polyethylene foam cushion
3	Redistributed polyethylene foam cushion
4	Impact absorber (paper honeycomb, balsa wood, char)

Figure 6-14 Packaging Material Regions

6.3.4.2.1 Impact Absorber

Thermal testing and analysis demonstrate that the impact absorber material (paper honeycomb, balsa wood) may undergo complete or partial combustion during a fire. The chemical composition of impact absorber material is carbon (C), hydrogen (H), and oxygen (O). Char is produced in the absence of oxygen by the slow pyrolysis of the impact absorber material. Charring is a chemical process of incomplete combustion a solid when subjected to high heat. The resulting residue matter is called char. By the action of heat, charring removes hydrogen and oxygen from the solid, so that the remaining char is composed primarily of carbon. The resulting char is 85% to 90% carbon with the remainder consisting of volatile chemicals and ash.

A void space with some residual ash would result in the volume normally occupied by impact absorber when complete combustion occurs, but in the absence of oxygen a char may form. Water or void is assumed to fill the void space left by the complete combustion of impact absorber material. Carbon at the density of the original material is assumed to remain if incomplete combustion of the impact absorber material were to occur.

The number of scattering collisions necessary to slow a neutron to thermal energies is inversely proportional to ξ. Better moderators are characterized by large values ξ, large scattering cross sections, Σ_s, and small absorption cross section, Σ_a. A measure of the moderating power of a material is the moderating ration,

$$\text{Moderating ratio} = \xi\Sigma_s/\Sigma_a$$

Carbon is a better moderator than the water because moderating ratio for carbon almost 3 times larger than for water (H2O).

The effect on neutron multiplication would depend on the ratio of scattering to absorption in the packaging material and interspersed moderation. The presence of materials with a moderating ratio that is larger than water may result in either an increase or decrease in neutron multiplication in the fuel. Neurons available for absorption in the fissile material (U-235) or neutron absorber (Cr) increase when carbon is present. Neutron absorbers in the packaging material compete with the fissile material for absorption of neutrons. Stainless steel in the packaging structure is a neutron absorber that is assumed to remain intact for transport conditions, and as such the stainless steel absorption increases when carbon is present. At the same time, the neutrons not absorbed by the stainless steel are available to increase the multiplication in the fissile material.

The neutron multiplication increases for a single package for normal and accident transport conditions where the package is subject to moderation and close reflection with full density water. The damaged package array multiplication factor decreases when carbon or water is an interspersed moderator or internal moderator.

6.3.4.2.2 Polyethylene Foam

Polyethylene foam that may melt and provide moderation within the fuel bundle is considered for accident transport conditions. The effect of moderation by packing materials that are part of the contents is evaluated by assuming that these materials are uniformly distributed on the fuel rod outer surface regardless of the condition of transport.

Thermal evaluation demonstrates that temperatures for a fire during the accident transport condition in the inner container is above the melting point range of 120-130°C (248 to 266°F) and ignition temperature of 349°C (660°F) for polyethylene materials. The polyethylene foam either remains in place, melts, or combusts depending on the duration of the fire. Melting polyethylene may slump into the void space in between fuel rods in a fuel bundle, and water may fill the remaining void space during immersion in water. The effect of polyethylene is considered in the demonstration of maximum reactivity for the contents. If temperatures in the inner container do

not exceed the melt temperature of polyethylene either due to a short duration fire or absence of a fire in the accident condition, the foam would remain intact.

The assessment of the fuel types for an accident transport condition is done assuming the thermal input is sufficient to melt the polyethylene. An increase in the dimension for the polyethylene radius ($\Delta POLYR$) from normal packing material ($POLYR_N$) is determined assuming that all the foam cushion material redistributes uniformly onto the fuel rods. The nominal volume of packaging foam cushion is 53,190 cm^3 ($V_{FOAM\ CUSHION}$) with a maximum density assumed to be 0.08 g/ cm3. Assuming an apparent density that is the same as for the normal packing materials ($\rho_{POLYR\text{-}N}$), the volume of polyethylene for the accident condition ($V_{POLYR\text{-}A}$) is determined as follows:

$$Equivalent\ volume\ of\ polyethylene\ foam\ cushion$$

$$V_{POLYR} = \frac{\rho_{POLY\ FOAM} V_{POLY\ FOAM}}{\rho_{POLYR}},\ where$$

$$V_{POLY\ FOAM} = 53190\ cm^3\ is\ total\ volume\ of\ packaging\ foam\ material$$

$$\rho_{POLY\ FOAM} = 0.080\ g/cm^3$$

$$V_{POLYR}\ is\ total\ volume\ of\ packaging\ foam\ cushion\ wrapped\ uniformly\ on\ each\ fuel\ rod$$

The volume of packing material is used to determine a uniform poly thickness ($POLYR_A$) around each fuel rod is calculated as follows:

$$Area\ of\ fuel\ rod\ with\ polyethylene = Area\ of\ polyethylene + Area\ of\ fuel\ rod$$

$$\pi(POLYR_A)^2 = \frac{V_{POLYR_A}}{\sum_i N_i H_i} + \pi(FUELR)^2,\ where$$

$$N\ is\ number\ of\ fuel\ rods\ with\ active\ fuel\ height\ H$$

$$POLYR_A = \sqrt{\frac{V_{POLYR_A}}{\pi \sum_i N_i H_i} + (FUELR)^2}$$

The outer radius for the polyethylene ($POLYR_A$) used to represent the packing materials for an accident condition is summarized in Table 6-18. The outer radius for the polyethylene ($POLYR_N$)

used to represent the routine packing material for the contents (cluster separators and plastic sheath) and apparent densities are summarized in Table 6-16.

Table 6-16 Polyethylene for Accident Transport Conditions

Fuel Type	Foam Cushion $V_{FOAM\ CUSHION}$ (cm^3)	Normal Condition (from Table 6-14) $V_{POLY\text{-}N}$ (cm^3)	Accident Condition $V_{POLYR\text{-}A}$ (cm^3)	$\sum_i N_i H_i$	POLYR$_A$ (cm)	$\Delta POLYR$[1] (cm)
GE12B	4495.92	8602.88	13098.80	35263.4	0.6176	0.0338
GE14C	4495.29	8561.81	13057.10	33131.2	0.6234	0.0357
GE14G	4495.03	8544.71	13039.74	32297.8	0.6258	0.0364
GNF2	4495.29	8561.81	13057.10	32614	0.6250	0.0362
SVEA	4630.22	704.89	5335.11	34840	0.5393	0.0410

Note 1: ΔPOLYR is the increase in polyethylene radius from Table 6-16 for normal packing materials (POLYRA-POLYRN) that is attributed to the melting of the polyethylene foam cushion packing material.

6.3.4.2.3 Structural Stainless Steel

Stainless steel is present in large quantities as the main structural packaging material. A significant amount of neutron elastic scatter occurs due to the iron and neutron absorption occurs due to chromium and nickel content. Only the sheet stainless steel is included in the model and all other structural stainless steel (angle, channel, and inner container support) is omitted.

6.3.4.2.4 Summary of Most Reactive Configuration for Packaging Materials

The packaging configurations are evaluated using the most reactive of the GNF fuel types and SVEA fuel bundle in the packaging configurations for the individual package and package array. The evaluation of effect of packaging materials is in Appendix 6.9.6 and the effects are summarized in Table 6-17 as an average Δk_{eff} for the fuel types and confinement boundaries (nominal, fuel channel, and inner container). The effects show no significant dependence on the fuel type, but there is a small dependence on the pitch associated with the confinement boundary. However, the effect of the packaging configuration on Δk_{eff} differs significantly between the individual package and package array.

Table 6-17 Summary of Effects of Packaging Materials

Packaging Configuration	Individual Package (GE14C or SVEA)	Δk_{eff}	Package Array (GNF2 or SVEA)	Δk_{eff}
Reference	Water (1,2,3,4)	–	Void (1,2,4)	–
Thermal Insulator	AlSi (1) Water (2,3,4)	-0.0423	AlSi (1) Void (2,4)	-0.0014
Normal Condition Polyethylene	Poly (2), Water (1,3,4)	-0.0638	Poly (2), Void (1,4)	-0.0062
Accident Condition Polyethylene	Pack Material (3), Water (1,2,4)	+0.0040	Pack Material (3), Void (1,2,4)	+0.0030
Accident Condition Impact Limiter	Char (4), Water (1,2,3)	-0.0026	Char (4), Void (1,2)	-0.0016

The *Reference* packaging configurations used for the package evaluations are *Water (1,2,3,4)* for the individual package and *Void (1,2,4)* for the package array. With exception of the A*ccident Condition Polyethylene* packaging configuration, the effect of the packaging materials relative to water or void is to decrease k_{eff}. Instead of including the accident condition polyethylene foam cushion redistribution explicitly, an uncertainty of +0.004 Δk_{eff} will be added to k_u for the individual package accident evaluations and an uncertainty of +0.003Δk_{eff} will be added to k_u for the package array accident evaluations.

6.4 INDIVIDUAL PACKAGE IN ISOLATION

6.4.1 Configuration

For the individual package, inner space of the packaging including the volume for the alumina silica thermal insulator, balsa wood and paper honeycomb is assumed to be filled with water. The individual package is reflected with 20 cm of full density water.

6.4.2 Results

6.4.2.1 Contents

6.4.2.1.1 Fuel Bundle or Fuel Assembly

The most reactive type of fuel bundle and fuel assembly contents without BA rods (GE14C, GNF2, and SVEA) are assessed in the individual package. Fuel assembly and fuel bundle contents are assessed without BA rods as the neutron absorption provided by the gadolinia is not needed to ensure that an individual package is subcritical under conditions consistent with normal and accident transport conditions. Normal packing materials (cluster separators and sheathing) are present as polyethylene around each rod for all transport conditions, as they provide additional moderation in the fuel. Water in the package void space provides greater reflection than that provided by the packaging materials.

Table 6-18 Individual Package, Normal Conditions of Transport

	GE14C		GNF2		SVEA	
Contents	k_p	σ_p	k_p	σ_p	k_p	σ_p
Fuel assembly or Fuel bundle						
Full density water in void space	0.80397	0.00041	0.80009	0.00032	0.80053	0.00038
No water in void space	0.54336	0.00032	0.53882	0.00028	0.53680	0.00034

Table 6-19 Individual Package, Accident Conditions of Transport

	GE14C		GNF2		SVEA	
Contents	k_p	σ_p	k_p	σ_p	k_p	σ_p
Fuel assembly						
Full density water in void space	0.80825	0.00035	0.81203	0.00040	0.82325	0.00043
No water in void space	0.54611	0.00031	0.54402	0.00032	0.54591	0.00038
Fuel bundle						
Full density water in void space	0.92011	0.00039	0.92442	0.00047	0.91905	0.00039
No water in void space	0.74882	0.00048	0.75328	0.00039	0.74274	0.00035

6.4.2.1.2 Fuel Rods

Fuel rods may be transported either packaged in a rod container or as a cluster of fuel rods without a rod container. The individual package with fuel rod contents is evaluated using the BWR_G3 fuel rod category. Three fuel rod containers are evaluated: rod pipe, rod box, and protective case. For fuel rod shipment without a rod container, a maximum of 25 fuel rods in each compartment of the inner container is permissible. For a rod container, the number of fuel rods is limited by the capacity of the rod container. The contents are evaluated through the optimum rod pitch within a fuel rod container and for a cluster of 25 fuel rods to the maximum pitch of the IC. Normal packing materials (polyethylene sleeve) are present for all transport conditions, and wrap each individual fuel rod.

The routine and normal condition of transport is for the fuel rods to be close packed, represented by a pitch of the nominal fuel rod outer diameter with normal packing materials included. Accident conditions of transport are representative of the fuel lattice expansion of the active fuel length to the confinement boundaries of either the rod container for fuel rods in a rod container or the IC for clustered rods without a rod container.

Table 6-20 Individual Package, Fuel Rods without Rod Container

Pitch (cm)	k_p	σ_p
Close packed	0.37341	0.00027
1.3	0.63034	0.00031
1.6	0.6465	0.00029

Table 6-21 Individual Package, Fuel Rods with Container

	Rod Container					
	5 in. Rod Pipe		WEC Rod Box		Protective Case	
Pitch (cm)	k_p	σ_p	k_p	σ_p	k_p	σ_p
Close packed	0.49967	0.00032	0.55954	0.0003	0.43476	0.00025
0.6	--	--	--	--	0.46224	0.00028
0.65	--	--	--	--	0.45823	0.00029
0.7	--	--	--	--	0.4745	0.00029
0.75	--	--	--	--	0.4635	0.00029
0.8	0.59841	0.00031	0.58564	0.0003	0.46341	0.00028
0.85	0.61146	0.00031	0.60846	0.0003	0.45864	0.00028
0.9	0.60266	0.00035	0.5934	0.00031	0.44895	0.00031
0.95	0.57231	0.00029	0.56062	0.00031	0.43947	0.00026
1.0	0.57395	0.00035	0.56448	0.00035	0.42648	0.00028
1.05	0.57524	0.00031	0.56312	0.0003	0.41493	0.00026
1.1	0.56728	0.0003	0.5333	0.00039	0.39034	0.00025

6.4.2.2 Uncertainties

6.4.2.2.1 Material and Fabrication Tolerances

Uncertainty due to material and fabrication tolerances is calculated using the TSUNAMI sensitivity coefficients ($\Delta k/k / \Delta\Sigma/\Sigma$) and relative tolerance (V/V) of the material determined in Section 6.3.3.3. The sensitivity coefficient is edited in TSUNAMI as the relative change in keff per increase in relative change in $\Delta\Sigma/\Sigma$. The dimensional tolerance is $\pm\Delta V/V$, therefore only the positive values of $\Delta k/k$ are considered to obtain that maximum total uncertainty.

Table 6-22 Uncertainties, Individual Package in Isolation

Material ID	Material	$\Delta k/k$ /$\Delta\Sigma/\Sigma$	Material Uncertainty Relative (dimension)	$\Delta V/V$	Percent change $\Delta k/k$
1	UO2 (nominal rod pitch)	1.0104E-03	0.2%	0.4%	4.0416E-04
3	ZIRC2 (nominal rod pitch)	3.2946E-05	1%	10%	3.2946E-04
4	Water (nominal rod pitch)	1.1149E-03	1% Note 1	2%	2.2298E-03
11	UO2 (expanded rod pitch)	1.4993E-01	0.2%	0.4%	5.9972E-02
13	Zirc2 (expanded rod pitch)	-7.9375E-04	1%	10%	1.4933E-03
14	Water (expanded rod pitch)	1.7380E-01	1% Note 1	2%	3.4760E-01
19	Water (fuel bundle water rod)	-1.1213E-03	1% Note 1	2%	2.2460E-03
20	SS304	-4.5057E-03	10% [8]	10%	4.5057E-02
21	Polyethylene (nominal rod pitch)	6.6627E-04	1% Note 2	10%	6.6627E-03
23	Polyethylene (expanded rod pitch)	3.1575E-02	1% Note 2	10%	3.1575E-01
30	Water (within package and reflector)	-6.2795E-03	Note 3	NA	NA
Total					0.78174

Note 1: Water displaces variance in cladding or water tube thickness.
Note 2: Polyethylene uncertainty is for the nominal packing material. An additional 0.004 Δk_{eff} is added to the accident cases to account for the redistribution of the foam cushion in a fire event.
Note 3: Water at full density results in the maximum k_{eff}.

6.4.2.2.2 Geometric or Material Representations

6.4.2.2.2.1 Spacing within Outer Container

The rubber vibro-isolating devices are also assumed to degrade or melt when exposed to an external fire, allowing the inner container to shift downward about 2.54 cm. Maximum temperature inside the outer container is 800°C and the ignition temperature for rubber is between 260° – 316°C. The inner container horizontal position within the outer container remains the same as the normal condition model, since the stainless steel fixture assemblies remained intact following the 9-meter drop.

The effect of shifting the position of the inner container is assessed by positioning the inner container in a corner of the outer container and evaluating k_{eff} for the single package. Table below demonstrates that the effect of position of the inner container within the outer container is to decrease k_{eff} for the single package configuration.

Table 6-23 Single Package, Spacing of Inner Container within Outer Container

		Confinement Boundary					
		Nominal		Fuel Channel		Inner Container	
Fuel Type		k_p	Δk_p	k_p	Δk_p	k_p	Δk_p
GE14C	Centered	0.80397	-0.00014	0.80825	-0.00091	0.92011	-0.00151
	Shifted	0.80383		0.80734		0.9186	
SVEA	Centered	0.80053	-0.00045	0.82325	-0.00054	0.91905	-0.00059
	Shifted	0.80008		0.82271		0.91846	

Note:
Statistical uncertainty, σ_p, in the calculation of k_p is less than 0.00030.

6.4.2.3 Summary

The total uncertainty, Δk_u, for the package array under accident transport conditions is a sum of applicable uncertainties as follows:

Table 6-24 Uncertainties for Individual Package

Uncertainty	Δk_u
Material and fabrication tolerances	0.0078
Polyethylene foam cushion redistribution (Note 1)	0.004

Note 1: Applies only to accident conditions of transport for fuel assembly, fuel bundle, or fuel rods without rod container.

Table 6-25 Individual Package, Normal and Accident Conditions of Transport, Summary

Contents Description	k_p	σ_p	Δk_u	Maximum k_p
Normal Conditions of Transport				
Fuel Assembly or Fuel bundle without BA Rods (Table 6-18, Full density water in void space, GE14C)	0.80397	0.00041	0.0078	0.8126
Fuel Rods with Rod Container (Table 6-21, close packed, WEC Rod Box)	0.55954	0.0003	0.0078	0.5679
Fuel Rods without Rod Container (Table 6-20, close packed)	0.37341	0.00027	0.0078	0.3817
Accident Conditions of Transport				
Fuel Assembly without BA Rods (Table 6-19, Full density water in void space, SVEA)	0.82325	0.00043	0.0118	0.8437
Fuel Bundle without BA Rods (Table 6-19, Full density water in void space, GNF2)	0.92442	0.00047	0.0118	0.9372
Fuel Rods with Rod Container (Table 6-21, 0.85 pitch, 5 inch rod pipe)	0.61146	0.00031	0.0078	0.6199
Fuel Rods without Rod Container (Table 6-20, 1.6 cm pitch)	0.6465	0.00029	0.0118	0.6589

6.5 PACKAGE ARRAYS UNDER NORMAL CONDITIONS OF TRANSPORT

6.5.1 Configuration

The demonstration of maximum reactivity showed void in the inner space of the packaging including the volume for the normal packaging materials (alumina thermal insulator, balsa wood and paper honeycomb) results in the highest k_{eff} for an infinite array. A number N is derived from the evaluation of packages under accident conditions of transport. At least five times N packages is shown to be subcritical without the normal packaging materials, with no moderation between the packages and the package arrangement reflected on all sides by 20 cm of water.

6.5.2 Results

6.5.2.1 Contents

6.5.2.1.1 Fuel Bundle or Fuel Assembly without BA Rods

The most reactive type of fuel bundle and fuel assembly contents without BA rods are GE14G, GNF2, and SVEA. Fuel assembly and fuel bundle contents assessed without BA rods is evaluated since the neutron absorption provided by the gadolinia is not needed to ensure that a small package array is subcritical under conditions consistent with normal and accident transport conditions. Normal packing materials (cluster separators and sheathing) are present as redistributed polyethylene around each rod for all transport conditions, as they provide additional moderation in the fuel.

Table 6-26 Package Array (without BA Rods)

		GE14G		GNF2		SVEA	
Array Size	5N	k_p	σ_p	k_p	σ_p	k_p	σ_p
Fuel Bundle without BA Rods	100	0.54045	0.00029	0.53970	0.00025	0.35710	0.00020
Fuel Assembly without BA Rods	169	0.57419	0.00025	—	—	—	—

6.5.2.1.2 Fuel Bundle or Fuel Assembly with BA Rods

The most reactive type of fuel bundle and fuel assembly contents with BA rods are GE14C, GNF2, and SVEA. Normal packing materials (cluster separators and sheathing) are present as redistributed polyethylene around each rod for all transport conditions, as they provide additional moderation in the fuel.

Table 6-27 Package Array (with BA Rods)

		GE14G		GNF2		SVEA	
Array Size	5N	k_p	σ_p	k_p	σ_p	k_p	σ_p
Fuel Bundle with 8 BA Rods	361	0.57334	0.00027	0.57509	0.00025	0.36130	0.00019
Fuel Assembly with 8 BA Rods	169	—	—	0.59044	0.00027	—	—

6.5.2.1.3 Fuel Rods

Fuel rods may be transported either packaged in a rod container or as a cluster of fuel rods without a rod container. The package array with fuel rod contents is evaluated using the BWR_G3 fuel rod category. Three fuel rod containers are evaluated: rod pipe, rod box, and protective case. For fuel rod shipment without a rod container, a maximum of 25 fuel rods in each compartment of the inner container is permissible. For a rod container, the number of fuel rods is limited by the capacity of

the rod container. The routine and normal condition of transport is for the fuel rods to be close packed, represented by a pitch of the nominal fuel rod outer diameter with normal packing materials included. The rod container generating the peak reactivity along with the fuel rod cluster without a rod container are evaluated for the normal transport conditions.

Table 6-28 Package Array (Fuel Rods)

		BWR_G3	
Array Size	**5N**	k_p	σ
Fuel Rods with Rod Container	361	0.4952	0.00022
Fuel Rods without Rod Container	361	0.21649	0.00015

6.5.2.2 Uncertainties

6.5.2.2.1 Material and Fabrication Tolerances

Uncertainty due to material and fabrication tolerances is calculated using the TSUNAMI sensitivity coefficients ($\Delta k/k/\Delta\Sigma/\Sigma$) and relative tolerance ($\Delta V/V$) of the material determined in Section 6.3.3.3. The sensitivity coefficient is edited in TSUNAMI as the relative change in keff per increase in relative change in $\Delta\Sigma/\Sigma$. The dimensional tolerance is $\pm\Delta V/V$, therefore only the positive values of $\Delta k/k$ is considered to obtain that maximum total uncertainty.

Table 6-29 Uncertainties, Package Array under Normal Transport

Material ID	Material	$\Delta k/k$ /$\Delta\Sigma/\Sigma$	Material uncertainty Relative (dimension)	$\Delta V/V$	Percent change $\Delta k/k$
1	UO (nominal rod pitch)	1.9882E-01	0.2%	0.4%	7.9528E-02
3	ZIRC2 (nominal rod pitch)	-6.7521E-03	1%	10%	6.7521E-02
6	UO2- Gd2O3 (nominal rod pitch)	5.1753E-04	0.2%	0.4%	2.0701E-04
8	ZIRC2 (nominal rod pitch)	-6.2467E-04	1%	10%	6.2467E-03
20	SS304	-1.6258E-01	10% [8]	10%	1.6258
21	Polyethylene (nominal rod pitch)	2.9957E-01	1% Note 1	10%	2.9951
30	Water (within package and reflector)	-3.9301E-02	Note 2	NA	–
Total					4.7744

Note 1: Polyethylene uncertainty is for the nominal packing material.
Note 2: Water at full density results in the maximum k_{eff}.

6.5.2.3 Summary

The total uncertainty, Δk_u, for the package array under accident transport conditions is a sum of uncertainties as follows:

Table 6-30 Total Uncertainty, Package Array, Normal Transport Conditions

Uncertainty	Δk_u
Material and fabrication tolerances	0.048

Table 6-31 Package Array under Normal Transport, Summary

Contents	5N	k_p	σ_p	Δk_u	Maximum k_p
Fuel Bundle without BA Rods (Table 6-26, GE14G)	100	0.54045	0.00029	0.0480	0.5891
Fuel Bundle with 8 BA Rods (Table 6-27, GNF2)	361	0.57509	0.00025	0.0480	0.6236
Fuel Assembly without BA Rods (Table 6-26, GE14G)	169	0.57419	0.00025	0.0480	0.6227
Fuel Assembly with 8 BA Rods (Table 6-27, GNF2)	529	0.59044	0.00027	0.0480	0.6390
Fuel Rods with Rod Container (Table 6-28, BWR_G3)	361	0.85982	0.00038	0.0480	0.9086
Fuel Rods without Rod Container (Table 6-28, BWR_G3)	361	0.88940	0.00033	0.0480	0.9381

6.6 PACKAGE ARRAYS UNDER ACCIDENT CONDITIONS OF TRANSPORT

6.6.1 Configuration

A number N is derived, such that two times N packages is subcritical with no moderation between packages and the package arrangement reflected on all sides by 20 cm of water.

6.6.2 Results

6.6.2.1 Contents

6.6.2.1.1 Fuel Assembly or Fuel Bundle

The most reactive type of fuel bundle and fuel assembly contents without BA rods (GE14C, GNF2, and SVEA) and contents with BA rods (GE14G, GNF2, and SVEA) are assessed in the package array. Fuel assembly and fuel bundle contents are assessed with and without BA rods with expansion of 50 cm of the active fuel length. Normal packing materials (cluster separators and sheathing) are present as redistributed polyethylene around each rod, as they provide additional moderation in the fuel. An array size of 2N is determined for the fuel assembly with and without the BA rods and likewise for the fuel bundle. The confinement boundary for the fuel assembly is the dimension of the fuel channel where as the fuel bundle may expand to the extent of the inside of the inner container. The fuel rod pitch resulting from expansion to the inside dimension of the inner container is near the optimum pitch as shown in the demonstration of maximum reactivity.

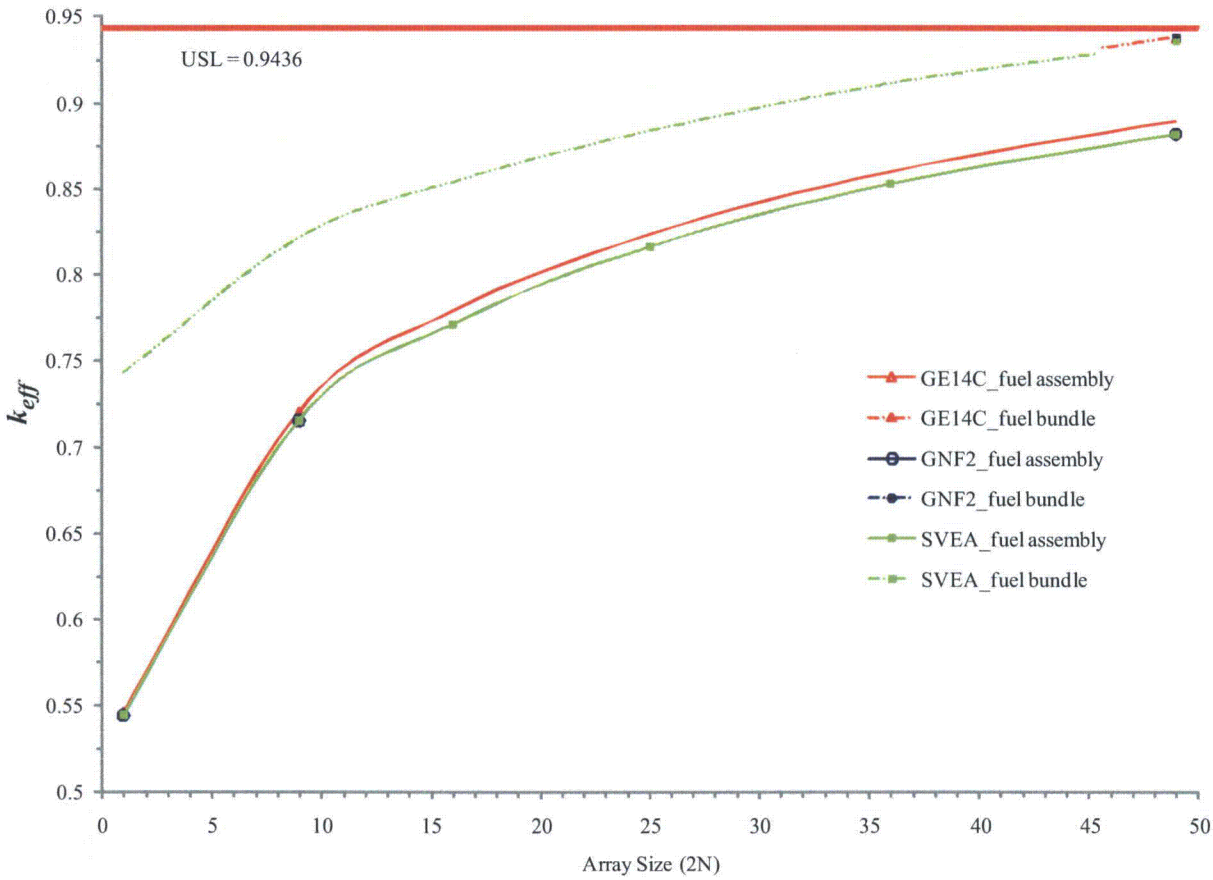

Figure 6-15 Fuel Assembly and Fuel Bundle w/o BA Rods

Table 6-32 Fuel Bundle w/o BA Rods

	GE14C		GNF2		SVEA	
Array Size	k_p	σ_p	k_p	σ_p	k_p	σ_p
1x1	0.74882	0.00048	0.75328	0.00039	0.74274	0.00035
3x3	0.82482	0.0004	0.82820	0.00049	0.82146	0.00035
4x4	0.85698	0.00038	0.85913	0.00044	0.85384	0.00038
5x5	0.88767	0.00035	0.88900	0.00040	0.88375	0.00038
6x6	0.91429	0.00035	0.91476	0.00037	0.91155	0.00039
7x7	0.93771	0.00033	0.93743	0.00038	0.93507	0.00045

Table 6-33 Fuel Assembly w/o BA Rods

	GE14C		GNF2		SVEA	
Array Size	k_p	σ_p	k_p	σ_p	k_p	σ_p
1x1	0.54611	0.00031	0.54402	0.00032	0.54591	0.00038
3x3	0.72028	0.00038	0.71527	0.00034	0.71764	0.00038
4x4	0.77855	0.00034	0.77078	0.00035	0.77556	0.00036
5x5	0.82299	0.00033	0.81568	0.00036	0.82139	0.00033
6x6	0.85982	0.00038	0.85237	0.00033	0.85798	0.00032
7x7	0.88940	0.00033	0.88135	0.00036	0.88845	0.00038

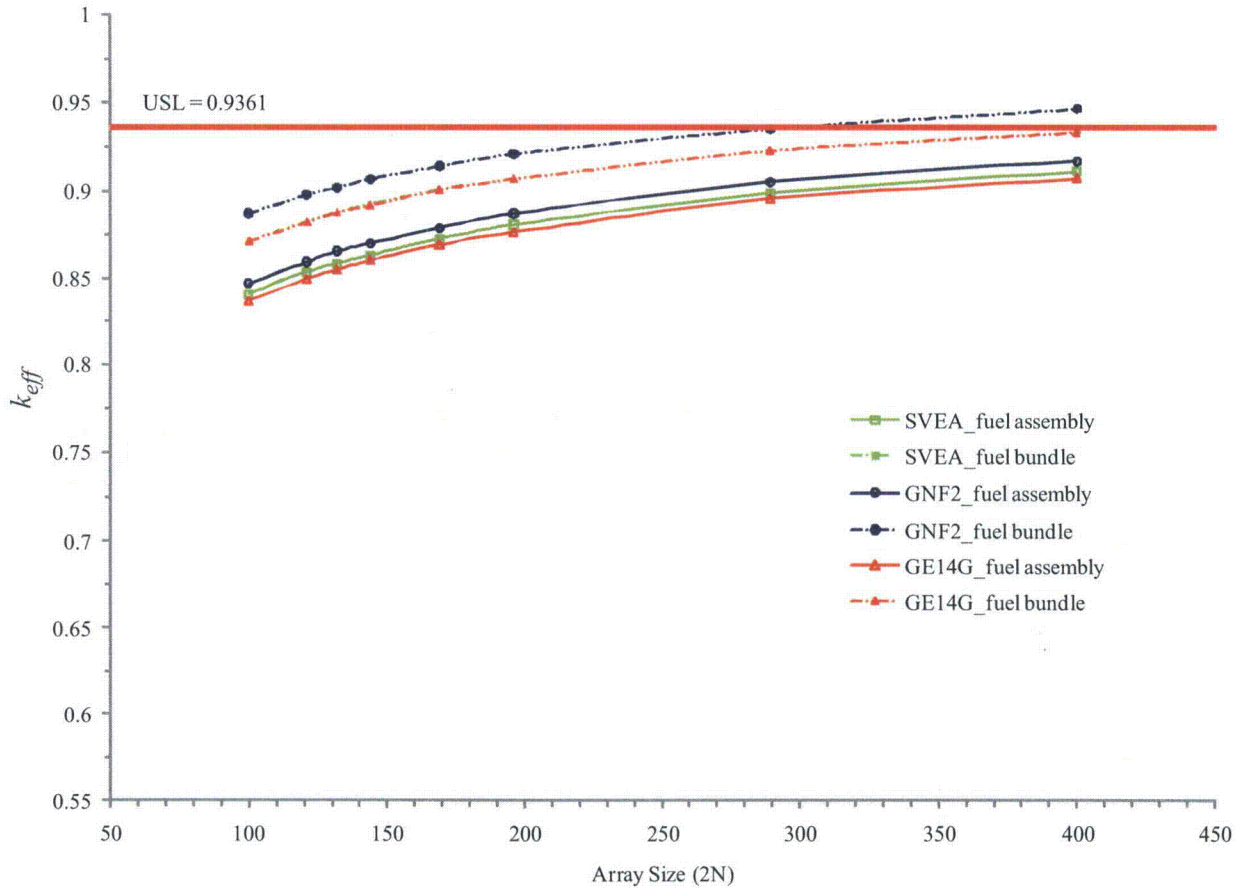

Figure 6-16 Fuel Assembly and Fuel Bundle w/BA Rods

Table 6-34 Fuel Assembly w/ BA Rods

	GE14G		GNF2		SVEA	
Array Size	k_p	σ_p	k_p	σ_p	k_p	σ_p
10x10	0.83676	0.00034	0.84677	0.00033	0.84075	0.00032
11x11	0.84923	0.00037	0.85930	0.00034	0.85351	0.00034
11x12	0.85456	0.00039	0.86559	0.00032	0.85819	0.00040
12x12	0.86000	0.00034	0.86997	0.0003	0.86311	0.00033
13x13	0.86899	0.00035	0.87873	0.00032	0.87244	0.00032
14x14	0.87633	0.0004	0.88698	0.00032	0.88056	0.00036
17x17	0.89530	0.0003	0.90458	0.00032	0.89869	0.00035
20x20	0.90699	0.00035	0.91695	0.00034	0.91105	0.00045

Table 6-35 Fuel Bundle w/ BA Rods

	GE14G		GNF2		SVEA	
Array Size	k_p	σ_p	k_p	σ_p	k_p	σ_p
10x10	0.87118	0.00040	0.88708	0.00035	0.87151	0.00036
11x11	0.88182	0.00031	0.89753	0.00037	0.88250	0.00032
11x12	0.88741	0.00032	0.90176	0.00035	0.88805	0.00030
12x12	0.89156	0.00033	0.90647	0.00035	0.89250	0.00031
13x13	0.90022	0.00037	0.91382	0.00035	0.90071	0.00030
14x14	0.90635	0.00042	0.92084	0.00039	0.90666	0.00037
17x17	0.92230	0.00035	0.93511	0.00032	0.92320	0.00033
20x20	0.93292	0.00032	0.94662	0.00036	0.93395	0.00033

6.6.2.1.2 Fuel Rods

Fuel rods may be transported either packaged in a rod container or as a cluster of fuel rods without a rod container. The package array with fuel rod contents is evaluated using the BWR_G3 fuel rod category. Three fuel rod containers are evaluated: rod pipe, rod box, and protective case. For fuel rod shipment without a rod container, a maximum of 25 fuel rods in each compartment of the inner container is permissible. For a rod container, the number of fuel rods is limited by the capacity of the rod container. The contents are evaluated through the optimum rod pitch within a fuel rod container and for a cluster of 25 fuel rods to the maximum pitch of the IC.

During accident conditions the rod container confines the fuel rods to fixed geometry, where as a cluster of fuel rods are confined only by the inner container. Accident conditions of transport are representative of the fuel lattice expansion of the active fuel length to the confinement boundaries of either the rod container for fuel rods in a rod container or the IC for clustered rods without a rod container. Normal packing materials (polyethylene sleeve) are present for all transport conditions.

Table 6-36 144 Package Array, Fuel Rod Containers

Rod Container	5 in. Pipe		WEC Box		Protective Case	
Pitch	k_p	σ_p	k_p	σ_p	k_p	σ_p
Rod OR	0.60923	0.0003	0.77937	0.00032	0.49095	0.00024
0.7	--	--	--	--	0.60148	0.00034
0.75	--	--	--	--	0.60755	0.00033
0.8	0.85776	0.00032	0.79613	0.00033	0.61028	0.00031
0.85	0.86587	0.00034	0.82499	0.00036	0.60722	0.00033
0.9	0.85738	0.00039	0.79481	0.00036	0.59915	0.00031
0.95	0.83027	0.00038	0.75036	0.00034	0.5858	0.00029
1.0	0.82909	0.00037	0.7607	0.00037	0.56908	0.00035
1.05	0.82336	0.00039	0.7525	0.00035	--	--
1.1	0.80669	0.00035	0.70763	0.00033	--	--

Table 6-37 144 Package Array, No Rod Containers

Rod Container	No Container	
Pitch	k_p	σ_p
Rod OR	0.41576	0.00026
1.3	0.72854	0.00035
1.6	0.75877	0.00031

6.6.2.2 Uncertainties

6.6.2.2.1 Material and Fabrication Tolerances

Uncertainty due to material and fabrication tolerances is calculated using the TSUNAMI sensitivity coefficients ($\Delta k/k / \Delta\Sigma/\Sigma$) and relative tolerance (V/V) of the material determined in Section 6.3.3.3. The sensitivity coefficient is edited in TSUNAMI as the relative change in keff per increase in relative change in $\Delta\Sigma/\Sigma$. The dimensional tolerance is $\pm\Delta V/V$, therefore only the positive values of $\Delta k/k$ is considered to obtain that maximum total uncertainty

Table 6-38 Uncertainties, Package Array with BA Rods (144) Under Accident Transport

Material ID	Material	$\Delta k/k$ /$\Delta\Sigma/\Sigma$	Material Uncertainty Relative (dimension)	$\Delta V/V$	Percent Change $\Delta k/k$
1	UO (nominal rod pitch)	1.5312E-01	0.2%	0.4%	6.1248E-02
3	ZIRC2 (nominal rod pitch)	-3.6914E-03	1%	10%	3.6914E-02
4	Water (nominal rod pitch)	1.7931E-01	1% Note 1	10%	3.5862E-01
6	UO2- Gd2O (nominal rod pitch)	-4.8343E-03	0.2%	0.4%	1.9357E-04
8	ZIRC2 (nominal rod pitch)	-1.3759E-04	1%	10%	1.3759E-03
9	Water (nominal rod pitch)	-5.2224E-03	1% Note 1	10%	1.0445E-02
11	UO2 (expanded rod pitch)	1.1595E-02	0.2%	0.4%	4.6426E-04
13	Zirc (expanded rod pitch)	-1.8084E-04	1%	10%	1.8084E-03
14	Water (expanded rod pitch)	1.0761E-02	1% Note 1	10%	2.1522E-02
16	UO2- Gd2O3 (expanded rod pitch)	-3.4918E-04	0.2%	0.4%	1.3981E-05
18	Zirc2 (expanded rod pitch)	-8.1600E-06	1%	10%	8.1600E-05
19	Water (fuel bundle water rod)	1.9983E-03	1% Note 1	10%	3.9966E-03
20	SS304	-7.7313E-02	10% [5]	10%	7.7313E-01
21	Polyethylene (nominal rod pitch, w/o BA)	7.0405E-02	1% Note 2	10%	7.0405E-01
22	Polyethylene (nominal rod pitch, BA)	-3.5932E-03	1% Note 2	10%	3.5932E-02
23	Polyethylene (expanded rod pitch, w/o BA)	-3.5932E-03	1% Note 2	10%	3.5932E-02
24	Polyethylene (expanded rod pitch, BA)	-2.3556E-04	1% Note 2	10%	2.3556E-03
30	Water (inter package and reflector)	-1.4503E-02	Note 3	NA	NA
Total					2.0479

Note 1: Water displaces variance in cladding or water tube thickness.
Note 2: Polyethylene uncertainty is for the nominal packing material. An additional 0.002 Δk_{eff} is added to the accident cases to account for the redistribution of the foam cushion in a fire event.
Note 3: Water at optimum density results in the maximum k_{eff}.

Table 6-39 Uncertainties, Package Array without BA Rods (36) Under Accident Transport

Material ID	Material	$\Delta k/k$ /$\Delta\Sigma/\Sigma$	Material Uncertainty Relative (dimension)	$\Delta V/V$	Percent change $\Delta k/k$
1	UO (nominal rod pitch)	1.1918E-01	0.2%	0.4%	4.7672E-02
3	ZIRC2 (nominal rod pitch)	-2.6090E-03	1%	10%	2.6090E-02
4	Water (nominal rod pitch)	2.3911E-01	1% Note 1	10%	4.7822E-01
11	UO2 (expanded rod pitch)	7.5298E-03	0.2%	0.4%	4.6426E-04
13	Zirc (expanded rod pitch)	-1.3288E-04	1%	10%	1.3288E-03
14	Water (expanded rod pitch)	1.0515E-02	1% Note 1	10%	2.1030E-02
19	Water (fuel bundle water rod)	2.6808E-03	1% Note 1	10%	5.3616E-03
20	SS304	-6.8641E-02	10% [5]	10%	6.8641E-01
21	Polyethylene (nominal rod pitch, w/o BA)	8.9592E-02	1% Note 2	10%	8.9592E-01
23	Polyethylene (nominal rod pitch, BA)	5.5821E-03	1% Note 2	10%	5.5821E-02
30	Water (inter package and reflector)	-1.8877E-02	Note 3	NA	–
Total					2.2183

Note 1: Water displaces variance in cladding or water tube thickness.
Note 2: Polyethylene uncertainty is for the nominal packing material. An additional 0.002 Δk_{eff} is added to the accident cases to account for the redistribution of the foam cushion in a fire event.
Note 3: Water at optimum density results in the maximum k_{eff}.

6.6.2.2.2 Geometric or Material Representations

6.6.2.2.2.1 Spacing within Outer Container

The rubber vibro-isolating devices are also assumed to degrade or melt when exposed to an external fire, allowing the inner container to shift downward about 2.54 cm. Maximum temperature inside the outer container is 800°C and the ignition temperature for rubber is between 260° – 316°C. The inner container horizontal position within the outer container would be the same as the normal condition model, since the stainless steel fixture assemblies remained intact following the 9-meter drop.

The effect of a shift in the position of the inner container is assessed by positioning the inner container in a corner of the outer container and evaluating k_{eff} for the infinite array. Table below demonstrates that the effect of position of the inner container within the outer container is less than 0.005 Δk_{eff} for the package array configuration.

Table 6-40 Package Array (Infinite), Spacing of Inner Container within Outer Container

Region Configuration		Confinement Boundary					
		Nominal		Fuel Channel		Inner Container	
Material (Region)		k_p	Δk_p	k_p	Δk_p	k_p	Δk_p
GNF2	Centered	1.13173	0.00248	1.13417	0.00272	1.13883	0.00324
	Shifted	1.13421		1.13689		1.14207	
SVEA	Centered	1.1185	0.00293	1.12180	0.0031	1.12392	0.0031
	Shifted	1.12143		1.1249		1.12702	

Note:
Statistical uncertainty, σ_p, in the calculation of k_p is less than 0.00030.

6.6.2.2.2.2 Package Spacing

The container deformation modeled for the package array includes the damage from the 9-meter drop onto an unyielding surface that causes container deformation is considered by varying the outside dimensions of the outer container. The outer container height and width is reduced by 2.4 cm is consistent with the damage observed during the 9-meter drop. Table below demonstrates that the effect of decreasing the spacing by 2.5 cm is less than 0.015 Δk_{eff} for the package array.

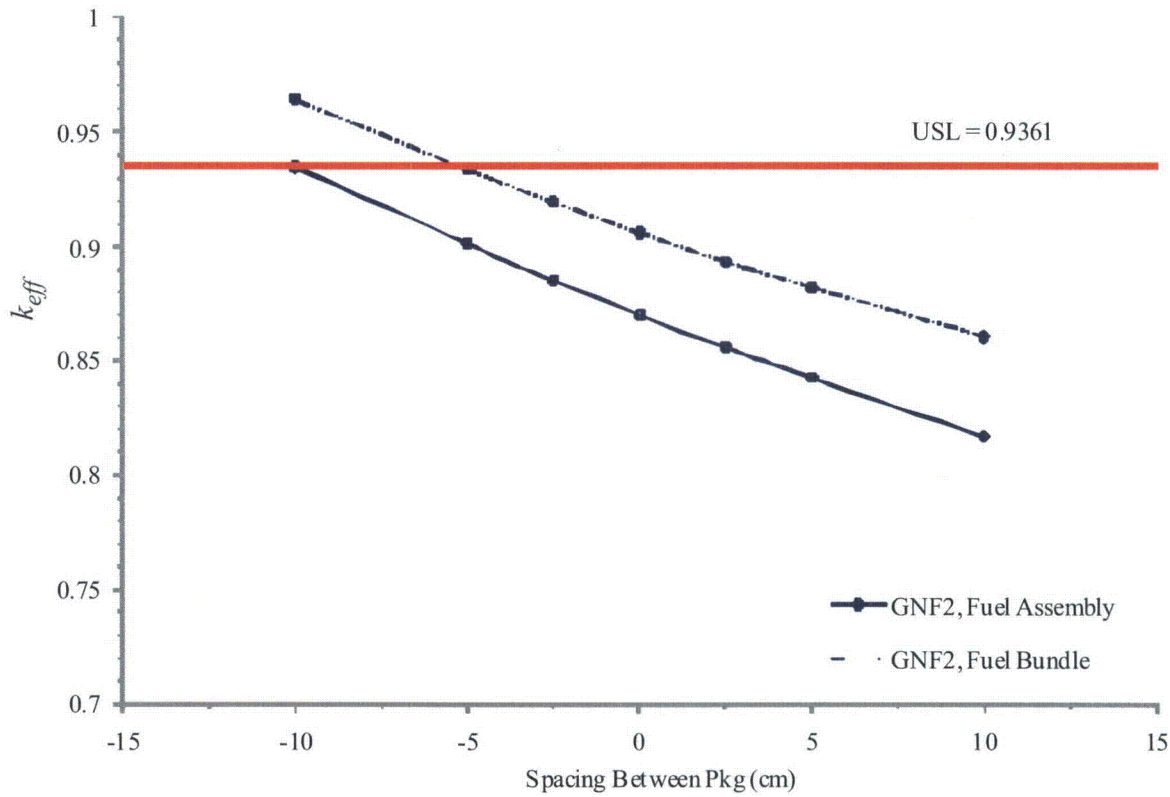

Figure 6-17 Package Array w/BA Rods, OC Dimensional Variation

Table 6-41 Package Array (GNF2) w/ BA Rods, OC Dimensional Variation

Confinement Boundary Spacing (cm)	Fuel Assembly			Fuel Bundle		
	k_p	σ_p	Δk_p	k_p	σ_p	Δk_p
10	0.81669	0.00034	-0.05328	0.86034	0.00034	-0.04613
5	0.8427	0.00035	-0.02727	0.8824	0.00033	-0.02407
2.5	0.85579	0.00037	-0.01418	0.89368	0.00034	-0.01279
0	0.86997	0.0003	0	0.90647	0.00035	0
-2.5	0.88532	0.00033	0.01535	0.91982	0.00036	0.01335
-5	0.90159	0.00038	0.03162	0.93409	0.00031	0.02762
-10	0.93518	0.00038	0.06521	0.96431	0.00029	0.05784

6.6.2.2.2.3 Moderation between Packages

The array is slightly undermoderated at zero water density, and increasing the moderator density (0.01 to 0.1) there is a small peaking effect on k_{eff}. As the water density increases further, the neutron absorption comes into effect, neutron interaction between packages decreases, and k_{eff} decreases to a minimum and rises again due to increased reflection provided by more interspersed water. The array k_{eff} at full-density moderation is less than the k_{eff} of the flooded and reflected single unit, indicating that the edge-to-edge spacing of the packages is not sufficient to permit full reflection.

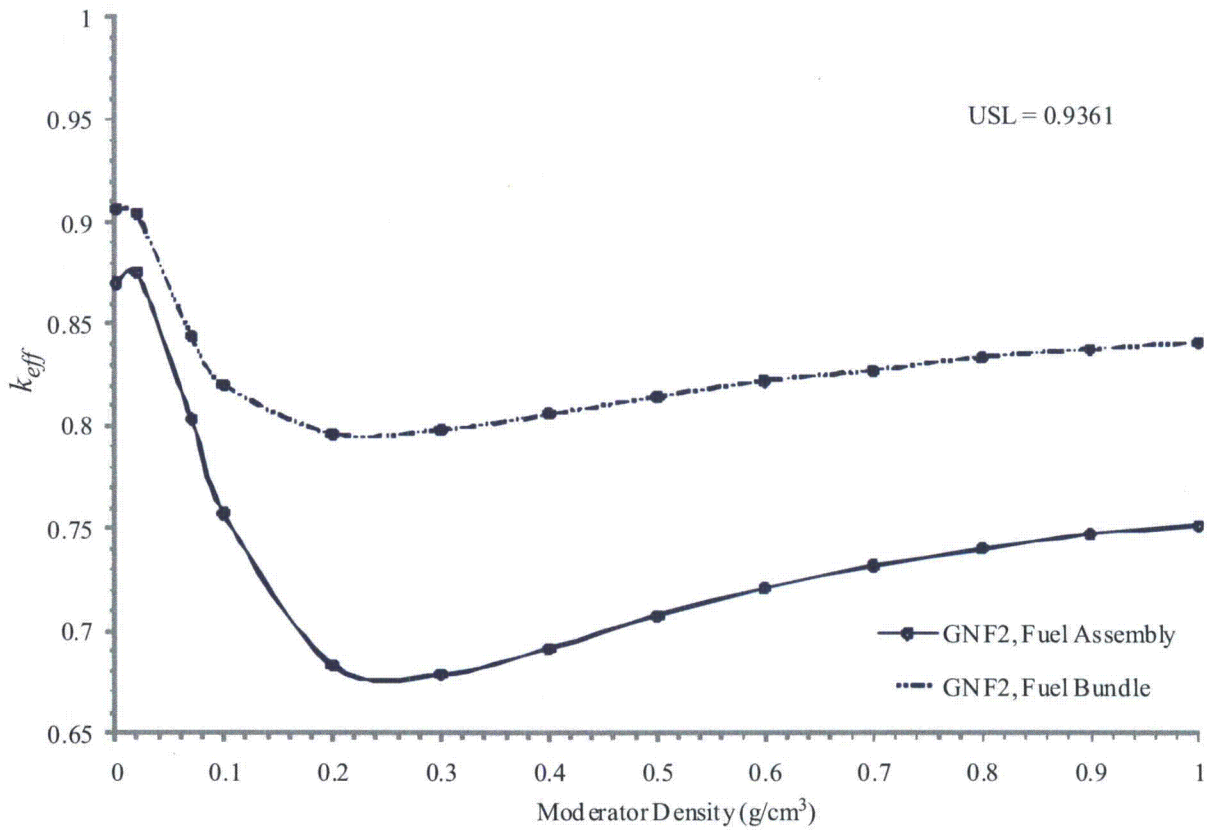

Figure 6-18 Package Array w/BA Rods, Moderation Variation

Table 6-42 Package Array (GNF2) w/ BA Rods, Moderation Variation

Confinement Boundary Moderation Density (g/cm^3)	Fuel Assembly		Fuel Bundle	
	k_p	σ_p	k_p	σ_p
0	0.86997	0.0003	0.90647	0.00035
0.02	0.87518	0.00036	0.9042	0.00031
0.07	0.80317	0.00038	0.84432	0.00039
0.1	0.75722	0.00036	0.82032	0.00033
0.2	0.68317	0.00034	0.79603	0.00036
0.3	0.67818	0.00033	0.79778	0.00035
0.4	0.69146	0.00043	0.80541	0.00038
0.5	0.7073	0.00035	0.81398	0.00039
0.6	0.72064	0.00033	0.8221	0.00035
0.7	0.73156	0.00035	0.82731	0.00037
0.8	0.73996	0.0004	0.83389	0.00045
0.9	0.74725	0.00038	0.83779	0.00036
1.0	0.75109	0.00033	0.8411	0.00035

6.6.2.3 Summary

The total uncertainty, Δk_u, for the package array under accident transport conditions is a sum of uncertainties as follows:

Table 6-43 Total Uncertainty, Package Array, Accident Transport Conditions

Uncertainty	Δk_u
Inner container spacing within outer container	0.005
Outer container dimensions	0.015
Polyethylene foam cushion redistribution (Note 1)	0.004
Material and fabrication tolerances	0.022
Total	0.046

Note 1: Applies only to accident conditions of transport for fuel assembly, fuel bundle, or fuel rods without rod container.

Table 6-44 Accident Conditions, Package Array, Summary

Contents	2N	k_p	σ_p	Δk_u	*Maximum* k_{eff}
Fuel Assembly without BA Rods (Table 6-33, GE14C, 7×7)	49	0.88940	0.00033	0.046	0.9361
Fuel Assembly with 8 BA Rods (Table 6-34, GNF2, 14×14)	196	0.88698	0.00032	0.046	0.9337
Fuel Bundle without BA Rods (Table 6-32, GE14C, 5×5)	25	0.88900	0.00040	0.046	0.9358
Fuel Bundle with 8 BA Rods (Table 6-35, GNF2, 10×10)	100	0.88708	0.00035	0.046	0.9345
Fuel Rods with Rod Container (Table 6-36, Rod Pipe, 0.85 cm pitch)	144	0.86587	0.00034	0.044	0.9106
Fuel Rods without Rod Container (Table 6-37, 1.6 cm pitch)	144	0.75877	0.00031	0.046	0.8054

6.7 FISSILE MATERIAL PACKAGES FOR AIR TRANSPORT

RAJ-II does not satisfy the requirements for fissile material package designs to be transported by air specified in 10 CFR 71.55(f).

6.7.1 Configuration

Not applicable.

6.7.2 Results

Not applicable.

6.8 BENCHMARK EVALUATIONS

The criticality safety critical experiment benchmarks were computed using SCALE 6 CSAS6 and the 238GROUPNDF7 cross-section library. Critical experiments were selected to represent the materials and geometry of the package. The USLSTATS methodology [6] is used to determine an Upper Subcritical Limit (USL).

6.8.1 Applicability of Benchmark Experiments

Critical experiment cases were selected from NUREG/CR-6361 [6] to evaluate the performance of the SCALE codes and cross-section libraries for heterogeneous systems with similarity to the package configurations. Critical experiments performed for actual BWR fuel configurations with

gadolinia oxide neutron absorber rods were also included in the bias evaluation [7]. These experiments are low-enriched light-water-reactor (LWR) lattices. The series of experiments demonstrates the performance of both the cross sections and the SCALE resonance cross-section processing methodology. The critical experiments span a range of moderation and fuel pin arrangements that are applicable in evaluating LWR fuel storage and transport and a BWR reactor core configuration with BA rods. A summary of the critical experiments is provided in Appendix 6.9.7.

TSUNAMI in SCALE 6 is used to calculate sensitivity and uncertainty data for each of the critical experiments and the package. TSUNAMI-IP is used to calculate global indices that assess the similarity of the package and critical experiments on a system wide basis for all nuclides and reactions. The integral index, c_k, is calculated for each package configuration (individual package and package array) with the contents (fuel bundle or fuel assembly and fuel rods). The interpretation of the correlation coefficient, c_k, is the following, a value of 0.0 represents no correlation between the package configuration and critical experiment and a value of 1.0 represents full correlation between the systems. Each package configuration has different sensitivities that affect the bias determination.

6.8.2 Bias Determination

Benchmarks with c_k greater than 0.80 were included to predict a USL for each package configuration. USLSTATS produces a non-linear extrapolation to a trend value of 1.0 for c_k. Two statistical approaches are used to determine USL for a set of critical experiments representing the package application: USL Method 1 determines a confidence band with administrated margin and USL Method 2 determines a single-sided tolerance limit. An administrative margin to ensure subcriticality, Δk_m, is considered sufficient if USL_1 is less than USL_2. Pooled descriptive statistics for k_c values are used to evaluate a lower single-sided tolerance limit and confidence band. for the gadolinia oxide benchmarks because the number of experiments with c_k greater than 0.80 is too small to produce a statistically significant regression analysis. For both USLSTATS and pooled descriptive statistics, the confidence level ($1-\gamma$) is 95%, confidence on the proportion of (α) is 95%, and proportion of population falling above the lower tolerance interval (ρ) is 99.5%. A k_m of at least 0.02 is sufficient for all package configurations, however, a recommended value of 0.05 is used to calculate USL_1. [8]

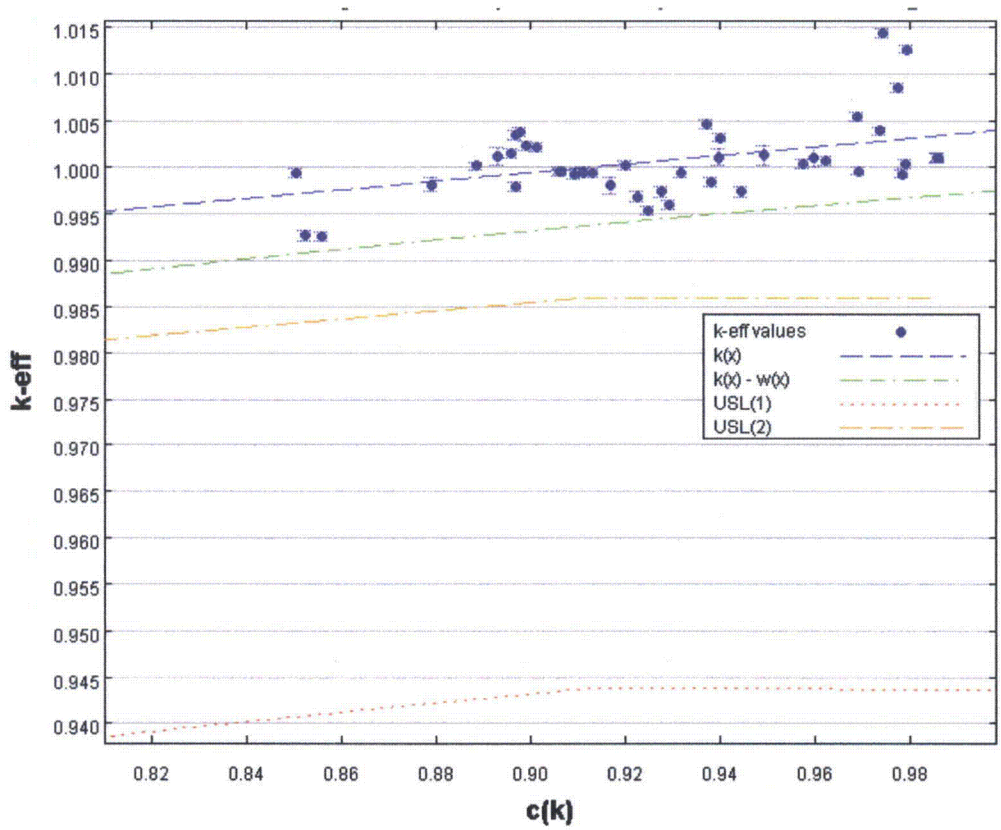

Figure 6-19 Fuel Bundle or Fuel Assembly no Gad Rods, Individual Package

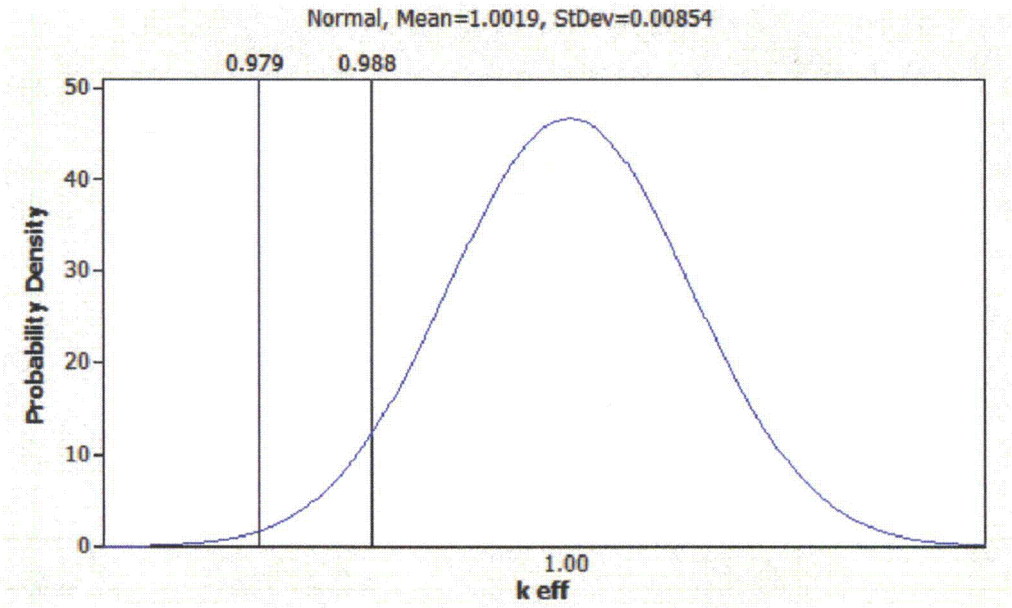

Figure 6-20 Fuel Bundle or Fuel Assembly with Gad Rods, Package Array

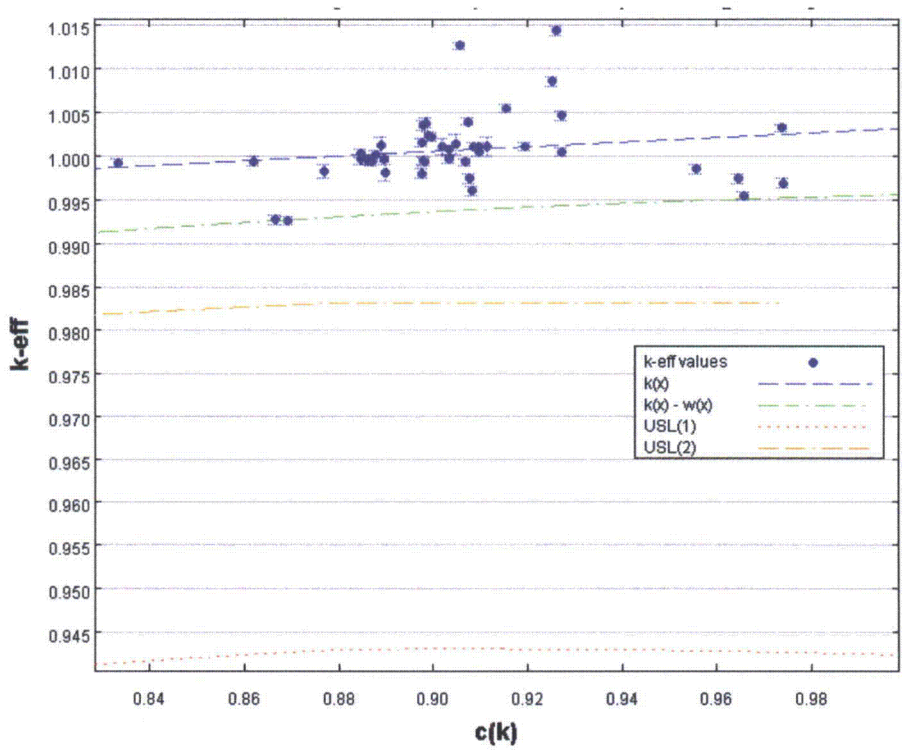

Figure 6-21 Fuel Bundle or Fuel Assembly no Gad Rods, Package Array

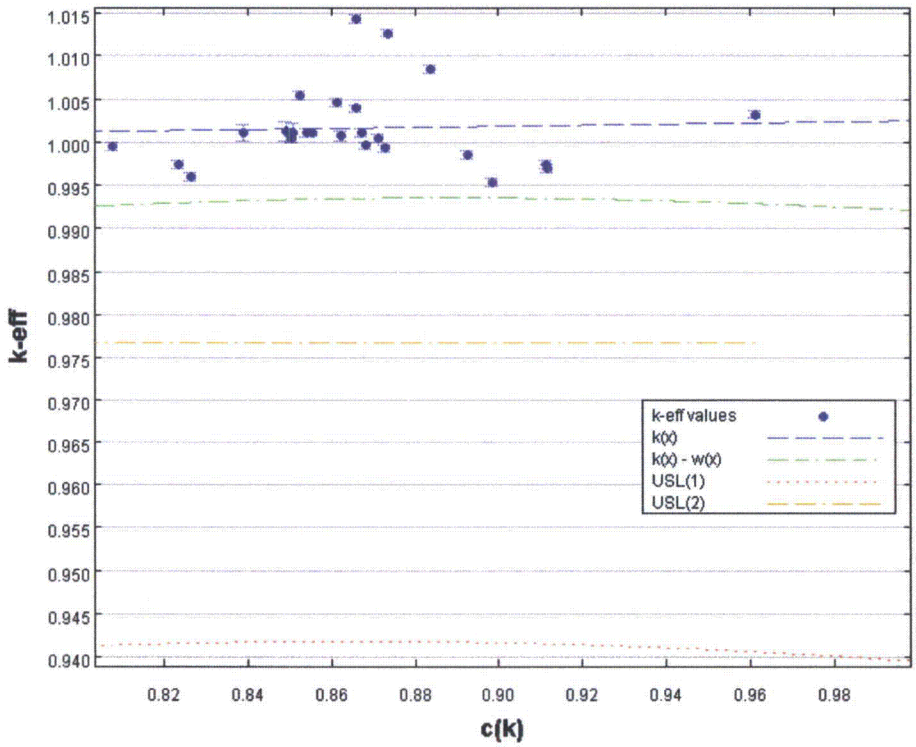

Figure 6-22 Fuel Rods, Individual Package

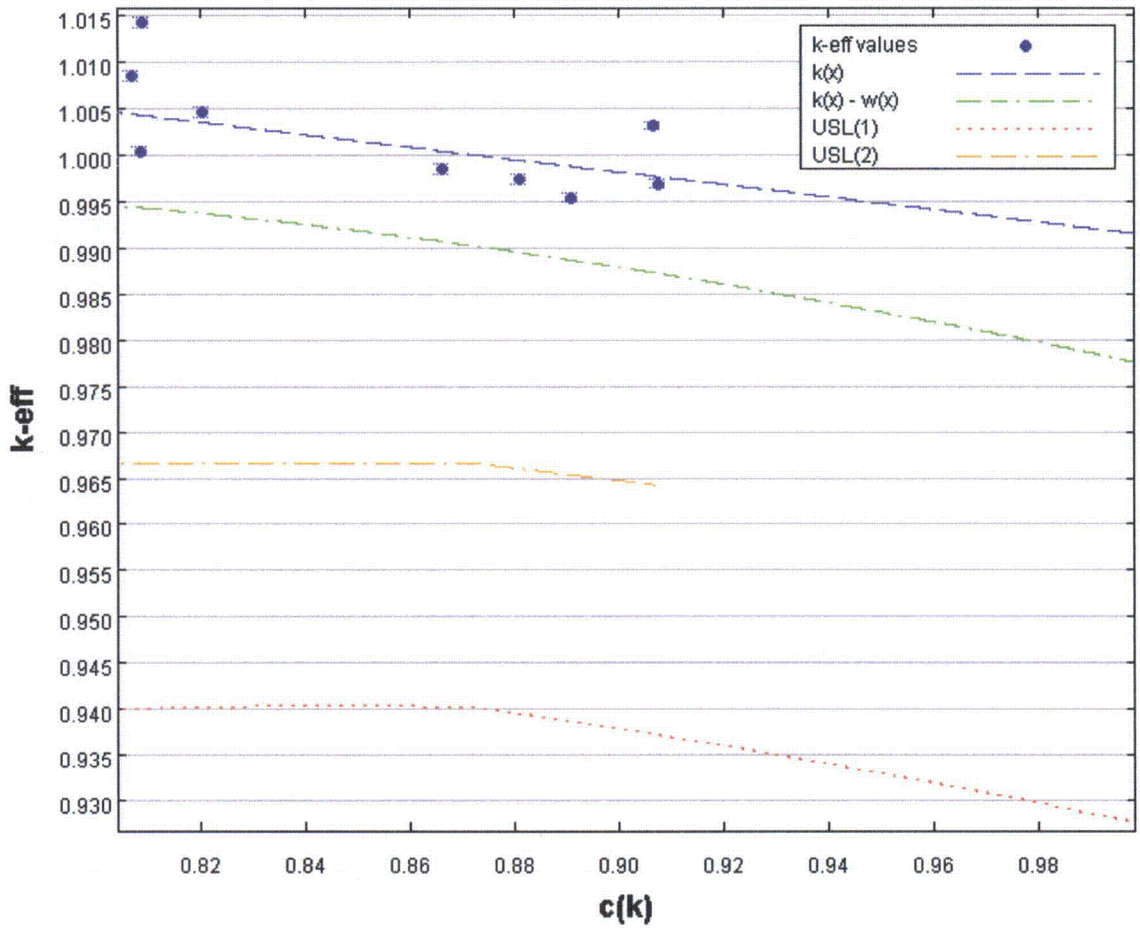

Figure 6-23 Fuel Rods, Package Array

Table 6-45 USL Summary for Δk_m=0.05 Evaluated at c(k)=1.0

Package Configuration	$USL_1=k_c-\Delta k_c-\Delta k_m$	$USL_2=k_c-\Delta k_c$
Fuel Bundle or Fuel Assembly no Gad Rods, Individual Package	0.9424	0.9831
Fuel Bundle or Fuel Assembly with Gad Rods, Package Array	0.9361	0.9771
Fuel Bundle or Fuel Assembly no Gad Rods, Package Array	0.9436	0.9860
Fuel Rods, Individual Package	0.9396	0.9769
Fuel rods, Package Array	0.9275	0.9580

6.9 APPENDIX

6.9.1 References

1. ANSI/ANS-8.17-2004: "Nuclear Criticality Safety in Operations with Fissionable Materials Outside Reactors," American Nuclear Society, La Grange Park, Illinois.

2. ASTM 996-04, "Standard Specification for Uranium Hexafluoride Enriched to Less Than 5% ^{235}U," ASTM International, West Conshohocken, PA.

3. SCALE: *A Modular Code System for Performing Standardized Computer Analyses for Licensing Evaluations*, ORNL/TM-2005/39, Version 6, Vols. I–III, January 2009. Available from Radiation Safety Information Computational Center at Oak Ridge National Laboratory as CCC-750.

4. NUREG/CR-6686, ORNL/TM-1999/322, "*Experience with the SCALE Criticality Safety Cross Section Libraries*," 1997.

5. ASTM A480 / A480M-10, "Standard Specification for General Requirements for Flat-Rolled Stainless and Heat-Resisting Steel Plate, Sheet, and Strip."

6. NUREG/CR-6361,ORNL/TM-13211, "Criticality Benchmark Guide for Light-Water-Reactor Fuel in Transportation and Storage Packages," March 1997.

7. J. Zino, V. Mills, D. Dixon, "Low Enriched UO_2 Pin Lattice in Water Critical Benchmark Evaluations with ENDF/B-VII Nuclear Data," *ANS Topical Meeting on Advances in Reactor Physics*, PHYSOR2006, Vancouver, BC (September 2006).

8. NUREG 5661, ORNL/TM-11936, "Recommendations for the Criticality Safety Evaluation for Transportation Packages," April 1997.

6.9.2 Input Files

6.9.2.1 Individual Package

Small Array 6x6, GNF2 w/o Gad rods, expansion to IC boundary, k_{eff}=0.91476, CSI=2.78

```
=csas6 parm=(centrm)
GNF2 bottom lattice pitch = 1.8247 cm
v7-238
read composition
 uo2          1 1 300
                                  92235 5
                                  92238 95              end
 h2o          2 1 300   end
 zirc2        3 1 300   end
 h2o          4 1 300   end
 h2o          5 1 300   end
 poly(H2O) 21 den=0.947 1 300   end
 uo2          6 1 300
                                  92235 5
                                  92238 95              end
Gd            6 0 5.2463E-04 end
O             6 0 2.7701E-03 end
 h2o          7 1 300   end
 zirc2        8 1 300   end
 h2o          9 1 300   end
 poly(H2O) 22 den=0.947 1 300   end
 uo2          11 1 300
                                  92235 5
                                  92238 95              end
 h2o          12 1 300   end
 zirc2        13 1 300   end
 h2o          14 1 300   end
 h2o          15 1 300   end
 poly(H2O) 23 den=0.947 1 300   end
 uo2          16 1 300
                                  92235 5
                                  92238 95              end
Gd            16 0 5.2463E-04 end
O             16 0 2.7701E-03 end
 h2o          17 1 300   end
 zirc2        18 1 300   end
 h2o          19 1 300   end
 poly(H2O) 24 den=0.947 1 300   end
 ss304        20  1 300   end

h2o          30 1 300   end

end composition
read celldata
  multiregion cylindrical right_bdy=white end   1 0.444       0 0.453       3 0.513       21
0.5888       4 0.7306       end zone
  multiregion cylindrical right_bdy=white end   6 0.444       0 0.453       8 0.513       22
0.5888       9 0.7306       end zone
   multiregion cylindrical right_bdy=white end   11 0.444         0 0.453         13 0.513
23 0.5888       14 1.0295  end zone
```

```
  multiregion cylindrical right_bdy=white end    16 0.444          0 0.453          18 0.513
24 0.5888       19 1.0295   end zone
end celldata

read parameter
 gen=550
 npg=10000
 htm=no
end parameter

read geometry
unit 1
com='5 wt% UO2 full length rod'
 cylinder 1    0.444            381             0
 cylinder 2   0.453            381             0
 cylinder 3    0.513            381             0
   cylinder 10  0.5888        381             0
 cuboid 4     4p0.6475    381             0
 media 1 1 1
 media 0 1 -1 2
 media 3 1 -1 -2 3
  media 21 1 -1 -2 -3 10
 media 4 1 -1 -2 -3 -10 4
 boundary 4
unit 2
 com='water rod'
 cuboid 1   4p0.6475    381             0
 media  4 1 1
 boundary 1
unit 6
com='5 wt% UO2 rod with 1.5          wt% GdO2'
 cylinder 1    0.444           381             0
 cylinder 2   0.453           381             0
 cylinder 3    0.513           381             0
   cylinder 10    0.5888          381             0
 cuboid 4     4p0.6475    381             0
 media 6 1 1
 media 0  1 -1 2
 media 8 1 -1 -2 3
  media 22 1 -1 -2 -3 10
 media 9 1 -1 -2 -3 -10 4
 boundary 4
unit 7
com='5 wt% UO2 partial length rod'
 cylinder 1    0.444            259.10    0
 cylinder 2   0.453            259.10    0
 cylinder 3    0.513            259.10    0
  cylinder 10    0.5888          259.10    0
 cuboid 4     4p0.6475    381             0
 media 1 1 1
 media 0 1 -1 2
 media 3 1 -1 -2 3
 media 21 1 -1 -2 -3 10
 media 4 1 -1 -2 -3 -10 4
 boundary 4
unit 8
com='5 wt% UO2 partial length rod'
 cylinder 1    0.444            137.20    0
 cylinder 2   0.453            137.20    0
 cylinder 3    0.513            137.20    0
   cylinder 10    0.5888          137.20    0
```

```
 cuboid 4     4p0.6475    381             0
 media 1 1 1
 media 0 1 -1 2
 media 3 1 -1 -2 3
  media 21 1 -1 -2 -3 10
 media 4 1 -1 -2 -3 -10 4
 boundary 4
unit 9
com='single assembly-normal top'
 cuboid 1    4p6.4163     381            50.001
 array 1 1 place 5 5 1 -0.6475 -0.6475 0
 cuboid 2    4p 8.8000     381            50.001
 media 0            1 -1  2
 boundary 2
unit 10
com='single assembly-normal bottom'
 cuboid 1    4p6.4163     0.001           0
 array 1 1 place 5 5 1 -0.6475 -0.6475 0
 cuboid 2    4p 8.8000     0.001           0
 media 0            1 -1  2
 boundary 2
unit 11
com='5 wt% UO2 full length rod'
 cylinder 1    0.444            381             0
 cylinder 2   0.453            381             0
 cylinder 3    0.513            381             0
 cylinder 10    0.5888           381             0
 cuboid 4     4p0.9124    381             0
 media 11 1 1
 media 0 1 -1 2
 media 13 1 -1 -2 3
  media 23 1 -1 -2 -3 10
 media 14 1 -1 -2 -3 -10 4
 boundary 4
unit 12
 com='water rod'
 cuboid 1  4p0.9124    381             0
 media 19  1 1
 boundary 1
unit 16
com='5 wt% UO2 rod with 1.5          wt% GdO2'
 cylinder 1    0.444           381             0
 cylinder 2   0.453           381             0
 cylinder 3    0.513           381             0
 cylinder 10    0.5888          381             0
 cuboid  4     4p0.9124    381             0
 media 16 1 1
 media 0  1 -1 2
 media 18 1 -1 -2 3
 media 24 1 -1 -2 -3 10
 media 19 1 -1 -2 -3 -10 4
 boundary 4
unit 17
com='5 wt% UO2 partial length rod'
 cylinder 1    0.444            259.10    0
 cylinder 2   0.453            259.10    0
 cylinder 3    0.513            259.10    0
 cylinder 10    0.5888           259.10    0
 cuboid 4     4p0.9124    381             0
 media 11 1 1
 media 0 1 -1 2
```

```
 media 13 1 -1 -2 3
  media 23 1 -1 -2 -3 10
 media 14 1 -1 -2 -3 -10 4
 boundary 4
unit 18
com='5 wt% UO2 partial length rod'
 cylinder 1    0.444            137.20    0
 cylinder 2   0.453            137.20    0
 cylinder 3    0.513            137.20    0
 cylinder 10    0.5888           137.20    0
 cuboid 4     4p0.9124    381             0
 media 11 1 1
 media 0 1 -1 2
 media 13 1 -1 -2 3
   media 23 1 -1 -2 -3 10
 media 14 1 -1 -2 -3 -10 4
 boundary 4
unit 19
com='single assembly damaged section'
 cuboid 1     4p 8.8000      50.001         0.001
 array 2 1  place 5 5 1 -0.9124 -0.9124 0
 cuboid 2    4p 8.8000     50.001         0.001
 media 0            1 -1  2
 boundary 2
unit 21
 com='20 cm tall water box'
 cuboid 1    4p 8.8000     20  0
 media 0            1  1
 boundary 1
unit 22
 com='basic GNF2 assembly stack up'
 cuboid 1     4p 8.8000  381             0
 array 3 1  place 1 1 1 0 0 0
 boundary 1

unit 100
com='single fuel assembly in left half inner container'
 cuboid 1     4p8.8          419.25           -38.25
 hole 22 origin x=0 y=0 z=0
 media 0  1  1
 cuboid 2  2p8.9          8.8          -8.9          419.35       -38.35
 media 20 1 -1  2
 boundary 2
unit 101
com='single fuel assembly in right half inner container'
 cuboid 1     4p8.8          419.25           -38.25
 hole 22 origin x=0 y=0 z=0
 media 0  1  1
 cuboid 2  2p8.9          8.8          -8.9          419.35       -38.35
 media 20 1 -1  2
 boundary 2

unit 102
com='individual RAJ-II package'
 cuboid 1 2p17.8         8.8          -8.9          419.35       -38.35
 array 4 1 place 1 1 1 -8.9          0 0
 ypplane 6  8.9           8.8
 media 20 1  6  2
 cuboid 2  2p22.80 2p13.90 424.35        -43.35
 media 0  1  -1 2 -6
 cuboid 3  2p22.95 2p14.05  424.5         -43.5
```

```
 media 20 1  -1 -2  3
' shock absorbers
 cuboid 10 2p25   2p16.3 429.1         -48.1
 media 0 1  -1 -2 -3 10
 cuboid 11 2p35.8 2p32.0 429.1         -48.1
 media 0 1 -1 -2 -3 -10 11
 cuboid 4  2p35.8 2p32.0 443.7         -62.7
 media 0  1  -1 -2 -3 -10 -11 4
 cuboid 5  2p36.0 2p32.2  443.9         -62.9
 media 20 1  -1 -2 -3 -10 -11 -4  5
 boundary 5

 global
unit 103
com='pkg array 6x6'
cuboid 1     396.0    -36.0    354.2    -32.2      443.9         -62.9
 array 5 1  place 1 1 1 0 0 0
cuboid 2     416.0    -56.0     374.2    -52.2     463.9         -82.9
 media 30 1  -1 2
boundary 2

end geometry

read array

ara=5 nux=6 nuy=6 nuz=1 typ=square
com='Package array'
 fill
   36R102
 end fill

ara=1 nux=10 nuy=10 nuz=1 typ=square
com='array for nominal GNF2 lattice'
 fill
    1    1    1    1    7    7    1    1    1    1
    1    1    1    1    1    1    1    1    1    1
    1    1    1    1    1    1    1    1    1    1
    1    1    1    1    8    2    2    1    1    1
    7    1    1    8    8    2    2    1    1    7
    7    1    1    2    2    8    8    1    1    7
    1    1    1    2    2    8    1    1    1    1
    1    1    1    1    1    1    1    1    1    1
    1    1    1    1    1    1    1    1    1    1
    1    1    1    1    7    7    1    1    1    1
 end fill

ara=2 nux=10 nuy=10 nuz=1 typ=square
com='array for expanded GNF2 lattice'
 fill
    11    11    11    11    17    17    11    11    11    11
    11    11    11    11    11    11    11    11    11    11
    11    11    11    11    11    11    11    11    11    11
    11    11    11    11    18    12    12    11    11    11
    17    11    11    18    18    12    12    11    11    17
    17    11    11    12    12    18    18    11    11    17
    11    11    11    12    12    18    11    11    11    11
    11    11    11    11    11    11    11    11    11    11
    11    11    11    11    11    11    11    11    11    11
    11    11    11    11    17    17    11    11    11    11
 end fill
```

```
ara=3 nux=1 nuy=1 nuz=3 typ=square
com='array for complete fuel assembly'
 fill
  10
  19
   9
 end fill

ara=4 nux=2 nuy=1 nuz=1 typ=square
com='Left and right sides of inner boxes'
 fill
   100 101
 end fill

end array

read bounds
all=void
end bounds

end data
end
```

6.9.2.2 Package Array

Large Array 12x12, GNF2 w/ Gad rods, expansion to IC boundary, k_{eff}=0.90647, CSI=0.69

```
=csas6 parm=(centrm)
GNF2 bottom lattice pitch = 1.8247 cm
v7-238
read composition
 uo2         1 1 300
                                92235 5
                                92238 95            end
 h2o         2 1 300   end
 zirc2       3 1 300   end
 h2o         4 1 300   end
 h2o         5 1 300   end
 poly(H2O) 21 den=0.947 1 300   end
 uo2         6 1 300
                                92235 5
                                92238 95            end
Gd           6 0 5.2463E-04 end
O            6 0 2.7701E-03 end
 h2o         7 1 300   end
 zirc2       8 1 300   end
 h2o         9 1 300   end
 poly(H2O) 22 den=0.947 1 300   end
 uo2         11 1 300
                                92235 5
                                92238 95            end
 h2o         12 1 300   end
 zirc2       13 1 300   end
 h2o         14 1 300   end
 h2o         15 1 300   end
 poly(H2O) 23 den=0.947 1 300   end
```

```
 uo2          16 1 300
                                92235 5
                                92238 95              end
Gd            16 0 5.2463E-04 end
O             16 0 2.7701E-03 end
 h2o          17 1 300   end
 zirc2        18 1 300   end
 h2o          19 1 300   end
 poly(H2O) 24 den=0.947 1 300   end
 ss304        20  1 300   end

h2o          30 1 300   end

end composition
read celldata
  multiregion cylindrical right_bdy=white end   1 0.444       0 0.453       3 0.513       21
0.5888       4 0.7306       end zone
  multiregion cylindrical right_bdy=white end   6 0.444       0 0.453       8 0.513       22
0.5888       9 0.7306       end zone
   multiregion cylindrical right_bdy=white end    11 0.444         0 0.453         13 0.513
23 0.5888       14 1.0295  end zone
   multiregion cylindrical right_bdy=white end    16 0.444         0 0.453         18 0.513
24 0.5888       19 1.0295   end zone
end celldata

read parameter
 gen=550
 npg=10000
 htm=no
end parameter

read geometry
unit 1
com='5 wt% UO2 full length rod'
 cylinder 1    0.444            381             0
 cylinder 2   0.453            381             0
 cylinder 3    0.513            381             0
   cylinder 10  0.5888          381             0
 cuboid 4     4p0.6475    381             0
 media 1 1 1
 media 0 1 -1 2
 media 3 1 -1 -2 3
  media 21 1 -1 -2 -3 10
 media 4 1 -1 -2 -3 -10 4
 boundary 4
unit 2
 com='water rod'
 cuboid 1   4p0.6475    381             0
 media  4 1 1
 boundary 1
unit 6
com='5 wt% UO2 rod with 1.5          wt% GdO2'
 cylinder 1    0.444           381             0
 cylinder 2   0.453           381             0
 cylinder 3    0.513           381             0
   cylinder 10    0.5888          381             0
 cuboid 4     4p0.6475    381             0
 media 6 1 1
 media 0  1 -1 2
 media 8 1 -1 -2 3
```

```
 media 22 1 -1 -2 -3 10
 media 9 1 -1 -2 -3 -10 4
 boundary 4
unit 7
com='5 wt% UO2 partial length rod'
 cylinder 1    0.444            259.10    0
 cylinder 2   0.453            259.10    0
 cylinder 3    0.513            259.10    0
  cylinder 10    0.5888          259.10    0
 cuboid 4     4p0.6475    381             0
 media 1 1 1
 media 0 1 -1 2
 media 3 1 -1 -2 3
 media 21 1 -1 -2 -3 10
 media 4 1 -1 -2 -3 -10 4
 boundary 4
unit 8
com='5 wt% UO2 partial length rod'
 cylinder 1    0.444            137.20    0
 cylinder 2   0.453            137.20    0
 cylinder 3    0.513            137.20    0
   cylinder 10    0.5888           137.20    0
 cuboid 4     4p0.6475    381             0
 media 1 1 1
 media 0 1 -1 2
 media 3 1 -1 -2 3
  media 21 1 -1 -2 -3 10
 media 4 1 -1 -2 -3 -10 4
 boundary 4
unit 9
com='single assembly-normal top'
 cuboid 1    4p6.4163     381            50.001
 array 1 1 place 5 5 1 -0.6475 -0.6475 0
 cuboid 2    4p 8.8000     381            50.001
 media 0            1 -1  2
 boundary 2
unit 10
com='single assembly-normal bottom'
 cuboid 1    4p6.4163     0.001           0
 array 1 1 place 5 5 1 -0.6475 -0.6475 0
 cuboid 2    4p 8.8000     0.001           0
 media 0            1 -1  2
 boundary 2
unit 11
com='5 wt% UO2 full length rod'
 cylinder 1    0.444            381             0
 cylinder 2   0.453            381             0
 cylinder 3    0.513            381             0
 cylinder 10    0.5888           381             0
 cuboid 4     4p0.9124    381             0
 media 11 1 1
 media 0 1 -1 2
 media 13 1 -1 -2 3
  media 23 1 -1 -2 -3 10
 media 14 1 -1 -2 -3 -10 4
 boundary 4
unit 12
 com='water rod'
 cuboid 1  4p0.9124    381             0
 media 19  1 1
```

```
 boundary 1
unit 16
com='5 wt% UO2 rod with 1.5          wt% GdO2'
 cylinder 1    0.444           381              0
 cylinder 2   0.453           381              0
 cylinder 3    0.513           381              0
 cylinder 10    0.5888          381              0
 cuboid  4     4p0.9124    381             0
 media 16 1 1
 media 0  1 -1 2
 media 18 1 -1 -2 3
 media 24 1 -1 -2 -3 10
 media 19 1 -1 -2 -3 -10 4
 boundary 4
unit 17
com='5 wt% UO2 partial length rod'
 cylinder 1    0.444            259.10    0
 cylinder 2   0.453            259.10    0
 cylinder 3    0.513            259.10    0
 cylinder 10    0.5888           259.10    0
 cuboid 4     4p0.9124    381             0
 media 11 1 1
 media 0 1 -1 2
 media 13 1 -1 -2 3
  media 23 1 -1 -2 -3 10
 media 14 1 -1 -2 -3 -10 4
 boundary 4
unit 18
com='5 wt% UO2 partial length rod'
 cylinder 1    0.444            137.20    0
 cylinder 2   0.453            137.20    0
 cylinder 3    0.513            137.20    0
 cylinder 10    0.5888           137.20    0
 cuboid 4     4p0.9124    381             0
 media 11 1 1
 media 0 1 -1 2
 media 13 1 -1 -2 3
   media 23 1 -1 -2 -3 10
 media 14 1 -1 -2 -3 -10 4
 boundary 4
unit 19
com='single assembly damaged section'
 cuboid 1     4p 8.8000      50.001         0.001
 array 2 1  place 5 5 1 -0.9124 -0.9124 0
 cuboid 2    4p 8.8000     50.001         0.001
 media 0            1 -1  2
 boundary 2
unit 21
 com='20 cm tall water box'
 cuboid 1    4p 8.8000     20  0
 media 0            1  1
 boundary 1
unit 22
 com='basic GNF2 assembly stack up'
 cuboid 1     4p 8.8000  381             0
 array 3 1  place 1 1 1 0 0 0
 boundary 1

unit 100
com='single fuel assembly in left half inner container'
```

```
 cuboid 1     4p8.8          419.25           -38.25
 hole 22 origin x=0 y=0 z=0
 media 0  1  1
 cuboid 2  2p8.9          8.8          -8.9          419.35       -38.35
 media 20 1 -1  2
 boundary 2
unit 101
com='single fuel assembly in right half inner container'
 cuboid 1     4p8.8          419.25           -38.25
 hole 22 origin x=0 y=0 z=0
 media 0  1  1
 cuboid 2  2p8.9          8.8          -8.9          419.35       -38.35
 media 20 1 -1  2
 boundary 2

unit 102
com='individual RAJ-II package'
 cuboid 1 2p17.8         8.8          -8.9          419.35       -38.35
 array 4 1 place 1 1 1 -8.9          0 0
 ypplane 6  8.9          8.8
 media 20 1  6  2
 cuboid 2  2p22.80 2p13.90 424.35        -43.35
 media 0  1  -1 2 -6
 cuboid 3  2p22.95 2p14.05  424.5         -43.5
 media 20 1  -1 -2  3
' shock absorbers
 cuboid 10 2p25   2p16.3 429.1         -48.1
 media 0 1  -1 -2 -3 10
 cuboid 11 2p35.8 2p32.0 429.1         -48.1
 media 0 1 -1 -2 -3 -10 11
 cuboid 4  2p35.8 2p32.0 443.7         -62.7
 media 0  1  -1 -2 -3 -10 -11 4
 cuboid 5  2p36.0 2p32.2  443.9         -62.9
 media 20 1  -1 -2 -3 -10 -11 -4  5
 boundary 5

 global
unit 103
com='pkg array 12x12'
cuboid 1     828.0    -36.0     740.6    -32.2      443.9         -62.9
 array 5 1  place 1 1 1 0 0 0
cuboid 2     848.0    -56.0     760.6    -52.2     463.9         -82.9
 media 30 1  -1 2
boundary 2

end geometry

read array

ara=5 nux=12 nuy=12 nuz=1 typ=square
com='Package array'
 fill
   144R102
 end fill

ara=1 nux=10 nuy=10 nuz=1 typ=square
com='array for nominal GNF2 lattice'
 fill
    1    1    1    1    7    7    1    1    1    1
    1    6    6    1    1    1    1    1    1    1
```

```
    1    6    6    6    1    1    1    6    1    1
    1    1    6    1    8    2    2    1    1    1
    7    1    1    8    8    2    2    1    1    7
    7    1    1    2    2    8    8    1    1    7
    1    1    1    2    2    8    1    1    1    1
    1    1    6    1    1    1    1    1    1    1
    1    1    1    1    1    1    1    1    1    1
    1    1    1    1    7    7    1    1    1    1
 end fill

ara=2 nux=10 nuy=10 nuz=1 typ=square
com='array for expanded GNF2 lattice'
 fill
    11    11    11    11    17    17    11    11    11    11
    11    16    16    11    11    11    11    11    11    11
    11    16    16    16    11    11    11    16    11    11
    11    11    16    11    18    12    12    11    11    11
    17    11    11    18    18    12    12    11    11    17
    17    11    11    12    12    18    18    11    11    17
    11    11    11    12    12    18    11    11    11    11
    11    11    16    11    11    11    11    11    11    11
    11    11    11    11    11    11    11    11    11    11
    11    11    11    11    17    17    11    11    11    11
 end fill

ara=3 nux=1 nuy=1 nuz=3 typ=square
com='array for complete fuel assembly'
 fill
  10
  19
   9
 end fill

ara=4 nux=2 nuy=1 nuz=1 typ=square
com='Left and right sides of inner boxes'
 fill
   100 101
 end fill

end array

read bounds
all=void
end bounds

end data
end
```

6.9.3 Gad Worth Evaluation and Pattern Selection Specifications

A set of BA rod locations is chosen to demonstrate a maximum credible reactivity for each fuel design. Constraints imposed on selection of BA locations for the package evaluation are consistent with actual fuel design objectives, and as such recognize that certain arrangements are not allowed. These constraints result in a demonstration of a maximum reactivity configuration for credible fuel designs only, not every conceivable arrangement of BA rods in the fuel lattice. The constraints

that are considered in selecting the BA rod locations for the purpose of the criticality assessment are summarized by the following rules with reference to Figure 6-24:

1. Rule of symmetry – BA rods shall be in positions that are symmetric across the major geometric diagonal defined from the control blade corner where:

    a. On the diagonal symmetry may be one or more individual BA rods.

    b. Off the diagonal symmetry shall be two BA rod positions. The average value of the two symmetric BA rod positions is tabulated and then corresponding least worth average pairs are selected.

2. No BA rod shall be located in the outermost edge or corner location of the fuel rod lattice

3. Partial length fuel rods shall not be BA rods.

4. At least one BA rod shall be located in three of the four fuel lattice quadrants.

5. Eight (8) Gad rods shall be selected.

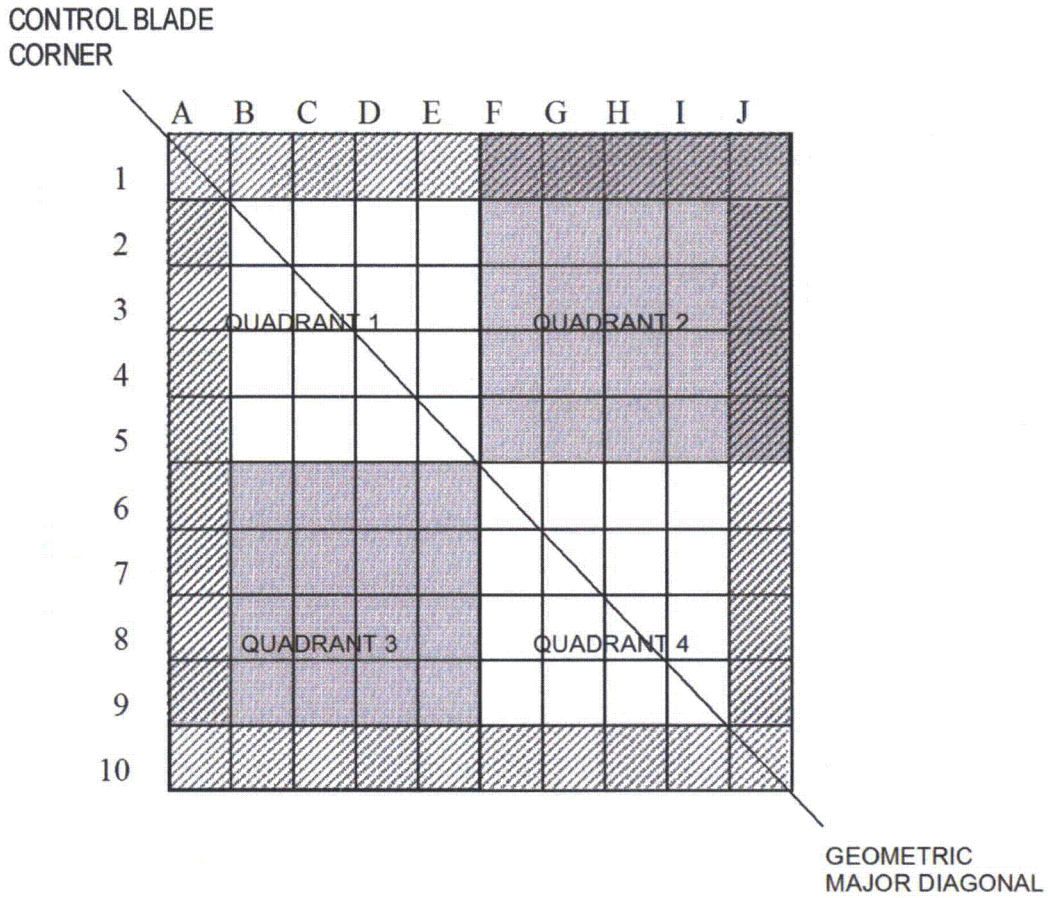

Figure 6-24 Fuel Lattice Description

A fuel lattice quadrant is defined by dividing the rows and columns of rods into four square lattices with equal numbers of rods referred to as quadrants. There are three zones considered in the selection of BA rod pairs that consist of two individual rods in positions that are symmetric across the geometric major diagonal.

ZONE A	Allowable rods in QUADRANT 1
ZONE B	Allowable rods in QUADRANT 2 and QUADRANT 4
ZONE C	Allowable rods in QUADRANT 3

Constraints placed on possible BA rod locations such that the locations chosen for the package evaluation are not necessarily the least worth BA rod locations. For example, the constraint requiring at least one BA rod to be located in three of the four fuel lattice or the rule of symmetry may result in selection of BA rod locations that may not be the least worth locations. In addition to fuel design constraints, lattice locations at the edge of the fuel bundle are not allowed, since these BA locations would be ineffective for transport conditions resulting in partial moderation in the fuel lattice.

As an example, the SVEA design is utilized here to demonstrate the application of the BA rod pattern selection process, through evaluation of the ^{157}Gd sensitivity coefficients of the infinite array results (displayed in Figure 6-25). Each rod position is associated with a material identification number assigned by the computer model (SCALE6/CSAS6).

A	B	C	D	E	F	G	H	I	J	
20	19	18	17	16	15	14	13	12	11	1
30	29 -2.2832E-03	28 -1.9420E-03	27 -1.9970E-03	26 -2.5205E-03	25 -2.6090E-03	24 -1.9613E-03	23 -1.9569E-03	22 -2.2919E-03	21	2
40	39 -1.9138E-03	38 -1.6502E-03	37 -1.7774E-03	36 -2.7852E-03	35 -2.6734E-03	34 -1.8492E-03	33 -1.6404E-03	32 -1.9248E-03	31	3
50	49 -1.9415E-03	48 -1.8267E-03	47 -2.7053E-03	46	45	44 -2.8217E-03	43 -1.8826E-03	42 -1.9808E-03	41	4
60	59 -2.5325E-03	58 -2.6794E-03	57	56	55	54	53 -2.7371E-03	52 -2.5971E-03	51	5
70	69 -2.5999E-03	68 -2.8032E-03	67	66	65	64	63 -2.8647E-03	62 -2.6076E-03	61	6
80	79 -1.9551E-03	78 -1.8649E-03	77 -2.8835E-03	76	75	74 -2.6898E-03	73 -1.8627E-03	72 -1.9603E-03	71	7
90	89 -1.8588E-03	88 -1.6393E-03	87 -1.8683E-03	86 -2.7777E-03	85 -2.7629E-03	84 -1.7999E-03	83 -1.6416E-03	82 -1.9201E-03	81	8
100	99 -2.3131E-03	98 -1.9008E-03	97 -1.9490E-03	96 -2.5318E-03	95 -2.5503E-03	94 -1.9825E-03	93 -1.9316E-03	92 -2.2942E-03	91	9
110	109	108	107	106	105	104	103	102	101	10

Figure 6-25 SVEA ^{157}Gd Sensitivity Results for Demonstration of Gad Pattern Selection

Step 1:

Select top 10 least worth Gad rod positions presented in ascending order of increasing worth

Location	Material ID	Worth
C8	88	-1.6393E-03
H3	33	-1.6404E-03
H8	83	-1.6416E-03
C3	38	-1.6502E-03
D3	37	-1.7774E-03
G8	84	-1.7999E-03
C4	48	-1.8267E-03
G3	34	-1.8492E-03
B8	89	-1.8588E-03
H7	73	-1.8627E-03

The individual rod locations will be used later in the process when selecting a single BA rod.

Step 2:

Averaging of BA rod pairs symmetric about the major diagonal

Starting in QUADRANT 1, calculate the average worth of rod pairs that are symmetric across and along the major diagonal. Rank the pairs in ascending order. Group the pairs by ZONE and rank the pairs within each ZONE based on average worth, with the least average worth being one.

The selection of the Gad rod pattern containing 8 Gad rods for each fuel design utilizes the least worth average among symmetric pairs to determine the least worth average per quadrant.

ZONE A

Location	Overall Rank	Zone Rank	Material ID	Average Worth
B3, C2	9	2	39, 28	-1.9279E-03
B2, C3	10	3	29, 38	-1.9667E-03
C4, D3	2	1	48, 37	-1.8021E-03
B 4, D2	11	4	49, 27	-1.9693E-03

ZONE B

Location	Overall Rank	Zone Rank	Material ID	Average Worth
C7, G3	4	2	78, 34	-1.8571E-03
C8, H3	1	1	88, 33	-1.6399E-03
D8, H4	5	3	87, 43	-1.8755E-03
B8, H2	6	4	89, 23	-1.9079E-03
C9, I3	7	5	98, 32	-1.9128E-03

ZONE C

Location	Overall Rank	Zone Rank	Material ID	Average Worth
G8, H7	3	1	84, 73	-1.8313E-03
G9, I7	13	4	94, 72	-1.9714E-03
H9, I8	8	2	93, 82	-1.9259E-03
H8, I9	12	3	83, 92	-1.9679E-03

Step 3:

Averaging of pairs per quadrant

Calculate the average worth of the 2 lowest ranked pairs in each ZONE from Step 2.

2 Lowest Rank Pairs (4 BA Rods)

ZONE	Rank	Locations	Average Worth
A	2	(C4, D3), (B3, C2)	-1.8650E-03
B	1	(C7, G3), (C8, H3)	-1.7485E-03
C	3	(G8, H7), (H9, I8)	-1.8786E-03

Select the lowest ranked ZONE BA rod pairing and calculate the average of the 3 lowest ranked pairs in that ZONE.

3 Lowest Rank Pairs (6 BA Rods)

ZONE	Locations	Average Worth
B	(C7, G3), (C8, H3) (D8, H4)	-1.8120E-03

Compare the 3 pair average to the averages for the 2 pair averages in the other two ZONES (A and C). If the 3 pair average is less than the 2 pair averages for the other two ZONES, these six BA rods locations are used. Otherwise, only the four BA rod locations defined by the 2 pair averages are used. In this example, the six BA rods locations in ZONE B are selected.

Step 4:

Select the remaining BA Rods

If six BA rods were defined by Step 3, then select the remaining two BA rod locations from the other ZONES. Otherwise, select remaining four BA rod locations by choosing two pairs of BA rods identified in Step 2 from the remaining ZONES. When selecting ZONE pairs, three quadrants must contain BA rods. Hence, if ZONE A or C has six BA rods, the remaining two BA rods must be in ZONE B, and vice versa for ZONE B. For this example the remaining two BA rod locations are D3 and C4 from ZONE A.

The eight BA rod locations selected based on the constraint design rules for this example are C7, G3, C8, H3, D8, H4, D3 and C4, shown in Figure 6-25 as the circled positions.

The following figures display the infinite array calculation results as Gad worth mapping for each rod position used to determine the BA rod positions shown in Table 6-9. The locations are determined for an infinite array of fuel bundles to represent the package array. Figure 6-26 through 6-32 show the ^{157}Gd relative worth for each viable BA rod position for each fuel design, respectively.

A	B	C	D	E	F	G	H	I	
30	29	28	27	26	25	24	23	21	1
40	39	38	37	36	35	34	33	31	2
		-2.8687E-03	-2.9344E-03		-2.8888E-03	-2.8962E-03			
50	49	48	47	46	45	44	43	41	3
	-2.8710E-03	**-2.3726E-03**	**-2.7637E-03**	-4.2530E-03	-3.7378E-03	**-2.7012E-03**	-2.9438E-03		
60	59	58	57	56	55	54	53	51	4
	-2.9418E-03	**-2.7749E-03**	-5.1526E-03			-3.8046E-03	-2.9352E-03		
70	69	68	67	66	65	64	63	61	5
		-4.1847E-03				-4.1314E-03			
80	79	78	77	76	75	74	73	71	6
	-2.9932E-03	-3.8200E-03			-4.9856E-03	**-2.7358E-03**	-2.8504E-03		
90	89	88	87	86	85	84	83	81	7
	-2.9742E-03	**-2.7225E-03**	-3.7998E-03	-4.1931E-03	-2.8040E-03	**-2.3654E-03**	-2.7906E-03		
100	99	98	97	96	95	94	93	91	8
		-2.9049E-03	-3.0433E-03		-2.8228E-03	**-2.7729E-03**			
110	109	108	107	106	105	104	103	101	9

Figure 6-26 GE11 Infinite Array ^{157}Gd Worth Mapping

A	B	C	D	E	F	G	H	I	
30	29	28	27	26	25	24	23	21	1
40	39	38	37	36	35	34	33	31	2
		-2.9681E-03	-2.9988E-03		-3.0154E-03	-2.9091E-03			
50	49	48	47	46	45	44	43	41	3
	-2.8647E-03	-2.4009E-03	-2.9143E-03	-4.3027E-03	-3.9003E-03	-2.7552E-03	-2.9734E-03		
60	59	58	57	56	55	54	53	51	4
	-2.9313E-03	-2.9115E-03	-5.1685E-03			-3.8306E-03	-3.0288E-03		
70	69	68	67	66	65	64	63	61	5
		-4.2148E-03				-4.2809E-03			
80	79	78	77	76	75	74	73	71	6
	-3.0686E-03	-3.8157E-03			-5.0960E-03	-2.8326E-03	-3.0122E-03		
90	89	88	87	86	85	84	83	81	7
	-3.0563E-03	-2.8165E-03	-3.8706E-03	-4.2439E-03	-2.8237E-03	-2.3687E-03	-2.8705E-03		
100	99	98	97	96	95	94	93	91	8
		-3.0163E-03	-3.0381E-03		-2.9009E-03	-2.9083E-03			
110	109	108	107	106	105	104	103	101	9

Figure 6-27 GE13 Infinite Array ^{157}Gd Worth Mapping

A	B	C	D	E	F	G	H	I	J	
20	19	18	17	16	15	14	13	12	11	1
----------	----------	----------	----------	----------	----------	----------	----------	----------	----------	
30	29	28	27	26	25	24	23	22	21	2
----------	----------	-2.3374E-03	----------	-2.1258E-03	-2.2150E-03	----------	-2.4818E-03	----------	----------	
40	39	38	37	36	35	34	33	32	31	3
----------	-2.3327E-03	-1.8085E-03	-1.8722E-03	-2.0616E-03	-2.8751E-03	-3.0322E-03	-2.1823E-03	-2.5760E-03	----------	
50	49	48	47	46	45	44	43	42	41	4
----------	----------	-1.8807E-03	-1.9750E-03	-3.2649E-03			-3.0571E-03	----------	----------	
60	59	58	57	56	55	54	53	52	51	5
----------	-2.2506E-03	-2.0863E-03	-3.3233E-03	----------			-2.7776E-03	-2.2151E-03	----------	
70	69	68	67	66	65	64	63	62	61	6
----------	-2.3276E-03	-2.8974E-03			----------	-3.3790E-03	-2.1064E-03	-2.2151E-03	----------	
80	79	78	77	76	75	74	73	72	71	7
----------	----------	-3.1364E-03			-3.2133E-03	-1.9640E-03	-1.8362E-03	----------	----------	
90	89	88	87	86	85	84	83	82	81	8
----------	-2.5162E-03	-2.2559E-03	-3.1257E-03	-2.8858E-03	-2.1266E-03	-1.8351E-03	-1.7918E-03	-2.4034E-03	----------	
100	99	98	97	96	95	94	93	92	91	9
----------	----------	-2.5166E-03	----------	-2.3097E-03	-2.1642E-03	----------	-2.3955E-03	----------	----------	
110	109	108	107	106	105	104	103	102	101	10
----------	----------	----------	----------	----------	----------	----------	----------	----------	----------	

Figure 6-28 GE12B Infinite Array ^{157}Gd Worth Mapping

A	B	C	D	E	F	G	H	I	J	
20	19	18	17	16	15	14	13	12	11	1
30	29	28	27	26	25	24	23	22	21	2
		-2.3785E-03		-2.2125E-03	-2.2811E-03		-2.5762E-03			
40	39	38	37	36	35	34	33	32	31	3
	-2.3989E-03	-1.8013E-03	-1.8702E-03	-2.0900E-03	-2.8133E-03	-3.0490E-03	-2.1646E-03	-2.5341E-03		
50	49	48	47	46	45	44	43	42	41	4
		-1.9050E-03	-1.9805E-03	-3.3408E-03			-3.0840E-03			
60	59	58	57	56	55	54	53	52	51	5
	-2.2089E-03	-2.0779E-03	-3.3136E-03				-2.8359E-03	-2.1960E-03		
70	69	68	67	66	65	64	63	62	61	6
	-2.2610E-03	-2.9902E-03				-3.2675E-03	-2.1312E-03	-2.1960E-03		
80	79	78	77	76	75	74	73	72	71	7
		-3.0613E-03			-3.2973E-03	-1.9944E-03	-1.8596E-03			
90	89	88	87	86	85	84	83	82	81	8
	-2.4873E-03	-2.2072E-03	-2.9936E-03	-2.8439E-03	-2.1377E-03	-1.8831E-03	-1.8708E-03	-2.3632E-03		
100	99	98	97	96	95	94	93	92	91	9
		-2.5105E-03		-2.2954E-03	-2.1768E-03		-2.4843E-03			
110	109	108	107	106	105	104	103	102	101	10

Figure 6-29 GE14C Infinite Array ^{157}Gd Worth Mapping

A	B	C	D	E	F	G	H	I	J	
20	19	18	17	16	15	14	13	12	11	1
30	29	28 -2.3475E-03	27	26 -2.1807E-03	25 -2.2801E-03	24	23 -2.5352E-03	22	21	2
40	39 -2.3782E-03	38 -1.7594E-03	37 -1.8283E-03	36 -2.0559E-03	35 -2.8931E-03	34 -3.0639E-03	33 -2.1635E-03	32 -2.5084E-03	31	3
50	49	48 -1.8295E-03	47 -1.9320E-03	46 -3.2653E-03	45	44	43 -3.0236E-03	42	41	4
60	59 -2.2551E-03	58 -2.1481E-03	57 -3.2801E-03	56	55	54	53 -2.8283E-03	52 -2.3333E-03	51	5
70	69 -2.2970E-03	68 -2.9581E-03	67	66	65	64 -3.4120E-03	63 -2.1087E-03	62 -2.2160E-03	61	6
80	79	78 -3.1614E-03	77	76	75 -3.3156E-03	74 -1.9639E-03	73 -1.8451E-03	72	71	7
90	89 -2.4753E-03	88 -2.2456E-03	87 -3.1001E-03	86 -2.9069E-03	85 -2.1385E-03	84 -1.8758E-03	83 -1.8110E-03	82 -2.3899E-03	81	8
100	99	98 -2.5054E-03	97	96 -2.3674E-03	95 -2.2446E-03	94	93 -2.4310E-03	92	91	9
110	109	108	107	106	105	104	103	102	101	10

Figure 6-30 GE14G Infinite Array ^{157}Gd Worth Mapping

A	B	C	D	E	F	G	H	I	J	
20	19	18	17	16	15	14	13	12	11	1
----------	----------	----------	----------	----------	----------	----------	----------	----------	----------	
30	29	28	27	26	25	24	23	22	21	2
----------	-1.9111E-03	-1.6956E-03	-1.7315E-03	-1.8216E-03	-1.8196E-03	-1.7923E-03	-1.7811E-03	-2.0002E-03	----------	
40	39	38	37	36	35	34	33	32	31	3
----------	-1.6842E-03	-1.4429E-03	-1.5534E-03	-2.0559E-03	-2.6179E-03	-2.4072E-03	-1.7405E-03	-1.7657E-03	----------	
50	49	48	47	46	45	44	43	42	41	4
----------	-1.6861E-03	-1.5876E-03	-2.3578E-03	----------			-2.4737E-03	-1.8370E-03	----------	
60	59	58	57	56	55	54	53	52	51	5
----------	-1.8004E-03	-2.1164E-03	----------	----------			-2.6166E-03	-1.8971E-03	----------	
70	69	68	67	66	65	64	63	62	61	6
----------	-1.8391E-03	-2.6220E-03			----------	----------	-2.0930E-03	-1.7944E-03	----------	
80	79	78	77	76	75	74	73	72	71	7
----------	-1.8564E-03	-2.5225E-03			----------	-2.3865E-03	-1.5977E-03	-1.6805E-03	----------	
90	89	88	87	86	85	84	83	82	81	8
----------	-1.7658E-03	-1.7595E-03	-2.4646E-03	-2.7683E-03	-2.1578E-03	-1.5964E-03	-1.4504E-03	-1.6828E-03	----------	
100	99	98	97	96	95	94	93	92	91	9
----------	-2.0328E-03	-1.7463E-03	-1.7932E-03	-1.8544E-03	-1.7722E-03	-1.7209E-03	-1.7192E-03	-1.9664E-03	----------	
110	109	108	107	106	105	104	103	102	101	10
----------	----------	----------	----------	----------	----------	----------	----------	----------	----------	

Figure 6-31 GNF2 Infinite Array ^{157}Gd Worth Mapping

A	B	C	D	E		F	G	H	I	J	
20	19	18	17	16		15	14	13	12	11	1
30	29	28	27	26		25	24	23	22	21	2
	-2.2832E-03	-1.9420E-03	-1.9970E-03	-2.5205E-03		-2.6090E-03	-1.9613E-03	-1.9569E-03	-2.2919E-03		
40	39	38	37	36		35	34	33	32	31	3
	-1.9138E-03	**-1.6502E-03**	**-1.7774E-03**	-2.7852E-03		-2.6734E-03	**-1.8492E-03**	**-1.6404E-03**	-1.9248E-03		
50	49	48	47	46		45	44	43	42	41	4
	-1.9415E-03	**-1.8267E-03**	-2.7053E-03				-2.8217E-03	-1.8826E-03	-1.9808E-03		
60	59	58	57	56		55	54	53	52	51	5
	-2.5325E-03	-2.6794E-03						-2.7371E-03	-2.5971E-03		
70	69	68	67	66		65	64	63	62	61	6
	-2.5999E-03	-2.8032E-03						-2.8647E-03	-2.6076E-03		
80	79	78	77	76		75	74	73	72	71	7
	-1.9551E-03	-1.8649E-03	-2.8835E-03				-2.6898E-03	**-1.8627E-03**	-1.9603E-03		
90	89	88	87	86		85	84	83	82	81	8
	-1.8588E-03	**-1.6393E-03**	-1.8683E-03	-2.7777E-03		-2.7629E-03	**-1.7999E-03**	**-1.6416E-03**	-1.9201E-03		
100	99	98	97	96		95	94	93	92	91	9
	-2.3131E-03	-1.9008E-03	-1.9490E-03	-2.5318E-03		-2.5503E-03	-1.9825E-03	-1.9316E-03	-2.2942E-03		
110	109	108	107	106		105	104	103	102	101	10

Figure 6-32 SVEA Infinite Array ^{157}Gd Worth Mapping

6.9.4 Fuel Bundle Lattice Expansion Evaluation

The effect on k_{eff} of increasing the lattice pitch in the fuel bundle is evaluated for a configuration that represents the individual package and package array. The effect is evaluated with and without the normal packing materials. The individual package evaluation is done without BA rods where as the package array evaluation is done with BA rods.

The sensitivity of k_{eff} to changes in lattice pitch is greater for an individual package configuration than for the package array configuration. The difference in sensitivity is due to the confinement of the lattice expansion to a 50 cm axial length. For the individual package configuration, the expanded lattice accounts for a major portion of the fissions occurring in a fully water reflected system. In the package array configuration, k_{eff} is influenced by the neutron interaction between fuel bundles, where about one-eighth of the length is an expanded lattice and the remainder is at nominal pitch.

6.9.4.1 Individual Package

An assessment is done with no burnable absorber rods for the individual package. The optimum k_{eff} occurs in a fuel rod pitch range of 1.9 to 2.3 cm. The optimum pitch corresponds to a packaging dimension that exceeds the dimension of the inner container (Figure 6-33 and 6-34, Tables 6-10 and 6-11). There is no significant effect on the range for optimum pitch due to inclusion of the normal packing material in the individual package. The 10X10 fuel types (GE12B, GE14C, GE14G, GNF2, and SVEA96) are the most reactive over the range of lattice expansion. The SVEA96, GNF2, and GE14G are the most reactive fuel bundle contents for the individual package.

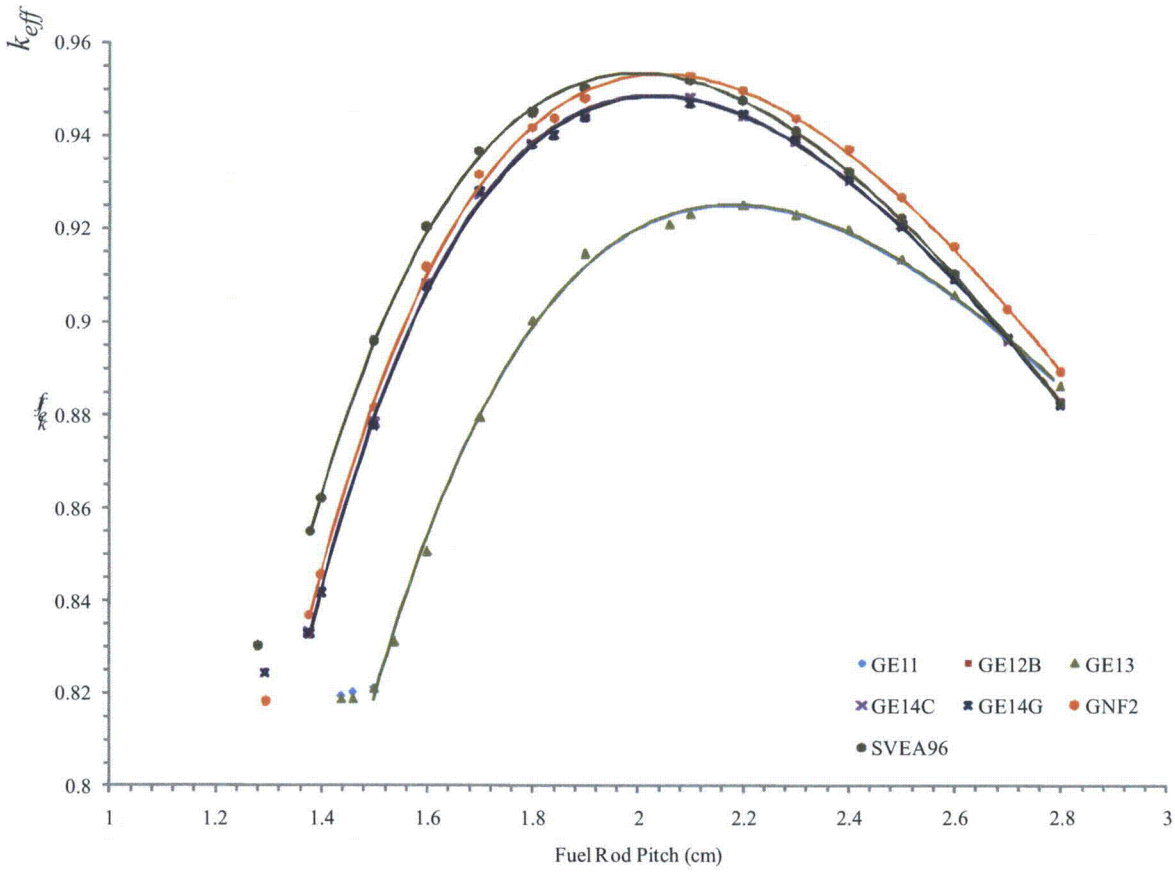

Figure 6-33 Lattice Expansion, Individual Package, without Normal Packing Materials

Table 6-46 Lattice Expansion, Individual Package, without Normal Packing Materials

Fuel Type	GE11		GE12B		GE13		GE14C		GE14G		GNF2		SVEA	
Pitch	k_{eff}	σ	k_{eff}	σ	k_{eff}	σ	k_{eff}	σ	k_{eff}	σ	k_{eff}	σ	k_{eff}	σ
Nominal	0.8195	0.00035	0.8239	0.00038	0.8188	0.00038	0.82447	0.00042	0.8244	0.00038	0.81825	0.00035	0.83026	0.0004
Fuel Channel	0.83223	0.00044	0.83207	0.00035	0.83122	0.00038	0.83322	0.00041	0.83287	0.0004	0.83683	0.00037	0.85492	0.00039
Inner Container	0.92183	0.00037	0.94028	0.00034	0.92069	0.00041	0.94009	0.00041	0.9399	0.00038	0.94373	0.0004	0.94525	0.00033
1.4			0.84136	0.0004			0.84183	0.00044	0.84177	0.00039	0.84553	0.00036	0.86214	0.00042
1.46	0.82043	0.00037			0.81882	0.00034								
1.5	0.82139	0.0004	0.87886	0.00038	0.82107	0.00035	0.8783	0.0004	0.87766	0.00034	0.88167	0.00042	0.89579	0.00035
1.6	0.85092	0.0004	0.9076	0.00049	0.85067	0.0004	0.90794	0.00038	0.90737	0.00039	0.91168	0.00037	0.92024	0.00035
1.7	0.87757	0.0004	0.92775	0.00036	0.87945	0.00037	0.92738	0.00042	0.9279	0.00041	0.93149	0.00043	0.9366	0.00035
1.8	0.90055	0.00035	0.93844	0.00039	0.90006	0.0037	0.93816	0.00047	0.93785	0.00039	0.94164	0.00042	0.94475	0.00035
1.9	0.91429	0.00037	0.94411	0.0004	0.9144	0.00037	0.94439	0.00037	0.94377	0.00039	0.94805	0.00037	0.95022	0.0004
2.1	0.923	0.00036	0.94795	0.00035	0.92287	0.00046	0.94813	0.0004	0.94688	0.0004	0.95271	0.00039	0.95184	0.00043
2.2	0.92426	0.00037	0.94464	0.0004	0.92481	0.00037	0.944	0.00037	0.94448	0.00033	0.94968	0.00036	0.94759	0.00042
2.3	0.92266	0.00037	0.93891	0.00038	0.92268	0.00039	0.93833	0.00035	0.93891	0.00038	0.94347	0.00039	0.9409	0.00039
2.4	0.9187	0.00033	0.92995	0.00033	0.91948	0.00037	0.93006	0.00032	0.93054	0.00033	0.93694	0.00048	0.93218	0.00036
2.5	0.91233	0.00038	0.92022	0.00044	0.9131	0.00047	0.92052	0.00038	0.92029	0.00035	0.92655	0.00032	0.92206	0.0004
2.6	0.90537	0.00045	0.90922	0.00037	0.90559	0.00031	0.9092	0.00036	0.90897	0.00039	0.91587	0.00038	0.91017	0.00035
2.7	0.896	0.00035	0.89648	0.00033	0.89626	0.00039	0.89586	0.00041	0.89622	0.00035	0.90267	0.0004	0.89614	0.00037
2.8	0.88591	0.00032	0.88275	0.00036	0.88606	0.00038	0.88237	0.00031	0.88205	0.00038	0.88913	0.0003	0.8825	0.00033

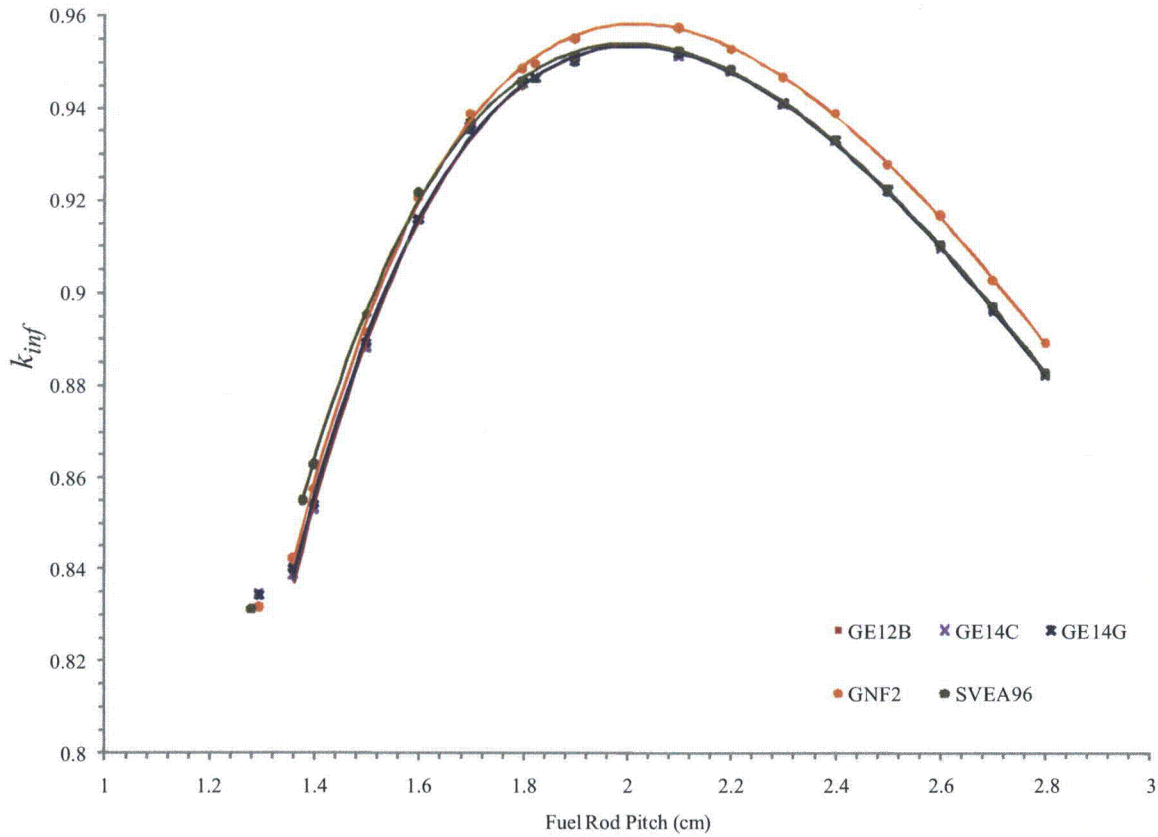

Figure 6-34 Lattice Expansion, Individual Package, with Normal Packing Materials

Table 6-47 Lattice Expansion, Individual Package, with Normal Packing Materials

Fuel Type	GE12B		GE14C		GE14G		GNF2		SVEA	
Pitch	k_{eff}	σ	k_{eff}	σ	k_{eff}	σ	k_{eff}	σ	k_{eff}	σ
Nominal	0.83474	0.00035	0.83477	0.00039	0.83426	0.00035	0.83166	0.00032	0.83121	0.00037
Fuel Channel	0.83817	0.00037	0.83885	0.00037	0.84013	0.00034	0.84232	0.00037	0.85499	0.00038
Inner Container	0.94573	0.00037	0.94631	0.00037	0.9465	0.00037	0.94968	0.00041	0.94491	0.00038
1.4	0.85246	0.00039	0.85318	0.00041	0.85406	0.00037	0.85731	0.0004	0.86285	0.00042
1.5	0.88782	0.00043	0.88819	0.00046	0.88926	0.00039	0.89147	0.0004	0.89524	0.00036
1.6	0.91625	0.00037	0.9158	0.00034	0.91579	0.00043	0.92044	0.00044	0.92157	0.00035
1.7	0.93562	0.00045	0.93568	0.00035	0.93504	0.0004	0.93868	0.00041	0.93685	0.00042
1.8	0.94455	0.00043	0.94523	0.00036	0.94581	0.00042	0.9486	0.00038	0.94541	0.00041
1.9	0.95041	0.00039	0.95099	0.00038	0.94993	0.00043	0.95505	0.00038	0.9512	0.00042
2.1	0.9519	0.00043	0.95132	0.00034	0.95163	0.00033	0.95735	0.00035	0.95232	0.00032
2.2	0.9473	0.00033	0.94782	0.00036	0.94797	0.00032	0.95265	0.00032	0.94839	0.00035
2.3	0.9407	0.00038	0.94047	0.00036	0.94084	0.00037	0.94664	0.00038	0.94095	0.00035
2.4	0.93258	0.00037	0.93266	0.00033	0.93282	0.00034	0.93859	0.00035	0.93298	0.0004
2.5	0.92219	0.00037	0.92208	0.0004	0.92173	0.00035	0.92759	0.00036	0.92226	0.00041
2.6	0.90996	0.00036	0.90953	0.00039	0.91011	0.00035	0.9166	0.00038	0.91008	0.00035
2.7	0.89685	0.00032	0.89687	0.0004	0.89597	0.00034	0.90267	0.00033	0.897	0.00033
2.8	0.88224	0.00039	0.88229	0.00035	0.88226	0.00035	0.88921	0.00036	0.8825	0.00033

6.9.4.2 Package Array

The package array assessment is done with eight, 2 weight percent Gd_2O_3 burnable absorber rods in three quadrants. Neutron absorber is most effective at the larger fuel rod pitch and results in the optimum k_{eff} in a fuel rod pitch in a range of 1.5 to 2.0 cm that corresponds to the confinement provided by the inner container (Figure 6-16 and 6-17, Tables 6-12 and 6-13). The presence of BA rod neutron absorber shifts the optimum pitch within the inner container confinement boundaries. The 10X10 fuel types (GE12B, GE14C, GE14G, GNF2, and SVEA96) are the most reactive over the range of lattice expansion. The GE and GNF fuel types include more normal packing material than the SVEA, but the SVEA fuel has more moderation with the fuel lattice due to the design of the coolant flow channels within the lattice. These differences result in changes in an increase in k_{eff} for the GE and GNF2 fuel types when the normal packing material is included that is not seen for the SVEA96 fuel type. The cluster separator packing material is not included when the GE and GNF fuel type contents is shipped as a fuel assembly (fuel bundle with channel installed). SVEA96 fuel bundles are always shipped with the channel installed. Although there are not large differences in the reactivity of the 10X10 fuel designs, the SVEA96, GNF2, and GE14G are the most reactive fuel bundle contents for the package array configuration.

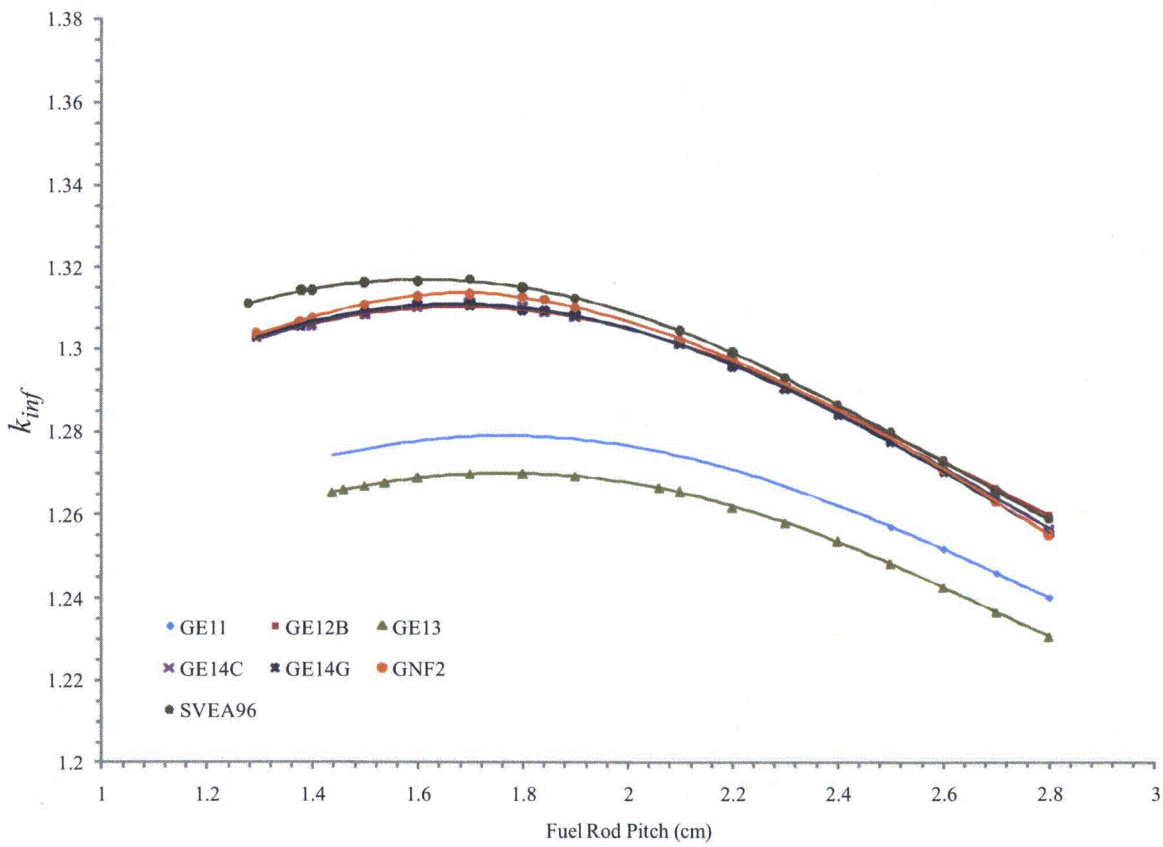

Figure 6-35 Lattice Expansion, Infinite Package Array, without Normal Packing Materials

Table 6-48 Lattice Expansion, Infinite Package Array, without Normal Packing Materials

Fuel Type	GE11		GE12B		GE13		GE14C		GE14G		GNF2		SVEA	
Pitch	k_{inf}	σ	k_{inf}	σ	k_{inf}	σ	k_{inf}	σ	k_{inf}	σ	k_{inf}	σ	k_{inf}	σ
Nominal	1.27444	0.00028	1.30242	0.00031	1.26548	0.00027	1.30279	0.0003	1.30309	0.00028	1.30377	0.00026	1.31122	0.00027
Fuel Channel	1.27663	0.00031	1.30564	0.00027	1.2676	0.00026	1.30577	0.00025	1.30572	0.0003	1.30675	0.00029	1.31454	0.00031
Inner Container	1.27518	0.00027	1.30941	0.00033	1.26639	0.00025	1.30922	0.00027	1.30948	0.0003	1.31218	0.00026	1.3149	0.00028
1.4			1.30623	0.00027			1.30591	0.0003	1.30666	0.00027	1.30784	0.00025	1.31451	0.0003
1.46	1.27468	0.00027			1.26595	0.00028								
1.5	1.27602	0.00031	1.30851	0.00026	1.26692	0.00027	1.30861	0.00026	1.30908	0.00026	1.31089	0.00031	1.31642	0.00027
1.6	1.27807	0.00026	1.31018	0.0003	1.26894	0.00027	1.31061	0.00029	1.31107	0.00026	1.31294	0.0003	1.31668	0.00029
1.7	1.27891	0.00028	1.31038	0.0003	1.26971	0.00027	1.31146	0.00031	1.31094	0.00029	1.31361	0.00029	1.31725	0.00029
1.8	1.27906	0.00028	1.30993	0.00027	1.2697	0.0003	1.31043	0.00029	1.30938	0.00032	1.3127	0.00028	1.31511	0.00026
1.9	1.27835	0.00035	1.30802	0.00029	1.26917	0.00027	1.30783	0.00028	1.30833	0.00027	1.31028	0.00029	1.31256	0.00026
2.1	1.27393	0.00028	1.30116	0.00029	1.26552	0.00028	1.30135	0.0003	1.30126	0.00029	1.30214	0.00029	1.30449	0.00026
2.2	1.27078	0.00026	1.29625	0.00027	1.26171	0.00029	1.29646	0.00029	1.29582	0.0003	1.29739	0.00026	1.29913	0.00027
2.3	1.26693	0.00027	1.29162	0.00026	1.25797	0.00028	1.2906	0.00027	1.29049	0.00026	1.29119	0.00027	1.29288	0.00027
2.4	1.26267	0.00026	1.28522	0.0003	1.25358	0.00029	1.28432	0.00028	1.28409	0.0003	1.28543	0.00026	1.28629	0.00029
2.5	1.2569	0.00029	1.27954	0.00028	1.24822	0.00027	1.27828	0.00026	1.27753	0.00026	1.27854	0.00028	1.27973	0.0003
2.6	1.25169	0.00027	1.27272	0.00027	1.24241	0.00027	1.27112	0.00026	1.27013	0.00029	1.27081	0.00028	1.27294	0.00036
2.7	1.24592	0.00028	1.26587	0.00026	1.23656	0.00026	1.26421	0.00028	1.26322	0.00029	1.26331	0.00027	1.26579	0.00029
2.8	1.24006	0.00028	1.25986	0.00028	1.23057	0.00025	1.25647	0.00032	1.25554	0.00029	1.25512	0.00027	1.25897	0.00026

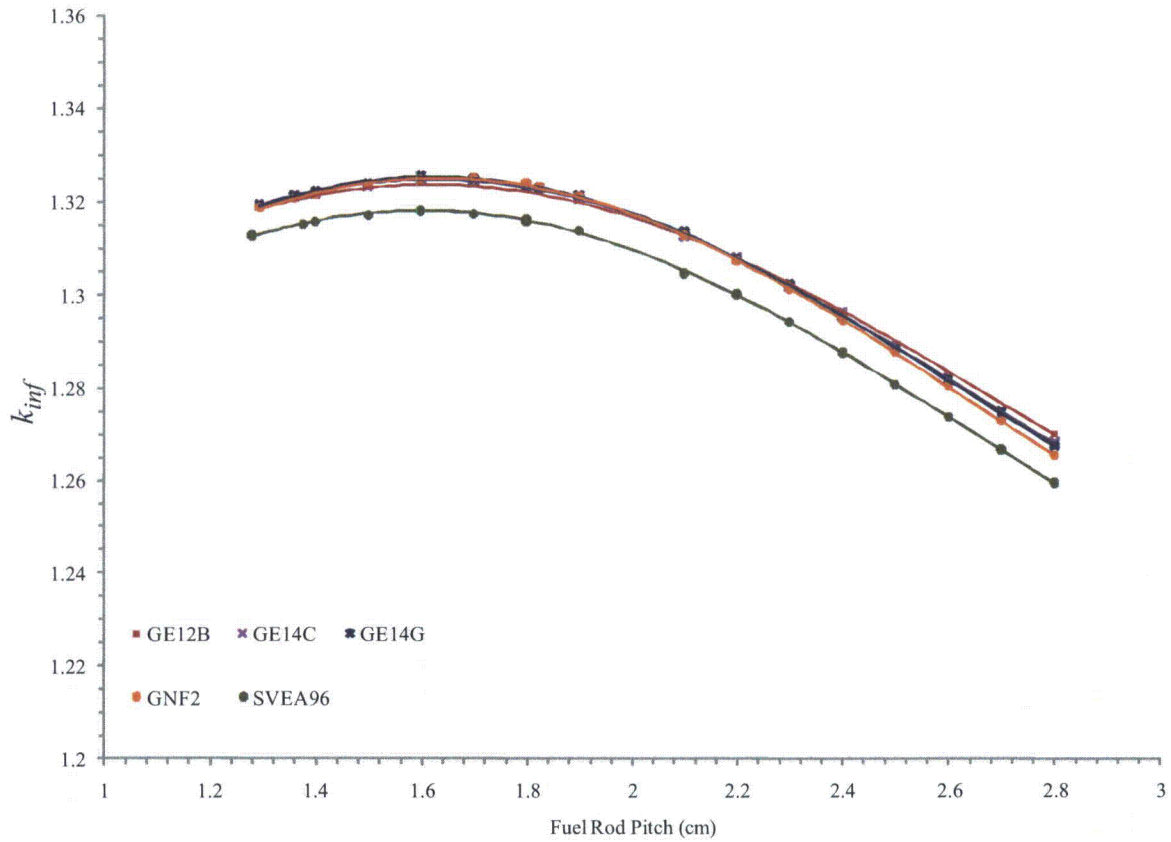

Figure 6-36 Lattice Expansion, Infinite Package Array, with Normal Packing Materials

Table 6-49 Lattice Expansion, Infinite Package Array, with Normal Packing Materials

Fuel Type	GE12B		GE14C		GE14G		GNF2		SVEA	
Pitch	k_{inf}	σ	k_{inf}	σ	k_{inf}	σ	k_{inf}	σ	k_{inf}	σ
Nominal	1.31829	0.00033	1.31883	0.00029	1.31934	0.00028	1.31874	0.00027	1.31264	0.00026
Fuel Channel	1.32024	0.00028	1.3212	0.00029	1.32129	0.00031	1.32057	0.00029	1.31497	0.00028
Inner Container	1.32136	0.00028	1.32279	0.00026	1.32286	0.00027	1.32309	0.00027	1.31604	0.00026
1.4	1.32097	0.00028	1.32175	0.00026	1.32211	0.00027	1.32146	0.00029	1.31555	0.00026
1.5	1.32312	0.00027	1.32341	0.0003	1.32391	0.00031	1.32353	0.0003	1.31703	0.00026
1.6	1.32298	0.00029	1.3246	0.0003	1.32554	0.0003	1.32487	0.00027	1.318	0.00028
1.7	1.32326	0.00027	1.32434	0.00026	1.32489	0.00029	1.32495	0.0003	1.31723	0.00028
1.8	1.32231	0.00029	1.32343	0.00028	1.3233	0.00027	1.3238	0.00027	1.31558	0.00027
1.9	1.31943	0.00027	1.32043	0.00025	1.32117	0.00029	1.32114	0.0003	1.31364	0.00027
2.1	1.31229	0.00028	1.31237	0.00027	1.31355	0.00026	1.31265	0.00028	1.3046	0.0003
2.2	1.30805	0.00026	1.30775	0.00028	1.30762	0.00032	1.30718	0.00027	1.30011	0.00028
2.3	1.30253	0.00026	1.3017	0.00028	1.30223	0.00027	1.30125	0.00028	1.29415	0.00028
2.4	1.29644	0.00028	1.29601	0.00025	1.29514	0.00028	1.29452	0.00027	1.28758	0.00027
2.5	1.28997	0.00026	1.28881	0.00028	1.2884	0.00027	1.2877	0.0003	1.28072	0.00032
2.6	1.28359	0.00031	1.28232	0.00027	1.28204	0.00027	1.28056	0.00027	1.27378	0.00027
2.7	1.27693	0.00025	1.2749	0.00035	1.27484	0.00033	1.27296	0.0003	1.26664	0.0003
2.8	1.27002	0.00032	1.2681	0.00028	1.26743	0.00028	1.26529	0.00027	1.25937	0.00027

6.9.5 Fuel Rod Contents Evaluation

The fuel rod contents are evaluated by calculating an infinite k_{eff} for a range of fuel rod pitches that encompasses peak reactivity to determine a maximum reactivity. The fuel rod designs are categorized by cylindrical dimensions and evaluated based on category dimensions, as shown in Table 6-50. The longest fuel length of the fuel types per category is used to represent that particular fuel rod category. An optimum configuration of fuel rod pitch and diameter as determined by this evaluation is used in the package assessment for transport of fuel rods.

Table 6-50 Fuel Rod Parameters

Fuel Category	Fuel OR	Gap OR	Clad OR	Fuel Length	Fuel Types
BWR_W1	0.424	0.4315	0.492	390	SVEA
BWR_G1	0.478	0.4875	0.599	370.84	GE11, GE13
BWR_G2	0.438	0.447	0.513	405.5	GE12B, GE14C, GE14G
BWR_G3	0.444	0.453	0.513	381	GNF2
PWR_W1	0.4374	0.4463	0.508	365.76	14OFA
PWR_W2	0.4647	0.4742	0.5359	365.76	14STD, 15OFA
PWR_W3	0.4839	0.4928	0.5588	347.218	CE14
PWR_W4	0.4096	0.4178	0.475	381	16STD, CE16 NGF, 17STD
PWR_W5	0.3922	0.4001	0.4572	365.76	16NGF, 17OFA, VV6
PWR_W6	0.4128	0.4216	0.4851	381	CE16NVA
PWR_W7	0.4128	0.4216	0.4851	381	CE16VA, CE16

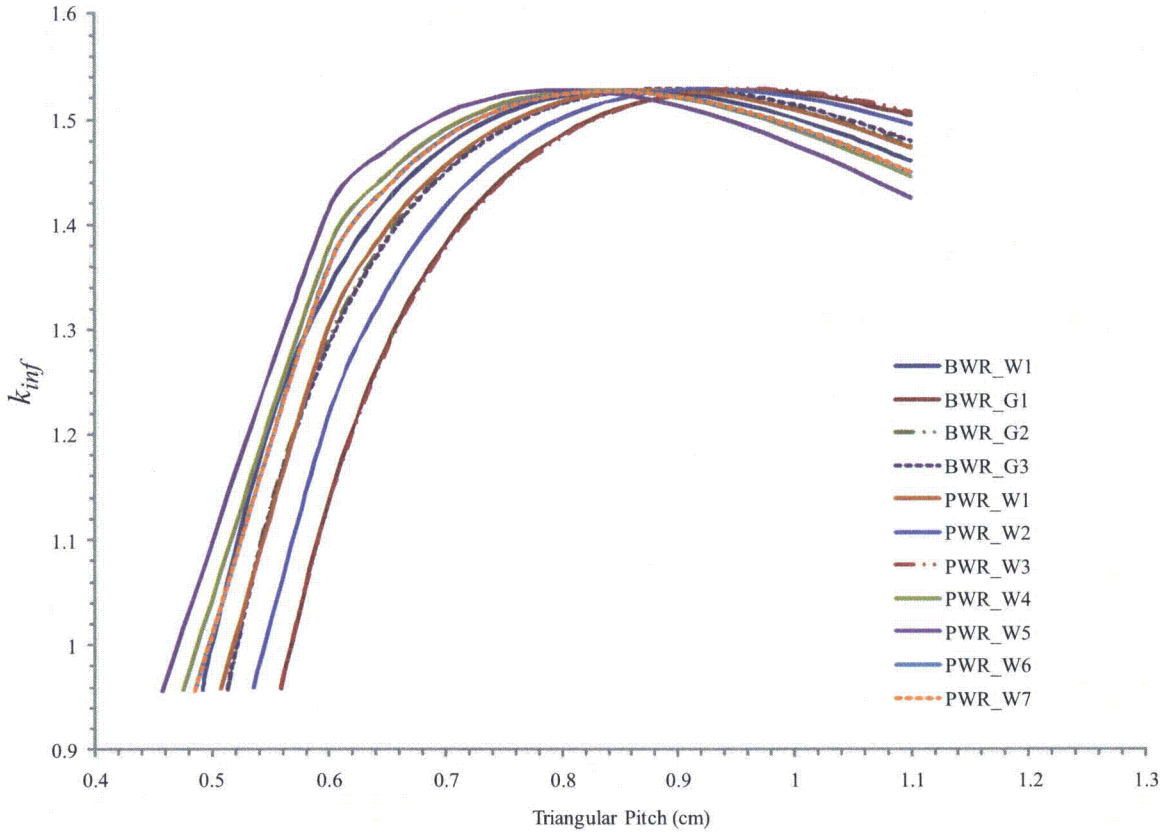

Figure 6-37 Rod Fuel Infinite Array Comparison

Table 6-51 Fuel Rod Infinite Array Comparison (k_{inf})

Fuel Type	BWR_W1	BWR_G1	BWR_G2	BWR_G3	PWR_W1	PWR_W2	PWR_W3	PWR_W4	PWR_W5	PWR_W6	PWR_W7
Rod OR	0.95768	0.95902	0.95792	0.95939	0.9587	0.9602	0.96001	0.95801	0.957	0.95708	0.95684
0.6	1.33954	1.13639	1.28849	1.28455	1.29977	1.2151	1.13445	1.37752	1.41322	1.35947	1.3589
0.65	1.42166	1.28401	1.38782	1.38419	1.39485	1.33633	1.2807	1.44705	1.47046	1.43558	1.43512
0.7	1.47346	1.38005	1.4512	1.4484	1.45572	1.4155	1.37682	1.48985	1.5041	1.48263	1.4823
0.75	1.5047	1.44317	1.49085	1.48906	1.49376	1.46717	1.44055	1.51424	1.52127	1.50999	1.50979
0.8	1.52113	1.48405	1.51385	1.5131	1.51565	1.49976	1.48222	1.52531	1.52641	1.52326	1.52318
0.85	1.52685	1.50908	1.52463	1.52489	1.52563	1.51847	1.5081	1.52624	1.5225	1.52604	1.52608
0.9	1.52411	1.52194	1.52616	1.52738	1.52656	1.52672	1.52182	1.51983	1.51164	1.52083	1.52097
0.95	1.51487	1.52663	1.52052	1.52264	1.52046	1.52689	1.52731	1.50729	1.49537	1.5094	1.50964
1.0	1.5005	1.52387	1.50925	1.51219	1.50882	1.5207	1.52532	1.49006	1.47486	1.49308	1.49341
1.05	1.48206	1.51554	1.49349	1.4972	1.49276	1.50943	1.51771	1.4691	1.45101	1.4729	1.47331
1.1	1.46038	1.50273	1.47415	1.47857	1.47318	1.49408	1.50556	1.4452	1.42456	1.44966	1.45015

6.9.6 Effect on Packaging Materials

The effect of packaging materials is evaluated by calculating the effect that the material has on k_p relative to a reference configuration as follows:

Individual package	Water in all void space and water in regions normally filled with thermal insulator, foam cushion, and impact limiter. Establishes a reference value for k_{eff} that maximizes neutron reflection for the confinement system.
Package array	Void in regions normally filled with thermal insulator, foam cushion, and impact limiter. Water filled in the fuel region. Establish a reference value for k_{eff} for neutron interaction between packages.

For both the individual package and package array the fuel bundle is moderated with full density water and polyethylene representing the cluster separators and plastic sheath is always present in Region 3 for the evaluations.

The packaging configurations are described as follows:

Water	Full density water in all spaces inside packaging that is normally void, thermal insulator, packing material, or impact limiter. Reference package configuration for individual package is described as Water (1,2,3,4)
Void	Void in all spaces inside packaging that is normally thermal insulator, packing material, or impact limiter. Reference package configuration for package array is described as Void (1,2,4).
AlSi (1)	Thermal insulator between the inner and outer walls of the inner container
Poly (2)	Foam cushion is intact and limits the expansion of fuel rods inside the inner container.
Pack Material (3)	Cluster separators and plastic sheath plus the melted foam cushion in the fuel bundle.
Char (4)	Char in regions normally occupied by impact limiter material (balsa wood or cardboard) in the outer container.

The effect of the packaging material is characterized by the difference in k_{eff} as follows:

$$\Delta k_p = k_p \text{ (Reference)} - k_p \text{ (Packaging Configuration)}$$

6.9.6.1 Individual Package

The effect of the packaging material for an individual package is evaluated using GE14C and SVEA fuel bundle contents. Figures 6-36 and 6-37 show the effects of the packaging materials on an individual package for the following packaging material configurations:

AlSi(1), Water (2,3,4)
Poly(2), Water (1,3,4)
Pack Material (3), Water (1,2,4)
Char (4), Water(1,2,3)

The effects of the packaging materials as summarized in Table 6-33 have some dependence on the fuel rod pitch associated with the confinement boundary dimension. All configurations with exception of the foam cushion redistribution to the fuel rod, *Pack Material (3), Water (1,2,4),* result in a decrease in k_p.

Table 6-52 Packaging Material Effects, Single Package

Fuel Type	Packaging Configuration Material (Region)	Confinement Boundary Nominal Δk_p	Fuel Channel Δk_p	Inner Container Δk_p	Δk_p *Average*
GNF2					
	AlSi (1) Water (2,3,4)	-0.02865	-0.03250	-0.06059	-0.04058
	Poly (2), Water (1,3,4)	-0.02959	-0.03220	-0.12701	-0.06293
	Pack Material (3), Water (1,2,4)	0.00542	0.00453	0.00322	0.00439
	Char (4), Water (1,2,3)	-0.00159	-0.00173	-0.00433	-0.00255
SVEA					
	AlSi (1) Water (2,3,4)	-0.03215	-0.03745	-0.06237	-0.04399
	Poly (2), Water (1,3,4)	-0.03204	-0.03639	-0.12581	-0.06475
	Pack Material (3), Water (1,2,4)	0.00587	0.00284	0.00195	0.00355
	Char (4), Water (1,2,3)	-0.00234	-0.00146	-0.00415	-0.00265
AVERAGE for SVEA and GNF2					
	AlSi (1) Water (2,3,4)	-0.03040	-0.03498	-0.06148	-0.04229
	Poly (2), Water (1,3,4)	-0.03082	-0.03430	-0.12641	-0.06384
	Pack Material (3), Water (1,2,4)	0.00565	0.00369	0.00256	0.00397
	Char (4), Water (1,2,3)	-0.00196	-0.00160	-0.00424	-0.00260

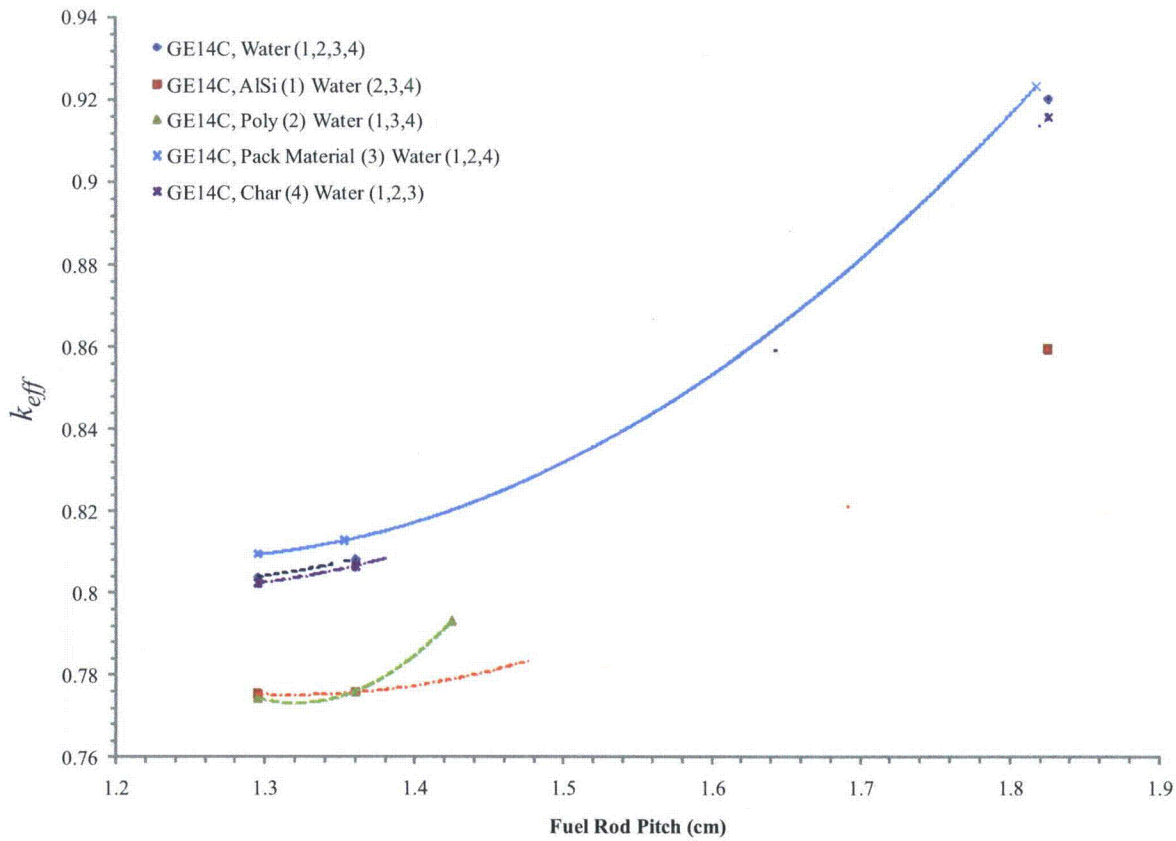

Packaging Configuration	Confinement Boundary					
	Nominal		Fuel Channel		Inner Container	
Material (Region)	k_p	σ_p	k_p	σ_p	k_p	σ_p
Water (1,2,3,4)	0.80397	0.00041	0.80825	0.00035	0.92011	0.00039
AlSi (1) Water (2,3,4)	0.77532	0.00034	0.77575	0.00031	0.85952	0.00034
Poly (2), Water (1,3,4)	0.77438	0.00033	0.77605	0.00033	0.7931	0.00036
Pack Material (3), Water (1,2,4)	0.80939	0.00033	0.81278	0.00037	0.92333	0.00036
Char (4), Water (1,2,3)	0.80238	0.00034	0.80652	0.00033	0.91578	0.00035

Figure 6-38 Packaging Material Effects, Single Package GE14C

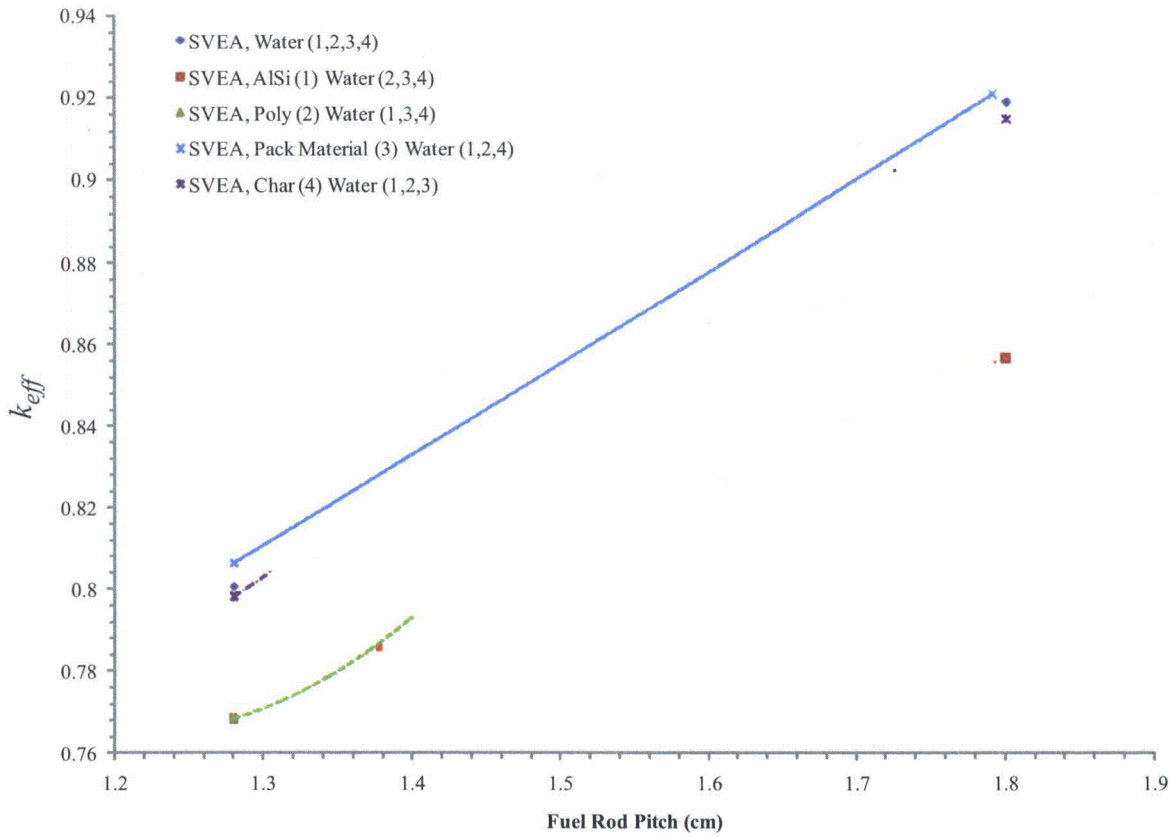

Packaging Configuration	Confinement Boundary					
	Nominal		Fuel Channel		Inner Container	
Material (Region)	k_p	σ_p	k_p	σ_p	k_p	σ_p
Water (1,2,3,4)	0.80053	0.00038	0.82325	0.00043	0.91905	0.00039
AlSi (1) Water (2,3,4)	0.76838	0.00036	0.7858	0.00036	0.85668	0.00039
Poly (2), Water (1,3,4)	0.76849	0.00038	0.78686	0.00035	0.79324	0.00036
Pack Material (3), Water (1,2,4)	0.80640	0.00041	0.82609	0.00039	0.921	0.00036
Char (4), Water (1,2,3)	0.79819	0.0004	0.82179	0.00046	0.9149	0.00038

Figure 6-39 Packaging Material Effects, Single Package SVEA

6.9.6.2 Package Array

The effect of the packaging material for the package array is evaluated using a GE14C and SVEA fuel bundle contents. Figures 6-38 and 6-39 show the effects of the packaging materials on a package array for the following packaging material configurations:

AlSi (1) Void (2,4)
Poly (2), Void (1,4)
Pack Material (3), Void (1,2,4)
Char (4), Void (1,2)

The effects of the packaging materials as summarized in Table 6-34 have some dependence on the fuel rod pitch associated with the confinement boundary dimension. All configurations with exception of the foam cushion redistribution to the fuel rod, *Pack Material (3), Water (1,2,4),* result in a decrease in k_p.

Table 6-53 Packaging Material Effects, Package Array

		Confinement Boundary			
Fuel Type	**Packaging Configuration Material (Region)**	**Nominal** Δk_p	**Fuel Channel** Δk_p	**Inner Container** Δk_p	Δk_p ***Average***
GNF2					
	AlSi (1) Water (2,3,4)	-0.00327	-0.00332	-0.00320	-0.00326
	Poly (2), Water (1,3,4)	-0.01314	-0.01346	-0.01601	-0.01420
	Pack Material (3), Water (1,2,4)	0.00324	0.00292	0.00221	0.00279
	Char (4), Water (1,2,3)	-0.00725	-0.00676	-0.00642	-0.00681
SVEA					
	AlSi (1) Water (2,3,4)	-0.00270	-0.00328	-0.00264	-0.00287
	Poly (2), Water (1,3,4)	-0.00812	-0.00909	-0.01003	-0.00908
	Pack Material (3), Water (1,2,4)	0.00396	0.00335	0.00231	0.00321
	Char (4), Water (1,2,3)	-0.00545	-0.00634	-0.00628	-0.00602
AVERAGE for SVEA and GNF2					
	AlSi (1) Water (2,3,4)	-0.00135	-0.00164	-0.00132	-0.00144
	Poly (2), Water (1,3,4)	-0.00570	-0.0062	-0.00662	-0.00617
	Pack Material (3), Water (1,2,4)	0.00360	0.00314	0.00226	0.00300
	Char (4), Water (1,2,3)	-0.00110	-0.00171	-0.00204	-0.00162

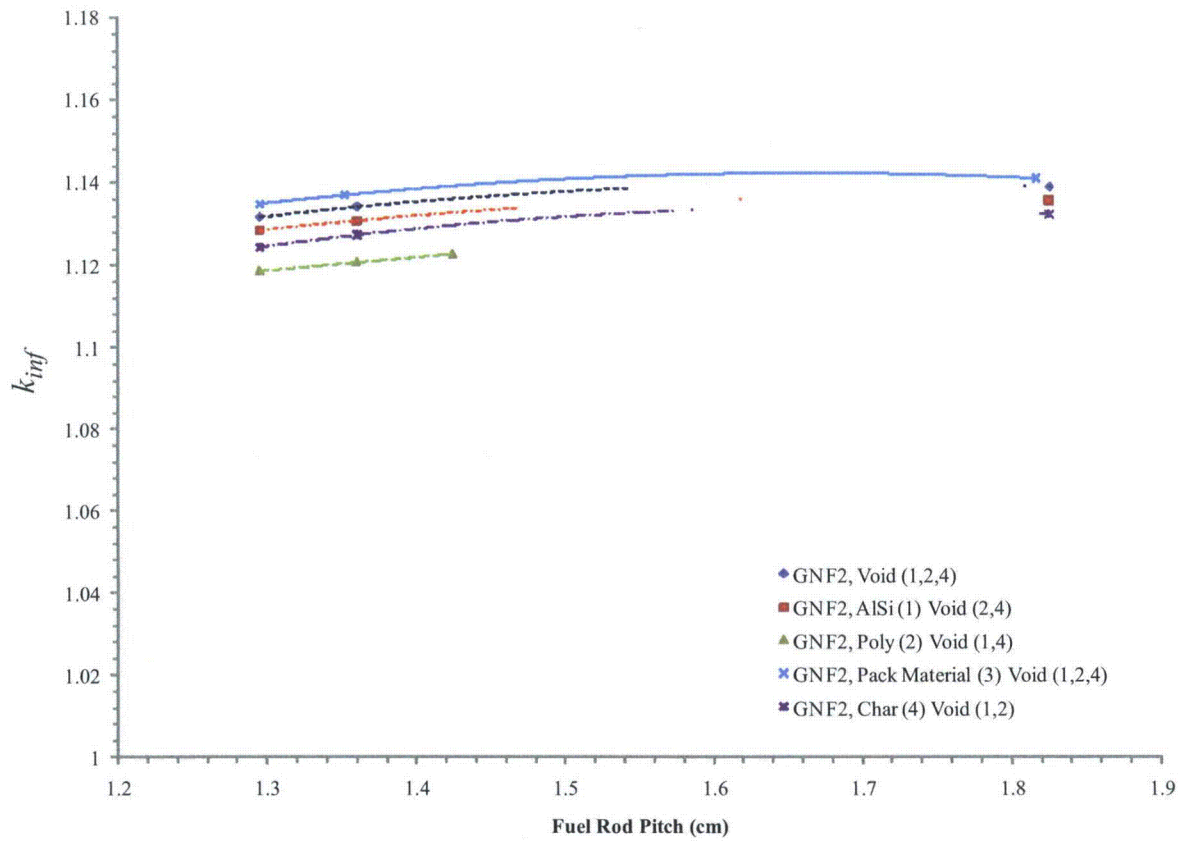

Packaging Configuration	Confinement Boundary					
	Nominal		Fuel Channel		Inner Container	
Material (Region)	k_p	σ_p	k_p	σ_p	k_p	σ_p
Water (1,2,3,4)	1.13173	0.00028	1.13417	0.00026	1.13883	0.00026
AlSi (1) Water (2,3,4)	1.12846	0.0003	1.13085	0.00025	1.13563	0.0003
Poly (2), Water (1,3,4)	1.11859	0.00026	1.12071	0.0003	1.12282	0.00032
Pack Material (3), Water (1,2,4)	1.13497	0.0003	1.13709	0.00025	1.14104	0.0003
Char (4), Water (1,2,3)	1.12448	0.00029	1.12741	0.00031	1.13241	0.00028

Figure 6-40 Packaging Material Effects, Package Array (Infinite), GNF2

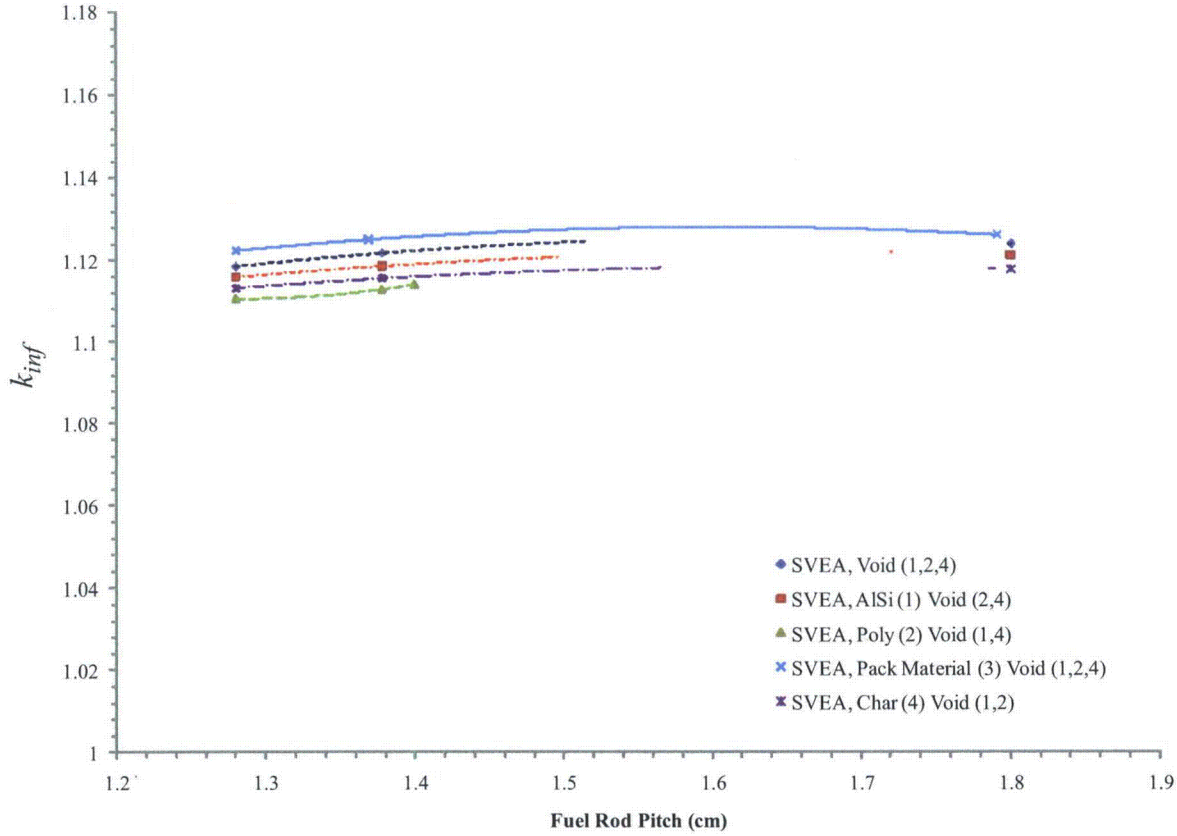

Packaging Configuration	Confinement Boundary					
	Nominal		Fuel Channel		Inner Container	
Material (Region)	k_p	σ_p	k_p	σ_p	k_p	σ_p
Water (1,2,3,4)	1.1185	0.00029	1.12180	0.00028	1.12392	0.00027
AlSi (1) Water (2,3,4)	1.11580	0.00027	1.11852	0.00025	1.12128	0.00026
Poly (2), Water (1,3,4)	1.11038	0.00026	1.11271	0.0003	1.11389	0.00026
Pack Material (3), Water (1,2,4)	1.12246	0.00035	1.12515	0.00028	1.12623	0.00029
Char (4), Water (1,2,3)	1.11305	0.00029	1.11546	0.00027	1.11764	0.00029

Figure 6-41 Packaging Material Effect, Package Array (Infinite), SVEA

6.9.7 Validation Details

Case No	Case Name	k_{eff}	± s	Enr. (wt%)	Ref.	AEG	EALF(ev)	Pitch (cm)	H2O/ fuel vol.	H/X	Plate matl.	Boron concen. (wt%)	Plate thick (cm)	No. of holes/ pin	Clad	Assembly separ. (cm)	Dancoff factor
1	ANS33AL1	1.0067	0.0029	4.74	5	199	0.2243	1.35	2.302	138.4	AL	-	.30	-	AL	5.0	0.20091
2	ANS33AL2	1.0168	0.0029	4.74	5	201	0.1913	1.35	2.302	138.4	AL	-	.30	-	AL	2.5	0.20091
3	ANS33AL3	1.0006	0.0029	4.74	5	202.2	0.1721	1.35	2.302	138.4	AL	-	.30	-	AL	10.0	0.20091
8	ANS33SLG	0.9932	0.0029	4.74	5	201	0.1903	1.35	2.302	138.4	-	-	-	-	AL	5.0	0.20091
20	BW1484C1	0.9966	0.0029	2.46		201.3	0.1853	1.636	1.84	204.5	-	-	-	-	AL	1.636	0.190713
21	BW1484C2	0.9983	0.0029	2.46		204.2	0.1466	1.636	1.84	204.5	-	-	-	-	AL	4.908	0.190713
24	BW1484SL	0.9992	0.0029	2.46	6	205	0.1365	1.636	1.841	216.1	-	-	-	-	AL	6.54	0.190713
32	BW1810B	0.9948	0.0029	2.46		198.3	0.2396	1.636	1.84	204.5	-	0.1171	-	0.032	AL	-	0.19044
33	BW1810CR	0.984	0.0029	4.02		194.2	0.3377	1.636	1.84	125.1	-	0.1499	-	0.039	AL	-	0.18662
34	BW1810D	0.9975	0.0005	4.02		194.5	0.3291	1.636	1.84	125.1	-	0.1653	-	0.032	AL	-	0.18662
35	BW1810E	0.9926	0.0029	4.02		194.5	0.3287	1.636	1.84	125.1	-	0.1579	-	0.034	AL	-	0.18662
45	EPRU65	1.0036	0.0029	2.35	7	197.7	0.2483	1.562	1.196	163.6	-	-	-	-	AL	-	0.277268
47	EPRU75	0.9994	0.0029	2.35	7	207.2	0.112	1.905	2.408	329.4	-	-	-	-	AL	-	0.116741
49	EPRU87	1.0027	0.0029	2.35	7	210.8	0.0823	2.210	3.687	504.2	-	-	-	-	AL	-	0.057303
	NC1_K6	0.999	0.013	3.00		2.00E+02	0.203	1.52	1.49	135.7	-	-	-	-	AL		0.243215
	NC10_K6	1.0094	0.0029	3.00		1.98E+02	0.2442	1.52	1.49	135.7	-	-	-	-	AL		0.243215
	NC11_K6	1.0024	0.0029	3.00		1.98E+02	0.2453	1.52	1.49	135.7	-	-	-	-	AL		0.243215
	NC12_K6	0.0125	0.0029	3.00		1.98E+02	0.2269	1.52	1.49	135.7	-	-	-	-	AL		0.243215
	NC13_K6	1.0071	0.0029	3.00		1.99E+02	0.2268	1.52	1.49	135.7	-	-	-	-	AL		0.243215
	NC14_K6	1.0071	0.0029	3.00		1.99E+02	0.2333	1.52	1.49	135.7	-	-	-	-	AL		0.243215
	NC15_K6	0.996	0.016	3.00		1.99E+02	0.2072	1.52	1.49	135.7	-	-	-	-	AL		0.243215
	NC2_K6	1.008	0.014	3.00		2.00E+02	0.2061	1.52	1.49	135.7	-	-	-	-	AL		0.243215
	NC3_K6	0.98	0.013	3.00		2.00E+02	0.2662	1.52	1.49	135.7	-	-	-	-	AL		0.243215
	NC4_K6	0.959	0.014	3.00		1.97E+02	0.2666	1.52	1.49	135.7	-	-	-	-	AL		0.243215
	NC5_K6	0.0966	0.013	3.00		1.97E+02	0.2547	1.52	1.49	135.7	-	-	-	-	AL		0.243215
	NC6_K6	1.0019	0.0029	3.00		1.97E+02	0.2286	1.52	1.49	135.7	-	-	-	-	AL		0.243215

Case No	Case Name	k_{eff}	± s	Enr. (wt%)	Ref.	AEG	EALF(ev)	Pitch (cm)	H2O/ fuel vol.	H/X	Plate matl.	Boron concen. (wt%)	Plate thick (cm)	No. of holes/ pin	Clad	Assembly separ. (cm)	Dancoff factor
	NC7_K6	1.0008	0.0029	3.00		1.98E+02	0.2327	1.52	1.49	135.7	-	-	-	-	AL		0.243215
	NC8_K6	0.9991	0.0029	3.00		1.99E+02	0.232	1.52	1.49	135.7	-	-	-	-	AL		0.243215
	NC9_K6	1.0138	0.0029	3.00		1.99E+02	0.2428	1.52	1.49	135.7	-	-	-	-	AL		0.243215
54	NSE71SQ	0.9969	0.0053	4.74	8	201.2	0.1879	1.26	1.823	110.0	-	-	-	-	AL	-	0.25704
55	NSE71W1	1.0082	0.0029	4.74	8	198.2	0.2398	1.26	1.823	110.0	-	-	-	.054	AL	-	0.25704
56	NSE71W2	0.9937	0.0051	4.74	8	199.3	0.2183	1.26	1.823	110.0	-	-	-	.152	AL	-	0.25704
	NSE71W2+FOD	1.0563	0.0007	4.74		200.1	0.2056	1.26	1.71	98.4	-	-	-	.152	AL	-	0.262591
	NSE71W2+H2O	1.0139	0.0053	4.74		201.6	0.181	1.26	1.82	105.0	-	-	-	.152	AL	-	0.25704
57	P2438AL	0.9931	0.0029	2.35	9	209.2	0.09545	2.032	2.918	398.7	AL	-	.625	-	AL	8.67	0.08633
58	P2438BA	0.9968	0.0029	2.35	9	208.8	0.09873	2.032	2.918	398.7	B	28.7	.713	-	AL	5.05	0.08633
60	P2438SLG	0.9968	0.0029	2.35	9	209.2	0.09541	2.032	2.918	398.7	-	-	-	-	AL	8.39	0.08633
61	P2438SS	0.9965	0.0029	2.35	9	209.1	0.09625	2.032	2.918	398.7	SS	-	.485	-	AL	6.88	0.25704
63	P2615AL	1.0007	0.0029	4.31	19	207.7	0.1129	2.540	3.883	256.1	AL	-	.625	-	AL	10.72	0.038898
64	P2615BA	1.0016	0.0029	4.31	19	207.6	0.1144	2.540	3.883	256.1	B	28.7	.713	-	AL	6.72	0.038898
68	P2615SS	0.9995	0.0029	4.31	19	207.6	0.1137	2.540	3.883	256.1	SS	-	.485	-	AL	8.58	0.038898
74	P2827SLG	0.985	0.012	2.35	10	209.2	0.09535	2.032	2.918	398.7	-	-	-	-	AL	8.31	0.08633
79	P3314AL	0.9985	0.0029	4.31	11	199	0.2299	1.892	1.60	105.4	AL	-	.625	-	AL	9.04	0.172843
80	P3314BA	1.0004	0.0029	4.31	11	195.1	0.3134	1.892	1.60	105.4	B	28.7	.713	-	AL	4.80	0.172843
81	P3314BC	0.9983	0.0029	4.31	11	202.7	0.1655	1.892	1.60	105.4	B	31.9	.231	-	AL	3.53	0.172843
82	P3314BF1	0.9949	0.0029	4.31	11	197.9	0.251	1.892	1.60	105.4	BF	-	.546	-	AL	3.60	0.172843
83	P3314BF2	0.9965	0.0029	4.31	11	198.5	0.2392	1.892	1.60	105.4	BF	-	.772	-	AL	4.94	0.200956
84	P3314BS1	0.9932	0.0029	2.35	11	198	0.2503	1.684	1.60	218.6	SS	1.1	.298	-	AL	3.86	0.200956
85	P3314BS2	0.9937	0.0029	2.35	11	199	0.2314	1.684	1.60	218.6	SS	1.6	.298	-	AL	3.46	0.200956
86	P3314BS3	0.986	0.017	4.31	11	199.2	0.2274	1.892	1.60	105.4	SS	1.1	.298	-	AL	7.23	0.200956
87	P3314BS4	0.9942	0.0029	4.31	11	196.2	0.2889	1.892	1.60	105.4	SS	1.6	.298	-	AL	6.63	0.200956
96	P3314SLG	0.9928	0.0029	4.31	11	196.2	0.2869	1.892	1.60	105.4	-	-	-	-	AL	10.86	0.172843
97	P3314SS1	0.9895	0.0029	4.31	11	202.1	0.7936	1.892	1.60	105.4	SS	-	.302	-	AL	3.38	0.200956
98	P3314SS2	0.9949	0.0029	4.31	11	202.2	0.1727	1.892	1.60	105.4	SS	-	.302	-	AL	11.55	0.200956
99	P3314SS3	0.9962	0.0029	4.31	11	195.2	0.3122	1.892	1.60	105.4	SS	-	.485	-	AL	4.47	0.200956

7.0 PACKAGE OPERATIONS

This chapter provides general instructions for loading and unloading and operation of the RAJ-II package. Specific detailed procedures based on and consistent with this application are used for the operation of the package. These procedures are maintained by the user of the package and may provide additional detail regarding the handling and operation of the package. Due to the low specific activity and low abundance of gamma emitting radionuclides, dose rates from the contents of the package when used as a Type A or Type B package are minimal. As a result of the low dose rates, there are no special handling requirements for radiation protection.

7.1 PACKAGE LOADING

This section delineates the procedures for loading a payload into the RAJ-II packaging. Hereafter, reference to specific RAJ-II packaging components may be found in Appendix 1.4.1.

7.1.1 Preparation for Loading

Prior to loading the RAJ-II with fuel, the packaging is inspected to ensure that it is in unimpaired physical condition. The inspection looks for damage, dents, corrosion, and missing hardware. Acceptable conditions are defined by the drawings in Section 1.3.2 as described in Section 8.1. Acceptance criteria and detailed loading procedures derived from this application are specified in user written procedures. These user procedures are specific to the authorized content of the package. Since the primary containment is the sealed fuel rod, radiation and contamination surveys are not required prior to loading. There is no required moderator, neutron absorbers or gaskets that require testing or inspection.

Defects that require repair will be fixed prior to shipping in accordance with approved procedures consistent with the quality program.

When used as a Type B package, verification that the primary containment (i.e., fuel rods have been leak checked) will be performed prior to shipping.

7.1.2 Loading of Contents

7.1.2.1 Outer Container Lid Removal

6. Remove the lid bolts.

7. Attach slings to the four lid lift attachment points on the lid.

8. Remove the outer lid.

7.1.2.2 Inner Container Removal

1. Release the inner clamp by removing the eight clamp bolts.

2. Remove the inner container from the outer container, and move it onto the packing table. Ensure that the inner container is lifted using the inner container handles and not the inner container lid handles.

3. Remove the bolts of the inner container lid and take the lid off.

7.1.2.3 Loading Fuel Assemblies into the RAJ-II

1. Clamp the inner container body to the packing table or up righting device, and remove the end lid.

2. Ensure that the following preparation work for packing has been completed if required.

   - The separators have been inserted.
   - The finger spring protectors have been attached.
   - The foam has been put in place.
   - The fuel assemblies have been covered with poly bags.

3. Stand the packing table upright. (The inner container body is fixed with clamps.)

4. Lift one fuel assembly and pack it in the inner container.

5. After packing one fuel assembly into the inner container, fit the securing fixtures of the fuel assembly. Then pack the other fuel assembly in the inner container

6. Lower the packing table back to the horizontal position from the upright position.

7. Attach the end lid of the inner container.

8. Check to ensure that the fuel assemblies are packaged in the container properly.

9. Attach the inner container lid and tighten the bolts securely (wrench tight or as defined in user procedures).

10. Place the inner container into the outer container.

11. Put on hold down clamps and tighten bolts.

12. Place the outer container lid on the package, and tighten the bolts securely (wrench tight or as defined in user procedures).

13. Install tamper-indicating devices on the outer container ends.

7.1.2.4 Loading Loose Rods in the Protective Case into the RAJ-II

1. Insert poly endcap spacers over each end or the fuel rod endcap (optional).

2. Sleeve (optional) each rod to be packed with a maximum of 5 mil polyethylene sleeve/tubing.

3. Insert up to 30, 10x10 design rods, 26, 9x9 design rods or 22, 8x8 design rods into the protective case and fill any empty space with empty tubing.

4. Place cushioning foam pads in protective case as needed to prevent sliding during shipment (optional).

5. Close the protective case and tighten bolts wrench tight.

7.1.2.5 Loading the Protective Case into the RAJ-II

1. Loose rods may be loaded in the protective case while either in the inner container or while removed from the inner container.

2. After packing the protective case(s) into the inner container, fit the securing fixtures for the case.

3. Check to ensure that the protective cases are packaged in the container properly.

4. Attach the inner container lid and tighten the bolts securely (wrench tight or as defined in user procedures).

5. Put on hold down clamps and tighten bolts.

6. Place the outer container lid on the package, and tighten the bolts securely (wrench tight or as defined in user procedures).

7. Install tamper-indicating devices on the outer container ends.

8. It is allowable to ship only one protective case in an RAJ-II inner.

7.1.2.6 Loading Loose Rods in the 5-Inch Stainless Steel Pipe into the RAJ-II

1. Sleeve (optional) each rod to be packed with a maximum of 5 mil polyethylene sleeve/tubing. The ends of the sleeves should be closed in a manner such as knotting or taping with the excess polyethylene trimmed away.

2. Place a cushioning foam pad in the capped end of the pipe (optional).

3. Insert up to 30, 10x10 design rods, 26, 9x9 design rods or 22, 8x8 design rods into the pipe and fill the empty space with empty zircaloy tubing with welded end plugs on both ends.

4. Place cushioning foam pads against the rod ends to block the rods from sliding during shipment (optional).

5. Close pipe with end cap.

6. Lift each 5-inch stainless steel pipe and pack it in the inner container.

7. Check to ensure that the 5-inch stainless steel pipe(s) is packaged in the container properly.

8. Attach the inner container lid and tighten the bolts securely (wrench tight or as defined in user procedures).

9. Place the outer container lid on the package, and tighten the bolts securely (wrench tight or as defined in user procedures).

10. Install tamper-indicating devices on the outer container ends.

11. It is allowable to ship one or two 5-inch pipes containing rods in an RAJ-II inner.

7.1.2.7 Loading Loose Rods (25 Maximum Per Side) into the RAJ-II

1. Sleeve (optional) each rod to be packed with a maximum of 5 mil polyethylene sleeve/tubing. The ends of the sleeves should be closed in a manner such as knotting or taping with the excess polyethylene trimmed away.

2. When only one rod per side is to be packed, no clamps are required. Block the rod in the lower corner of the container by evenly spacing 10 or more notched foam pads the length of the rod.

3. When 2 rods up to a maximum of 25 rods are to be packed, banding with steel clamps is not required for criticality safety purposes. If banding is chosen, position 10 or more open steel clamps evenly in each side of the inner container in which loose rods are place.

4. Place foam pads on top of the open clamps, lay the rods on top of the foam.

5. Close and tighten the clamps so the foam surrounds the array of rods. Tighten each clamp until the foam collapses slightly.

6. Place foam pads against the ends of the rods, above the rods and beside the rods to block the rods from moving during shipment.

7. Repeat the above steps for the other side of the inner container, if required.

8. Fill each side (if used) with foam pads so as to minimize movement during shipment.

9. Attach the inner container lid and tighten the bolts securely (wrench tight or as defined by user procedure).

10. Place the outer container lid on the package, and tighten the bolts securely (wrench tight as defined by user procedure).

11. Install tamper-indicating devices on the outer container ends.

7.1.3 Preparation for Transport

When used as a type B package leak testing of the rods (primary containment) is performed during the manufacturing process. Verification of successful leak testing is done prior to shipment. There are no surface temperature measurements required for this package.

Procedure: (These steps may be performed in any sequence.)

1. Complete the necessary shipping papers in accordance with Subpart C of 49 CFR 172.

2. Ensure that the RAJ-II package markings are in accordance with 10 CFR 71.85(c) and Subpart D of 49 CFR 172. Package labeling shall be in accordance with Subpart E of 49 CFR 172. Package placarding shall be in accordance with Subpart F of 49 CFR 172.

3. Survey the surface of the package for potential contamination and dose rates.

4. Transfer the package to the conveyance and secure using tie-downs secured to the package.

7.2 PACKAGE UNLOADING

7.2.1 Receipt of Package from Carrier

Radiation and contamination surveys are performed upon receipt of the package and the packages are inspected for significant damage. There are no fission gases, coolants or solid contaminants to be removed.

7.2.2 Removal of Contents

After freeing the tie downs, the RAJ-II package is lifted from the carrier either by fork lift or by the use of lifting slings placed around the package. If lifted by forklift, the forks are placed at the designated lift locations and the package is lifted. If slings lift the package, a sling is placed under each end of the package at the lifting angles that prevent the sling from sliding. Care should be taken to ensure that the slings are placed in the correct location depending on whether the package is loaded or empty.

7.2.2.1 Outer Container Lid Removal

1. Remove the lid bolts.
2. Attach slings to the four sling fittings on the lid.
3. Remove the outer lid.

7.2.2.2 Inner Container Removal

1. Release the inner clamp by removing the eight clamp bolts.
2. Remove the inner container from the outer container, and move it onto the packing table. Ensure that the inner container is lifted using the appropriate inner container handles and not the inner container lid handles.
3. Remove the bolts of the inner container lid and take the lid off.

7.2.2.3 Unloading Fuel Assemblies from the RAJ-II

1. Clamp the inner container body to the packing table or up righting device, and remove the end lid.
2. Stand the packing table upright. (The inner container body is fixed with clamps.)
3. Attach the lifting device to the assembly and remove the securing fixture.
4. Lift one fuel assembly at a time from the package.
5. Repeat for other assembly.

7.2.2.4 Removing / Unloading Protective Case or 5-Inch Stainless Steel Pipe from the RAJ-II

1. Remove the outer container and inner container lids as described in Sections 7.2.2.1 and 7.2.2.2.

2. The inner container may be removed or left in place while removing the protective case or 5-inch pipe.

3. Remove the 5-inch stainless steel pipe with a sling or remove the cover from the protective case.

4. Remove the rods from the 5-inch pipe or protective case.

7.3 PREPARATION OF EMPTY PACKAGE FOR TRANSPORT

Empty RAJ-II's are prepared and transported per the requirements of 49 CFR 173.428. Prior to shipping as an empty RAJ-II, the packaging is surveyed to assure that contamination levels are less than the 49 CFR 173.433(a) limit. The RAJ-II is visually verified as being empty. The packaging is inspected to assure that it is in an unimpaired condition and is securely closed so that there will be no leakage of material under conditions normally incident to transportation.

Any labels previously applied in conformance with subpart E of part 172 of this subchapter are removed, obliterated, or covered and the "Empty" label prescribed in 49 CFR 172.450 of this subchapter is affixed to the packaging.

7.4 OTHER OPERATIONS

The following are considered normal routine maintenance items and do not require QA or Engineering evaluation for replacement. Material must be of the same type as original equipment parts.

- Wooden Bolster Assemblies
- Bolster Bolting
- Delrin Inserts
- Polyethylene Container Guides
- Gaskets
- Shock Absorbers (Paper Honeycomb)
- Fork Pocket Rubber Protective Pads
- Outer Container Stopper #2 (Rubber Pad)
- Safety Walk
- Plastic Plugs
- Lid Tightening Bolts (Outer, Inner and End Lid)

- Inner Container End Face Lumber (Upper)
- Inner Container End Face Lumber (Lower "Y" Block)
- Inner Container Polyethylene Foam
- Heliserts

When deviations to items other than those listed above are identified, the RAJ-II shall be removed from service, and the item(s) shall be identified as non-conforming material, and dispositioned in accordance with written procedures including the 10 CFR 71, Subpart H approved QA Plan.

7.5 APPENDIX

No additional information is required. Loading and unloading this package is a relatively simple and routine operation. The weights, contamination levels and radiation dose rates do not impose significant hazards or operations outside normal material handling.

Note: The regulatory provided, such as 49 CFR and 10 CFR, are the current requirements. If regulatory change, the new are applicable. This applies throughout the SAR.

8.0 ACCEPTANCE TESTS AND MAINTENANCE PROGRAM

8.1 ACCEPTANCE TESTS

Per the requirements of subpart G of 10 CFR 71, this section discusses the inspections and tests to be performed prior to first use of the RAJ-II. The RAJ-II is to be manufactured under a Quality Assurance Program meeting the requirements of 10 CFR 71 subpart H and 10 CFR 21.

8.1.1 Visual Inspections and Measurements

Prior to the first use of the RAJ-II for the shipment of licensed material, the RAJ-II will be inspected to ensure that it is conspicuously and durably marked with its model number, serial number, gross weight and package identification number assigned by NRC. Prior to applying the model number, it will be determined that the RAJ-II was fabricated in accordance with the drawings reference in the NRC Certificate of Compliance.

Critical dimensions related to quality are those with tolerances on the drawings called out in Appendix 1.3.2. Data for these dimensions shall be recorded and verified in accordance with the quality plan. Dimensions are to be taken in an unloaded, horizontal condition. Documentation of these measurements is to be compiled in a data pack. This data pack will be checked for completeness for each RAJ-II as part of the acceptance program. Dimensions without tolerances may vary to ensure form, function and fit by the fabricator.

RAJ-II's are inspected to ensure that there are no missing parts (nuts, bolts, shock absorbers, gaskets, plugs, etc.) or components and that there is no shipping damage on receipt.

The inner and outer container shall be weighed and recorded in the data pack to verify compliance to the maximum weights as called out on the drawings in Appendix 1.3.2.

8.1.2 Weld Examinations

RAJ-II packaging materials of construction and welds shall be examined in accordance with requirements delineated on the drawings in Appendix 1.3.2, per the requirements of 10 CFR 71.85(a). This includes 100% VT and liquid penetrant (LP) examination of the horizontal (loaded position – 4 places) lifting lugs and the vertical lifting lugs (2 places) for the inner container, and both outer container sling hold angles (4 places). All such required VT and LP examinations shall occur after the double load test (below).

The non-destructive examination personnel qualification and certification shall be in accordance with either The American Society for Non-destructive Testing (ASNT) SNT-TC-1A (recommended practice) or Japanese Society for Non-destructive Inspection (JSND) Japanese Industrial Standard (JIS) JIS Z 2305 latest revision.

8.1.3 Structural and Pressure Tests

The RAJ-II is not pressurized and is structurally the same as the test units.

All outer and inner containers shall be load tested at twice their maximum design weight. The maximum design weight for the inner container is 992 kg, and that for the outer is 1614 kg. Each shall be tested by an approximately equally distributed weight, and shall be held for a minimum of 2 minutes. Afterwards the affected welds shall have a VT and LP examination, per the above.

The inner container shall be tested horizontally only at the loaded (outside) lifting lugs. The vertical lugs can be tested in either the horizontal position (via hydraulics) or vertically.

The outer container shall be checked by fork lift or other suitable device at the fork lift pockets, and then again via slings at the two sling hold angle positions (three tests total).

Record of load tests and VT and PT examinations shall be in the data packs.

8.1.4 Leakage Tests

No leak tests of the packaging are required. The fuel rod weld joints are examined at the time of fuel fabrication and leak tested to ensure they are sealed. The welding and leak testing of fuel rods is performed during manufacturing using a qualified process. This process assures that the fuel is acceptable for use in a nuclear reactor core and is tightly controlled. The acceptable leak rate is less than 1×10^{-7} atm-cc/s. The inner and outer container are not relied on for containment, and do not require leak testing.

8.1.5 Component and Material Tests

The RAJ-II packaging does not contain gaskets that perform a safety function or pressure boundary, and as such, do not require testing. Neither the inner nor outer container lids are required to provide an air or water tight seal.

The packaging does not contain neutron absorbers that would require testing. No component tests are required.

Material testing or certifications from the suppliers of material for this container must show compliance to the properties found in Tables 2-2 and 2-3, or to other properties that satisfactorily indicate compliance to the properties found in these tables and that are approved by the licensee.

8.1.6 Shielding Tests

The RAJ-II packaging does not contain shielding and therefore shielding tests are not required.

8.1.7 Thermal Tests

The alumina silicate thermal properties will be assured by procuring this material with a certified pedigree that shows compliance to the properties in Table 3-1. This procurement is done consistent with the QA program.

8.1.8 Miscellaneous Tests

There are no additional or miscellaneous tests are required prior to the use of the RAJ-II packaging.

8.2 MAINTENANCE PROGRAM

8.2.1 Structural and Pressure Tests

Prior to each use of the RAJ-II, the packaging is visually inspected to assure that the packaging is not damaged and that the components parts are in place. The containers are constructed primarily from stainless steel making it corrosion resistant. Since the packaging is not relied on for containment, there are no pressure test requirements for the inner or outer containers that comprise the packaging. When used as a Type B package, each fuel rod is leak checked and the successful results of the test are checked before shipment.

The RAJ-II packaging is maintained consistent with a 10 CFR 71 subpart H QA program. Containers that do not conform to the license drawings are removed from service until they are brought back into compliance. Repairs are performed in accordance with the approved procedures and consistent with the quality assurance program.

Leakage Tests

Containment is provided by the fuel rod for Type B shipments. Each loaded fuel rod is leak checked to assure that the rod is leak tight. Neither the inner or outer container is credited with providing leak protection. Therefore, no leak test of the packaging is required.

8.2.2 Component and Material Tests

There are no prescribed component tests or replacement requirements for this packaging. The packaging does not use neutron absorbers or shielding that would require testing or maintenance. Replacement parts shall meet the requirements in Table 2-3 by either testing or certifications from suppliers. The compressive strength of any replacement balsa wood shall be no less than 10.8 MPa, and the foam polyethylene shall be no greater than +/- 25% from nominal. The density of the paper honeycomb shall be no greater than +/- 25% from nominal. The density of the foam polyethylene shall be no greater than +10/-25% from nominal.

8.2.3 Thermal Tests

The alumina silicate thermal material is sealed within the stainless steel plates of the container wall. The packaging is visually inspected prior to use to assure that the alumina silicate is contained. No thermal testing is required.

8.2.4 Miscellaneous Tests

There are no additional or miscellaneous tests are required for the use of this packaging. The RAJ-II packaging is inspected prior to each use and maintained consistent with the license drawings. The package is inspected to verify that there are no missing parts or handling damage prior to shipping. As noted on the drawings localized deformation in the shell is permitted up to 25.4 mm and the lids of both containers need not provide an air tight seal. The packaging is repaired in accordance with drawings found in Section 1.3.2 under a Quality Assurance Program meeting 10 CFR 71 subpart H. Rework does not need to meet the 10CFR71 requirement, as long as any replacement parts meet the requirements in Table 2-3.

Foam cushioning material may have up to 5% of the total volume removed for packing purposes, handling or as a result of tears or punctures to the foam.

Small dents, tears and rounding (or damage) of corners on paper honeycomb are acceptable providing the volume of material missing or damaged is less than 10% for the individual piece.

8.3 APPENDIX

No appendix for this section.